INACTIVATION MECHANISMS OF ADENOVIRUS FROM EXPOSURE TO POLYCHROMATIC ULTRAVIOLET LIGHT IRRADIATION

BY

BERNARDO VAZQUEZ BRAVO

DISSERTATION

Submitted in partial fulfillment of the requirements
for the degree of Doctor of Philosophy in Environmental Engineering in Civil Engineering
in the Graduate College of the
University of Illinois at Urbana-Champaign, 2018

Urbana, Illinois

Doctoral Committee:

Professor Benito J. Mariñas, Chair
Professor Joanna L. Shisler
Professor Thanh H. Nguyen
Professor Wen-Tso Liu

ABSTRACT

Ultraviolet (UV) light is a drinking water treatment technology that has gained popularity as an alternative to control chlorine-resistant pathogens and comply with regulations on disinfection byproduct formation. Human adenovirus (HAdV) is found in water sources around the world and can cause respiratory, urinary, gastrointestinal, and eye infections. HAdV has emerged as a waterborne pathogen of concern due to its resilience against UV light inactivation. The ultraviolet disinfection guidance manual for the Long-Term 2 Enhanced Surface Water Treatment Rule in the United States has established a fluence (UV dose) of 186 mJ/cm^2 to inactivate 99.99% of viruses based on adenovirus inactivation.

There are different sources of UV light that are commercially available but the most commonly used are monochromatic low-pressure (LP) and polychromatic medium-pressure (MP) UV lamps. MP UV light is found more effective at inactivating human adenovirus than LP UV light. While LP UV disinfection has been largely studied, MP UV inactivation has been less investigated and the mechanisms by which MP UV inactivates adenovirus are not fully understood.

The main goal of this research was to obtain a better understanding of the inactivation mechanisms that make MP UV light more effective than LP UV to control human adenovirus. In this research work the inactivation kinetics of human adenovirus type 2 (HAdV-2) after exposure to narrow wavelength bandwidths of polychromatic UV irradiation within the 200-300 nm range were characterized. Quantitative polymerase chain reaction (qPCR) and reverse transcriptase qPCR assays were used to elucidate stages in the adenovirus replication cycle that were disrupted after exposure to three UV wavelength ranges with peak emissions at 224, 254 and 280 nm.

This research determined that association of HAdV-2 to the host cells was not inhibited by UV treatment at any of the wavelengths analyzed even after exposure to a fluence that would produce a reduction in virus infectivity greater than 99.99%. In contrast, early and late gene transcription, and viral DNA

replication were inhibited to different extents by UV irradiation at all three peak emissions, which suggested that different mechanisms might be dominating such disruptions for each wavelength range.

The findings of this work help to better understand the mechanisms by which polychromatic MP UV light inactivate human adenovirus and which components of the virus are affected by UV irradiation emitted at different wavelengths. This research provides valuable information that can be used to develop more effective and efficient treatment approaches that incorporate UV light technologies for water disinfection.

Additionally, the presence of synergistic effects with the sequential application of polychromatic UV irradiation at different wavelength ranges, as well as the simultaneous application of monochromatic LP UV light and monochloramine were investigated. No explicit synergy was detected in any of the sequential configurations assessed. In contrast, the simultaneous application of LP UV light and monochloramine showed synergy between these two disinfectants; this aspect indicated potential for this configuration as an alternative to be further evaluated to control adenovirus in water treatment processes.

My lifelong gratitude for the support from all the wonderful people and organizations I had the privilege to interact and collaborate with throughout the duration of my graduate studies.

A todos ustedes, muchas gracias.

TABLE OF CONTENTS

CHAPTER 1: INTRODUCTION 1

CHAPTER 2: BACKGROUND INFORMATION 9

CHAPTER 3: ADENOVIRUS REPLICATION CYCLE DISRUPTION FROM EXPOSURE TO POLYCHROMATIC ULTRAVIOLET IRRADIATION 20

CHAPTER 4: SEQUENTIAL APPLICATION OF POLYCHROMATIC ULTRAVIOLET LIGHT TO INACTIVATE HUMAN ADENOVIRUS 66

CHAPTER 5: SIMULTANEOUS APPLICATION OF MONOCHROMATIC LOW-PRESSURE ULTRAVIOLET LIGHT AND MONOCHLORAMINE TO HUMAN ADENOVIRUS 76

CHAPTER 6: CONCLUSIONS AND FUTURE WORK 97

APPENDIX A: INACTIVATION OF COXSACKIEVIRUS B5 AND MURINE NOROVIRUS 1 FROM EXPOSURE TO POLYCHROMATIC ULTRAVIOLET LIGHT 109

APPENDIX B: RAW DATA 123

CHAPTER 1: INTRODUCTION

1.1 Preface

Chlorine disinfection is the water treatment technique most commonly used worldwide (Crittenden et al., 2012). However, when chlorine reacts with natural organic compounds in the water it can form toxic, regulated disinfection by-products (DBPs) that cause adverse health effects (Crawford et al., 2005). Ultraviolet (UV) light disinfection is a treatment approach with increasing application in water systems due to its effectiveness to inactivate chlorine-resistant pathogens (virus, bacteria, and protozoa) such as *Cryptosporidium parvum* oocyst; a protozoan parasite that infects the cell lining of the digestive tract causing the diarrheal disease cryptosporidiosis (Casemore, 1990). In addition, UV light does not seem to generate regulated DBPs at the fluences (UV doses) that are commonly applied for water treatment purposes (Crittenden et al., 2012).

The most common types of UV light sources for water disinfection are monochromatic low-pressure (LP) UV and polychromatic medium-pressure (MP) UV mercury-vapor lamps. LP UV lamps emit almost all of their radiation at 253.7 nm, whereas MP UV lamps emit radiation at a wide range of wavelengths including those that are considered to have germicidal properties (200-300 nm).

Cryptosporidium parvum oocyst has been shown to be similarly affected by emissions from either LP or MP UV, and is more susceptible to UV radiation compared to bacteria and viruses (Linden et al., 2001). Viruses are challenging to control in water treatment processes due to their small size and diversity of susceptibility to different disinfectants. Therefore, it is important to perform analyses on different types of viruses to assess what the similarities and differences are among them. These analyses can provide important information regarding the mechanism of inactivation that might be unique to certain viruses or shared among different types of pathogens.

The fact that facilities have incorporated UV light as an alternative disinfection technology induced concern about emerging pathogens that are susceptible to chlorine but resistant to UV inactivation. Human adenovirus (HAdV) is a non-enveloped, icosahedral, double-stranded (ds) DNA virus with a capsid or protein coat surrounding its genome. Due to its known public health risk, adenovirus has been included in the US Environmental Protection Agency's Contaminant Candidate List Four (CCL 4) as one of the microbial contaminants listed for future regulation (USEPA, 2016). Different viruses that are included in the EPA's CCL4 have shown different sensitivities to commonly used disinfectants including free chlorine, monochloramine, and UV irradiation. Even different serotypes of the same virus can show different sensitivities to the same disinfectant (Shirasaki et al., 2017).

Human adenoviruses (HAdVs) are the second-leading cause of childhood gastroenteritis worldwide (Fongaro et al., 2013). Adenovirus has become a waterborne pathogen of concern due to its relatively high resistance to UV light inactivation and has, consequently, determined the current drinking water UV disinfection requirements. The Long Term 2 Enhanced Surface Water Treatment Rule (LT2ESWTR) established a fluence of 186 mJ/cm^2 required for a 4-log (99.99%) inactivation of all viruses. This parameter was determined based on results from several adenovirus inactivation studies performed with monochromatic LP UV light (Eischeid, 2009; USEPA, 2006). Although adenovirus has been shown to be highly resistant to monochromatic LP UV irradiation, polychromatic MP UV light has been reported to be more effective at inactivating this pathogen (Linden et al., 2007; Linden et al., 2009; Shin et al., 2009; Beck et al., 2014). MP UV light has been increasingly implemented in water treatment facilities due to its greater capability to control adenovirus; however, the fundamentals behind such enhanced effectiveness (compared to LP UV) are not fully understood.

Genome damage is considered the main inactivation mechanisms by which UV light renders a microorganism non-infectious (Bolton and Cotton, 2008). Typically, the effectiveness of UV disinfection is assessed using cell culture infectivity assays. Some studies have attributed the resistance of adenovirus

to UV light inactivation to the capability of the host cell to repair UV-induced genome damage (Eischeid et al., 2009; Guo et al., 2010). Direct DNA damage induced by LP UV and MP UV has been evaluated by PCR or qPCR assays (Eischeid et al., 2009; Rodriguez et al., 2013) and both UV light sources showed similar effectiveness to damage the adenovirus genome at similar UV doses. A recent study has shown different levels of UV-induced DNA damage from exposure to monochromatic UV radiation assessed in 10 nm increments within the 200-300 nm wavelength range, with those below 240 nm being the least effective at damaging the adenovirus genome despite seeing increased inactivation effectiveness compared with inactivation at wavelength ranges above 240 nm (Beck et al., 2014). This aspect showed the need to further investigate the inactivation mechanisms of the wavelengths below 240 nm since they could be causing a widespread damage to viral proteins (in addition to nucleotide damage) that contribute to the overall virus inactivation (Beck et al., 2014). The observations from these previous studies accentuate the importance of having a better understanding of the mechanisms that cause MP UV to be more effective to inactivate human adenovirus. Moreover, there is need for a better understanding about how structural modifications in the virus translate into infectivity inhibition. For this reason the goal of this research was to look at different steps in the virus replication cycle to determine at which point the regular progression of infection was blocked by UV disinfection.

By knowing the replication cycle step that is disrupted, the specific components involved in such step can be further analyzed to determine an indicator that can be targeted to detect and differentiate between infectious and non-infectious viruses. This information can be used to improve real time detection of infectious viruses to have better monitoring of water quality in treatment systems for contextualized applications in developed or developing countries scenarios.

1.2 Research Objectives

The general objective of this research was to advance the knowledge on the mechanisms by which polychromatic UV light inactivates human adenovirus. The approach implemented for this task was to look at inhibitions at particular steps of the adenovirus replication cycle after exposure to UV irradiation. Elucidating which step of the infection cycle is disrupted and what viral components are damaged by UV light emitted at a specific wavelength range can help to design more cost-effective technologies for water treatment in developed and developing countries.

The specific objectives of this research were:

1. Characterize the inactivation kinetics of human adenovirus type 2 after exposure to narrow wavelength bandwidths of polychromatic UV irradiation within the 200-300 nm range.
2. Employ molecular biology techniques to elucidate stages in the adenovirus replication cycle that are disrupted after exposure to a particular UV wavelength range to better understand the inactivation mechanisms of polychromatic UV disinfection.
3. Explore synergistic effects in the combination of different UV wavelength ranges, or the combination of UV light and monochloramine, to inactivate human adenovirus.

1.3 Scope

Background information on the fundamentals of water disinfection by UV light, as well as the adenovirus structure and replication cycle is included in Chapter 2. The research work on adenovirus inactivation by UV light is organized into three sections (Chapters 3 through 5), and a summary of findings and recommendations for future work are presented in Chapter 6. Although the central point of this research work was focused on human adenovirus, the inactivation kinetics of coxsackievirus B5 (CVB5) and murine norovirus 1 (MNV-1) after exposure to different wavelength ranges was also investigated. The action spectrum for CVB5 and MNV1 were developed and are presented in Appendix A of this document.

Adenovirus Replication Cycle Disruption from Exposure to Polychromatic Ultraviolet Irradiation (Chapter 3) [♪]

Polychromatic ultraviolet (UV) light with bandwidth of 20 nm and peak emission centered at 224, 254, or 280 nm (UV_{224}, UV_{254}, and UV_{280}, respectively) were used to inactivate human adenovirus type 2 (HAdV-2). Quantitative polymerase chain reaction (qPCR) and reverse transcriptase qPCR assays were used to elucidate the step in the HAdV-2 replication cycle that was disrupted after UV exposure. UV treatment at any of the wavelengths analyzed did not inhibit association of HAdV-2 to the host cells even after exposure to a fluence (UV dose) that would produce a virus inactivation efficiency, measured by plaque assay, greater than 99.99%. In contrast, UV irradiation at all three peak emissions disrupted early E1A gene transcription and viral DNA replication, but different mechanisms appeared to be dominating such disruptions. UV_{224} seemed to have little effect on the integrity of the viral genome but produced a structural transformation of the viral capsid that may inhibit the delivery of viral genome into the host cell nucleus. On the other hand, UV_{254} and UV_{280} did not affect the integrity of the viral capsid, but the mutations they produced on the viral genome might cause the inhibition of the early gene transcription and DNA replication after the viral genome successfully translocated into the host cell nucleus.

Sequential Application of Polychromatic Ultraviolet Light to Inactivate Human Adenovirus (Chapter 4)

Since different wavelengths may affect predominantly different targets in the genome or viral proteins it is possible that certain combinations of wavelengths might result in an enhanced disinfection effect for particular waterborne pathogens. The sequential application of polychromatic UV light from the three different regions of the germicidal range (200-300 nm) was evaluated to assess synergistic effects to inactivate human adenovirus type 2 (HAdV-2). This work was done using a MP UV lamp and bandpass

[♪] Abstract from Vazquez-Bravo, B.; Gonçalves, K.; Shisler, J. L.; Mariñas, B. J. Adenovirus Replication Cycle Disruption from Exposure to Polychromatic Ultraviolet Irradiation, *Environ. Sci. Technol.*, **2018**, *52* (6), pp 3652–3659.

filters with peak transmittance at 224, 254, and 280 nm. The reduction in viral genome replication at 48 hours postinfection (hpi) assessed by qPCR was utilized to determine the levels of inactivation achieved by each sequential combination of UV wavelengths. No synergistic effects were observed by any combination of the three UV wavelength ranges analyzed. These results suggest that the level of inactivation achieved by a source that combines UV irradiation at multiple wavelengths (such as a MP UV source) would be the addition of the individual contributions from the photons emitted at all the wavelengths in the range covered for a given time.

Simultaneous Application of Monochromatic Low-Pressure Ultraviolet Light and Monochloramine to Inactivate Human Adenovirus (Chapter 5)

The simultaneous application of LP UV light and monochloramine to inactivate human adenovirus type 2 was evaluated (HAdV-2). Additionally, a possible mechanism of synergy was investigated. This work complemented the available data on the sequential configuration of these treatment techniques and helped to improve the understanding of the inactivation mechanisms by different disinfectants. Explicit synergism was observed with the simultaneous application of LP UV light and monochloramine. The presence of monochloramine made LP UV light about twice as effective to inactivate HAdV-2 compared to the level of inactivation achieved by LP UV acting independently. This information can help to develop alternative disinfection strategies for water treatment facilities that currently use both LP UV light and monochloramine as part of their treatment train. Moreover, this knowledge can also contribute on the design of innovative treatment approaches for application in developing countries scenarios where presence of ammonia in drinking water makes effective chlorination a challenge.

1.4 References

Beck, S. E.; Rodriguez, R. A.; Linden, K. G.; Hargy, T. M.; Larason, T. C.; Wright, H. B. Wavelength dependent UV inactivation and DNA damage of adenovirus as measured by cell culture infectivity and long range quantitative PCR. *Environ. Sci. Technol.* **2014**, *48* (1), 591– 598, DOI: 10.1021/es403850b

Bolton, J. R.; Cotton, C. A. *The Ultraviolet Disinfection Handbook*; American Water Works Association: Denver, CO, **2008**; pp 11– 40.

Casemore, D. Epidemiological aspects of human cryptosporidiosis. *Epidemiol. Infect*. **1990**, 104:1-28.

Crawford, M.; Banas, F.; Ross, M.; Ruby, D.; Nelson, J.; Boucher, R.; Allerman, A. Final LDRD Report: Ultraviolet water purification systems for rural environments and mobile applications. **2005**, SAND2005-7245.

Crittenden, J. C.; Trussell, R. R.; Hand, D. W.; Howe, K. J.; Tchobanoglous, G., Disinfection. In MWH's Water Treatment: Principles and Design, Third Edition, John Wiley & Sons, Inc.: **2012**; pp 903-1032

Eischeid, A. C.; Meyer, J. N.; Linden, K. G. UV disinfection of adenoviruses: Molecular indications of DNA damage efficiency. *Appl. Environ. Microbiol.* **2009**, *75* (1), 23– 28, DOI: 10.1128/AEM.02199-088.

Fongaro, G.; Nascimento, M. A. do; Rigotto, C, et al. Evaluation and molecular characterization of human adenovirus in drinking water supplies: viral integrity and viability assays. *Virology Journal*. **2013**; 10:166. DOI:10.1186/1743-422X-10-166.

Guo, H. L.; Chu, X. N.; Hu, J. Y. Effect of host cells on low- and medium-pressure UV inactivation of adenoviruses. *Appl. Environ. Microbiol.* **2010**, *76* (21), 7068– 7075, DOI: 10.1128/AEM.00185-10

Linden, K. G.; Thurston, J.; Schaefer, R.; Malley, J. P. Enhanced UV inactivation of adenoviruses under polychromatic UV lamps. *Appl. Environ. Microbiol.* **2007**, *73* (23), 7571– 7574, DOI: 10.1128/AEM.01587-07

Linden, K. G.; Shin, G. A.; Lee, J. K.; Scheible, K.; Shen, C. Y.; Posy, P. Demonstrating 4-log adenovirus inactivation in a medium-pressure UV disinfection reactor. *J. - Am. Water Works Assoc.* **2009**, *101* (4), 90–99, DOI: 10.1002/j.1551-8833.2009.tb09876.x

Linden, K. G.; Shin, G. A.; Sobsey, M. D. Comparative effectiveness of UV wavelengths for the inactivation of Cryptosporidium parvum oocysts in water. *Water. Sci. Technol*. **2001,** *43*(12): 171- 174.

Rigotto, C.; Victoria, M.; Moresco, V.; Kolesnikovas, C. K. M.; Correa, A. A.; Souza, D. S. M.; Miagostovich, M.; Simões, C. M.; Barardi, C. R. Assessment of adenovirus, hepatitis A virus and rotavirus presence in environmental samples in Florianópolis South Brazil. *J Appl Microbiol*. **2010**; *109*:1979–1987.

Rodriguez, R. A.; Bounty, S.; Linden, K. G. Long-range quantitative PCR for determining inactivation of adenovirus 2 by ultraviolet light. *J. Appl. Microbiol.* **2013**, *114* (6), 1854– 65, DOI: 10.1111/jam.12169

Shin, G. A.; Lee, J. K.; Linden, K. G. Enhanced effectiveness of medium-pressure ultraviolet lamps on human adenovirus 2 and its possible mechanism. *Water Sci. Technol.* **2009**, *60* (4), 851– 857, DOI: 10.2166/wst.2009.414

Shirasaki, N.; Matsushita, T.; Matsui, Y.; Murai, K.; Aochi, A. Elimination of representative contaminant candidate list viruses, coxsackievirus, echovirus, hepatitis A virus, and norovirus, from water by coagulation processes. *Journal of Hazardous Materials*. **2017**, 326, 110–119.

USEPA. Drinking Water Contaminant Candidate List 4: Final. In *Federal Register*, Vol. 81, No. 222; Washington, DC, **2016**, pp 81099– 81114.

USEPA (U.S. Environmental Protection Agency). *Ultraviolet Disinfection Guidance Manual for the Final Long Term 2 Enhanced Surface Water Treatment Rule*; Washington, DC, **2006**.

CHAPTER 2: BACKGROUND INFORMATION

2.1 Ultraviolet Light

Light is transmitted in packets of energy called photons but it also has a frequency and wavelength, thus light holds both particle and wave properties (Bolton and Cotton, 2008). Ultraviolet (UV) light can be generated by applying a voltage through a gas mixture that results in a discharge of photons (USEPA, 2006). When a photon is absorbed by a molecule such molecule is raised to an excited state from which a chemical reaction may happen (Bolton and Cotton, 2008). The UV light range is divided into four regions; UVA (315-400 nm), UVB (280-315 nm), UVC (200-280 nm), and vacuum UV (100-200 nm) (USEPA, 2006). UVC can be absorbed by nucleic acids and proteins (Bolton and Cotton, 2008). UV *irradiance* (sometimes called UV intensity, and usually measured in mW/cm^2 or W/m^2) is the amount of UV light incident on a nearly flat surface area, however if the target surface is almost spherical the term *fluence rate* is more adequate (Bolton et al., 2015). When using a collimated-beam system to assess the inactivation of a microorganism within a very shallow water layer, fluence rate and irradiance are practically interchangeable (Bolton and Cotton, 2008). For collimated-beam experiments the term irradiance is more commonly used in the water treatment industry. Integrating irradiance (or fluence rate) over time the fluence, or UV dose (mJ/cm^2 or J/m^2), is obtained (Bolton and Cotton, 2008).

2.2 Water Disinfection by UV Light

Ultraviolet light disinfection has gained increased interest as a technology to incorporate in water treatment systems due to its proven effectiveness against chlorine-resistant pathogens, such as *Cryptosporidium parvum* (USEPA, 2006). UV disinfection is a physical processes and since no chemicals are involved the water quality after UV treatment does not greatly change, nor are significant levels of regulated disinfection by-products generated (Bolton and Cotton, 2008). The USEPA's Long Term 2 Enhanced Surface Water Treatment Rule (LT2ESWTR) indicates a minimum of 4-log (99.99%) removal or inactivation of viruses, and the UV dose required to reach this level of inactivation was set at

186 mJ/cm^2 based on the inactivation of adenovirus by monochromatic low-pressure (LP) UV light (USEPA, 2006). Human adenovirus (HAdV) has been included on the U.S. Environmental Protection Agency (USEPA)'s Contaminant Candidate List Four (CCL 4) for potential future regulation (USEPA, 2016). HAdV is commonly present in sewage and has been detected in surface waters, storm water, coastal waters and swimming pools; detection is usually performed with a combination of cell-culture based methods and molecular techniques (Rigotto et al., 2011).

LP UV lamps have been the predominant technology utilized for drinking water disinfection in water treatment plants (Bolton and Cotton, 2008). These lamps emit monochromatic UV light at 253.7 nm and operate at an internal mercury-vapor pressure of 0.13 to 1.3 Pa (2×10^{-5} to 2×10^{-4} psi) with moderate temperature of about 40 ºC (USEPA, 2006). Polychromatic medium-pressure (MP) lamps emit UV light at a wider range of wavelengths (200-800 nm) compared to LP UV lamps, including those considered to have germicidal properties (200-300 nm). MP UV lamps operate at temperatures in the range of 600-900 ºC an internal mercury-vapor pressure of 13,000 to 1,300,000 Pa (2 to 200 psi) generating polychromatic UV light (USEPA, 2006).

In practice, temperature and pH do not seem to affect the performance and inactivation rates obtained by UV disinfection (AWWA, 1999). A main drawback of UV disinfection is the lack of disinfectant residual capacity after treatment, and for this reason free chlorine or monochloramine is usually applied after UV disinfection to have disinfectant residual in the distribution system (Bolton and Cotton, 2008). Some disadvantages of UV disinfection include the need for constant electric power supply, the presence of mercury in UV lamps that can be hazardous in the event of a lamp breakage, and the challenge to monitor the fluence (UV dose) constantly in UV reactors (Bolton and Cotton, 2008). The effectiveness of UV disinfection can be assessed by determining the dose-response behavior for a particular microorganism using a collimated-beam system, however, the characterization and quantification of UV doses in full scale reactors remains a challenge (NWRI, 2012). The design fluence for UV disinfection systems

depends on the local regulations for pathogen removal or inactivation, and the presence of other barriers such as microfiltration, ultrafiltration, or reverse osmosis prior to the UV disinfection step (NWRI, 2012).

Historically, absorption of UV photons by DNA or RNA has been identified as the main inactivation mechanism against pathogenic microorganisms (Bolton and Cotton, 2008). What is considered as the germicidal range (200-300 nm) of the UV spectrum is delimited by the fact that UV light emitted below 200 nm does not penetrate water and UV light emitted above 300 nm is not absorbed by DNA (Crittenden et al., 2012). Recent work has shown that at different wavelengths mechanisms other than absorption of UV radiation by nucleic acids might be playing a more predominant role in the inactivation of certain microorganisms, such as adenovirus (Beck et al., 2014). UV light does not have the same disinfection capacity at all wavelengths and thus there is need to better understand the factors delineating the germicidal effectives of different wavelengths within the 200-300 nm range (Crittenden et al., 2012).

2.3 Fundamentals of UV Light Inactivation Mechanisms

Nucleotides and proteins absorb UV light in the range of 200-300 nm. In DNA the absorption of a UV photon by one of two adjacent thymine bases results in a chemical bond between the two bases called a thymine dimer. For RNA viruses a similar dimerization reaction takes place between uracil bases. These dimers disrupt the structure of the DNA or RNA, and is considered to be the fundamental mechanism of UV disinfection (Bolton and Cotton, 2008). The absorbance spectrum of DNA or RNA have a peak near 260 nm and a minimum around 230-240 nm (USEPA, 2006). In addition to pyrimidine dimers, pyrimidine (6-4) pyrimidone photoproducts, and protein-DNA cross-links are other types of DNA mutations that can contribute to microorganism inactivation (USEPA, 2006). Single and/or double-strand breaks, and DNA-DNA cross-links can also happen but they are about 1000 times less likely to occur compared to pyrimidine dimers (USEPA, 2006). Below 230 nm proteins dominate the absorbance of UV light relative to nucleotides and the opposite occurs above 230 nm (Bolton and Cotton, 2008). Tryptophan, tyrosine, and phenylalanine are three amino acids that absorb UV light significantly above

210 nm and they depict a small absorption peak at ~280 nm, tryptophan being the strongest absorber of the three at this wavelength (Bolton and Cotton, 2008).

2.4 Human Adenovirus

Adenoviruses are composed by a linear double-stranded DNA (dsDNA) genome inside an icosahedral protein shell (~ 90 nm in diameter) with fiber proteins at each of the vertices of the icosahedron that aid the virus to bind to host-cells (Berk, 2013). Respiratory disease, conjunctivitis, and gastroenteritis are the most common self-limiting infections caused by adenovirus, however in neonates and immunosuppressed individuals, adenoviruses can cause fatal pneumonia, hepatitis, and/or encephalitis (Berk, 2013). Adenoviruses are responsible for ~7% of upper respiratory tract infection cases in children under 5 years of age, and for about 10% of pneumonias of childhood (Wold and Ison, 2013). There are seven species of human adenovirus (A, B, C, D, E, F, and G) among which 57 types are distributed (Wold and Ison, 2013). Human adenovirus type 2 is classified within species C along with adenoviruses type 1, 5 and 6, being types 2 and 5 the most widely used for structural studies of adenoviruses (Berk, 2013). Viral myocarditis, most commonly known to be caused by enterovirus infections (e.g. by coxsackievirus), might be significantly caused as well by adenoviruses; in children with myocarditis or dilated cardiomyopathy, adenoviruses were detected in 8-36% of the patients, with adenovirus type 2 being the most predominant type detected (Wold and Ison, 2013). Adenovirus has become a waterborne pathogen of concern due to its high resistance to monochromatic low-pressure UV light inactivation, compared to other viruses potentially present in drinking water, and this aspect has driven the development of the current regulations for UV disinfection (Oguma et al., 2015).

2.4.1 Virion Structure

Adenovirus particles have a mass of ~150×10^6 Da from which 13% is DNA and 87% is protein. The virion is comprised by 12 proteins numbered II-IX, IIIa, IVa, μ, terminal protein, and the p23 viral protease (Berk, 2013). The icosahedral capsid is formed by 240 capsomers of hexon trimers, 12

pentameric penton capsomers at each vertex, and 12 fibers protruding from each penton. The minor capsid proteins IIIa, VIII, and IX stabilize interactions between hexon trimers. Polypeptides VII, VI, and μ contact the viral genome and likely condense it within the core (Berk, 2013). Protein VI associates with protein V connecting the capsid to the DNA-protein core. The terminal protein is covalently bound to the 5' ends of the viral DNA and serves as a primer for DNA replication (Berk, 2013)

The DNA of human adenovirus type 2 (HAdV-2) was the first adenovirus genome to be fully sequenced and consists of 35,937 base pairs (bp) (Berk, 2013). HAdV genomes contain five early transcription units (E1A, E1B, E2, E3, and E4), four intermediate transcription units (IX, Iva2, L4 intermediate, and E2 late), and one late transcription unit (major late). Intermediate transcription units are transcribed at the same time that DNA replication takes place, the late transcription unit generates five families of late mRNAs (L1-L5) transcribed by RNA polymerase II (Berk, 2013). The E1A unit encodes two proteins that activate transcription and induce the host cell to enter S phase; E1B encodes two proteins that block apoptosis; E2 encodes three proteins that operate in DNA replication; E3 encodes products that regulate the response of the host to infection, and the late family of mRNAs drive the production and assembly of capsid components (Berk, 2013). Figure 2.1 shows a transmission electron microscopy (TEM) image of human adenovirus 2 (HAdV-2).

2.4.2 Replication Cycle

Human adenovirus type 2 initiates its replication cycle by associating to the host cell using the fiber knob of its fiber-like projections to attach with high affinity to the coxsackie-adenovirus receptor (CAR) protein located in the host cell membrane (Berk, 2013). Next, the arg-gly-asp (RGD) loop domains of the penton base protein of the virus attach to the αvβ3 and αvβ5 integrins in the host cell (Berk, 2013; Greber et al., 1999). Viral internalization is triggered via receptor-mediated endocytosis and in epithelial cells, such as A549 cells, the fibers detach from the viral particle during internalization (Greber et al., 1999). Inside the endosomes the vertices of the viral particle dissociate and internal capsid proteins IIIa, VI, and

VIII are released; protein VI lyses the endosome and the partially uncoated capsid is released into the cytosol (Berk, 2013). Viral internalization takes place within 10-15 min postinfection (Greber et al., 1999). The viral capsid is then transported to the nuclear pore complex by dynein motor proteins via microtubules and it reaches the nucleus about 60 minutes after infection (Berk, 2013). Once at the nuclear membrane the viral particle further disassembles and by 2 hours postinfection the viral DNA and associated protein VII is imported into the nucleus by the importins Trasportin and Imp7 (Greber et al., 1999: Berk, 2013).

Three main goals are pursued during the early phase of adenovirus gene transcription: (1) cause the host to enter the S phase cycle to provide an adequate environment for viral replication; (2) set up systems to avoid antiviral defenses of the host; (3) and synthesize products needed for viral DNA replication (Berk, 2013). The E1A region is the first one to be transcribed once the viral DNA reaches the nucleus, then transcription of the E1B, E2 early, E3, and E4 regions takes place (Berk, 2013). HAdV-2 initiates DNA replication about 6 hours after infection, and requires a set of 3 replication proteins: terminal protein (pTP, used as primer of DNA synthesis), the viral DNA polymerase (Ad Pol), and the ssDNA binding protein (DBP) (Berk, 2013). Two stages are involved in the viral DNA replication: first, only one of the two parental strands of DNA serves as template for DNA synthesis leaving a displaced parental DNA, and then a complement to the displaced single strand is synthesized during the second stage (Berk, 2013). After the translation of viral late mRNAs, hexon and penton capsomers are assembled in the cytoplasm and then imported into the nucleus where the viral DNA is packaged into the capsids resulting in a complete virion (Berk, 2013). Lastly, the cleavage of precursors of proteins VI, VII, VIII, μ, and terminal protein by a viral protease completes the formation of infectious particles. The E3 11.6-kD protein is expressed at high levels during the late phase of infection and its accumulation kills the cells and promotes their lysis. About 100,000 progeny virions are released form a cell at the end of a replication cycle (Berk, 2013). Typically, by 48 hours postinfection a productive viral replication cycle is completed (Jogler et al., 2006; Berk, 2013). Figure 2.2 shows a simplified graphic representation of the different

steps involved in the adenovirus replication cycle. Figure 2.3 includes transmission electron microscopy (TEM) images of A549 cells infected with HAdV-2 where HAdVs can be observed in the outer cell membrane and then next to the cell nucleus (at around 0 and 2 hours postinfection, respectively).

2.5 Figures

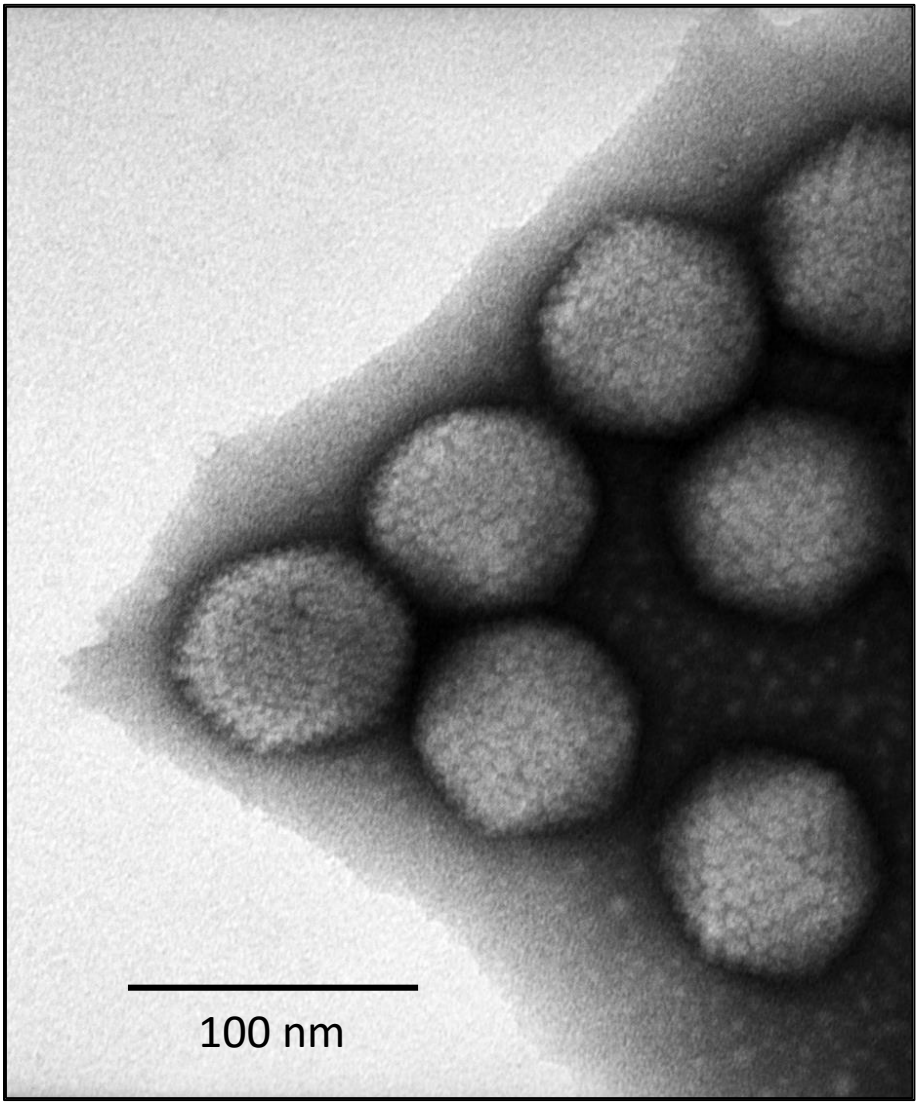

Figure 2.1. TEM image of human adenovirus type 2.

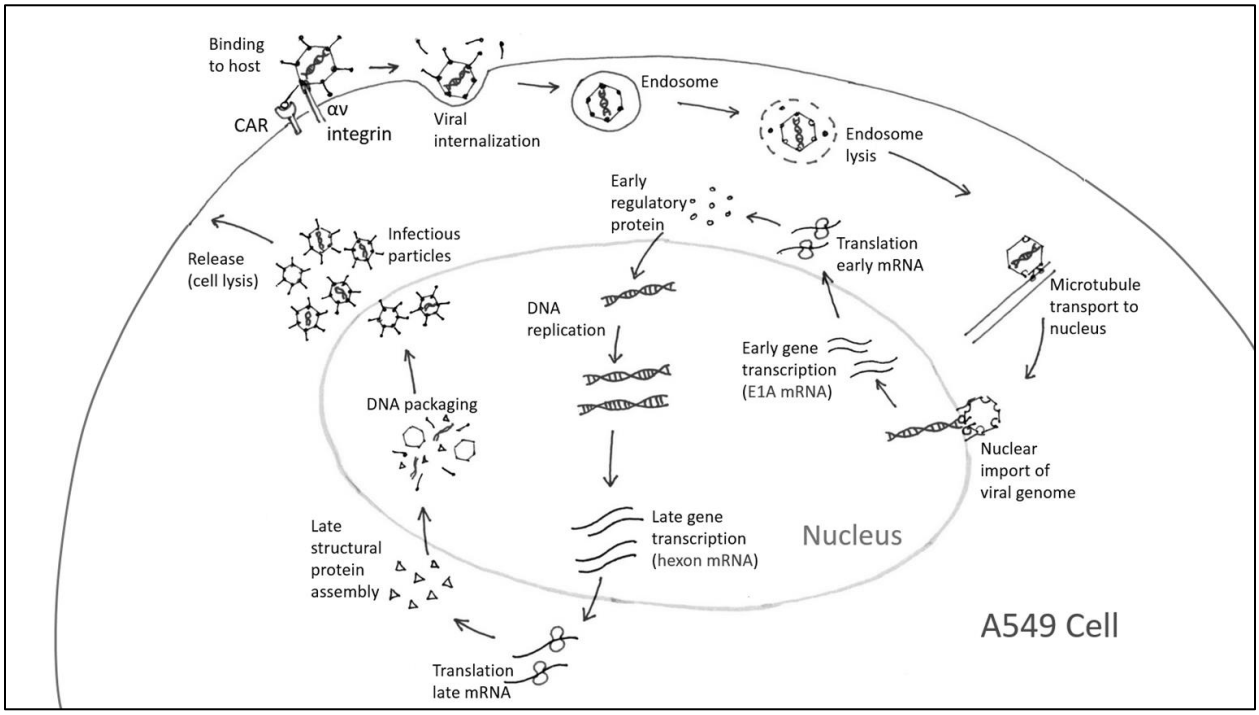

Figure 2.2. Graphic representation of the HAdV replication cycle.

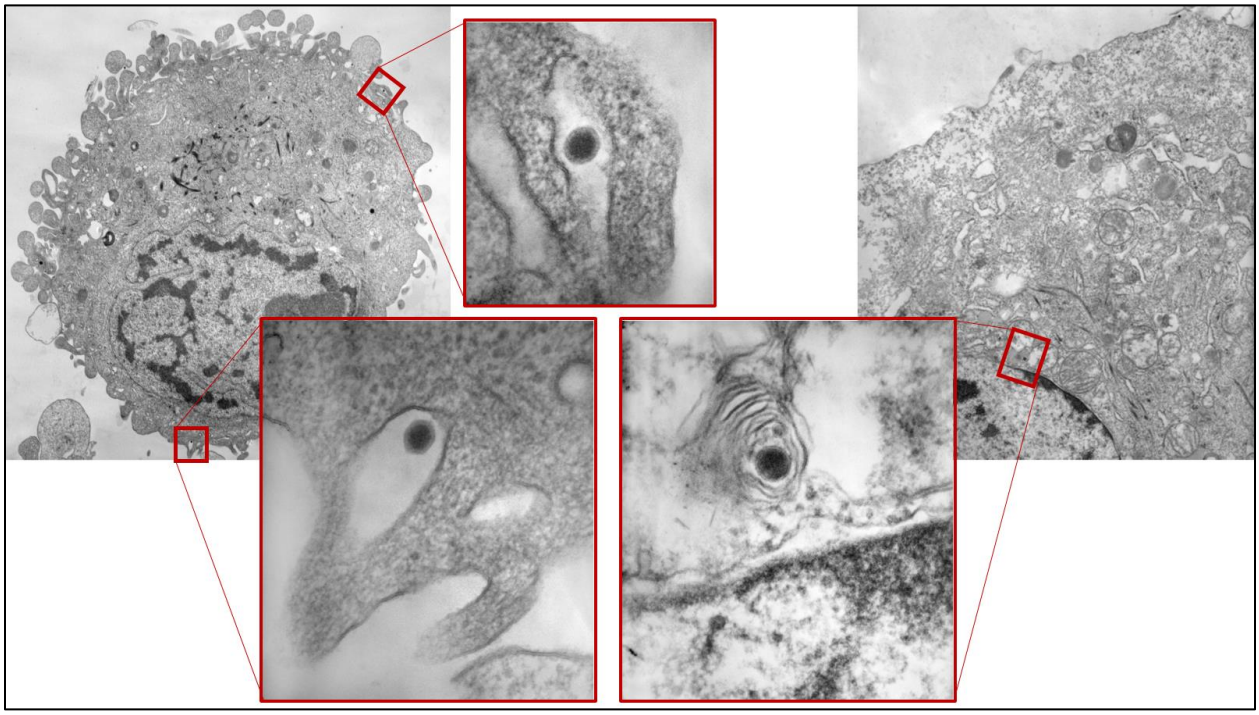

Figure 2.3. TEM image of A549 cells infected with HAdV-2. At ~0 hours postinfection (hpi), HAdV-2 can be observed in the outer cell membrane (left). By ~2 hpi HAdV-2 can be observed next to the cell nucleus (right).

2.6 References

American Water Works Association (AWWA), Water Quality and Treatment, A Handbook of Community Water Supplies, McGraw-Hill, Inc., 5TH edition, **1999**.

Beck, S. E.; Rodriguez, R. A.; Linden, K. G.; Hargy, T. M.; Larason, T. C.; Wright, H. B. Wavelength dependent UV inactivation and DNA damage of adenovirus as measured by cell culture infectivity and long range quantitative PCR. *Environ. Sci. Technol.* **2014**, *48* (1), 591– 598, DOI: 10.1021/es403850b

Berk, A. J. Adenoviridae. In *Fields Virology*, 6th ed.; Knipe, D. M., Howley, P. M., Eds.; Lippincott Williams & Wilkins: Philadelphia, PA, **2013**; pp 1704– 1735.

Bolton, J. R.; Cotton, C. A. *The Ultraviolet Disinfection Handbook*; American Water Works Association: Denver, CO, **2008**; pp 11– 40.

Bolton, J. R.; Mayor-Smith, I.; and Linden, K. G. Rethinking the concepts of fluence (UV dose) and fluence rate: The importance of photon-based units – A Systemic Review. *Photochem. Photobiol*. **2015**, **91**, 1252–1262.

Crittenden, J. C.; Trussell, R. R.; Hand, D. W.; Howe, K. J.; Tchobanoglous, G., Disinfection. In MWH's Water Treatment: Principles and Design, Third Edition, John Wiley & Sons, Inc.: **2012**; pp 903-1032

Greber, U. F.; Nakano, M. Y.; Maarit Suomalainen, M. *Adenovirus Entry into Cells*, *Methods in Molecular Medicine*, Vol 21; Adenovirus Methods and Protocols; World, W. S. M.; Humana Press, Inc.: Totowa, NJ,**1999**; pp 217– 230

Jogler, C.; Hoffmann, D.; Theegarten, D.; Grunwald, T.; Überla, K.; Wildner, O. Replication Properties of Human Adenovirus In Vivo and in Cultures of Primary Cells from Different Animal Species. *Journal of Virology* **2006**, *80* (7), 3549– 3558, DOI: 10.1128/JVI.80.7.3549-3558.2006

National Water Research Institute (NWRI) in collaboration with Water Research Foundation (WRF), *Ultraviolet Disinfection Guidelines for Drinking Water and Water Reuse*, Third edition, August **2012**,

Oguma, K.; Rattanakul, S.; Bolton, J. R. Application of UV light-emitting diodes to adenovirus in water. *J. Environ. Eng.* **2016**, *ISNN*, 0733– 9372, DOI: 10.1061/(ASCE)EE.1943-7870.0001061

Rigotto, C.; Hanley, K.; Rochelle, P. A.; De Leon, R.; Barardi, C. R.; Yates, M. V. Survival of adenovirus types 2 and 41 in surface and ground waters measured by a plaque assay. *Environ. Sci. Technol.* **2011**, *45*(9), 4145– 4150, DOI: 10.1021/es103922r

USEPA. Drinking Water Contaminant Candidate List 4: Final. In *Federal Register*, Vol. 81, No. 222; Washington, DC, **2016**, pp 81099– 81114.

USEPA (U.S. Environmental Protection Agency). *Ultraviolet Disinfection Guidance Manual for the Final Long Term 2 Enhanced Surface Water Treatment Rule*; Washington, DC, **2006**.

Wold, W. S. M.; Ison, M. G. Adenoviruses. In *Fields Virology*, 6th ed.; Knipe, D. M., Howley, P. M., Eds.; Lippincott Williams & Wilkins: Philadelphia, PA, **2013**; pp 1732– 1767.

CHAPTER 3: ADENOVIRUS REPLICATION CYCLE DISRUPTION FROM EXPOSURE TO POLYCHROMATIC ULTRAVIOLET IRRADIATION [♪]

3.1 Introduction

Water disinfection with ultraviolet (UV) light is gaining popularity due to its effectiveness to inactivate chlorine-resistant pathogens while forming lower levels of toxic disinfection byproducts (DBPs) compared to chlorination, the most common water disinfection approach currently used throughout the world (Sirikanchana et al., 2008; Eischeid et al., 2011). Two common types of UV light sources for water disinfection are monochromatic low-pressure (LP) and polychromatic medium-pressure (MP) UV mercury-vapor lamps. LP UV lamps emit light at 254 nm, whereas MP UV lamps emit light with a wide wavelength range that includes those (200–300 nm) with germicidal properties (Eischeid et al., 2011).

Adenovirus is a waterborne pathogen of concern because it has the highest resistance to LP UV inactivation among all waterborne pathogens found in drinking water and thus it is considered a benchmark in regulations (Oguma et al., 2016; USEPA, 2006). Adenovirus is a nonenveloped, icosahedral, double-stranded (ds) DNA virus with a capsid or protein coat surrounding the genome. There are more than 50 adenovirus serotypes causing different diseases (Wold and Ison, 2013), and many of them have been found in recreational and drinking water sources around the world (Oguma et al., 2016; Nascimento et al., 2015; Jiang, 2006; Rigotto et al., 2011). Due to its known public health risk, adenovirus is included in the United States Environmental Protection Agency (USEPA)'s Contaminant Candidate List Four (CCL 4) (USEPA, 2016). The USEPA established a fluence of 186 mJ/cm^2 required for a 4-log inactivation of viruses based on the resistance of adenovirus to LP UV light (USEPA, 2006).

[♪] Adapted from Vazquez-Bravo, B.; Gonçalves, K.; Shisler, J. L.; Mariñas, B. J. Adenovirus Replication Cycle Disruption from Exposure to Polychromatic Ultraviolet Irradiation, *Environ. Sci. Technol.*, **2018**, *52* (6), pp 3652–3659.

MP UV light is found to be more effective than LP UV light at inactivating adenovirus when using tissue culture systems to assess virus replication (Linden et al., 2007; Linden et al., 2009; Shin et al., 2009; Beck et al., 2014). Polymerase chain reaction (PCR) or quantitative PCR (qPCR) assays have shown that both LP UV and MP UV irradiation have similar capacity to damage the adenovirus genome, and yet, infectivity assays reveal the occurrence of different inactivation kinetics with the two light sources (Eischeid et al., 2009; Rodriguez et al., 2013). It has been suggested that irradiation emitted by a MP UV lamps inactivates adenoviruses by damaging the viral genome, the viral proteins, or both (Beck et al., 2014; Eischeid et al., 2009). However, the actual mechanisms by which polychromatic MP UV inactivates adenovirus are unknown. Because different wavelengths could preferentially target different regions of the genome or proteins in the capsid, it is important to elucidate the mechanisms of inactivation by different wavelengths within the germicidal range of 200–300 nm. For these reasons, we chose to examine the effect that specific wavelengths have on several steps of the viral replication cycle that might render the virus noninfectious.

Adenovirus has a dsDNA genome with ~36 kb pairs surrounded by an icosahedral capsid with 240 hexon protein trimers, 12 pentameric penton proteins at each vertex, and 12 fiber protein trimers protruding from each penton. Adenovirus uses its fiber-like projections to attach to a host cell receptor such as the coxsackie-adenovirus receptor (CAR) (Berk, 2013). Next, the RGD loop domains of the penton base protein attach to αvβ integrins in the host cell (Berk, 2013; Greber et al., 1999), triggering viral internalization by endocytosis (Greber et al., 1999). Inside the endosomes, the vertices of the viral particle dissociate, and protein VI lyses the endosome, releasing the viral particle into the cytosol (Berk, 2013). The viral particle interacts with microtubules, transporting them toward the nucleus (Berk, 2013). Upon reaching the nuclear membrane, the viral particle further disassembles, and by ~2 hours postinfection (hpi), the viral DNA and associated protein VII is imported into the nucleus (Berk, 2013; Greber et al., 1999). Inside the nucleus, the E1A gene quickly undergoes transcription, followed by genome replication, which initiates about 6 h after infection, approximately at the same time as late gene

transcription to produce structural proteins such as hexon. Typically, by 48 hpi, a productive viral replication cycle is completed (Berk et al., 2013; Jogler et al., 2006).

Ethidium monoazide bromide (EMA) (Invitrogen, ThermoFisher Scientific, Inc., Waltham, MA) was used to analyze if UV irradiation affected the integrity of the adenovirus capsid. EMA is a fluorescent nucleic acid stain that covalently binds to nucleic acids after exposure to visible light (Kim et al., 2011). When EMA binds to the viral genome, the affected genome region does not amplify by qPCR. EMA can access the adenovirus DNA only if the capsid has undergone a certain level of disruption. Therefore, PCR not amplifying the adenovirus DNA would signal damage of the adenovirus capsid to the extent that EMA internalizes after UV treatment. Previous work used qPCR coupled with EMA to assess the capsid integrity of HAdV-5 after exposure to UV irradiation with peak emissions in the 240–320 nm range (Sangsanont et al., 2014). Our research expands on this work by assessing narrower bandwidths within that wavelength range as well as the region of high UV absorbance by proteins (wavelength <240 nm).

Adenovirus inactivation experiments performed at different UV wavelengths served as a baseline for our novel molecular work assessing the inhibition of the adenovirus replication cycle. This analysis was important for better understanding the details of the inactivation capacity of MP UV compared to that of LP UV. qPCR and reverse transcriptase qPCR (RT-qPCR) were used to assess disruption of genome replication and early and late mRNA transcription. These findings can be the foundation to create more effective and efficient disinfection strategies that incorporate UV technologies. Additionally, by knowing what transformations result from exposure to different UV wavelengths, molecular sensors could be designed to distinguish transformed targets from those untransformed and therefore differentiate between infectious and noninfectious viruses. The major objective of this research is to elucidate using molecular techniques what steps in the adenovirus replication cycle were disrupted after exposure to UV radiation emitted in different regions of the MP UV spectrum.

3.2 Materials and Methods

3.2.1 Ultraviolet Light Irradiation Experiments

UV inactivation experiments were performed using a 1 kW Rayox collimated system operating with a polychromatic MP UV lamp (A300014, Calgon Carbon Co., Pittsburgh, PA). Bandpass filters (Andover Corporation, Salem, NH) with maximum peak transmittance at 224, 254, and 280 nm and bandwidth of about 10 nm at half of the maximum peak transmittance were used to isolate specific regions of UV radiation emitted by a polychromatic MP UV lamp. These nonoverlapping spectra were selected to represent different inactivation kinetics observed for three distinct regions within the germicidal range of 200–300 nm after performing preliminary experiments with 13 bandpass filters with maximum peak transmittance within the 218–297 nm range (Figure 3.1). Each filter was installed at the end of the collimator, and the spectral irradiance of the light passing through the filter was measured with a BLK-C-50 spectrometer (StellarNet Inc. Tampa, FL). The light intensity distribution across the irradiated water surface was measured with a 1400A radiometer and SEL 240 detector (International Light, Peabody, Massachusetts). The spectral irradiance was used as the weighting function to calculate the average fluence rate in the water sample following the standard protocol for a bench-scale UV apparatus using a polychromatic UV source by Bolton and Linden (2003). The radiometer readings were used to adjust for the nonuniformity of the light distribution across the irradiated surface (Petri factor). The average fluence rate calculations accounted for the variation of the sensitivity of the SEL 240 detector to measure the irradiance (sensor factor), and the UV absorbance between 200 and 300 nm of the water sample (UV-2700 Shimadzu spectrophotometer) adjusting for the water sample depth (water factor), distance of the suspension from the UV lamp (divergence factor), and water surface reflection (reflection factor). A recirculating water-jacketed reactor (23 °C) containing 20 mL of 1 mM carbonate buffer solution (CBS, Fisher Scientific) in Milli-Q water was dosed with HAdV-2 at concentrations of (6–20) × 10^5 plaque forming units (PFU) per mL and irradiated by UV light at the different band ranges. The fluence (UV dose) applied to HAdV-2 samples was controlled by varying the exposure time. All experiments were performed in duplicate.

3.2.2 Virus Propagation and Viability Assessment

Human lung A549 carcinoma cells (CCL-185) and human adenovirus type 2 (VR-846) were obtained from the American Type Culture Collection (Manassas, VA). A549 cells were used for adenovirus propagation and infectivity assessment with a soft agar overlay plaque assay. Cell culture growth, virus propagation, and infectivity assessment assays were performed following previously reported protocols (Sirikanchana et al., 2008; Page et al., 2010; Gall et al., 2015). Additional details are available in Text S1 of section 3.4.

3.2.3 Amplicon Integrity

To assess genome damage after UV light treatment, viral DNA was extracted from UV-treated and untreated virions following the extraction protocol for the DNeasy Blood & Tissue Kit (Qiagen, Valencia, CA). Primers previously designed to amplify different regions of the adenovirus genome (Rodriguez et al., 2013; Gall et al., 2015) were used to assess if such regions were amplifiable by qPCR after UV light exposure. The genome regions selected represent different steps during the replication cycle; the E1A gene is the first gene transcribed during an early phase, and the hexon gene is a late gene that is transcribed soon after viral genome replication begins (Berk, 2013). A 0.1-kilobase (kb) portion each of the E1A (nucleotides 673–778) and hexon (nucleotides 19 400–19 510) viral genes was subjected to qPCR amplification. Additionally, a 1.1-kb fragment (nucleotides 17 822–18 996) was PCR-amplified to target a larger section of the genome to compare the UV-induced effect observed with the 0.1-kb E1A and hexon amplicons. Details about the procedures followed and primer sets used are in Text S2 and Table 3.1 of section 3.4. Absolute copy numbers of the E1A and hexon amplicons as well as the 1.1-kb fragment were determined using the standard curves described in Text S5 of section 3.4.

3.2.4 Ethidium Monoazide Exposure

The inhibition of qPCR amplification due to EMA-DNA interactions was assessed by measuring the ratio of amplified DNA fragments present in UV-treated samples as compared to those present in the untreated sample. Protocols followed were from previous studies (Kim et al., 2011; Sangsanont et al., 2014; Parshionikar et al., 2010) with modifications detailed in Text S3 of section 3.4.

3.2.5 Viral Genome Replication in Host Cells and mRNA Transcription

HAdV-2 genome replication and mRNA transcription were quantified using previously reported protocols (Gall et al., 2015) (see Text S4 in section 3.4). Briefly, viruses were treated with light at each UV bandwidth and then inoculated onto cell host monolayers. After incubation for 90 min at 4 °C, the inocula was removed, and the monolayers were washed twice with 1 mL of ice-cold phosphate buffered saline (PBS) to remove unbound viruses. Viral genome replication and mRNA transcription in infected cells were monitored in the subsequent 48 h, a time by which one full replication cycle should occur (Berk, 2013). Total DNA or RNA was extracted from the A549 cellular monolayers with bound HAdV-2 at various times postinfection (0, 4, 12, 24, 36, and 48 h). qPCR was used to quantify 0.1-kb amplicons of the E1A and hexon genes as proxy of the whole genome (primer sets listed in Table 3.1 of section 3.4). The absolute copy numbers of viral E1A and hexon qPCR products were normalized per 100 β-actin copies and determined using the standard curves described in Text S5 of section 3.4. Cells infected with untreated virus sample were used as control. At time 0 hpi, the amplicon copies detected would correspond to attached viruses. RNA samples were reverse transcribed by PCR into cDNA before they were analyzed by qPCR (RT-qPCR) with the same primer sets used for DNA extracted samples to quantify E1A and hexon mRNA transcripts.

3.2.6 qPCR Data Analysis and Statistical Analysis

Quantification cycle (C_q) values obtained from the qPCR or RT-qPCR assays were used to determine the absolute copy numbers of each amplicon based on standard curves generated by amplifying 10-fold serial

dilutions of DNA positive controls as previously described (Rodriguez et al., 2013; Gall et al., 2015) (see also Text S5 of section 3.4). Analysis of covariance (ANCOVA) was used to compare the linear regression slopes and intercepts between relative decrease in DNA amplification, genome replication, or mRNA transcription with the virus inactivation assessed by plaque assay to determine if they were statistically similar ($P > 0.05$). Absolute copy numbers of genome fragments amplified by qPCR were analyzed using a *t* test (one-tailed with unequal variances) to determine if genomic amplicons detected in UV-treated samples were statistically different from those in the untreated sample.

3.3 Results and Discussion

3.3.1 Inactivation Kinetics of HAdV-2 Exposed to UV Irradiation

The sections of the MP UV spectra covered with each bandpass filter and the corresponding inactivation kinetics of HAdV-2 are shown in Figure 3.1. In general, the observed inactivation kinetics are in agreement with what was previously reported (Beck et al., 2014) using UV light emitted by a tunable laser adjusted at a similar set of wavelengths to inactivate HAdV-2. Both studies show similar tendencies contrasting the inactivation efficiency between UV irradiation emitted below and above 240 nm. This is confirmation that the enhanced effectiveness of MP UV light to inactivate HAdV is possibly due to protein damage by the lower wavelengths given that DNA absorption of UV light at wavelengths below 240 nm does not follow the action spectrum for adenovirus (Beck et al., 2014). The differences in the viral sensitivity at some of the nominal peak emissions between both studies could be due to the different UV light sources utilized (highly monochromatic irradiation provided by the laser-UV emitter compared to narrow polychromatic irradiation using the bandpass filters in this study). Wright et al., (2007) also reported differences in the dose response of bacteriophages obtained by filtered MP UV light using a 254 nm bandpass filter compared to the response obtained using a monochromatic LP UV lamp. This reproduction of results was important to confirm consistency with the published data and serve as basis for the novel molecular work on the adenovirus replication cycle that is the main objective of this study.

The analysis subsequently presented for the UV irradiation at the three regions selected will be referred to as the nominal peak transmittance of the filter used and indicated as UV_{224}, UV_{254}, and UV_{280}.

Pseudo first-order inactivation kinetics were used for analysis, and the results were consistent with what was reported previously (Beck et al., 2014): UV_{224} was most effective to inactivate HAdV-2 among the three wavelength ranges analyzed. UV_{224} (k = 0.181 cm^2/mJ, R^2 = 0.995) required a fluence of ~20 mJ/cm^2 to reach a HAdV-2 survival ratio $N/N_0 = 10^{-4}$, which corresponds to a 4-log (99.99%) adenovirus inactivation, as detected by plaque assay. In contrast, UV_{254} (k = 0.032 cm^2/mJ, R^2 = 0.994) showed slower kinetics requiring a fluence of ~125 mJ/cm^2 to achieve 4-log adenovirus inactivation as detected by plaque assay. For UV_{280} (k = 0.036 cm^2/mJ, R^2 = 0.986), an intermediate fluence of ~110 mJ/cm^2 was required to achieve 4-log HAdV-2 inactivation. ANCOVA determined that the linear regressions of the three wavelength ranges were significantly different ($P < 0.05$). Figure 3.2 shows the sections of the MP UV spectra covered using the UV_{224}, UV_{254}, and UV_{280} bandpass filters and their corresponding inactivation kinetics of HAdV-2 obtained in this study.

3.3.2 Effect of UV Light on Genomic DNA Amplification and Capsid Integrity

To understand the molecular basis of virus disinfection at each wavelength range used above, we first examined the extent of viral genome and capsid damage induced by the three UV wavelengths investigated in purified virions independent of infection. Figure 3.3 displays the combined ratios of E1A and hexon amplicons from UV-treated samples compared to the untreated samples (0.1-kb/0.1-kb_0) for UV_{224}, UV_{254}, and UV_{280}. For all the three wavelength ranges, relatively similar copy numbers of the E1A and hexon amplicons were detected in the UV-treated and untreated HAdV-2 samples (P > 0.05, t test). These data suggest that the 0.1-kb amplicons of E1A and hexon genes did not change significantly within the light fluence ranges investigated. However, it is important to note that these amplicons cover about 12.1 and 3.8% of the whole E1A and hexon genes, respectively, and damage to other regions of these genes could occur. Next, we further assessed genome damage using a 1.1-kb DNA

fragment following the protocols previously reported (Beck et al., 2014; Rodriguez et al., 2013), and the results (Figure 3.4) indicated that genome damage increased with treatment according to UV_{224} < UV_{254} < UV_{280}. These observations are consistent with previous reports that UV_{280} was the most effective of these three wavelength ranges at inducing genome damage (Beck et al., 2014).

An additional set of untreated and UV-treated viruses exposed to EMA assist in determining the structural integrity of viral capsids. Viruses that were in contact with EMA after UV_{224} exposure showed a decreased amplification of the E1A and hexon genes with increasing UV_{224} fluence (see Figure 3.3). This indicated that UV_{224} treatment of viruses altered the structure of the viral capsid such that it became increasingly permeable to EMA with increasing fluence. In contrast, EMA did not affect qPCR amplification of HAdV-2 genes from viruses treated with UV_{254} or UV_{280} (Figure 3.3). These results implied that UV_{254} and UV_{280} did not cause structural modifications to the viral capsid to the extent that UV_{224} did.

3.3.3 Effect of UV Light on Genome Replication

Given the limited effects on the 0.1-kb amplicons of E1A and hexon DNA by UV_{224}, UV_{254}, and UV_{280} for the range of fluence investigated, we used them to assess if the genome was effectively replicated during a normal virus lifecycle. The average number of E1A and hexon amplicons from two independent experiments was quantified throughout the duration of one full replication cycle (48 h). The resulting amounts of E1A and hexon-based amplicons are shown in Figures 3.5 and 3.6. By 48 hpi, the number of E1A and hexon amplicons increased by more than 3 orders of magnitude in the untreated samples. However, UV treatment of viruses resulted in a decreased amount of viral genome synthesis at all times tested, as determined by qPCR.

The relative ratios of E1A DNA copies present in UV-treated samples compared to the untreated sample ($E1A/E1A_0$) at the beginning and end of one replication cycle (0 and 48 hpi, respectively) are shown

in Figure 3.7. This relative quantification was compared with the virus inactivation kinetics achieved (N/N_0) for each UV range. Figure 3.7 shows that at 0 hpi, the copies of E1A amplicons were relatively the same in all UV-treated and untreated samples ($P > 0.05$, *t* test). The data in Figure 3.7 implied that UV_{224}, UV_{254}, and UV_{280} did not affect the ability of the virions to associate with the host cells, even after exposure to a fluence that resulted in a 4-log (99.99%) viral inactivation. Page et al., (2010) reported that only about 5% of HAdV-2 bind nonspecifically to host cells lacking CAR receptors; thus, most of the E1A-based qPCR signal is due to viruses that bound to CAR. Adenovirus uses its fiber-like projections to bind to CAR (Berk, 2013). Beck et al., (2018) reported little to no adenovirus fiber protein damage/degradation by UV light emitted at 220, 254, and 278 nm at similar fluence ranges to those used in this study for each case, which supports our findings that UV-treated viruses are able to bind to the host cells. By 48 hpi, the relative decrease in viral genome replication with increasing exposure to UV_{224}, UV_{254}, and UV_{280} matched the decrease in viral infectivity assessed by plaque assay (N/N_0); ANCOVA determined that the linear regression slopes and intercepts between the relative genome replication at 48 hpi ($E1A/E1A_0DNA$) and the virus inactivation measured by plaque assay (N/N_0) were not significantly different ($P > 0.05$). Collectively, these results indicated that UV_{224}, UV_{254}, and UV_{280} interrupted DNA synthesis or an earlier step in the replication cycle but did not inhibit virus association to the host cells. As expected, the relative quantification data for the hexon gene, shown in Figure 3.8, were similar to those for the E1A gene, supporting that the step inhibited was earlier in the replication cycle.

3.3.4 Effect of UV Light on mRNA Synthesis

Because DNA replication was disrupted, the effect of UV exposure on early gene transcription (E1A mRNA synthesis), which occurs prior to DNA synthesis, was analyzed next. Once again, HAdV-2 samples were incubated with host cells after various levels of exposure to UV irradiation at each target wavelength. At different times postinfection, cells were harvested, and transcription of the E1A gene was detected using RT-qPCR. The numbers of E1A mRNA determined for each wavelength as a function of fluence and postinfection time are shown in Figure 3.9.

The relative ratios of E1A mRNA transcripts from UV-treated samples compared to the untreated control ($E1A/E1A_0$) by the end of one viral replication cycle (48 hpi) quantified for each wavelength are displayed and compared to the decrease in virus infectivity measured by plaque assay (N/N_0) in Figure 3.10. ANCOVA determined that the linear regression slopes and intercepts between the relative expression levels of E1A mRNA and the reduction in viral infectivity (N/N_0) assessed by plaque assay were not significantly different ($P > 0.05$) for UV_{224}. This implied that UV_{224} inhibited adenovirus infection by blocking early E1A gene transcription or a prior step in the replication cycle.

In contrast, ANCOVA determined that the linear regressions of the relative expression of E1A mRNA synthesis for UV_{254} and UV_{280} did not match the corresponding virus inactivation levels (N/N_0) ($P < 0.05$ at both wavelengths). UV_{254} and UV_{280} produced a greater decrease in viral inactivation and relative DNA replication compared to the decrease in E1A mRNA synthesis. It is likely that at these two wavelength ranges, UV-induced mutations in the viral genome template from targeted regions that are not transcribed in the early phase of the replication cycle are preventing DNA synthesis and resulting in the higher decrease in DNA replication and infectivity observed.

3.3.5 Occurrence of DNA Damage Repair

Although a decrease in hexon mRNA synthesis was expected because it occurs at a similar time or shortly after DNA replication begins (Berk, 2013), the effect of UV treatment on this step was also assessed, and the results are included in Figure 3.11 (absolute values) and Figure 3.12 (relative ratios). A comparison of data sets in Figures 3.12 and 3.8 reveals that by 48 hpi for UV_{224} treatment, as expected, the hexon mRNA transcription data match the results obtained for hexon DNA amplicon replication. In contrast, ANCOVA determined that the relative levels of hexon mRNA transcription were significantly lower compared to those for hexon amplicon replication for both UV_{254} and UV_{280} treatment were significantly different ($P < 0.05$), with the discrepancy for UV_{280}being more pronounced. One possible explanation for these

differences in hexon mRNA transcription and hexon DNA replication observed by 48 hpi could be a delay associated with genome repair. An interesting finding was observed when the data for hexon mRNA transcription at various times postinfection prior to 48 h were plotted in relative quantification format as shown in Figure 3.12. A delayed increase in hexon mRNA synthesis is observed in UV treated viruses, particularly for the two wavelengths where genome damage was prevalent (UV_{254} and UV_{280}), which might be an indirect indication of genome repair taking place. Relatively speaking, UV_{224} (which produced the least damage to the viral genome from the three wavelength ranges analyzed by a fluence that caused a 4-log HAdV-2 inactivation) approached the reduction in infectivity assessed by plaque assay more readily. For the UV_{254} hexon mRNA transcription data, delays were apparent with respect to the 24 and 36 hpi curves at UV_{224} even though the transcription data nearly reached the viral inactivation curve by postinfection of 48 h. The levels of hexon mRNA transcription for UV_{280} were generally lower than those for UV_{254}, and by 48 hpi, the expression levels of hexon mRNA did not match the viral inactivation curve. It is likely that longer postinfection time would be required for viruses exposed to UV_{280} to produce the same relative levels of hexon mRNA copies as those observed for the genome copies and infectious viruses. The hexon mRNA synthesis data suggests that there might be damage and repair of other genome regions not used in this study but important for hexon mRNA synthesis. These observations highlight the need to look at other portions of the genome that are responsible for late mRNA transcription. One possibility is assessing the integrity of the genome region encoding the major late promoter (MLP), which is situated at an intermediate location between the two regions analyzed in this study (E1A and hexon genes) and from which most late mRNAs originate (Berk, 2013).

Similar trends were observed when the sets of DNA replication at postinfection times prior to 48 hpi were plotted in relative quantification format as shown in Figure 3.13. UV_{254} and UV_{280} seemed to require longer time than UV_{224} to reach the level of inactivation determined by plaque assay. This observation might be additional indication of genome repair taking place in the virus samples treated with UV_{254} and UV_{280}. In the relative quantification plots of the DNA replication data (Figure 3.13), the samples included

were those expressing genome copies to a level above the background baseline E1A and hexon DNA copies that would correspond to attached viruses (equivalent to time 0 hpi shown in Figures 3.5 and 3.6).

Finally, a comparison of the relative quantification of E1A mRNA synthesis at the different postinfection times assessed for the three wavelength ranges investigated is shown in Figure 3.14. Differently to DNA replication and hexon mRNA synthesis, the inhibition levels of E1A mRNA synthesis attained by increasing fluences in general did not significantly change at times investigated prior to 48 hpi, suggesting that genome repair might be happening predominantly after E1A mRNA transcription takes place (likely during DNA replication). As a whole, these observations suggest that different parts of the genome might have different sensitivities to damage induced by UV light at a particular wavelength range and that such damage might not be equally repaired in all regions of the genome that are affected. DNA damage repair during cell culture infectivity assays has been suggested as a possible explanation of the different adenovirus inactivation effectiveness of LP UV and MP UV light (Shin et al., 2009; Eischeid et al., 2009). Reports that quantum yields of the reduction in viral infectivity for double-stranded nucleic acid viruses are an order of magnitude lower compared to quantum yields for the formation of UV photoproducts of pyrimidines support the occurrence of repair in host cells (Rauth, 1965). Single and/or double-strand breaks and DNA–DNA cross-links can also happen but they are about 1000 times less likely to occur compared to pyrimidine dimers (USEPA, 2006). UV absorption of nucleotides is predominant at intermediate wavelengths, while proteins dominate the absorbance of UV light at wavelength below and above this intermediate range (Bolton and Cotton, 2008) (see Figure 3.2 showing intermediate range at 243–285 nm). This is consistent with our results at UV_{254} and UV_{280} having pronounced delays in genome replication and hexon mRNA synthesis. Different sensitivities of viruses to UV light have been attributed to differences in viral protein sensitivity and the fact that photons absorbed at different wavelengths in the germicidal range does not have the same inactivation quantum yield (Rauth, 1965). Mattle et al., (2015) discussed the inactivation quantum yield by sunlight (290–320 nm) for HAdV-2, indicating that although the adenovirus genome readily absorbs light in the UVB range, the

low inactivation quantum yield from UV exposure could be possible given that adenovirus could repair UV-induced genome damage inside the host. Our results provide valuable insight on genome repair taking place after UV exposure to different UV wavelengths, and this aspect should be further investigated in future studies.

3.3.6 Mechanistic Considerations

Collectively, the data obtained in this study suggest that different molecular mechanisms are involved in the HAdV-2 inactivation levels achieved by the different UV wavelength ranges analyzed. UV_{224} disinfection did not inhibit HAdV-2-host cell binding and had the lowest effect on the integrity of the viral genome among the three wavelength ranges analyzed but hampered viral gene transcription and viral genome replication. In addition, assays using EMA suggested that UV_{224} modified the viral capsid (see Figure 3.3). UV_{224} treatment of adenovirus resulted in conformational changes in the virus capsid that do not preclude binding to the host cell but prevent one of the subsequent steps of the infection cycle such as internalization to the cytoplasm, endosomal release, or genome translocation into the host cell nucleus. The adenovirus capsid is primarily formed by three major capsid proteins (hexon, fiber, and penton base) and several internal proteins (e.g., proteins VI and VII). One possibility is that during UV_{224} treatment, the penton base gets disrupted, thus blocking internalization of the attached virus. After the high-affinity binding of the fiber knob with CAR, RGD loop domains of penton base subunits associate with αv integrins on the host cell with 50-fold lower affinity than the interaction of fiber with CAR to promote endocytosis (Berk, 2013). Exposure to UV_{224} may further inhibit a successful interaction at this step if penton base is affected. Beck et al., (2018) indicated that a fluence of 38 mJ/cm^2 emitted at 220 nm reduced adenoviral penton and hexon protein quantities to ~31 and ~33%, respectively, of the original amounts. The authors also detected indication of protein aggregation with increasing fluence at this wavelength. Their results support the hypothesis that UV_{224} treatment might be predominantly disrupting the ability of the bound viruses to promote endocytosis and internalize into the host or that, if successfully internalized, it might not be able to release from the endosome due to

disruption of the capsid. Finally, if the virus reaches the nucleus, import of the genome might be inhibited due to disruption of protein VII as it mediates DNA import through the nuclear pore complex (Berk, 2013; Kremer and Nemerow, 2015). Inhibition of the virus replication cycle steps post binding and prior to early gene transcription should be assessed in future research to determine what viral protein modifications induced by UV_{224} rendered adenovirus noninfectious.

UV_{254} treatment of viruses also allowed virus–host cell binding, but it disrupted the viral genome to a greater extent than UV_{224} (Figure 3.4). The results from the EMA assay indicated that UV_{254} did not cause modifications to the viral capsid that would allow EMA permeation (Figure 3.3). This is consistent with the observations reported by Bosshard et al., (2013) in which UV_{254} did not cause degradation to structural proteins (hexon, fiber, and penton base) of HAdV-2. UV_{254} also hindered early E1A mRNA synthesis but not to the same level as the decrease in viral infectivity, as was the case with UV_{224}. For UV_{254} the inhibition of early gene transcription may be dominated by UV-induced mutations to the template E1A gene. It is possible that the UV_{254}-treated virus could translocate its mutated genome into the cell nucleus, and E1A mRNA transcription was inhibited proportionally to the level of UV-induced damage to the complete E1A gene region. Likely, the viral DNA was replicated depending on the level of mutations caused to the whole genome. Consequently, genome replication appeared to be the limiting step that ultimately produced the reduction in infectivity assessed by plaque assay after irradiation with UV_{254}. Adenovirus may be able to repair UV-induced damage to its genome using host cell repair mechanisms such as the nucleotide excision-repair process (Beck et al., 2014; Eischeid et al., 2009; Guo et al., 2010). Specifics about the effect of viral genome repair mechanisms and their repercussions in the viral replication cycle inhibitions require future exploration.

Finally, UV_{280} did not seem to inhibit viral binding association with the host cell either and showed capacity higher than that of UV_{254} to disrupt mRNA transcription under similar applied fluences. UV_{280} disrupted early mRNA synthesis to a greater extent than UV_{254}, as indicated by the steeper linear

regression slope of the E1A mRNA synthesis plot for UV_{280} (slope UV_{280} = −0.027, slope UV_{254} = −0.016) in Figure 3.10. Similar to UV_{254}, UV_{280} did not seem to be greatly affecting structural proteins, as indicated by the EMA results (Figure 3.3). However, UV_{280} was the most effective among the 3 wavelength ranges analyzed in blocking qPCR amplification of the 1.1-kb amplicon used (Figure 3.4). This suggests that the more effective HAdV-2 inactivation by UV_{280} (compared to UV_{254}) is likely dominated by a more effective induction of mutations on the viral genome (perhaps to DNA regions associated with core proteins) rather than modifications to structural proteins. Three amino acids (tryptophan, tyrosine, and phenylalanine) that regularly constitute proteins have UV absorption peaks at 280 nm, and although this peak is smaller relative to that for UV absorption of DNA, its presence may be contributing to the enhanced effectiveness that UV_{280}showed compared to UV_{254} (Bolton and Cotton, 2008). Further research is needed to elucidate if damage to a specific core protein or DNA–protein complex region contributes in the viral inactivation effect observed by UV_{280}.

3.3.7 Practical Implications

Some of the techniques utilized in this work allowed a relatively fast determination of virus inactivation levels attained by UV irradiation. For all 3 wavelengths, results for genome replication experiments by 48 hpi matched the decrease in virus infectivity achieved by each applied fluence when infectivity was assessed by plaque assay (which required 10 days to be completed). This convenient aspect could help inspect the effectiveness of water disinfection approaches more rapidly when using adenovirus as the target pathogen for monitoring virus inactivation by UV light.

The results from this study also contribute to a better understanding of the mechanisms by which UV irradiation emitted at different wavelengths renders HAdV-2 noninfectious. A complete understanding of this phenomenon will allow the development of more effective and efficient water disinfection strategies that incorporate UV technologies as well as rapid methods for detection and monitoring of pathogens in drinking water. In addition, our results confirmed better capacity of the 260–280 nm wavelength range,

UV_{270} being the most effective (Figure 3.1), to inactivate HAdV-2 compared to UV_{254}, making it an attractive alternative to be further explored to control viruses in drinking water. This work provided insightful information toward a better understanding of the mechanisms by which different regions of the MP UV spectrum inactivate human adenovirus during water disinfection.

3.4 Supporting Information

Text S1. Virus Propagation and Viability Assessment

Human lung A549 carcinoma cells (CCL-185) obtained from the American Type Culture Collection (Manassas, VA) were used for adenovirus propagation and viability assessment with a soft agar overlay plaque assay. Cell culture growth, virus propagation, and viability assessment assays were performed following previously reported protocols (Sirikanchana et al., 2008; Page et al., 2010; Gall et al., 2015). Briefly, A549 cell monolayers were propagated in T175 flasks using a nutrient media containing modified Ham's F12K growth media supplemented with 10% fetal bovine serum (FBS), 0.25 μg/mL amphotericin B, 100 units/mL penicillin, and 10 μg/mL streptomycin (Sigma-Aldrich, St. Louis, MO). The cell monolayers were incubated at 37 °C in a 5% CO_2 incubator until used for virus propagation or harvested to prepare T-25 or 6-well plates to perform HAdV-2 viability assessment by plaque assay. Viruses were propagated by inoculating cell monolayers in T-175 flasks with previously purified virus stock and incubated until cytopathic effect was observed. Viral release was induced by three freeze-thaw cycles. The suspension containing the lysed cells was centrifuged at 2000 rpm for 15 min and the supernatant was removed and passed through a 0.22 μm microfilter to remove large cellular debris. Concentration and purification of the virus was done through several washes with 1mM carbonate buffer solution (CBS) using a 300 kDa ultrafiltration membrane in an Amicon stirred cell. The concentrated virus stock was aliquoted and stored at -80 °C. Virus titer was determined by plaque assay using a nutrient mixture and soft agar overlay on A549 cell monolayers. Plaque formation was observed and quantified from 6 to 10 days postinfection.

Text S2. Amplicon Integrity

To assess genome damage after UV light treatment, viral DNA was extracted from UV-treated and untreated samples following the DNA extraction protocol from the DNeasy Blood & Tissue Kit (Qiagen, Valencia, CA). Primers designed to amplify different regions of the adenovirus genome were used to assess if such regions were amplifiable by qPCR after UV light exposure. The primer sets used can be found in Table 3.1 and were used after previous studies (Rodriguez et al., 2013; Gall et al., 2015).

The regions selected for analysis correspond to three viral DNA fragments, two of them 0.1-kilobase (kb) pairs long, and a third one 1.1-kb long. The first DNA fragment (106 bp) corresponds to the E1A gene located at the left-hand side of the adenovirus genome (nucleotides 673-778) and covers ~12.1% of the complete E1A gene (870 bp). The E1A gene is the first gene transcribed during an early phase in the replication cycle (Berk, 2013). The second DNA fragment (111 bp) is located within the hexon gene (nucleotides 19,400-19,510) covering ~3.8% of the complete hexon gene (2907 bp) which is a late gene that is transcribed soon after viral genome replication begins. The hexon gene is located in the central part of the adenovirus genome (Berk, 2013). The third DNA fragment amplified (1174 bp) is located in the central section of the genome (nucleotides 17,822-18,996) upstream of the hexon gene region. This section of the viral DNA was PCR-amplified to target a larger section of the genome to compare the UV-induced effect observed with the 0.1-kb E1A and hexon amplicons. The C_q values from the qPCR or RT-qPCR assays were used to determine relative log reductions or absolute copy numbers of each amplicon based on standard curves generated by amplifying 10-fold serial dilutions of DNA positive controls as described by Rodriguez et al., 2013, and Gall et al., 2015.

Table 3.1 Primers used for qPCR and RT-qPCR (after Rodriguez et al., 2013, and Gall et al., 2015).

Primer	Bases (bp)	Sequence	GC content	Tm °C[a]	Genomic Position[b]	Amplicon Length (bp)
E1A Forward	19	5'-GAACCACCTACCCTTCACG-3'	57.9%	55.2	673-778	106
E1A Reverse	20	5'-CCGCCAACATTACAGACTCG-3'	55.0%	56.0		
Hexon Forward	19	5'-AAAGCGGGCTACAAATAGG-3'	47.4%	52.6	19400-19510	111
Hexon Reverse	20	5'-CTTCGTTCCACTGAGATTCG-3'	50.0%	53.1		
β-actin Forward	19	5'-ATGAGGCTGGTGTAAAGCG-3'	52.6%	55.3	5528803-5528905	103
β-actin Reverse	19	5'-AGAACACGGCTAAGTGTGC-3'	52.6%	55.4		
Long range PCR forward	40	5'-CACGGAGAGATGGCTATGCGCGGCGGTATCCTGCCCCTCC-3'	67.5%	73.6	17822-18996	1174
Long range PCR reverse	28	5'CGTAGGTGCCACCGTGGGGTTTCTAAAC-3'	57.1%	64.3		
Long range qPCR forward	20	5'-CACGGAGAGATGGCTATGCG-3'	60.0%	57.9	Adapter	177
Long range qPCR reverse	19	5'-CAAGCGAGCGTGAGACTCC-3'	63.2%	58.3	17961-17979	

[a] Tm, melting temperature, based on 50 mM NaCl.
[b] Genomic position based on human adenovirus type 2 genome (NCBI accession AC_000007.1) for E1A and hexon, homo sapien chromosome 7 (NCBI accession NC_000007.14) for β-actin, and adenovirus 2 genome (NCBI accession number 56160492) for long range fragment (after Rodriguez et al., 2013, and Gall et al., 2015).

Text S3. Ethidium Monoazide Bromide Exposure

These experiments were performed following previously reported protocols (Parshionikar et al., 2010; Kim et al., 2011; Sangsanont et al., 2014). Briefly, a concentration of 1µg/mL EMA was mixed with 200 µL of UV-treated and untreated virus samples. After an incubation time of 1 hour at 4 °C in the dark, the samples were exposed for 5 minutes to a 650 Watt xenon lamp equipped with a filter to cut out all the irradiation below 400 nm. The samples were placed on ice at a distance of 15 cm away from the lamp to

prevent temperature increase during visible light exposure. Viral DNA was extracted using the DNeasy Blood & Tissue Kit (Qiagen, Valencia, CA) and qPCR amplification was performed using the same set of primers used to assess amplicon integrity (Table 3.1). The absolute number of 0.1-kb DNA fragments quantified by qPCR was determined using the equations from Text S5. The ratio of amplified 0.1-kb DNA fragments (E1A or hexon region) present in UV-treated samples compared to those present in the untreated sample ($E1A/E1A_0$, $Hexon/Hexon_0$) was evaluated with and without exposure to EMA to detect the effect of EMA binding to the DNA and inhibiting amplification of the targeted genome region. Control conditions of EMA-exposed virus samples without exposure to visible light, and virus samples exposed to visible light only were performed for all wavelengths and fluences investigated to assess if EMA or visible light by itself would have any effect on the disruption of the DNA amplification. No effect was observed on these control conditions (data not shown).

Text S4. Genome Replication in Host Cells and mRNA Transcription

HAdV-2 genomic DNA replication and mRNA transcription was performed following the protocols reported by Gall et al., (2015). Total DNA or RNA was extracted from A549 cells inoculated with viruses at different hours post-infection (hpi). The number of gene copies at each post-infection time was analyzed by qPCR, using primer sets previously designed (Gall et al., 2015), and quantified using the equations described in Text S5.

A confluent monolayer of A549 cells in T-25 flasks were placed at 4 ^{o}C for 60 min with media lacking fetal bovine serum (FBS). After this time, UV-treated and untreated viruses were allowed to bind to the host cell monolayer for 90 min at 4 ^{o}C with constant rocking. Then, the inocula was removed and the monolayers were washed twice with 1 mL of ice-cold phosphate buffer saline (PBS) to remove unbound viruses. Cells were dislodged using 0.25% trypsin and the enzymatic activity of trypsin was quenched using media with FBS. Detached cells were centrifuged at 300 x g for 5 min and supernatants were removed. Cell pellets were re-suspended in 180 µL of molecular biology grade water and 20 µL of 10x

PBS. DNA was extracted using the DNeasy Blood & Tissue Kit (Qiagen, Valencia, CA) following the protocol provided by the manufacturer. Total DNA from A549 cells with bound viruses was extracted at 0, 4, 12, 24, 36, and 48 hours p.i. The number of gene copies at each time point was quantified by qPCR, using the primer sets and protocols previously reported (Gall et al., 2015). Additionally, a primer set to amplify *β*-actin, a housekeeping gene of the host cell, was included to use as a normalizer (Table 3.1).

Total RNA was extracted from A549 cells inoculated with UV-treated and untreated virus at 4, 12, 24, 36 and 48 hours post-infection. RNA was extracted using the RNeasy Mini Kit (Qiagen, Valencia, CA) following the manufacturers' procedure and homogenized using QIAshredder spin columns. 20 µL of extracted RNA were digested with 2.5 µL of RNase-free DNase I stock solution to remove any contaminating DNA, and cleaned RNA samples were stored at -80 °C until they were processed into cDNA. Purified RNA was quantified using NanoDrop spectrophotometer (Thermo Scientific, Wilmington, DE) and 0.5 µg of total RNA from each sample was reverse transcribed into cDNA following the described protocol by Gall et al., (2015). cDNA was synthesized by PCR, and final samples were kept at 4 °C until they were analyzed by qPCR.

Text S5. PCR Data Analysis

For analysis of data generated from qPCR and RT-qPCR assays, relative and absolute quantification was used based on values obtained for the quantification cycle, $C_{q,}$ as has been previously described (Rodriguez et al., 2013; Gall et al., 2015).

Relative quantification

The relative expression level from infected cells, *R*, was determined using the $\Delta\Delta C_q$ method with the following equation:

$$R = 2^{-\Delta\Delta C_q} = 2^{-(\Delta C_{q,\text{sample}} - \Delta C_{q,\text{calibrator}})}$$

where the values ΔC_q are obtained as $\Delta C_q = (C_{q,N} - C_{q,\beta\text{-actin}})$.

Being "*N"* succeeding UV-treated samples (N_1, N_2, N_3 … etc.) or the untreated sample (N_0). For each analysis, the calibrator was the untreated virus sample (N_0). In this way for UV-treated sample 1: $\Delta C_{q\ sample\ 1} = (C_{q,\ N1} - C_{q,\beta\text{-actin}})$, and $\Delta C_{q,\ calibrator} = (C_{q,\ N0} - C_{q,\beta\text{-actin}})$.

The relative expression level, *R,* is represented as $E1A/E1A_0$ or $Hexon/Hexon_0$ for the relative quantity of DNA or mRNA for each gene fragment.

The log reduction of the 1.1-kb fragment was calculated by subtracting the $\log_{10}$ copies of the control sample (not exposed to UV light) to the $\log_{10}$ copies of UV-treated samples.

Absolute quantification

For absolute quantification, a standard curve generated from dilutions of purified PCR amplicons from each primer set was used to correlate C_q values to log-copies. The following equations were used to calculate the number of copies in a sample for each primer set:

E1A: $\log_{10}(\text{number of copies}) = -(0.2869 \times C_q) + 10.4533$ ($r^2 = 0.9980$)

Hexon: $\log_{10}(\text{number of copies}) = -(0.2718 \times C_q) + 10.3289$ ($r^2 = 0.9972$)

β-actin: $\log_{10}(\text{number of copies}) = -(0.2699 \times C_q) + 10.3617$ ($r^2 = 0.9989$)

1.1-kb: $\log_{10}(\text{number of copies}) = -(0.3060 \times C_q) + 14.7854$ ($r^2 = 0.9992$)

Utilizing a housekeeping gene is standard practice in qPCR when determining the relative quantity of a gene. To be used as a normalizer in the $\Delta\Delta C_q$ method, the housekeeping gene must be expressed at consistent levels throughout the viral infection. With this approach we normalize the increase in HAdV gene expression to a stable housekeeping gene present in the host cells. Through this normalization we are comparing treated to untreated viral samples (as well as the changing viral gene expression) to a stable gene expression (housekeeping gene) in the host cells (Livak and Schmittgen, 2001; Schmittgen et al., 2000; Winer et al., 1999). We used β-actin as a reference gene because of its constant and abundant expression (Livak and Schmittgen, 2001; Morse et al., 2005; Bas et al., 2004). The advantages of this method are the reliability and the reproducibility of results.

Text S6. Action Spectrum

The relative sensitivity of a microorganism to UV light emitted at different wavelengths is known as the inactivation action spectrum (Bolton and Cotton, 2008). For polychromatic sources it is important to take into account the relative germicidal effectiveness of UV light at different wavelengths and this is done by comparison with a reference wavelength. Usually a germicidal factor of 1 is assigned to UV emitted at 254 nm and it is used as the reference for other wavelengths.

For many microorganisms the action spectrum is not known, for this reason it is common practice to use the absorption spectrum of DNA as the germicidal factor to calculate the germicidal fluence from a polychromatic UV light (Bolton and Cotton, 2008). From the linear regression analysis for each inactivation curve presented in Figure 3.1, a kinetic constant was obtained and used to determine the spectral sensitivity of adenovirus relative to its inactivation at 254 nm. The action spectrum obtained in this work is shown in Figure 3.16. The spectrum showed that below 240 nm adenovirus is highly sensitive to UV light and its sensitivity increases as the wavelength decreases. Above 240 nm a relative peak was observed at ~270 nm. The enhanced effectiveness of MP UV light compared to LP UV is considered to be due to the effect of the wavelengths below 240 nm which seem to affect other components different to the viral genome (Beck et al., 2014).

The obtained action spectrum was compared to that previously reported by Beck et al., (2014) and in general both spectrums are consistent (Figure 3.17). For the wavelengths below 240 nm the spectrum from this work displays a relative sensitivity slightly lower compared to that reported by Beck et al., (2014). This difference can be due to the difference in UV sources utilized (narrow polychromatic emissions used in this work compared with the monochromatic emission from the tunable laser used by Beck et al., 2014), which can influence the relative sensitivities obtained. Still, both action spectrums are comparable and the data from this work complements and confirms the previously reported information.

Inactivation by the Full Spectrum of MP UV light

There is certain variability in the literature regarding the fluences required for a 4-log (99.99%) adenovirus inactivation using a MP UV source. Reported applied fluences range from ~25 to ~90 mJ/cm^2 (~40 mJ/cm^2, Linden et al., 2007; ~25 mJ/cm^2, Eischeid et al., 2009; ~60 mJ/cm^2, Shin et al., 2009; ~80 mJ/cm^2, Linden et al., 2009; 86 mJ/cm^2, Rochelle et al., 2010; ~50 mJ/cm^2, Rodriguez et al., 2013).

The different fluences reported in the literature can be due to variability in the methodology followed for determination of the average germicidal irradiance, as well as inherent differences in the virus stocks used and cell culture conditions employed for viability assessment. In this work a fluence of ~80 mJ/cm^2 of MP UV light was required to reach a 4-log reduction of adenovirus infectivity. This value was determined using the spectral irradiance of the MP UV lamp as the weighting function in the average fluence rate calculations. When using a polychromatic UV source, such as a MP UV lamp, weighting the average germicidal fluence using the UV absorption spectrum of nucleic acid is common practice in the water treatment industry (Bolton and Cotton, 2008). When the fluence was calculated using the absorption of DNA as the weighting factor, the fluence value for a 4-log adenovirus inactivation switched from ~80 to ~60 mJ/cm^2.

When the fluence was calculated using the action spectrum obtained in this work the value for a 4-log inactivation went to 169 mJ/cm^2, which is very similar to the required fluence for a 4-log adenovirus inactivation by LP UV light obtained in this work (164 mJ/cm^2). The inactivation kinetics of human adenovirus (HAdV) from exposure to LP UV have been characterized in the literature with reporting fluences needed to reach 4-log inactivation typically in the 160-180 mJ/cm^2 range (Malayeri et al., 2016).

Figure 3.18 shows the comparison of the adenovirus inactivation kinetics obtained by LP UV and that for MP UV calculated using 3 different weighting functions; 1) UV absorption of DNA, 2) the spectral irradiance, and 3) the action spectrum obtained in this work.

As shown in Figure 3.18, the kinetics from the LP UV and MP UV weighted by action spectrum are very similar; the linear regressions between these two data sets were not significantly different (ANCOVA, $P > 0.05$). These results confirm that the action spectrum obtained in this work is accurate. This analysis corroborated that, for adenovirus, using the absorption spectrum of DNA as the weighting function in the fluence calculations does not accurately account for its sensitivity to UV light at the wavelengths below 240 nm. When the relative effectiveness of different wavelengths provided by a polychromatic UV source are adequately accounted for, its inactivation response should be similar to the response of the reference wavelength (UV_{254}) (Beck et al., 2014). Ideally, the action spectrum of the target microorganisms for validation of UV systems should be used as the weighting factor for accurate fluence determinations, since the spectral sensitivity might differ from the absorption spectrum of nucleic acids,

3.5 Figures

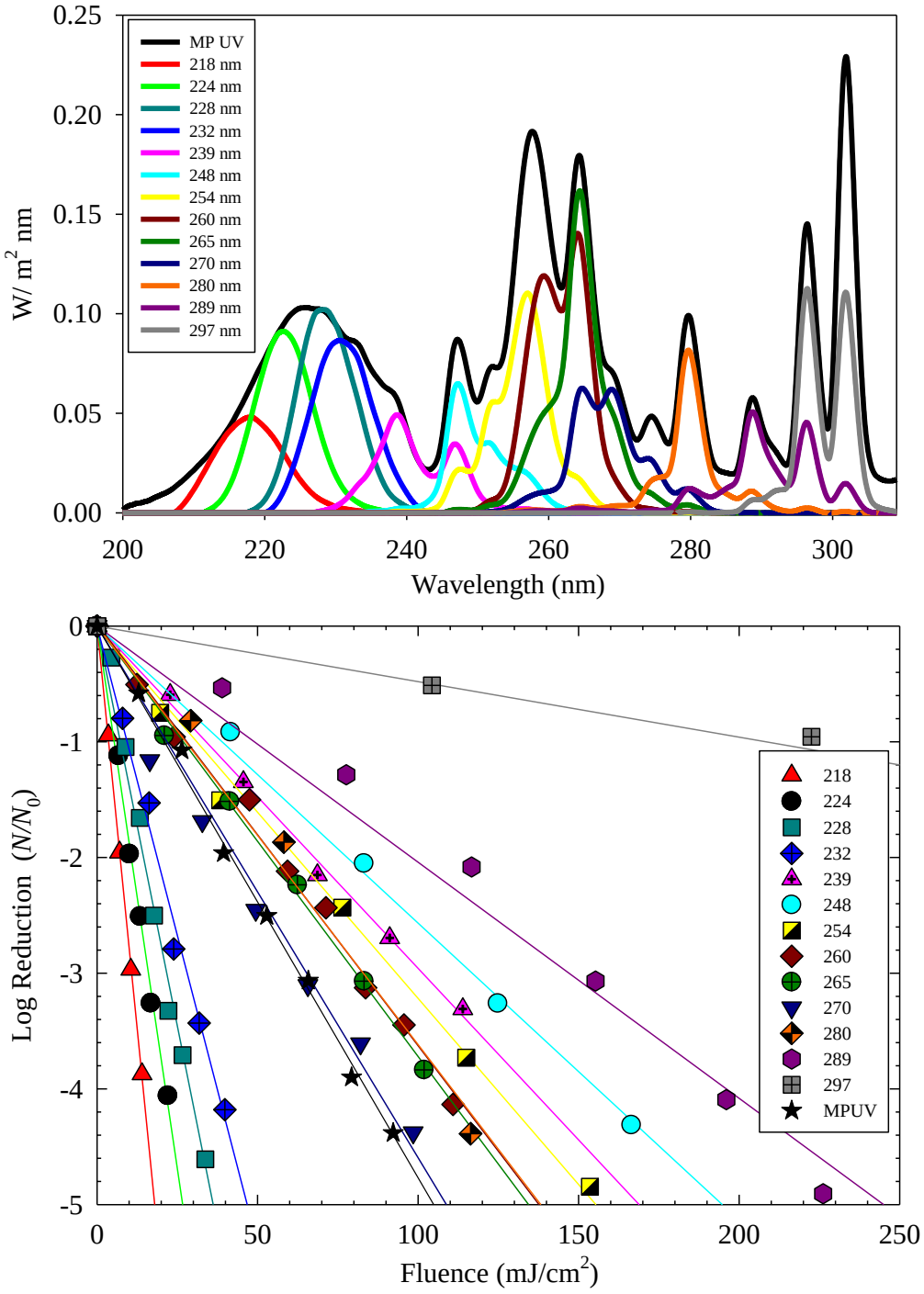

Figure 3.1. Top plot: Polychromatic MP UV spectrum and spectral irradiance of the different wavelength ranges provided by bandpass filters with peak UV emission from 218 to 297 nm. Bottom plot: Human adenovirus type 2 (HAdV-2) inactivation assessed by infectivity assay in A549 cells after exposure to UV irradiation using each of the bandpass filters.

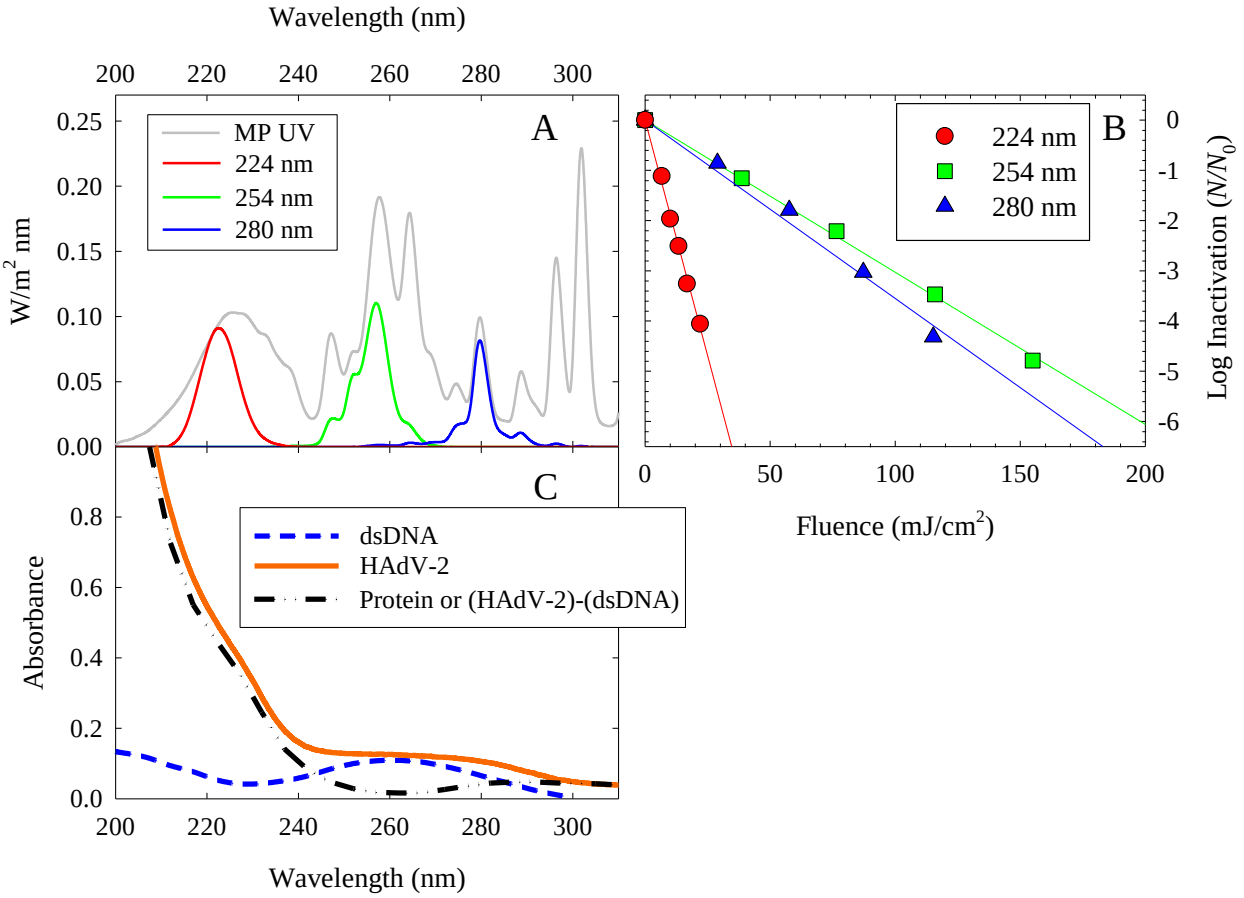

Figure 3.2. **(A)** Spectra of the MP UV light and each of the three non-overlapping range of wavelengths analyzed. **(B)** HAdV-2 inactivation assessed by infectivity assay in A549 cells after exposure to UV_{224}, UV_{254}, and UV_{280}. **(C)** UV absorption spectra of HAdV-2 and dsDNA, and a qualitative HAdV-2 protein. HAdV particles are 13% DNA and 87% protein (Berk, 2013).

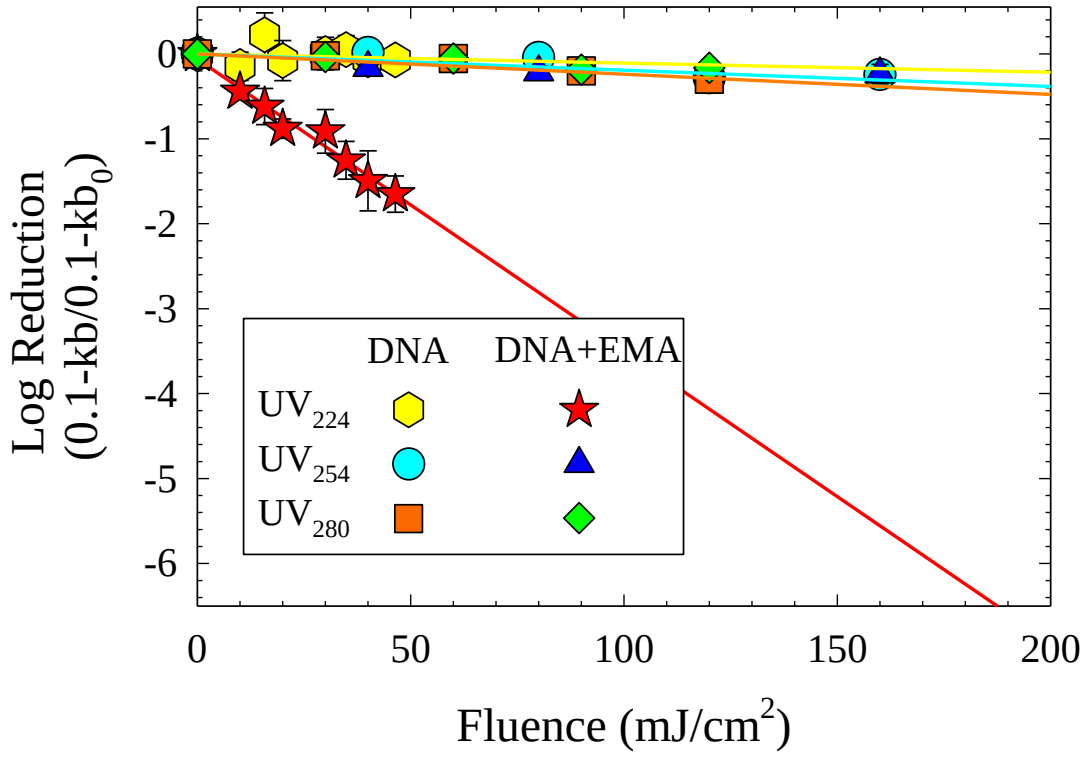

Figure 3.3. Relative combined average ratios of E1A and hexon DNA copy numbers (0.1-kb/0.1-kb_0) after increasing applied fluences of UV_{224}, UV_{254} and UV_{280}. The plots noted as "DNA + EMA" were obtained from UV-treated virus samples that were subsequently exposed to EMA. Viral DNA was extracted from purified virions immediately after exposure to UV irradiation, or after UV irradiation followed by EMA exposure. No cell infection took place in these sets of experiments. The E1A and hexon DNA copy numbers from UV-treated virus samples exposed and unexposed to EMA were quantified using qPCR. Error bars represent standard deviation of the mean.

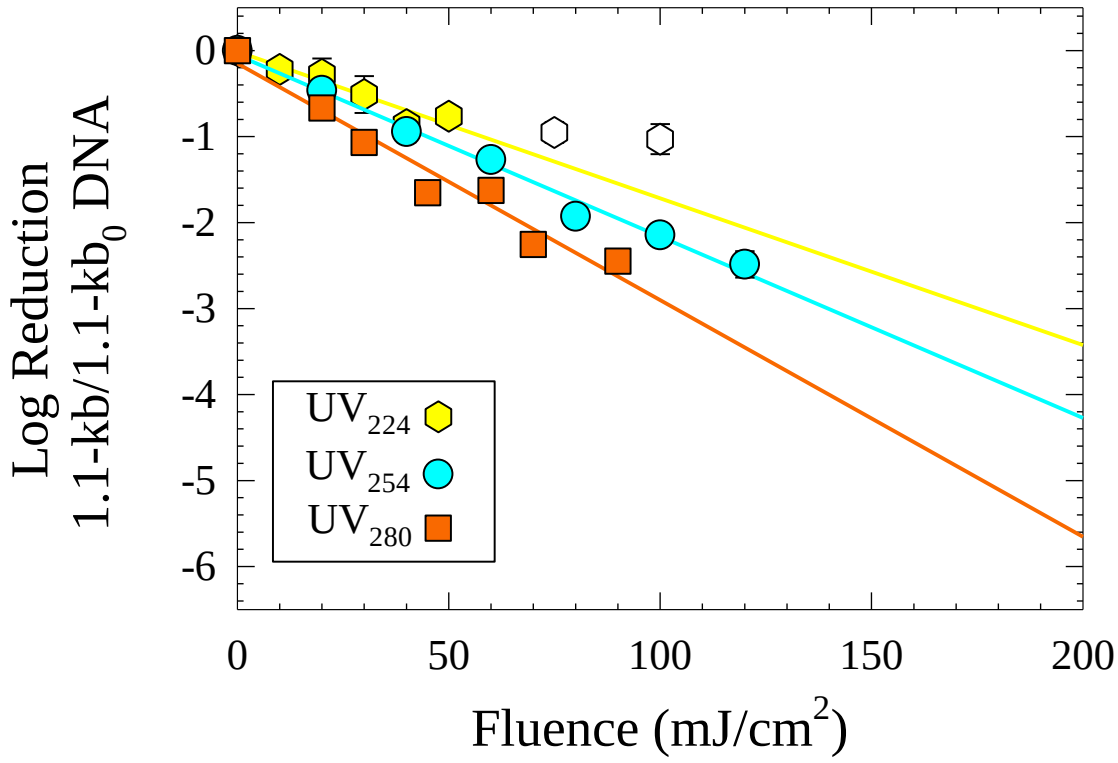

Figure 3.4. Decrease in amplification by qPCR of a 1.1-kb viral DNA fragment after increasing exposure to UV_{224}, UV_{254}, and UV_{280}. No cell infection took place in these sets of experiments. Error bars represent standard deviation of the mean. The white symbols for UV_{224} represent data points that were not included in statistical analysis due to indications of tailing. ANCOVA determined that the linear regressions of UV_{224} (k=0.017 cm^2/mJ, R^2=0.916) and UV_{254} (k=0.021 cm^2/mJ, R^2=0.988) were not significantly different ($P > 0.05$). The linear regression of UV_{254} and UV_{280} (k=0.029 cm^2/mJ, R^2=0.946) were significantly different ($P < 0.05$).

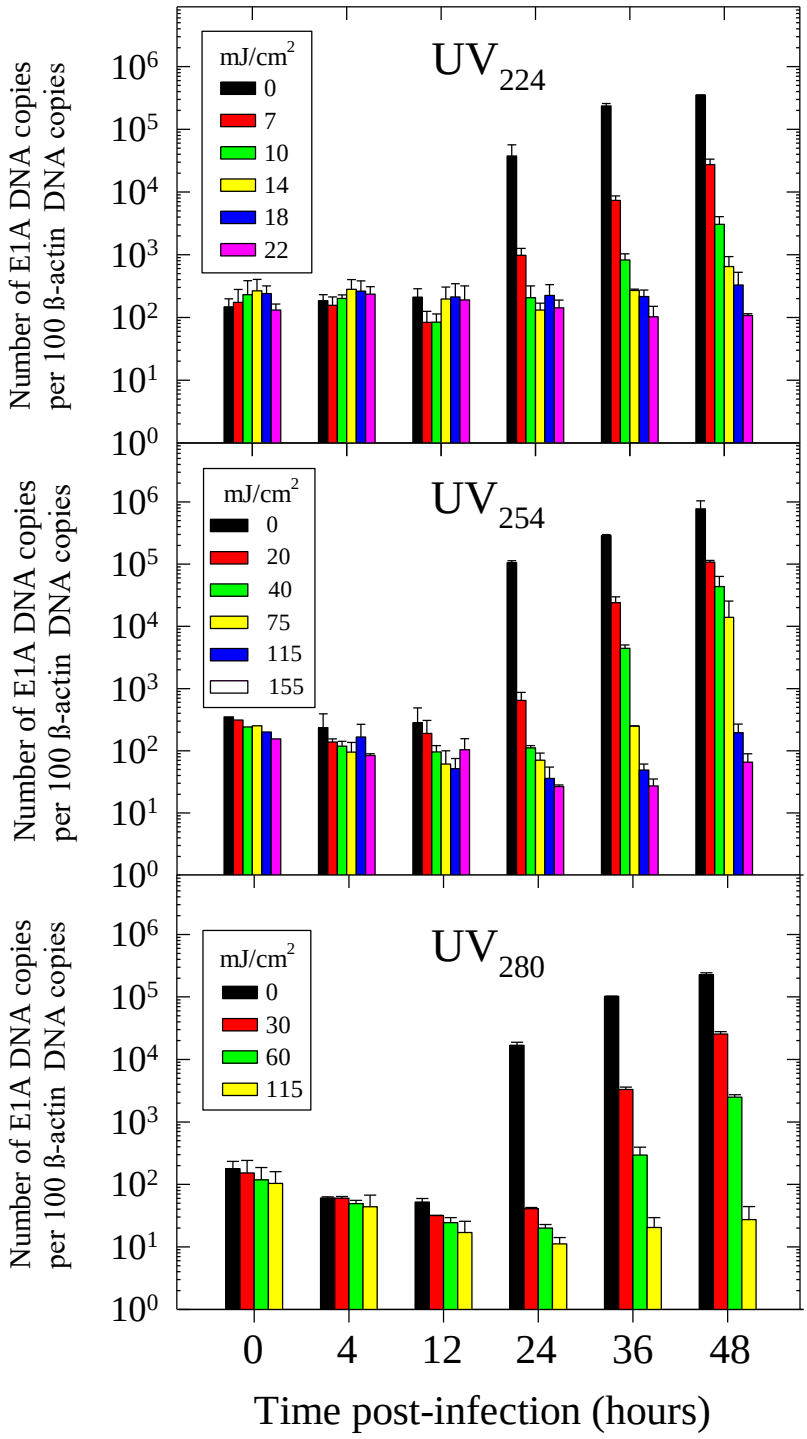

Figure 3.5. Absolute quantification of adenovirus E1A DNA copies (0.1-kb long) per 100 β-actin DNA copies measured from 0 to 48 hours postinfection (hpi) after increasing exposure to UV_{224}, UV_{254}, and UV_{280}. Error bars represent standard deviation of the mean.

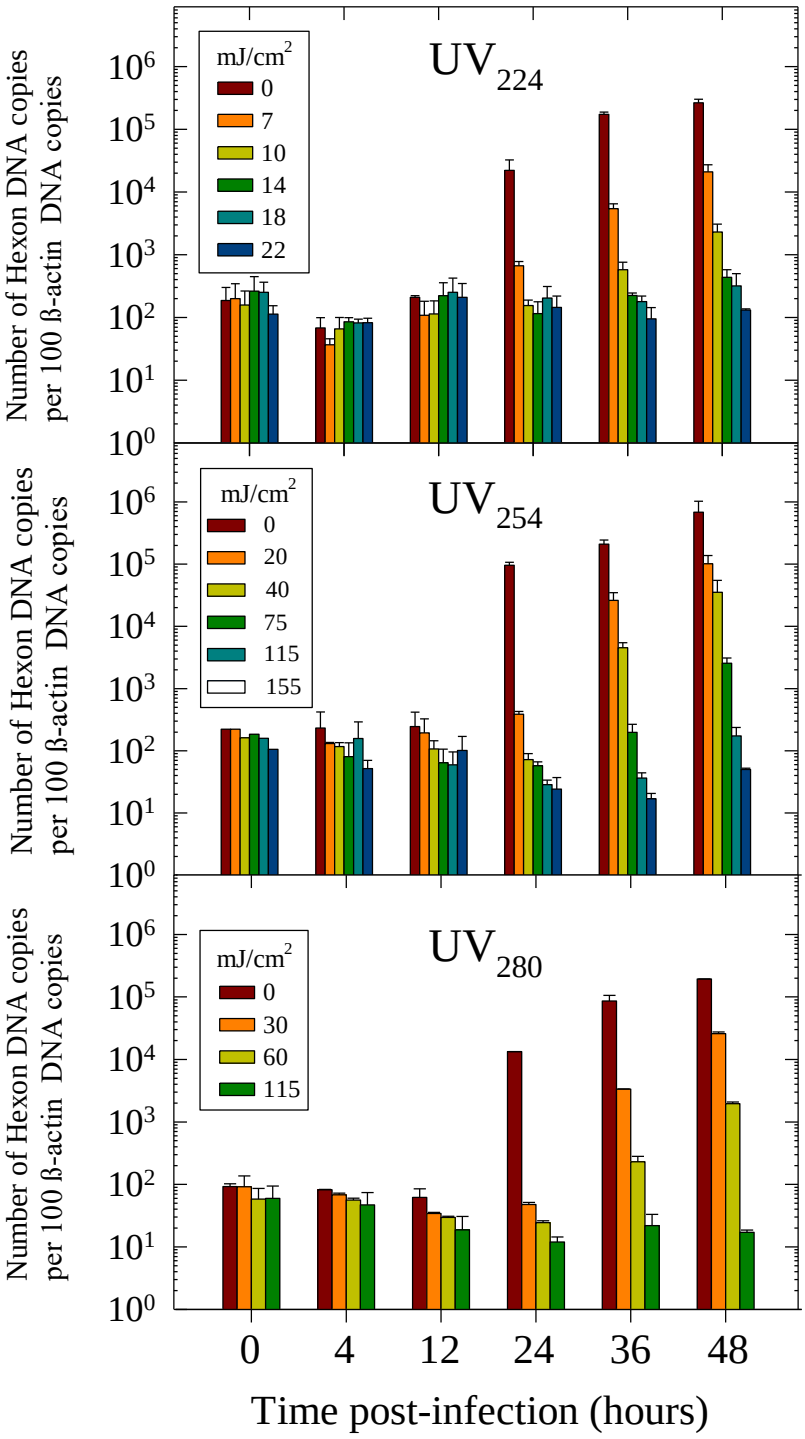

Figure 3.6. Absolute quantification of adenovirus Hexon DNA copies (0.1-kb long) per 100 β-actin DNA copies measured from 0 to 48 hours postinfection (hpi) after increasing exposure to UV_{224}, UV_{254}, and UV_{280}. Error bars represent standard deviation of the mean.

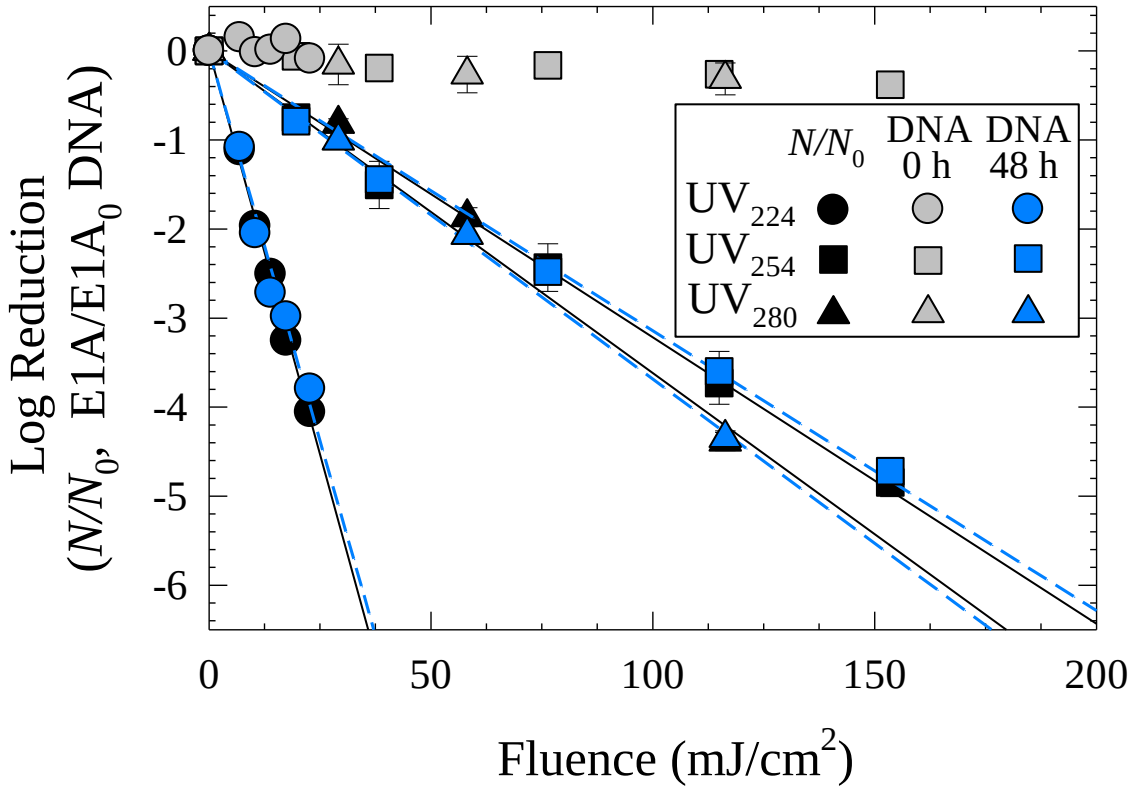

Figure 3.7. Relative expression level of E1A DNA (E1A/E1A$_0$) measured at 0 and 48 hpi (hours postinfection) normalized to the untreated sample is compared to the adenovirus survival ratio (N/N_0) determined by plaque assay, where N is the number of infectious viruses at any given time and N_0 the initial number of infectious viruses. Error bars represent the standard deviation of the mean. For each of the three conditions (UV$_{224}$, UV$_{254}$, and UV$_{280}$), the linear regression slopes and intercepts of the relative genome replication (E1A/E1A$_0$ DNA) at 48 hpi and the virus inactivation (N/N_0) were not significantly different (ANCOVA, $P > 0.05$).

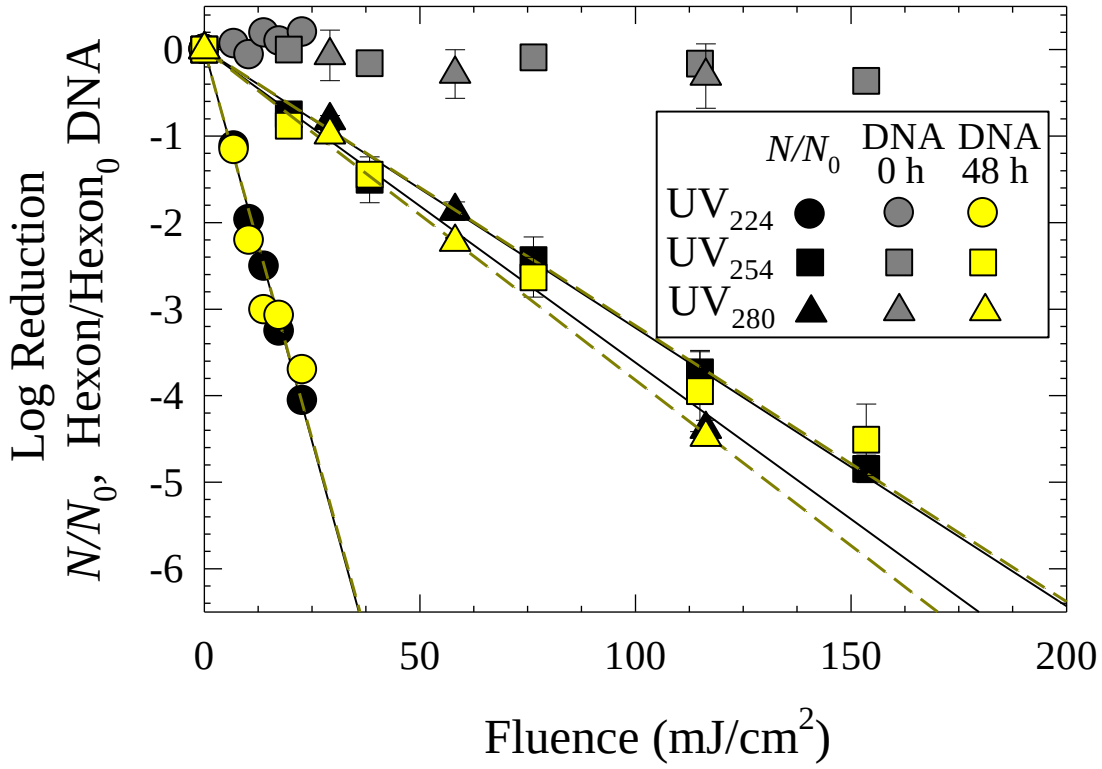

Figure 3.8. The relative expression level of Hexon DNA (*Hexon*/*Hexon*$_0$) measured at 0 and 48 hours post-infection (hpi) normalized to the untreated sample is compared to the adenovirus survival ratio (N/N_0) determined by plaque assay. Error bars represent standard deviation of the mean.

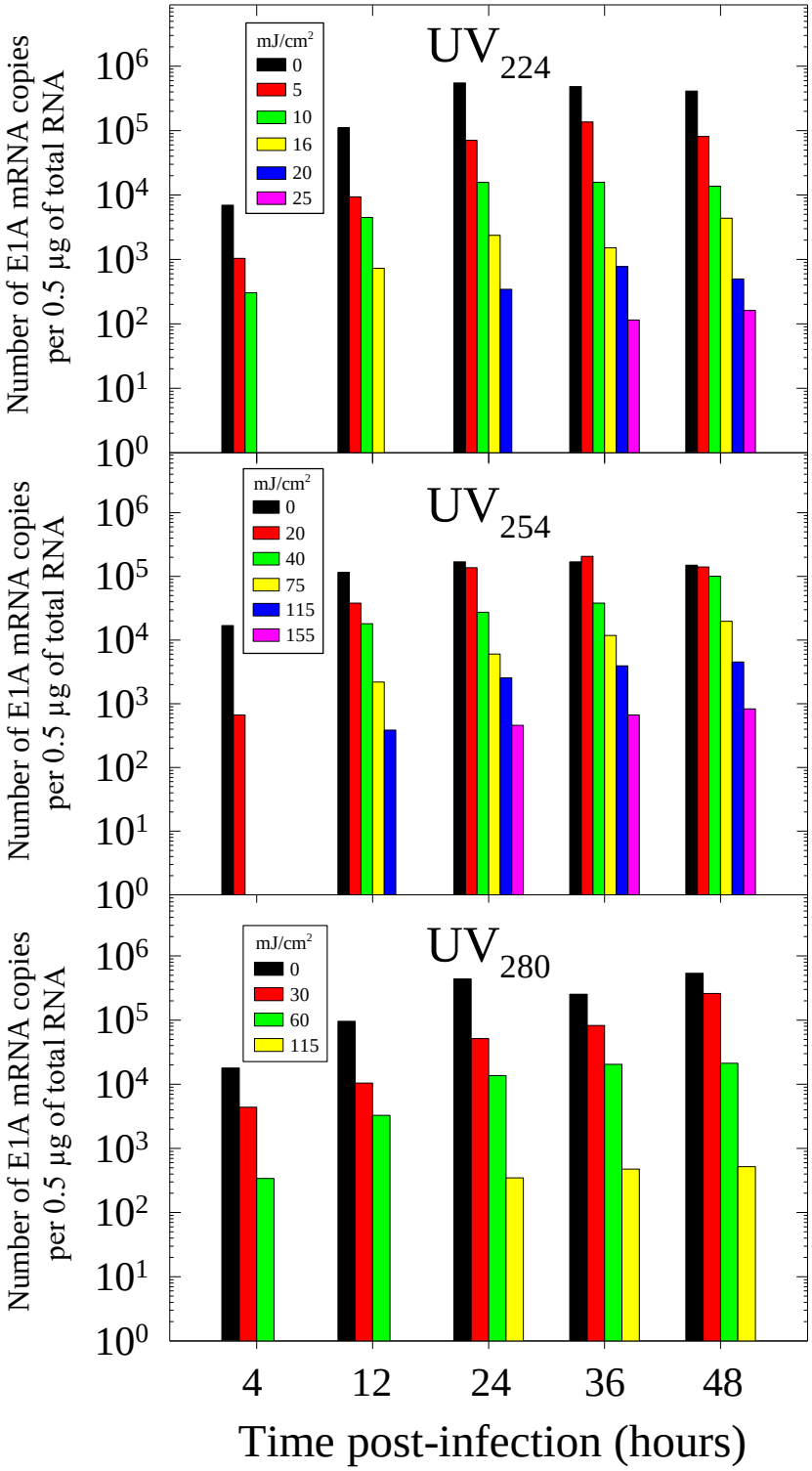

Figure 3.9. Absolute quantification of E1A mRNA copies per 0.5 µg of total RNA measured from 4 to 48 hours postinfection after increasing applied fluence at UV_{224}, UV_{254}, and UV_{280}

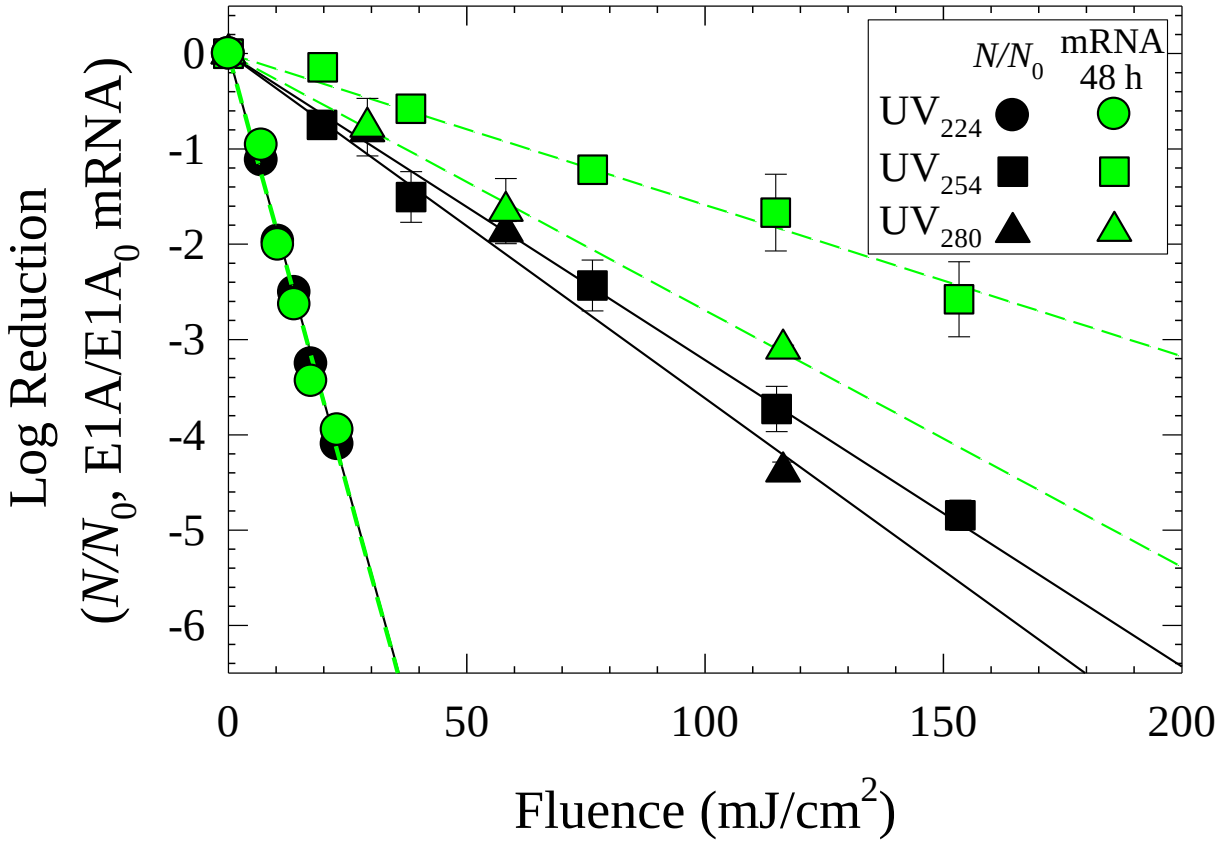

Figure 3.10. Relative expression level of E1A mRNA synthesis (E1A/E1A$_0$) at 48 hpi (hours postinfection) normalized to the untreated sample is compared to the adenovirus survival ratio (N/N_0) determined by plaque assay after exposure to UV_{224}, UV_{254}, and UV_{280}. Error bars represent the standard deviation of the mean. For UV_{254} and UV_{280}, the linear regression of the relative mRNA synthesis (E1A/E1A$_0$ mRNA) and the virus inactivation (N/N_0) were significantly different (ANCOVA, $P < 0.05$).

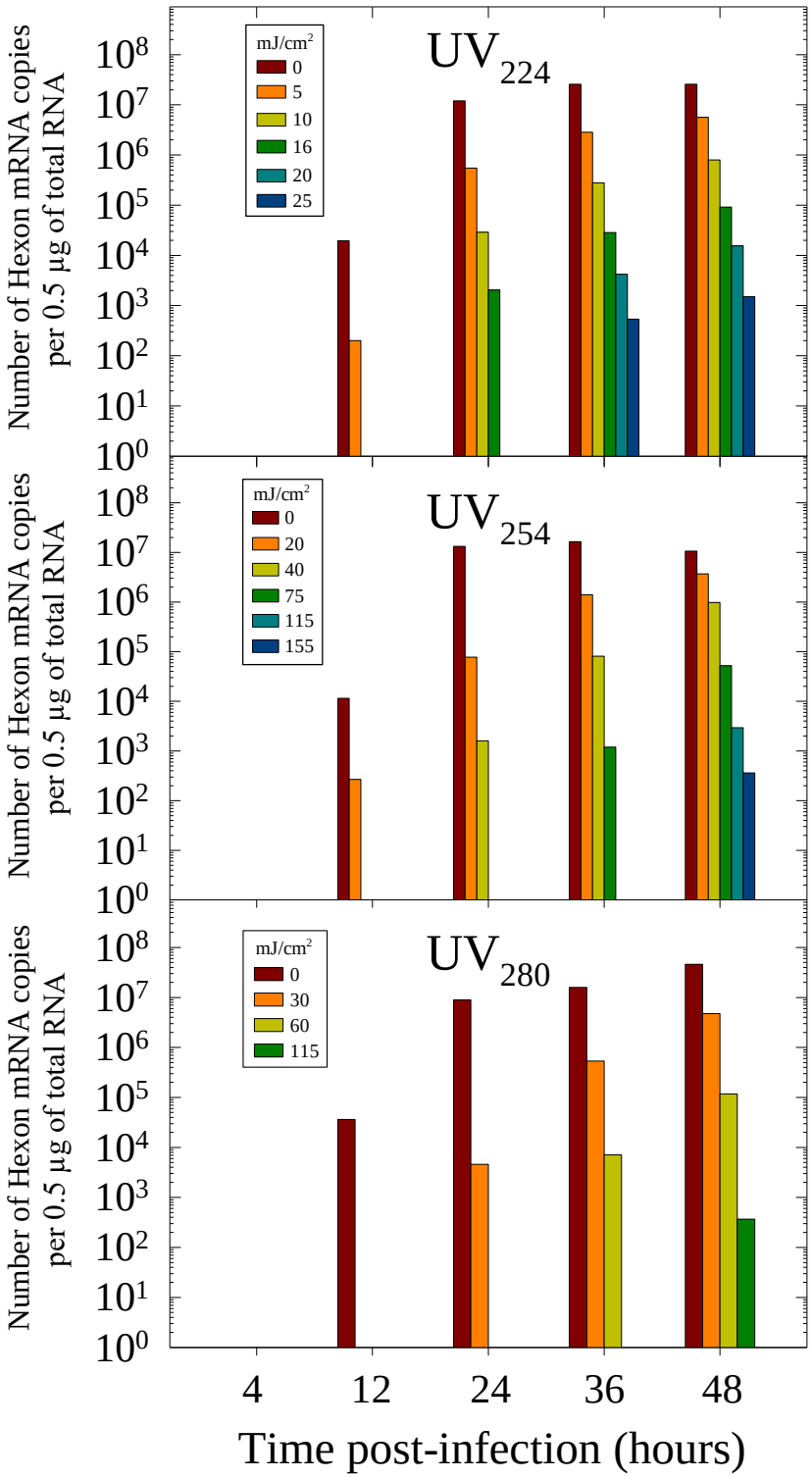

Figure 3.11. Absolute quantification of Hexon mRNA copies per 0.5 µg of total RNA measured from 4 to 48 hours postinfection after increasing applied fluence at UV_{224}, UV_{254}, and UV_{280}

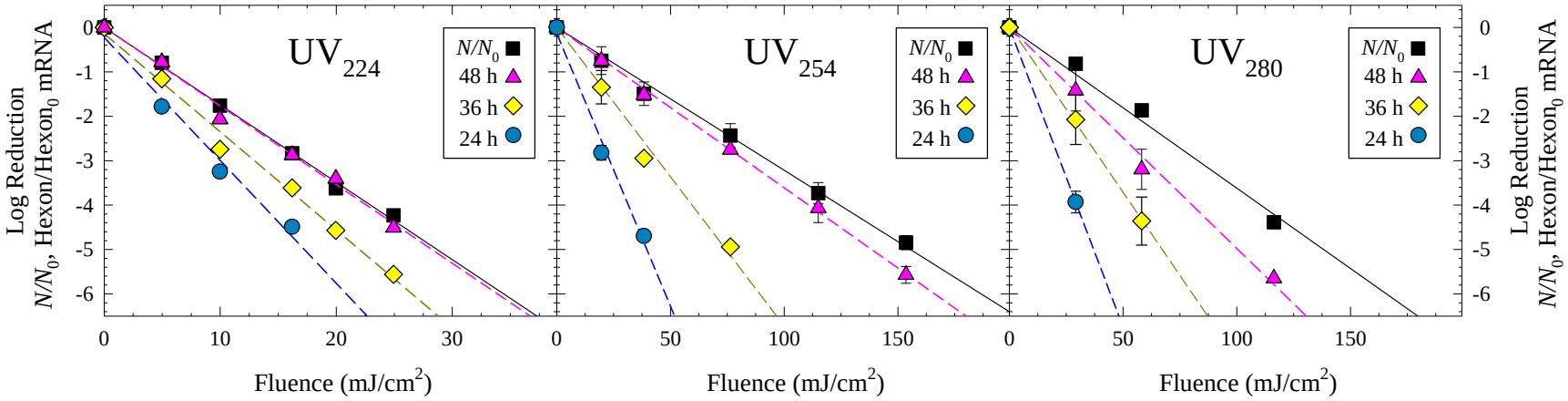

Figure 3.12. Relative expression level of Hexon mRNA synthesis (Hexon/Hexon$_0$) at 24, 36, and 48 hpi normalized to the untreated sample compared to the adenovirus survival ratio (N/N_0) determined by plaque assay after exposure to UV_{224}, UV_{254}, and UV_{280}. Error bars represent standard deviation of the mean.

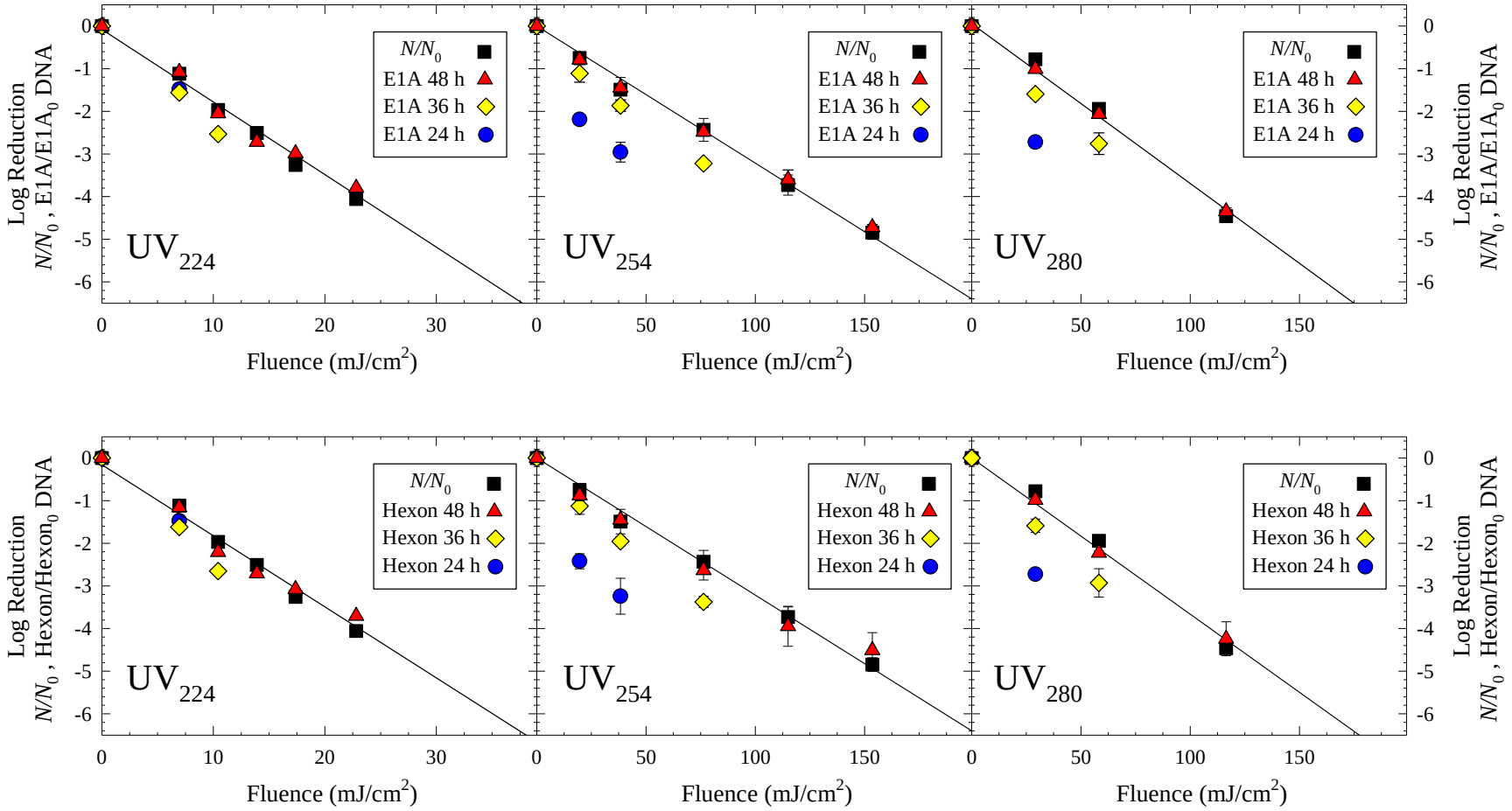

Figure 3.13. The relative expression level of E1A (top plots) and Hexon (bottom plot) amplicon replication (*E1A*/*E1A*$_0$ DNA, and *Hexon*/*Hexon*$_0$ DNA) at 24, 36, and 48 hours post-infection (hpi) normalized to the untreated sample is compared to the adenovirus survival ratio (N/N_0) determined by plaque assay after exposure to UV_{224}, UV_{254} and UV_{280}. Error bars represent standard deviation of the mean.

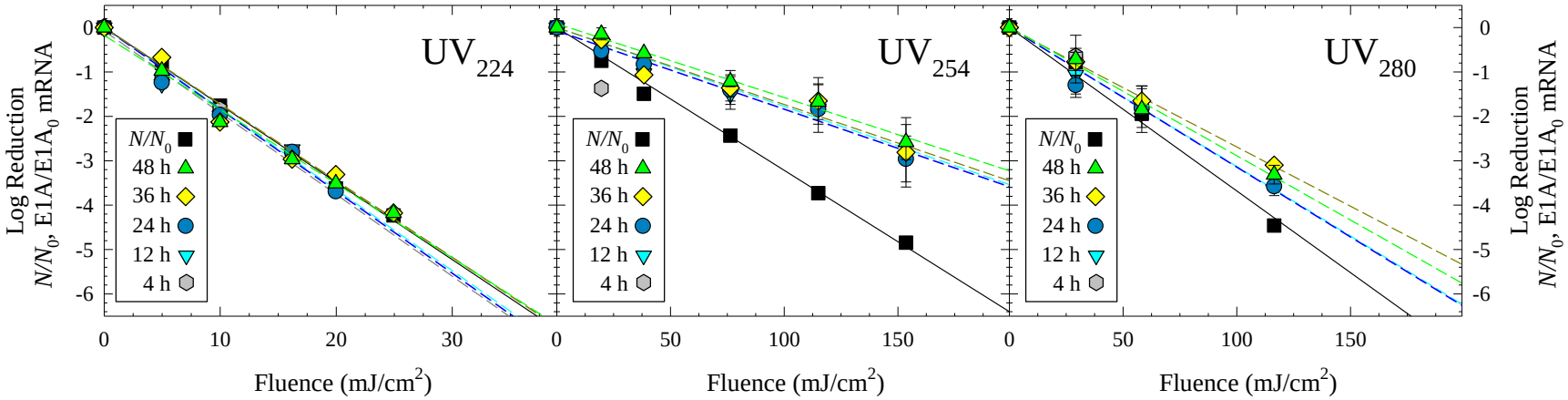

Figure 3.14. The relative expression level of E1A mRNA synthesis ($E1A/E1A_0$) at 4, 12, 24, 36, and 48 hours post-infection (hpi) normalized to the untreated sample is compared to the adenovirus survival ratio (N/N_0) determined by plaque assay after exposure to UV_{224}, UV_{254} and UV_{280}. Error bars represent standard deviation of the mean.

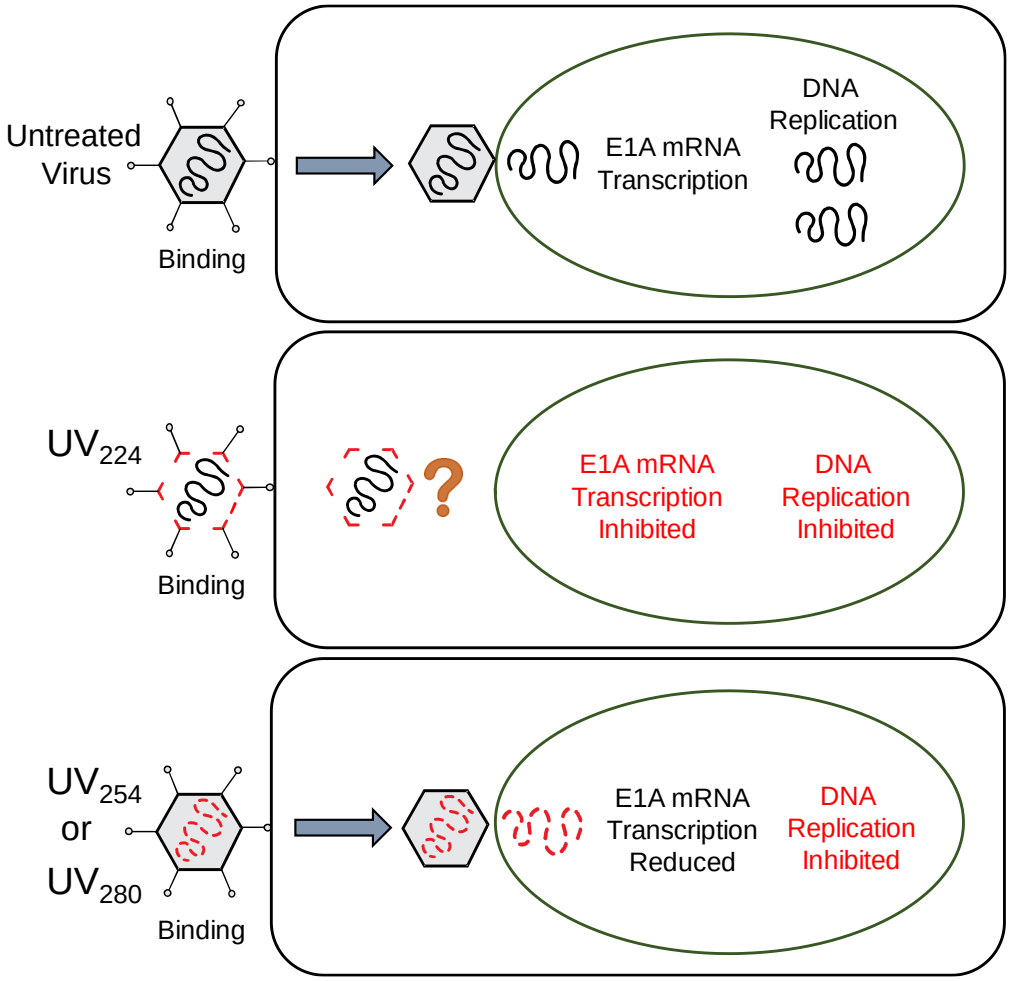

Figure 3.15. Summary of the HAdV-2 replication cycle inhibitions from exposure to UV_{224}, UV_{254} and UV_{280}.

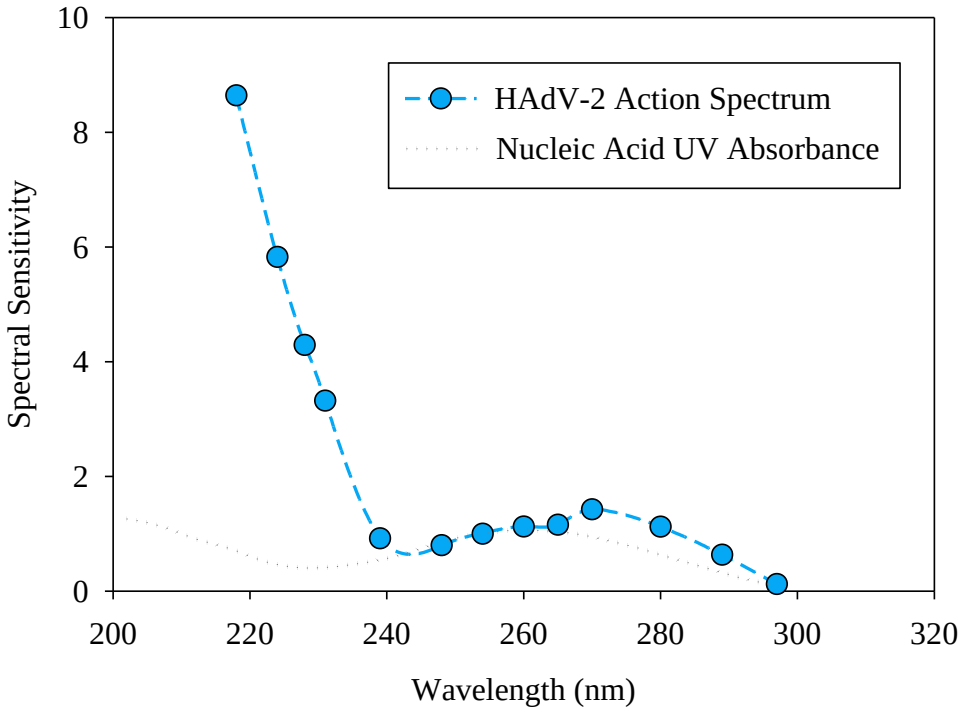

Figure 3.16. Human adenovirus type 2 action spectrum determined by inactivation after exposure to narrow bands of UV light within the range of 200-300 nm isolated with bandpass filters.

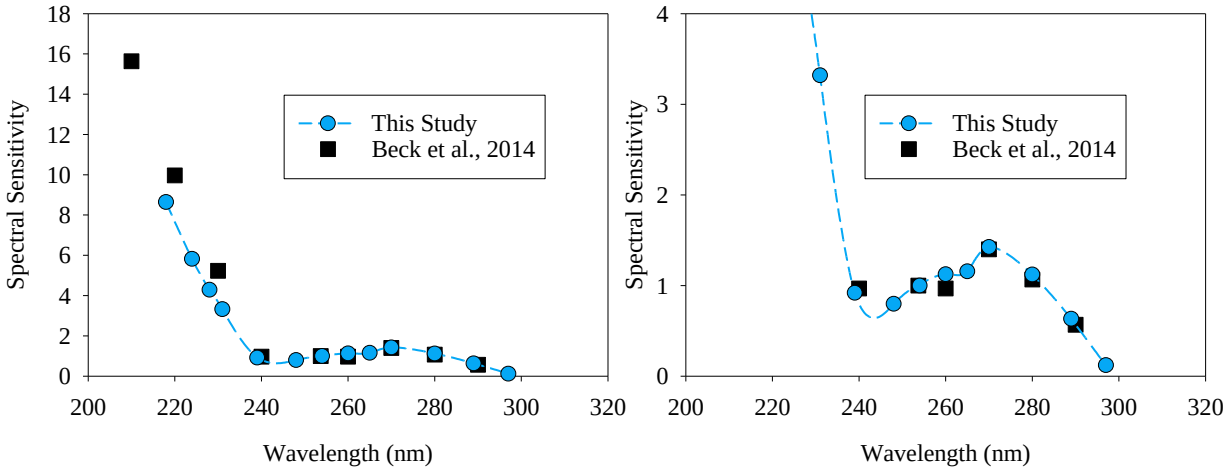

Figure 3.17. Human adenovirus type 2 action spectrum determined in this study compared with a previously published spectrum obtained using a laser UV emitter (Beck et al., 2014).

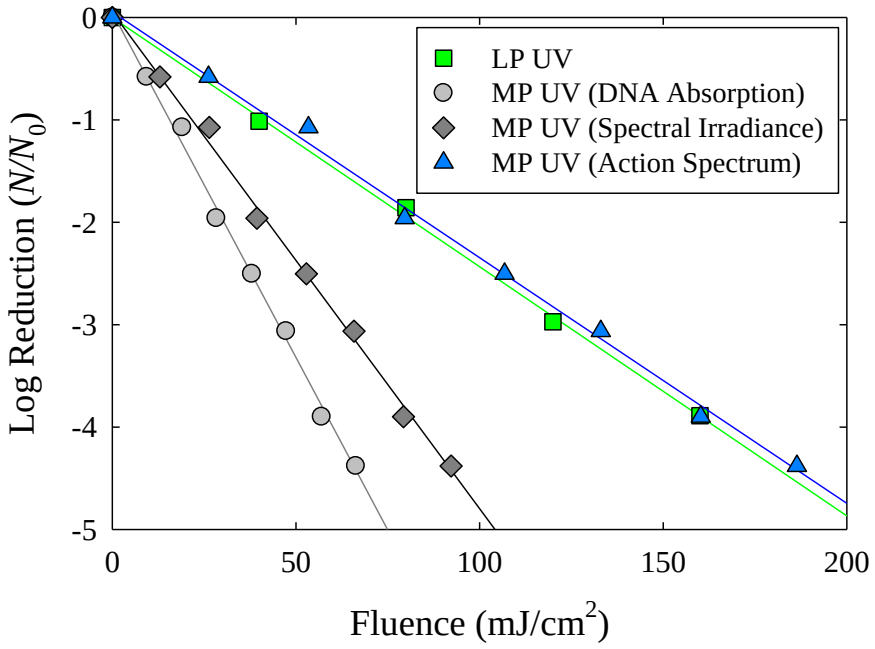

Figure 3.18. Comparison of HAdV-2 inactivation kinetics from exposure to LP UV and MP UV light. The different kinetics displayed from MP UV were obtained by using DNA absorption, spectral irradiance, or action spectrum as the weighting function in the fluence calculations. The linear regression between the relative reduction in viral infectivity caused by LP UV and that from MP UV weighted by the action spectrum were not significantly different (ANCOVA, $P > 0.05$).

3.6 References

Bas, A.; Forsberg, G.; Hammarström, S.; Hammarström, M. L.; Utility of the housekeeping genes 18S rRNA, beta-actin and glyceraldehyde-3-phosphate-dehydrogenase for normalization in real-time quantitative reverse transcriptase-polymerase chain reaction analysis of gene expression in human T lymphocytes. *Scand J Immunol*. **2004** Jun; *59*(6):566-73.

Beck, S. E.; Hull, N. M.; Poepping, C.; Linden, K. G. Wavelength-Dependent Damage to Adenoviral Proteins Across the Germicidal UV Spectrum. *Environ. Sci. Technol.* **2018**, *52*, 223– 229, DOI: 10.1021/acs.est.7b04602

Beck, S. E.; Rodriguez, R. A.; Linden, K. G.; Hargy, T. M.; Larason, T. C.; Wright, H. B. Wavelength dependent UV inactivation and DNA damage of adenovirus as measured by cell culture infectivity and long range quantitative PCR. *Environ. Sci. Technol.* **2014**, *48* (1), 591– 598, DOI: 10.1021/es403850b

Berk, A. J. Adenoviridae. In *Fields Virology*, 6th ed.; Knipe, D. M., Howley, P. M., Eds.; Lippincott Williams & Wilkins: Philadelphia, PA, **2013**; pp 1704– 1735.

Bolton, J. R.; Cotton, C. A. *The Ultraviolet Disinfection Handbook*; American Water Works Association: Denver, CO, **2008**; pp 11– 40.

Bolton, J. R.; Linden, K. G. Standardization of methods for fluence (UV dose) determination in bench-scale UV experiments. *J. Environ. Eng.* **2003**, *129* (3), 209– 215, DOI: 10.1061/(ASCE)0733-9372(2003)129:3(209)

Bosshard, F.; Armand, F.; Hamelin, R.; Kohn, T. Mechanisms of human adenovirus inactivation by sunlight and UVC light as examined by quantitative PCR and quantitative proteomics. *Appl. Environ. Microbiol.* **2013**, *79* (4), 1325– 1332, DOI: 10.1128/AEM.03457-12

Eischeid, A. C.; Meyer, J. N.; Linden, K. G. UV disinfection of adenoviruses: Molecular indications of DNA damage efficiency. *Appl. Environ. Microbiol.* **2009**, *75* (1), 23– 28, DOI: 10.1128/AEM.02199-08

Eischeid, A. C.; Thurston, J. A.; Linden, K. G. UV disinfection of adenovirus: Present state of the research and future directions. *Crit. Rev. Environ. Sci. Technol.* **2011**, *41* (15), 1375– 1396, DOI: 10.1080/10643381003608268

Gall, A. M.; Shisler, J. L.; Marinas, B. J. Analysis of the viral replication cycle of adenovirus serotype 2 after inactivation by free chlorine. *Environ. Sci. Technol.* **2015**, *49* (7), 4584– 4590, DOI: 10.1021/acs.est.5b00301

Greber, U. F.; Nakano, M. Y.; Maarit Suomalainen, M. *Adenovirus Entry into Cells, Methods in Molecular Medicine*, Vol 21; Adenovirus Methods and Protocols; World, W. S. M.; Humana Press, Inc.: Totowa, NJ,**1999**; pp 217– 230.

Guo, H. L.; Chu, X. N.; Hu, J. Y. Effect of host cells on low- and medium-pressure UV inactivation of adenoviruses. *Appl. Environ. Microbiol.* **2010**, *76* (21), 7068– 7075, DOI: 10.1128/AEM.00185-10

Jiang, S. C. Human adenoviruses in water: occurrence and health implications: a critical review. *Environ. Sci. Technol.* **2006**, *40* (23), 7132– 40, DOI: 10.1021/es060892o

Jogler, C.; Hoffmann, D.; Theegarten, D.; Grunwald, T.; Überla, K.; Wildner, O. Replication Properties of Human Adenovirus In Vivo and in Cultures of Primary Cells from Different Animal Species. *Journal of Virology* **2006**, *80* (7), 3549– 3558, DOI: 10.1128/JVI.80.7.3549-3558.2006

Kim, K.; Katayama, H.; Kitajima, M.; Tohya, Y.; Ohgaki, S. Development of a real-time RT-PCR assay combined with ethidium monoazide treatment for RNA viruses and its application to detect viral RNA after heat exposure. *Water Sci. Technol.* **2011**, *63* (3), 502– 507, DOI: 10.2166/wst.2011.249

Kremer, E. J.; Nemerow, G. R. Adenovirus tales: From the cell surface to the nuclear pore complex. *PLoS Pathog.* **2015**, *11* (6), e1004821, DOI: 10.1371/journal.ppat.1004821

Linden, K. G.; Thurston, J.; Schaefer, R.; Malley, J. P. Enhanced UV inactivation of adenoviruses under polychromatic UV lamps. *Appl. Environ. Microbiol.* **2007**, *73* (23), 7571– 7574, DOI: 10.1128/AEM.01587-07

Linden, K. G.; Shin, G. A.; Lee, J. K.; Scheible, K.; Shen, C. Y.; Posy, P. Demonstrating 4-log adenovirus inactivation in a medium-pressure UV disinfection reactor. *J. - Am. Water Works Assoc.* **2009**, *101* (4), 90–99, DOI: 10.1002/j.1551-8833.2009.tb09876.x

Livak, K. J.; Schmittgen, T. D. Analysis of relative gene expression data using real-time quantitative PCR and the 2(-Delta Delta C(T)) *Method. Methods*. **2001** Dec; *25*(4):402-8.

Mattle, M. J.; Vione, D.; Kohn, T. Conceptual Model and Experimental Framework to Determine the Contributions of Direct and Indirect Photoreactions to the Solar Disinfection of MS2, phiX174, and Adenovirus. *Environ. Sci. Technol.* **2015**, *49* (1), 334– 342, DOI: 10.1021/es504764u

Morse, D. L.; Carroll, D.; Weberg, L.; Borgstrom, M. C.; Ranger-Moore, J.; Gillies, R. J. Determining suitable internal standards for mRNA quantification of increasing cancer progression in human breast cells by real-time reverse transcriptase polymerase chain reaction. *Anal Biochem*. **2005** Jul 1; *342*(1):69-77.

Malayeri, A. H., Mohseni, M., Cairns, B., and Bolton, J. R., Fluence (UV Dose) Required to Achieve Incremental Log Inactivation of Bacteria, Protozoa, Viruses and Algae. *IUVA*, **2016**

Nascimento, M. A.; Magri, M. E.; Schissi, C. D.; Barardi, C. R. Recombinant adenovirus as a model to evaluate the efficiency of free chlorine disinfection in filtered water samples. *Virol. J.* **2015**, *12*, 30, DOI: 10.1186/s12985-015-0259-7

Oguma, K.; Rattanakul, S.; Bolton, J. R. Application of UV light-emitting diodes to adenovirus in water. *J. Environ. Eng.* **2016**, *ISNN*, 0733– 9372, DOI: 10.1061/(ASCE)EE.1943-7870.0001061

Page, M. A.; Shisler, J. L.; Marinas, B. J. Mechanistic aspects of adenovirus serotype 2 inactivation with free chlorine. *Appl. Environ. Microbiol.* **2010**, *76* (9), 2946– 2954, DOI: 10.1128/AEM.02267-09

Parshionikar, S.; Laseke, I.; Fout, G. S. Use of propidium monoazide in reverse transcriptase PCR to distinguish between infectious and noninfectious enteric viruses in water samples. *Appl. Environ. Microbiol.***2010**, *76*, 4318– 4326, DOI: 10.1128/AEM.02800-09

Rauth, A. M. Physical state of viral nucleic acid and sensitivity of viruses to ultraviolet light. *Biophys. J.* **1965**, *5* (3), 257– 273, DOI: 10.1016/S0006-3495(65)86715-7

Rigotto, C.; Hanley, K.; Rochelle, P. A.; De Leon, R.; Barardi, C. R.; Yates, M. V. Survival of adenovirus types 2 and 41 in surface and ground waters measured by a plaque assay. *Environ. Sci. Technol.* **2011**, *45*(9), 4145– 4150, DOI: 10.1021/es103922r

Rochelle, P.A., Blatchley III, E.R., Chan, P., Scheible, O.K., Shen, C.Y., Challenge Organisms for Inactivation of Viruses by Ultraviolet Treatment. Final Report. **2010**, Water Research Foundation and US EPA, Denver, CO.

Rodriguez, R. A.; Bounty, S.; Linden, K. G. Long-range quantitative PCR for determining inactivation of adenovirus 2 by ultraviolet light. *J. Appl. Microbiol.* **2013**, *114* (6), 1854– 65, DOI: 10.1111/jam.12169

Sangsanont, J.; Katayama, H.; Kurisu, F.; Furumai, H. Capsid-damaging effects of UV irradiation as measured by quantitative PCR coupled with ethidium monoazide treatment. *Food Environ. Virol.* **2014**, *6*,269– 275, DOI: 10.1007/s12560-014-9162-4

Schmittgen, T. D.; Zakrajsek, B. A.; Mills, A. G.; Gorn, V.; Singer. M. J.; Reed, M. W. Quantitative reverse transcription-polymerase chain reaction to study mRNA decay: comparison of endpoint and real-time methods. *Anal Biochem.* **2000** Oct 15; *285*(2):194-204.

Shin, G. A.; Lee, J. K.; Linden, K. G. Enhanced effectiveness of medium-pressure ultraviolet lamps on human adenovirus 2 and its possible mechanism. *Water Sci. Technol.* **2009**, *60* (4), 851– 857, DOI: 10.2166/wst.2009.414

Sirikanchana, K.; Shisler, J. L.; Marinas, B. J. Effect of exposure to UV-C irradiation and monochloramine on adenovirus serotype 2 early protein expression and DNA replication. *Appl. Environ. Microbiol.* **2008**, *74* (12), 3774– 3782, DOI: 10.1128/AEM.02049-07

USEPA. Drinking Water Contaminant Candidate List 4: Final. In *Federal Register*, Vol. 81, No. 222; Washington, DC, **2016**, pp 81099– 81114.

USEPA (U.S. Environmental Protection Agency). *Ultraviolet Disinfection Guidance Manual for the Final Long Term 2 Enhanced Surface Water Treatment Rule*; Washington, DC, **2006**.

USEPA (U.S. Environmental Protection Agency). *National Primary Drinking Water Regulations: Ground Water Rule, Final Rule*; Washington, DC, **2006**.

Winer, J.; Jung, C. K.; Shackel, I.; Williams, P. M. Development and validation of real-time quantitative reverse transcriptase-polymerase chain reaction for monitoring gene expression in cardiac myocytes in vitro. *Anal Biochem*. **1999** May 15; *270*(1):41-9.

Wold, W. S. M.; Ison, M. G. Adenoviruses. In *Fields Virology*, 6th ed.; Knipe, D. M., Howley, P. M., Eds.; Lippincott Williams & Wilkins: Philadelphia, PA, **2013**; pp 1732– 1767.

Wright, H. B.; Mackey, E. D.; Gaithuma, D.; Fonseca, C.; Baumberger, L.; Drzurny, T.; Clancy, J. L.;Hargy, T. M.; Fallon, K.; Cabaj, A.; Schmalweisser, A.; Bierman, A.; Gribbin, C. Optimization of UV Disinfection. *Awwa Research Foundation and NYSERDA* **2007**, 1

CHAPTER 4: SEQUENTIAL APPLICATION OF POLYCHROMATIC ULTRAVIOLET LIGHT TO INACTIVATE HUMAN ADENOVIRUS

4.1 Introduction

Human adenovirus is of relevance in the study of water disinfection due to its high resistance to UV light inactivation relative to other waterborne pathogens (Eischeid et al., 2009). The USEPA has established a fluence of 186 mJ/cm^2 required to inactivate 99.99 % of waterborne viruses based on adenovirus inactivation by monochromatic low-pressure (LP) UV light (USEPA, 2006). Polychromatic medium-pressure (MP) UV light has been reported more effective than LP UV to inactivate adenovirus (Linden et al., 2007; Linden et al., 2009; Eischeid et al., 2009; Shin et al., 2009).

As described in Chapter 3, UV light emitted by a polychromatic MP UV source at different wavelengths inhibits various HAdV-2 replication cycle events to different extents. This suggests the involvement of diverse inactivation mechanisms that are driven by the damage inflicted on different targets of the virus during MP UV light disinfection. Polychromatic MP UV light has been shown to be more effective than monochromatic LP UV light at damaging some viral proteins (Eischeid and Linden, 2011). The enhanced inactivation of adenovirus by MP UV light seems to be the result of damage to viral components other than its nucleic acid (Beck et al., 2014). Therefore, tailored UV systems could be designed incorporating UV light at wavelengths that are highly absorbed by nucleic acids (250-280 nm) and those where absorption of polypeptides is dominant (220-230 nm) (Beck et al., 2014; Beck et al., 2015; Beck et al., 2017). Since different wavelengths may affect predominantly different targets in the genome or viral proteins perhaps a certain combination of wavelengths might result in an enhanced inactivating effect for particular waterborne pathogens.

In this work the sequential application of polychromatic UV light from three different regions of the germicidal range (200-300 nm) was evaluated to assess synergistic effects at inactivating human

adenovirus type 2 (HAdV-2). This work was done using a MP UV lamp and bandpass filters with peak transmittance at 224, 254, and 280 nm. The reduction in viral genome replication at 48 hours postinfection (hpi) assessed by qPCR was utilized to determine the levels of inactivation achieved by each sequential combination of wavelengths.

4.2 Materials and Methods

4.2.1 UV Irradiation Experiments

The inactivation experiments were performed using a 1-kW Rayox collimated UV system operating with a polychromatic MP UV lamp (A300014, Calgon Carbon Co., Pittsburgh, PA). Bandpass filters with a bandwidth of about 10 nm at half of the maximum peak transmittance at 224, 254, and 280 nm (Andover Corporation, Salem, NH) were used to isolate specific regions from the full MP UV radiation spectrum. The presence of synergy by the sequential combination of the narrow band ranges provided with the bandpass filters was determined by comparison to the inactivation attained by each independent wavelength range as a control. The details on the fluence calculations were described in section 3.2.1 of Chapter 3. For the sequential application of UV_{254} and UV_{280} the fluence was determined using absorption of DNA as the weighting function in order to better discern the presence of synergistic effects by such combination.

4.2.2 Virus Propagation and Viability Assessment

Human lung A549 carcinoma cells (CCL-185) obtained from the American Type Culture Collection (Manassas, VA) were used for adenovirus propagation and viability assessment with a soft agar overlay plaque assay. Cell culture growth, virus propagation, and viability assays were performed following previously reported protocols (Sirikanchana et al., 2008; Page et al., 2010; Gall et al., 2015). Additional details are included in section 3.4 of Chapter 3 (Text S1).

4.2.3 Viral Genome Replication in Host Cells

HAdV-2 genome replication was quantified using previously reported protocols (Gall et al., 2015). Details are provided in section 3.2.5 of Chapter 3. Briefly, total DNA was extracted at 48 hours postinfection from A549 cellular monolayers that were inoculated with untreated and UV-treated HAdV-2. The number of E1A gene copies present at the time of DNA extraction was assessed by qPCR amplification, using primer sets listed in Table 3.1 of Chapter 3, and quantified using the standard curves presented in section 3.4 (Text S5) of Chapter 3.

4.2.4 qPCR Data Analysis and Statistical Analysis

Quantification cycle (C_q) values obtained from the qPCR assays were used to determine the relative decrease in DNA replication as described in section 3.2.6 of Chapter 3 (see also Text S5 of section 3.4). Analysis of covariance (ANCOVA) was used to compare the linear regression slopes between relative decrease in genome replication observed in the sequential experiments compared to their reference independent wavelength control in order to determine if they were statistically similar ($P > 0.05$), or a synergistic effect was observed.

4.3 Results and Discussion

The sequential application of narrow polychromatic UV light with peak emissions at 224, 254 and 280 nm was evaluated using the following combinations: UV_{224} followed by UV_{254} (UV_{224}+UV_{254}), UV_{224} followed by UV_{280} (UV_{224}+UV_{280}), and UV_{254} followed by UV_{280} (UV_{254}+UV_{280}). Each combination was also assessed in the reverse order. The results discussed in Chapter 3 indicated that for UV inactivation of HAdV-2 the reduction in viral infectivity and the inhibition of genome replication by 48 hours postinfection (hpi) was statistically similar (ANCOVA, $P > 0.05$). Thus, the log reduction of viable adenovirus provided by each combination of wavelengths was assessed by the disruption of E1A gene replication at 48 hpi. Nonetheless, the levels of inactivation of some of the combinations were assessed by plaque assay and the results obtained correlated well with those provided by the analysis of E1A gene

replication disruption at 48 hpi (Figure 4.1). These results corroborated that the assay to evaluate genome replication inhibition using qPCR quantification of the E1A gene amplicon can be used to determine the decrease in viral infectivity assessed by plaque assay produced by the UV treatment.

Figure 4.2 displays the log reduction of viral E1A DNA replication at 48 hpi from sequential exposure to UV_{224} followed by UV_{254} (UV_{224}+UV_{254}) and UV_{254} followed by UV_{224} (UV_{254}+UV_{224}). The reduction in E1A DNA replication provided by the independent application of each individual wavelength are included in the plot as controls for comparison. Figure 4.2 shows that in the sequential experiments when the exposure to the second wavelength range started the slope of the reduction in E1A gene replication shifted and followed the log reduction displayed by the second wavelength applied independently. The slope of the linear regression from each of the two distinct sections of the sequential experiment was not significantly different (ANCOVA, $P > 0.05$) to the slope of their corresponding control (independent wavelength without prior UV exposure). These results suggest that there is no synergy obtained by the sequential application of UV_{224} and UV_{254}. Pretreatment with either wavelength did not change the inactivation rate of the subsequent exposure. The data implies that the final level of inactivation achieved in the sequential UV tests is the summation of the individual contributions of each wavelength range during the complete duration of the experiment.

Figure 4.3 shows the results for the sequential exposure to UV_{224} and UV_{280}. Similarly to the results from the sequential combination of UV_{224} and UV_{254}, there was no explicit synergy observed with the combination of these two wavelengths. The slope of the linear regression from each of the two sections of the sequential experiment was not significantly different (ANCOVA, $P > 0.05$) to the slope of their corresponding control (no prior UV exposure to the other wavelength). This again, suggests an additive effect of the individual contributions of both wavelength ranges.

Finally, Figure 4.4 shows the results for the combination of UV_{254} and UV_{280}. A clear trend was difficult to observe in this combination since the dose-response curve for each individual wavelength was similar

when the spectral irradiance was used as the weighting function to calculate the average fluence rate in the water (see Figure 3.2). In this particular case the fluence displayed in Figure 4.4 was calculated using absorption of DNA as the weighting function in order to better observe the change in slopes from the sequential exposure experiments. Consistent with the two previous combinations, the final level of virus inactivation was the result from the individual contributions of both wavelength ranges.

The results obtained in this work indicate that there does not seem to be synergy among any combination of the wavelengths tested, which suggests that the effects of different wavelength ranges on the virus are independent from each other. This would imply that the virus inactivation by MP UV light (200-300 nm) is the addition of the individual effects from the wavelengths in the range covered during a given exposure time. This phenomenon is consistent with the second law of photochemistry (Stark-Einstein Law) which indicates a 1:1 correspondence between absorbed photons and yield of physical or chemical events (Bolton et al., 2015). The Stark-Einstein Law implies that photochemical events are independent of each other and therefore the extent of photochemical reaction is directly proportional to the total number of absorbed photons of all wavelengths (Bolton et al., 2015).

A recently published work assessed synergistic effects by the simultaneous application of polychromatic UV light with peak emissions at 260 and 280 nm using UV-C LEDs (Beck et al., 2017). Consistent to the results from this work, no synergy was observed by the 260|280 combination compared to the sum of their individual effects acting separately to inactivate HAdV-2 (Beck et al., 2017). The results from this work complement what was reported by Beck et al., 2017 indicating that the dual combination of different wavelength ranges in either configuration, simultaneous or sequential, does not provide synergism to inactivate HAdV-2. Collectively these data suggest that the inactivation obtained by the full spectrum of a polychromatic MP UV light is predominantly the result of the additive contributions from all the wavelengths over the range covered.

4.4 Figures

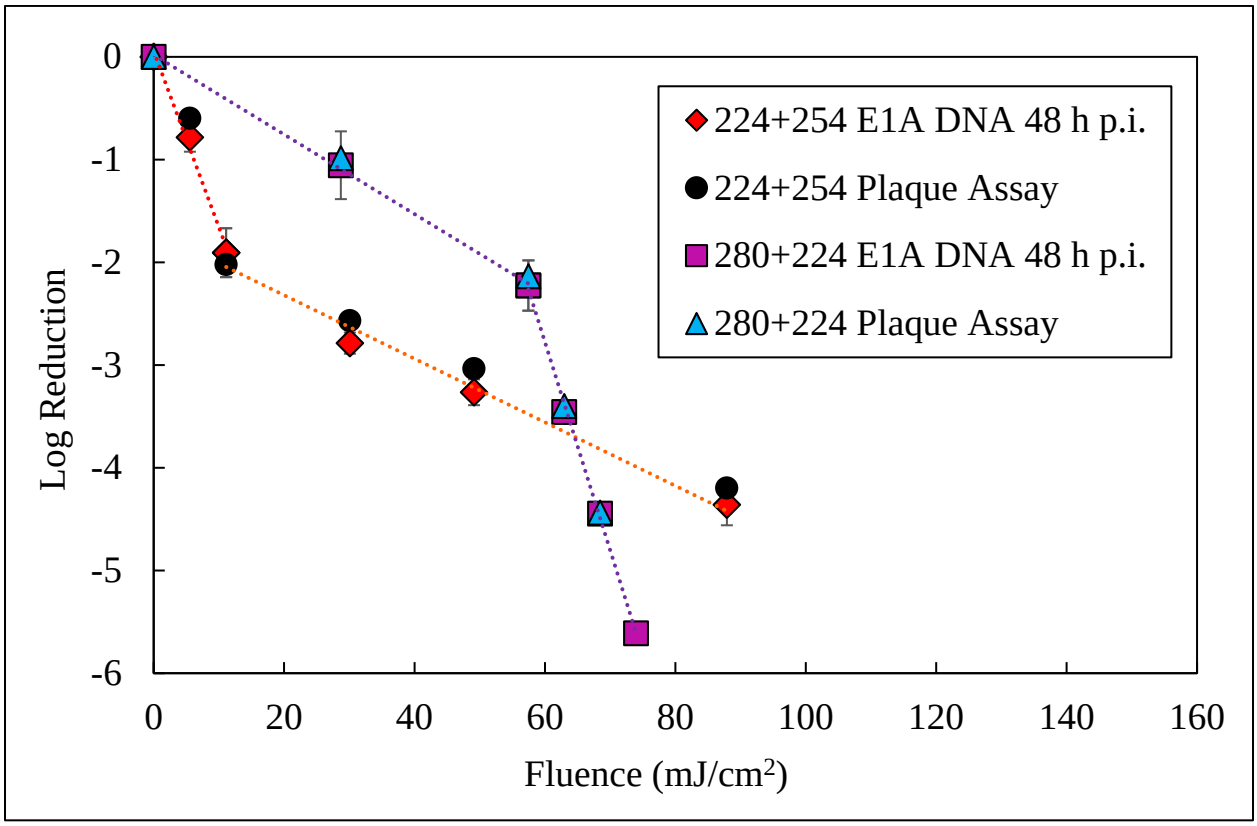

Figure 4.1. Comparison of HAdV-2 inactivation assessed by the relative reduction in the expression level of E1A DNA measured at 48 hours postinfection (hpi) normalized to the untreated sample ($E1A/E1A_0$), and the decrease in viral infectivity assessed by plaque assay (N/N_0) in A549 cells. The plot includes the experiments for the sequential application of UV_{224} followed by UV_{254} (224+254), and UV_{280} followed by UV_{224} (280+224).

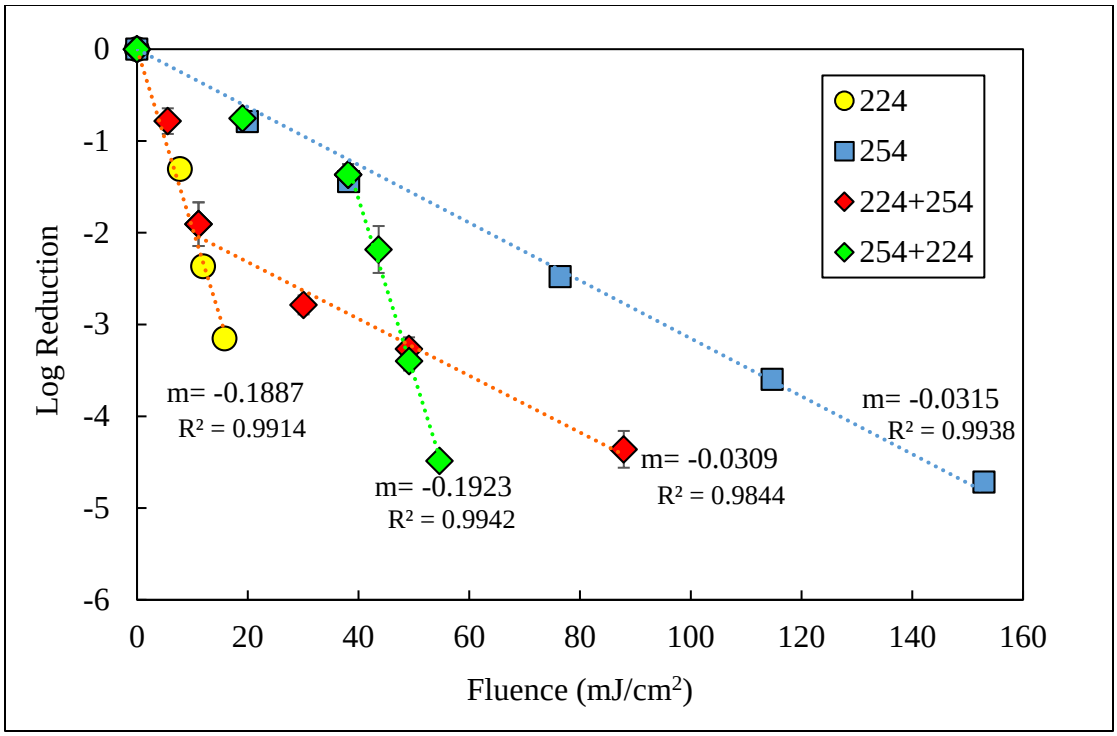

Figure 4.2. HAdV-2 inactivation assessed by the relative reduction in the expression level of E1A DNA ($E1A/E1A_0$) measured at 48 hours postinfection (hpi) normalized to the untreated sample. For the sequential experiments (UV_{224}+UV_{254}, and UV_{254}+UV_{224}) the linear regression slopes of the relative decrease in genome replication of each section was not significantly different (ANCOVA, $P > 0.05$) to the slope of their corresponding independent wavelength (without prior UV exposure at the other wavelength).

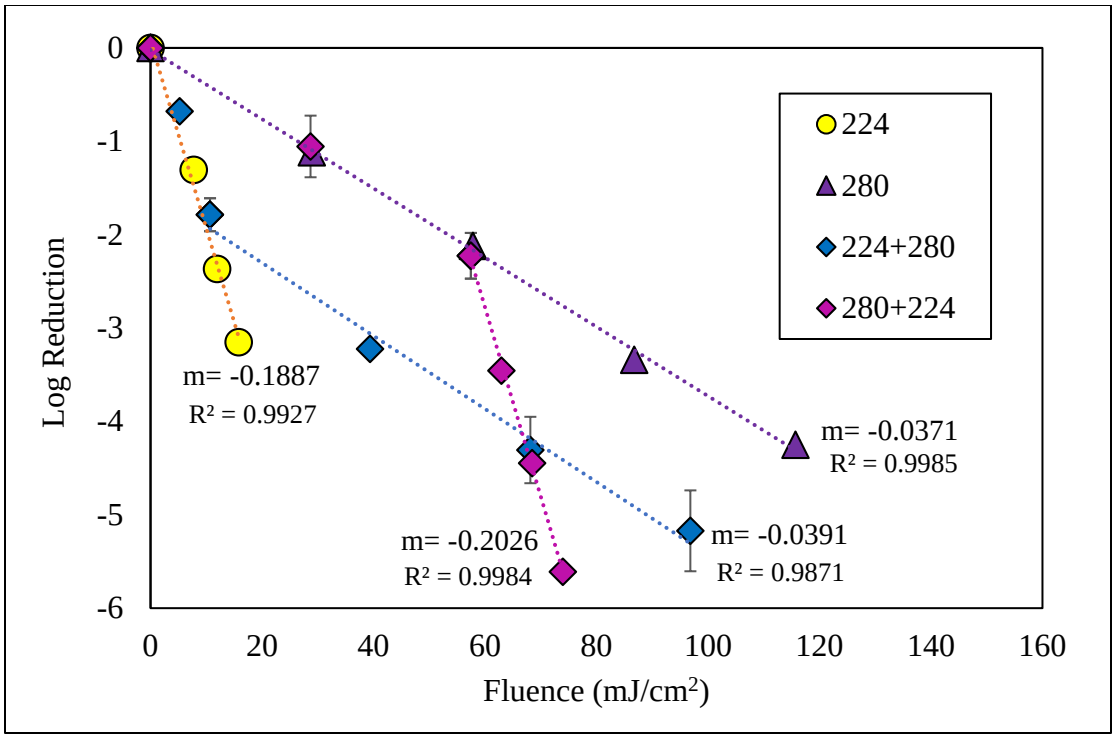

Figure 4.3. HAdV-2 inactivation assessed by the relative reduction in the expression level of E1A DNA (*E1A*/*E1A*$_0$) measured at 48 hours postinfection (hpi) normalized to the untreated sample. For the sequential experiments (UV_{224}+UV_{280}, and UV_{280}+UV_{224}) the linear regression slope of the relative decrease in genome replication of each section was not significantly different (ANCOVA, $P > 0.05$) to the slope of their corresponding independent wavelength (without prior UV exposure at the other wavelength).

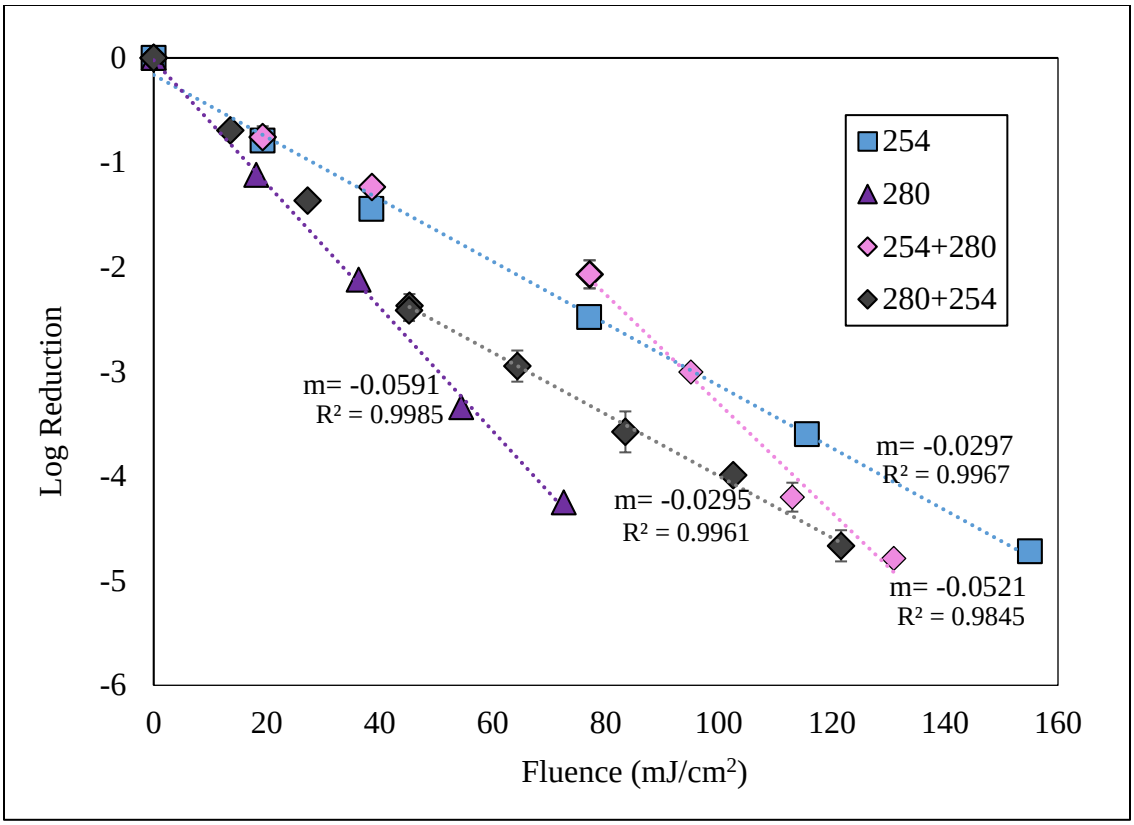

Figure 4.4. HAdV-2 inactivation assessed by the relative reduction in the expression level of E1A DNA (*E1A*/*E1A*$_0$) measured at 48 hours postinfection (hpi) normalized to the untreated sample. For the sequential experiments (UV_{254}+UV_{280}, and UV_{280}+UV_{254}) the linear regression slope of the relative decrease in genome replication of each section was not significantly different (ANCOVA, $P > 0.05$) to the slope of their corresponding independent wavelength without prior UV exposure. Fluences displayed were determined using UV absorption of DNA as the weighting function to calculate the average fluence rate in the water to better visualize trends.

4.5 References

Beck, S. E.; Rodriguez, R. A.; Linden, K. G.; Hargy, T. M.; Larason, T. C.; Wright, H. B. Wavelength dependent UV inactivation and DNA damage of adenovirus as measured by cell culture infectivity and long range quantitative PCR. *Environ. Sci. Technol.* **2014**, *48* (1), 591– 598, DOI: 10.1021/es403850b

Beck, S. E.; Ryu, H.; Boczek, L. A.; Cashdollar, J. L.; Jeanis, K. M.; Rosenblum, J. S.; Lawal, O. R.; Linden, K. G. Evaluating UV-C LED disinfection performance and investigating potential dual-wavelength synergy. *Water Research*. **2017,** 109, 207-216.

Beck, S. E.; Wright, H.; Hargy, T.; Larason, T. C.; Linden, K. G. Action spectra for validation of pathogen disinfection in medium-pressure ultraviolet (UV) systems. *Water Res*. **2015**, 70, 27-37.

Bolton, J. R.; Mayor-Smith, I.; Linden, K. G. Rethinking the Concepts of Fluence (UV Dose) and Fluence Rate: The Importance of Photon-based Units – A Systemic Review. *Photochemistry and Photobiology*. **2015**, 91: 1252–1262.

Eischeid, A. C.; Meyer, J. N.; Linden, K. G. UV disinfection of adenoviruses: Molecular indications of DNA damage efficiency. *Appl. Environ. Microbiol.* **2009**, *75* (1), 23– 28, DOI: 10.1128/AEM.02199-08

Eischeid, A. C.; Linden, K. G. Molecular Indications of Protein Damage in Adenoviruses after UV Disinfection. *Appl. Environ. Microbiol.* **2011**, *77*(3): 1145-1147.

Gall, A. M.; Shisler, J. L.; Marinas, B. J. Analysis of the viral replication cycle of adenovirus serotype 2 after inactivation by free chlorine. *Environ. Sci. Technol.* **2015**, *49* (7), 4584– 4590, DOI: 10.1021/acs.est.5b00301

Linden, K. G.; Thurston, J.; Schaefer, R.; Malley, J. P. Enhanced UV inactivation of adenoviruses under polychromatic UV lamps. *Appl. Environ. Microbiol.* **2007**, *73* (23), 7571– 7574, DOI: 10.1128/AEM.01587-07

Linden, K. G.; Shin, G. A.; Lee, J. K.; Scheible, K.; Shen, C. Y.; Posy, P. Demonstrating 4-log adenovirus inactivation in a medium-pressure UV disinfection reactor. *J. - Am. Water Works Assoc.* **2009**, *101* (4), 90–99, DOI: 10.1002/j.1551-8833.2009.tb09876.x

Page, M. A.; Shisler, J. L.; Marinas, B. J. Mechanistic aspects of adenovirus serotype 2 inactivation with free chlorine. *Appl. Environ. Microbiol.* **2010**, *76* (9), 2946– 2954, DOI: 10.1128/AEM.02267-09

Shin, G. A.; Lee, J. K.; Linden, K. G. Enhanced effectiveness of medium-pressure ultraviolet lamps on human adenovirus 2 and its possible mechanism. *Water Sci. Technol.* **2009**, *60* (4), 851– 857, DOI: 10.2166/wst.2009.414

Sirikanchana, K.; Shisler, J. L.; Marinas, B. J. Effect of exposure to UV-C irradiation and monochloramine on adenovirus serotype 2 early protein expression and DNA replication. *Appl. Environ. Microbiol.* **2008**, *74* (12), 3774– 3782, DOI: 10.1128/AEM.02049-07

USEPA (U.S. Environmental Protection Agency). *Ultraviolet Disinfection Guidance Manual for the Final Long Term 2 Enhanced Surface Water Treatment Rule*; Washington, DC, **2006**

CHAPTER 5: SIMULTANEOUS APPLICATION OF MONOCHROMATIC LOW-PRESSURE ULTRAVIOLET LIGHT AND MONOCHLORAMINE TO HUMAN ADENOVIRUS ♫

5.1 Introduction

Concern about adverse health effects of regulated disinfection by-products (DBPs) formed during water chlorination has driven the increased application of chloramines as secondary disinfectant since they formed fewer regulated DBPs (Gall et al., 2016). The USEPA (2016) indicates that more than 20% of Americans use drinking water treated with chloramines. However, chloramine has been shown to be significantly less effective than free chlorine to inactivate different microorganisms (Ballester and Malley, 2004; Gall et al., 2015; Gall et al., 2016). In addition, stringent regulations about DBP formation has caused the rise in utilization of alternative disinfection technologies like ultraviolet (UV) light that do not seem to produce known DBPs at the fluences commonly applied (USEPA, 2006). However, one of the main challenges with the implementation of UV light disinfection technologies is the lack of residual disinfectant in the treated water. A majority of the water supply systems in the US is required to provide a residual disinfectant in the distribution line to ensure safe drinking water reaching the households, and to prevent biofilm formation (Shin and Lee, 2010). Human adenovirus (HAdV) is known as the least susceptible virus to monochloramine inactivation and there is not a good understanding of the mechanism by which monochloramine renders adenovirus non-infectious (Gall et al., 2016). Also, human adenovirus is highly resistant to monochromatic low-pressure (LP) UV light inactivation and this aspect has determined the UV disinfection requirements in the current regulations (USEPA, 2006). Most waterborne pathogens of concern require 4 to 5 times lower fluences (UV doses) to reach a 4-log inactivation compared to that needed for human adenovirus (Malayeri et al., 2016). It has been suggested that human adenovirus could be used as a viral indicator for fecal contamination due to its prevalence in water sources and public health implications (Rattanakul et al., 2015).

♫ Adapted from Vazquez-Bravo, B.; Gonçalves, K.; Shisler, J. L.; Mariñas, B. J., Adenovirus Inactivation by Simultaneous Application of Ultraviolet Light and Monochloramine, (in preparation).

Although UV light and monochloramine are increasingly used in water treatment systems globally the available literature investigating potential synergism combining both disinfectants to inactivate human adenovirus is limited. The sequential application of UV light and monochloramine to inactivate HAdV-2 has been assessed in a few studies; however, different observations have been reported regarding potential presence of synergistic effects in the sequential application of these disinfectants. Ballester and Malley (2004) indicated that the sequential application of monochloramine and LP UV light resulted in higher HAdV-2 inactivation than the expected additive result from both disinfectants acting independently under the same experimental conditions. These authors also reported greater HAdV-2 inactivation when UV light was applied prior to monochloramine exposure, compared to the inactivation achieved when the disinfectants where applied in the reverse order. The results from Ballester and Malley (2004) would suggest a potential synergistic effect in the sequential application of these disinfectants. On the other hand, Baxter et al., (2007) reported no statistically significant difference in the inactivation rate of HAdV-2 by monochloramine when viruses were previously exposed to UV light compared to those that did not received prior UV treatment. The experiments from both of these studies were performed at pH 8 and 20-23 ºC.

In a more recent study (Shin and Lee, 2010), LP UV and medium-pressure (MP) UV light were used in sequential combination with monochloramine to inactivate HAdV-2. Shin and Lee (2010) showed that MP UV was more effective than LP UV to inactivate adenovirus, which is consistent with other studies that have assessed the capacity of both UV sources to inactivate HAdV-2 (Linden et al., 2007; Eischeid et al., 2009; Shin et al., 2009). Still, the inactivation provided by monochloramine was not enhanced by prior exposure to either MP UV or LP UV light. The experiments of Shin and Lee (2010) were performed at pH 8 at 5 ºC.

Due to the limited information available there is a need to further evaluate the presence of potential synergistic effects in the combined application of UV light and monochloramine to determine if a

particular configuration can enhance the individual contributions of both disinfectants. Although the sequential application has been previously assessed (Ballester and Malley, 2004; Baxter et al., 2007; Shin and Lee, 2010), to our knowledge, the simultaneous application of monochloramine and LP UV to inactivate human adenovirus has not been reported.

The main objective of this study was to assess the presence of synergy in the simultaneous application of LP UV light and monochloramine to inactivate HAdV-2. Additionally, a possible mechanism of synergy was investigated. This work complemented the available data on the sequential configuration of these treatment techniques and helped to improve the understanding of the inactivation mechanisms by these disinfectants. Furthermore, this knowledge can aid in the development of alternative disinfection strategies for water treatment facilities currently using both LP UV light and monochloramine as part of their treatment train, and also on the design of applications for developing countries scenarios where presence of ammonia in drinking water makes the implementation of free chlorine a challenge.

5.2 Materials and Methods

5.2.1 UV Irradiation Experiments

UV light inactivation experiments were performed using a 1-kW Rayox collimated UV system (A300014, Calgon Carbon Co., Pittsburgh, PA) operating with a 15-W low-pressure (LP) UV lamp providing monochromatic UV light at 254 nm. The applied fluence was determined following the recently published IUVA protocol for a LP UV lamp using a collimated beam system (Bolton, et al., 2015). A reactor with 20 mL of 1 mM carbonate buffer solution (CBS) was dosed with HAdV-2 at concentrations of ~2×10^6 plaque forming units (PFU) per mL and irradiated by LP UV light. Experiments were conducted at room temperature (23 ºC). A recirculating water-jacketed reactor was used to maintain the temperature constant throughout the duration of the experiment. Continuous stirring was provided by a magnetic stir bar and plate. The fluence (UV dose) applied to HAdV-2 samples was controlled by varying the exposure time.

5.2.2 Monochloramine Experiments

Monochloramine disinfection experiments were performed in batch reactors containing 20 mL of 1 mM carbonate buffer solution (CBS) dosed with HAdV-2 at concentrations of ~2×10^6 plaque forming units (PFU) per mL. Preformed monochloramine was prepared by mixing 50 mL of sodium hypochlorite solution and 50 mL of ammonium chloride solution. Monochloramine concentration was determined using the N, N-diethyl-p-phenylenediamine colorimetric method. Confirmation that monochloramine was the only chloramine species formed was done by measuring the absorbance from 200-400 nm using a UV-Vis spectrophotometer (Shimadzu, UV-2700). At exposure times set to match those at which the LP UV samples were taken, virus samples were withdrawn from the monochloramine reactor and mixed with 0.1% sodium thiosulfate to quench the monochloramine. Residual monochloramine concentration was measured at the times that virus samples were taken. Experiments were performed at pH 8.3 and 23 ºC. A recirculating water-jacketed reactor was used to maintain the temperature constant throughout the duration of the experiment. Initial monochloramine concentration was 4 mg/L as Cl_2.

5.2.3 Simultaneous LP UV and Monochloramine Experiments

The same conditions described for the monochloramine experiments in section 5.2.2 were used with the addition that the mixed monochloramine-virus solution was simultaneously exposed to LP UV light. At exposure times set to match those at which the LP UV and monochloramine samples were taken when used independently, virus samples were also taken from the UV-irradiated monochloramine reactor and residual monochloramine was quenched with 0.1% sodium thiosulfate. Monochloramine concentration was measured at the times that virus samples were taken. The presence of synergy by the simultaneous application of LP UV light and monochloramine was determined by comparison with the calculated level of virus inactivation attained when the effect of each disinfectant acting independently was added.

5.2.4 Virus Propagation and Viability Assessment

Human lung A549 carcinoma cells (CCL-185) obtained from the American Type Culture Collection (Manassas, VA) were used for adenovirus propagation and viability assessment with a soft agar overlay plaque assay or HAdV-2 genome amplification by qPCR from extracted DNA at 48 hours post-synchronized infection. Cell culture growth, virus propagation, and viability assays were performed following previously reported protocols (Sirikanchana et al., 2008; Page et al., 2010; Gall et al., 2015).

5.2.5 Amplicon Integrity

To assess genome damage after exposure to LP UV light, monochloramine, or their simultaneous application (LP UV | NH_2Cl), viral DNA was extracted from treated and untreated samples following the extraction protocol for the DNeasy Blood & Tissue Kit (Qiagen, Valencia, CA). Primers previously reported to amplify different regions of the adenovirus genome (Rodriguez et al., 2013; Gall et al., 2015) were used to assess if such regions were amplifiable by qPCR after treatment with each condition evaluated. The primer sets used can be found in Table 3.1 of Chapter 3.

5.2.6 Thermal Stability Assay Coupled with Ethidium Monoazide Bromide Exposure

Ethidium monoazide bromide (Invitrogen, Thermo Fisher Scientific, Inc., Waltham, MA) was used to analyze if the different treatment conditions assessed in this work affected the integrity of the adenovirus capsid. EMA is a fluorescent nucleic acid stain that covalently binds to nucleic acids after exposure to visible light (Kim et al., 2011). When EMA binds to the viral genome, the affected genome region cannot be amplified by qPCR. Previous studies have shown that the disassembly behavior exhibited by purified adenovirus particles upon heating is very similar to the disassembly behavior exhibited during the first steps of viral infection (Greber et al., 1993; Wiethoff et al., 2005). The approach used to detect the effects of the different treatment conditions investigated on the viral capsid integrity, as an indication of capsid protein transformation, was to assess the thermal stability of the capsid comparing untreated versus treated viruses. If a difference in thermal stability of treated versus untreated virions was observed, then

this would imply that such treatment altered the capsid proteins in a manner that destabilized the virus. Such mutagenesis of the capsid perhaps alters the virus's ability to bind to the cell, internalize or properly disassemble within the cytoplasm.

We developed a qPCR-based strategy that quantified viral genomes after virions were exposed to different temperatures in the presence of ethidium monoazide bromide (EMA). If the integrity of the capsid was compromised, EMA would enter the virion and covalently bind to DNA to prevent PCR amplification of the genome. Thus, the use of EMA coupled with a thermal stability assay can identify changes in capsid conformation. Control experiments at different temperatures determined that untreated virions remained impermeable to EMA up until 50 ºC and that this temperature alone did not affect the integrity of the genome (data not shown). If UV light, monochloramine, or the simultaneous application of both disinfectants makes the virions permeable to EMA at a temperature lower or higher than 50 ºC, it would be an indication of mutagenesis of capsid proteins induced by such treatment. It was decided to perform experiments at 37 ºC as a temperature to evaluate a shift in the thermal stability of the virus post-treatment. This temperature was selected for being the temperature at which cell monolayers are incubated during the infectivity assays and is also what is considered normal human body temperature. For each disinfection condition the inhibition of qPCR amplification due to EMA-DNA interactions at 37 ºC was assessed by measuring the ratio of amplified DNA fragments present in treated samples as compared to those present in the untreated sample. Details of the EMA protocol, with exception of the incubation step at 37 ºC, are included in section 3.4 of Chapter 3 (Text S3).

5.2.7 Analysis of Viral Replication Cycle Inhibition

Inhibition at different steps of the HAdV-2 replication cycle was quantified as previously reported (Gall et al., 2015). Details are provided in section 3.2.5 of Chapter 3. Briefly, total DNA or RNA was extracted at 48 hours postinfection from A549 cellular monolayers that were inoculated with untreated or treated HAdV-2 by LP UV, monochloramine, or the simultaneous application of both disinfectants. The

number of E1A or hexon gene copies present at the time of DNA or RNA extraction was assessed by qPCR amplification, using primer sets listed in Table 3.1 of Chapter 3, and quantified using the equations presented in section 3.4 of Chapter 3 (Text S5). RNA samples were reverse transcribed by PCR into cDNA before they were analyzed by qPCR (RT-qPCR).

5.2.8 qPCR Data Analysis and Statistical Analysis

Quantification cycle (C_q) values obtained from the qPCR assays were used to determine the relative decrease in DNA replication or qPCR amplification as previously described (Gall et al., 2015; Rodriguez et al., 2013). Analysis of covariance (ANCOVA) was used to compare the linear regression slopes between the relative decrease in genome replication calculated by the addition of the independent contributions of the two disinfectants used (additive effect), and the relative decrease in genome replication observed in the simultaneous experiments in order to determine if they were statistically similar ($P > 0.05$), or significantly different, which would suggest presence of synergy.

5.3 Results and Discussion

5.3.1 HAdV-2 Inactivation by LP UV, NH_2Cl, and simultaneous LP UV | NH_2Cl

The inactivation of HAdV-2 from exposure to low-pressure (LP) UV light, monochloramine (NH_2Cl), and the simultaneous application of both, UV light and monochloramine (LP UV | NH_2Cl) was assessed. All experiments were performed in carbonate buffer solution (CBS) at pH 8.3 and 23 ºC. An initial concentration of monochloramine was set to 4 mg/L as Cl_2 to consider the value on the regulatory limit of residual concentration and also be within the range that is commonly used in water treatment processes (2 - 6 mg/L as Cl_2) (Crittenden et al., 2012). Also, this condition was selected to complement and compare with previously reported data that evaluated the sequential application of LP UV and NH_2Cl (Ballester and Malley, 2004; Baxter et al., 2007).

Figure 5.1 (top plot) shows the log-reduction of HAdV-2 infectivity assessed by genome replication inhibition at 48 hours postinfection (hpi) using a 100-bp amplicon of the E1A gene. Figure 5.1 (top plot) displays the levels of adenovirus inactivation attained by each disinfectant acting independently (NH_2Cl, and LP UV) and also in their simultaneous application (LP UV | NH2Cl). For ease of comparison among treatments the horizontal axis displays the exposure time (in minutes) for each disinfectant. The top plot of Figure 5.1 includes the additive effect curve that was calculated by summation of the inactivation rate constants obtained using the linear regression analysis for each disinfectant independently. Figure 5.1 (top plot) indicates that the resulting inactivation curve from the simultaneous application of LP UV light and monochloramine (LP UV | NH2Cl) has a faster HAdV-2 inactivation rate compared with the calculated additive effect (LP UV + NH_2Cl). ANCOVA determined that the linear regressions of the calculated additive effect plot and that from the simultaneous application of both disinfectants obtained experimentally were significantly different. These results indicate that the simultaneous application of LP UV light and monochloramine inactivate HAdV-2 at a faster rate than the addition of their independent contributions, which suggests a synergistic interaction between both disinfectants.

Rattanakul, et al., (2015) observed synergy in the sequential application of free chlorine followed by LP UV to inactivate HAdV-5, but the authors did not see this effect in the simultaneous application of both disinfectants. It is possible that the fast rate at which free chlorine inactivates HAdV impeded the observation of synergy in the simultaneous experiments of Rattanakul et al., (2015). The conditions used in this work and the slow kinetics of HAdV-2 inactivation by monochloramine allowed the observation of a clear synergistic effect. By ~25 min when LP UV light was used independently a fluence of ~80 mJ/cm^2 was applied and about a 2-log reduction of HAdV-2 infectivity was reached. This is consistent with previously reported data using LP UV light to inactivate HAdV-2 (Baxter et al., 2007; Shin and Lee, 2010). When monochloramine was present, the same fluence of ~80 mJ/cm^2 reached a ~4-log HAdV-2 inactivation, in contrast to the 2-log reduction that was obtained by LP UV independently. By this time (~25 min), the monochloramine concentration decreased from 4 mg/L to about 2 mg/L (Figure 5.1,

bottom plot). In the experiments where monochloramine was not exposed to UV light, the monochloramine concentration decreased from 4 to ~3 mg/L by 25 min (Figure 5.1, bottom plot) but less than 0.5-log HAdV-2 inactivation was achieved (Figure 5.1, top plot). Exposure to LP UV light decreased the monochloramine concentration at a faster rate than the decrease in the absence of UV light. Still, there was residual 2 mg/L of monochloramine by the time the exposure to UV light ended.

5.3.2 Mechanism of Synergy

It has been previously shown that LP UV light does affect the integrity of the adenovirus genome (Rodriguez et al., 2013; Beck et al., 2014). On the other hand, monochloramine applied independently did not seem to affect the integrity of a 0.1-kb DNA fragment of the E1A and Hexon genes (Gall et al., 2016). In this work genome integrity was assessed with a 1.1-kb DNA fragment of the adenovirus genome using primers previously reported (Rodriguez et al., 2013). qPCR amplification of the 1.1-kb HAdV-2 genome fragment was not inhibited by monochloramine during the exposure times assessed using an initial NH_2Cl concentration of 4 mg/L as Cl_2. Simultaneous application of LP UV light and monochloramine did not cause greater genome disruption compared to the damaged produced by LP UV alone (Figure 5.2). Therefore, it is likely that the enhanced inactivation observed with the simultaneous application of LP UV light and monochloramine is due to damage to viral components other than the genome.

The HAdV-2 capsid integrity after exposure to the 3 disinfection conditions investigated (NH_2Cl, LP UV, and LP UV | NH_2Cl) was evaluated by its thermal stability in the presence of EMA. Figure 5.3 shows the results obtained when the most inactivated virus samples for each condition tested (<0.5-log inactivated by NH_2Cl, ~2-log inactivated by LP UV, and ~4-log inactivated by LP UV | NH_2Cl) were exposed to EMA while incubated at 37 ºC. A decrease in the qPCR amplification of viral genome would suggest a mutagenized capsid that resulted in a shift in the thermal stability of the virion, and allowed EMA-DNA interaction. Figure 5.3 shows that in the most inactivated sample of each condition (by ~25 min exposure

to each treatment), a decrease in qPCR amplification of about 80 % of the viruses that were exposed to simultaneous LP UV light and monochloramine was detected. In contrast, when each disinfectant was applied independently a decrease of about 10 % in qPCR amplification of the genome fragment analyzed was detected after the samples were incubated in the presence of EMA.

The HAdV-2 capsid is formed by a set of twelve proteins that are divided into three groups: major, minor and core proteins (Berk, 2013). The capsid proteins are responsible for packing, transporting, and delivering the viral genome into host cell nucleus, therefore, mutation of any one of these twelve proteins can impact the success of HAdV replication (Reddy and Nemerow, 2014). It has been previously reported that monochloramine does not inhibit the ability of the virus to bind to the host cell (Gall et al., 2016), and this research work has shown that UV_{254} does not inhibit this step in the replication cycle either (see Figures 3.7 and 3.8 of Chapter 3). Similarly, the simultaneous application of LP UV (emitted at 254 nm) and monochloramine did not inhibit association of the virus with the host cell (Figure 5.4). Collectively, the results suggest that while each disinfectant acting independently did not cause gross modifications on the viral capsid during the exposure times evaluated, the simultaneous application of both disinfectants produced a modification in the viral capsid that did not inhibit the ability of the virus to associate with the host cell but perhaps disrupted virus internalization or a subsequent step in the replication cycle.

Next, the disruption of early and late gene transcription was assessed for each condition using previously reported protocols (Gall et al., 2015). The three conditions analyzed (monochloramine, LP UV light, and the simultaneous application of LP UV and monochloramine) inhibited hexon mRNA synthesis to the same extent at which DNA replication was inhibited (Figure 5.5). In contrast, E1A mRNA transcription was reduced to a greater extent compared to the effect caused by LP UV independently or by monochloramine exposure alone (Figure 5.6). The greater decrease in E1A mRNA synthesis observed by simultaneous LP UV | NH_2Cl is possibly the result from a combination of genome damage induced by

the LP UV to the template E1A gene, and less number of viruses reaching/translocating their genome into the nucleus due to disruption of the timely-synchronized progression of the post-binding steps caused by conformational changes of the capsid proteins.

The results for LP UV on the analysis of early and late gene transcription are consistent with the work described in Chapter 3 using bandpass filters to isolate polychromatic UV light emitted by a MP UV lamp with peak transmittance at 254 nm. The observations from the condition in which monochloramine was applied independently are consistent with what was reported by Gall et al., 2016, who looked at replication cycle inhibitions of HAdV-2 by monochloramine. Collectively, the results suggest that the enhanced HAdV-2 inactivation observed by the simultaneous application of LP UV and monochloramine is likely produced by a conformational change of the viral capsid proteins that possibly disrupts viral internalization or a subsequent step in the replication cycle. Under this premise, viruses that were able to reach the cell nucleus and internalize their UV-damaged genome could continue the replication cycle but E1A mRNA transcription was reduced due to the UV-induced damage to the E1A gene template.

Patton et al., (2017) indicated that photolysis of monochloramine can generate the formation of hydroxyl radicals ($HO^{\bullet}$) or the chlorine dimer ($Cl_2^{\bullet -}$), which both contributed in the degradation of 1,4-dioxane for potable water reuse applications. It is possible that these radicals react with the viral capsid proteins in the simultaneous LP UV | NH_2Cl approach, causing a conformational change of the viral capsid that allowed the results shown in Figure 5.3, and that might drive the enhanced HAdV-2 inactivation observed.

5.3.3 Practical implications

The total exposure times used in the experiments displayed in Figure 5.1 are about 25 min. In scenarios encountered in water treatment plants the exposure times in UV reactors are much shorter with high UV intensities applied. For this reason, an exploratory experiment was performed where the UV light

intensity was increased to assess if the same synergistic effect would be observed with conditions closer to real scenarios in water treatment plants. Figure 5.7 shows the results obtained when the UV intensity was increased ~6 times and the kinetics observed were about 5 times faster (k=-0.826) than those displayed in Figure 5.1 (k=-0.163). These results suggest that enhanced HAdV inactivation by simultaneous application of LP UV light and monochloramine would be achieved in conditions encountered in real water treatment plant scenarios (high UV intensity in short contact time). At the experimental conditions used in this work (pH 8.3, 23 ºC, initial [NH_2Cl] = 4 mg/L as Cl_2), the presence of monochloramine made LP UV light as effective as MP UV light to control HAdV-2. A fluence of ~80 mJ/cm^2 of MP UV light generated a 4-log reduction of HAdV-2 infectivity, which was a similar fluence at which LP UV light reached the same level of HAdV-2 inactivation (4-log reduction) when it was applied simultaneously with monochloramine. This aspect can be advantageous to develop approaches that use LP UV lamps to control HAdV given that they are more energy efficient than MP UV lamps, which can reduce operational costs.

It was not intended in this study to provide a full characterization of inactivation kinetics caused by the simultaneous application of LP UV and monochloramine. The main objective of this work was to identify the presence of a synergistic effect with the simultaneous application of both disinfectants, and (if detected) explore a possible mechanism of synergism. There is need to investigate these synergistic effects in natural water samples with different levels of natural organic matter since results might differ due to non-specific reactions of the formed radicals with other organic matter in the water matrices. A complete characterization at different pH values and temperatures of interest in water treatment processes would complement this work to further evaluate practical applications of this simultaneous approach. Assessment of nitrogenous disinfection byproducts formation and their toxicological analysis during LP UV | NH_2Cl applications is an important aspect to be addressed, however it was outside of the scope of this work and should be investigated in future studies.

5.4 Figures

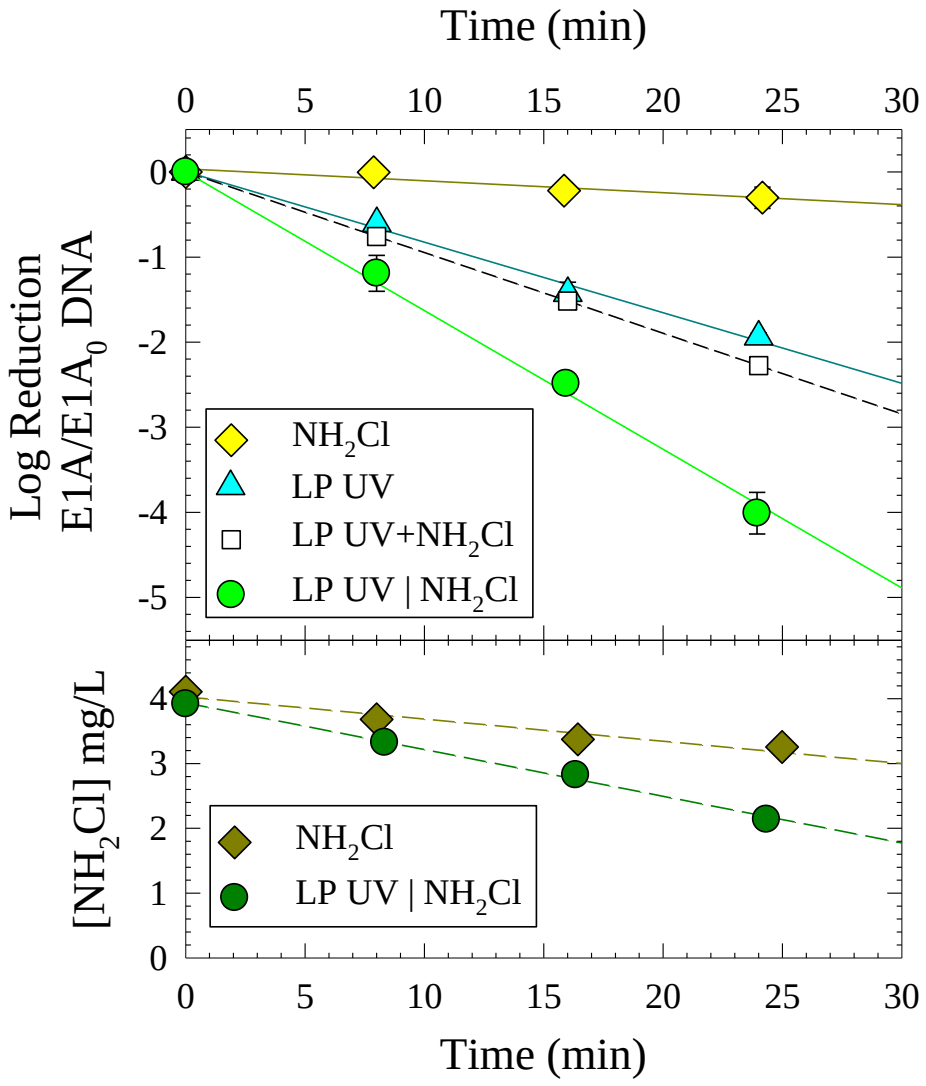

Figure 5.1. Relative expression level of E1A DNA synthesis ($E1A/E1A_0$) at 48 hours postinfection (hpi) normalized to the untreated sample after exposure to monochloramine independently (NH_2CL), low-pressure UV independently (LP UV), or the simultaneous application of both disinfectants (LP UV | NH_2CL). The additive effect from the independent contributions of both disinfectants was calculated by adding the reaction rate constants from both independent conditions and it is represented by the dashed line and squares in the top plot (LP UV+NH_2CL). The linear regressions of the relative decrease from the calculated additive effect and that from the simultaneous application of both disinfectants obtained experimentally were significantly different (ANCOVA, $P < 0.05$). These data suggest the presence of synergism in the simultaneous application of LP UV and NH_2CL to inactivate HAdV-2. Experiments were performed at pH 8.3, 23 °C, and initial NH_2CL concentration of 4 mg/L as Cl_2. The bottom plot shows the decrease in monochloramine concentration in the presence of HAdV-2 with and without exposure to LP UV light.

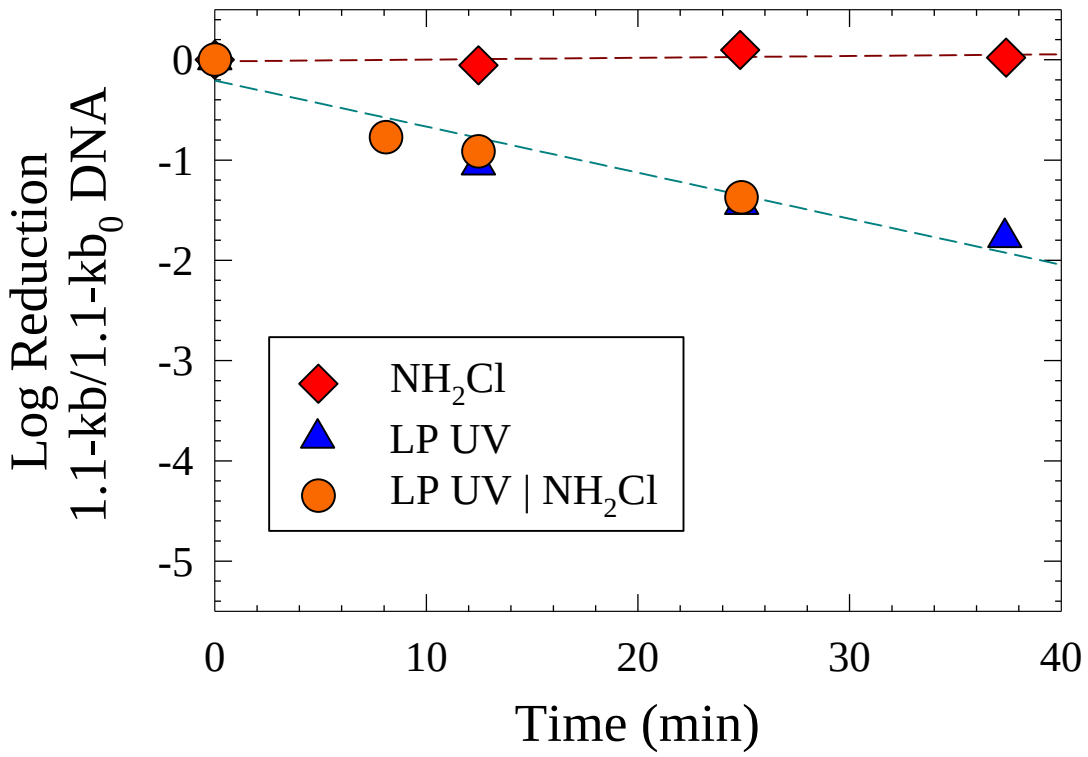

Figure 5.2. Decrease in amplification by qPCR of a 1.1-kb viral DNA fragment after increasing exposure to monochloramine independently (NH_2Cl), low-pressure UV light independently (LP UV), and the simultaneous combination of UV light and monochloramine (LP UV | NH_2Cl). No cell infection took place in these sets of experiments. The combined application of both disinfectants did not produce greater disruption of the genome fragment analyzed compared to LP UV alone. NH_2CL acting independently did not seem to affect the integrity of the 1.1-kb fragment amplified by qPCR.

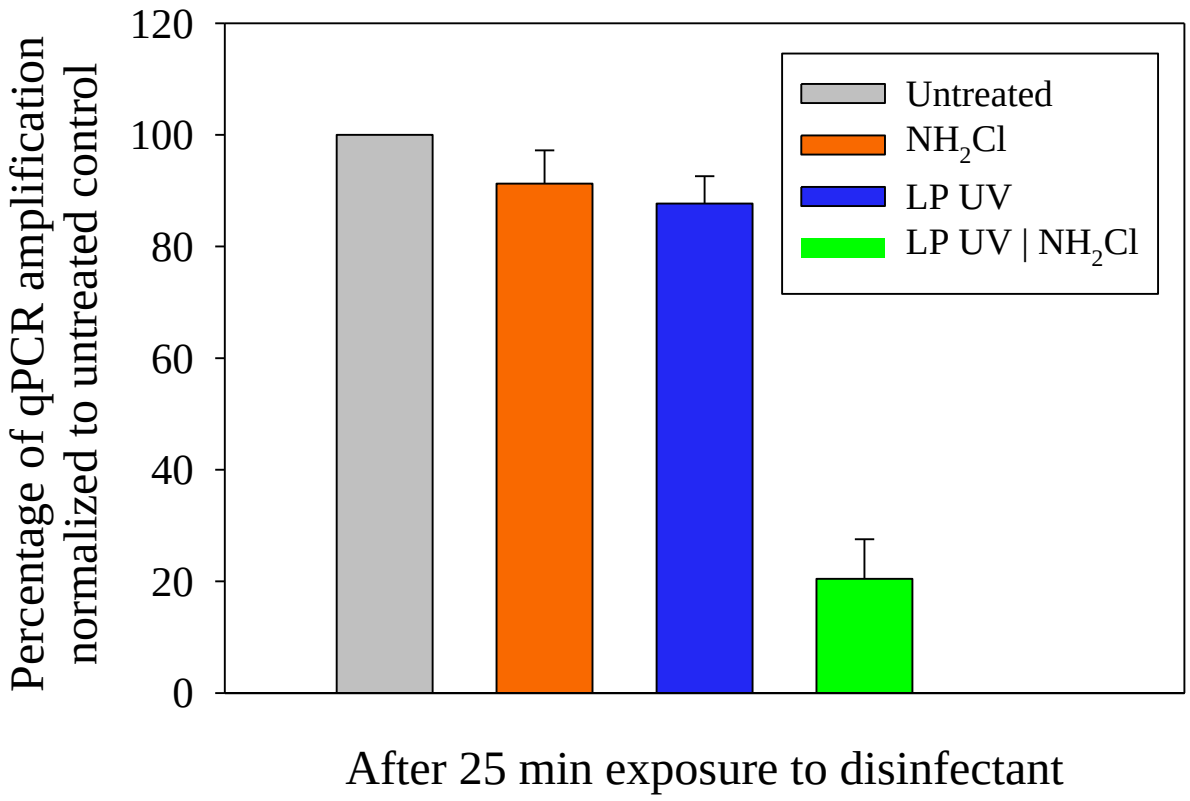

Figure 5.3. Assessment of viral capsid conformation caused by exposure to monochloramine (NH_2Cl), low-pressure UV light (LP UV) or the simultaneous application of both disinfectants (LP UV | NH_2Cl) by EMA assay performed at 37 °C. Indication that the capsid of ~80% of viruses was mutagenized in the most inactivated sample by simultaneous LP UV | NH_2CL was observed. About 10% of viruses in samples from the independent application of each disinfectant were permeable to EMA after treatment.

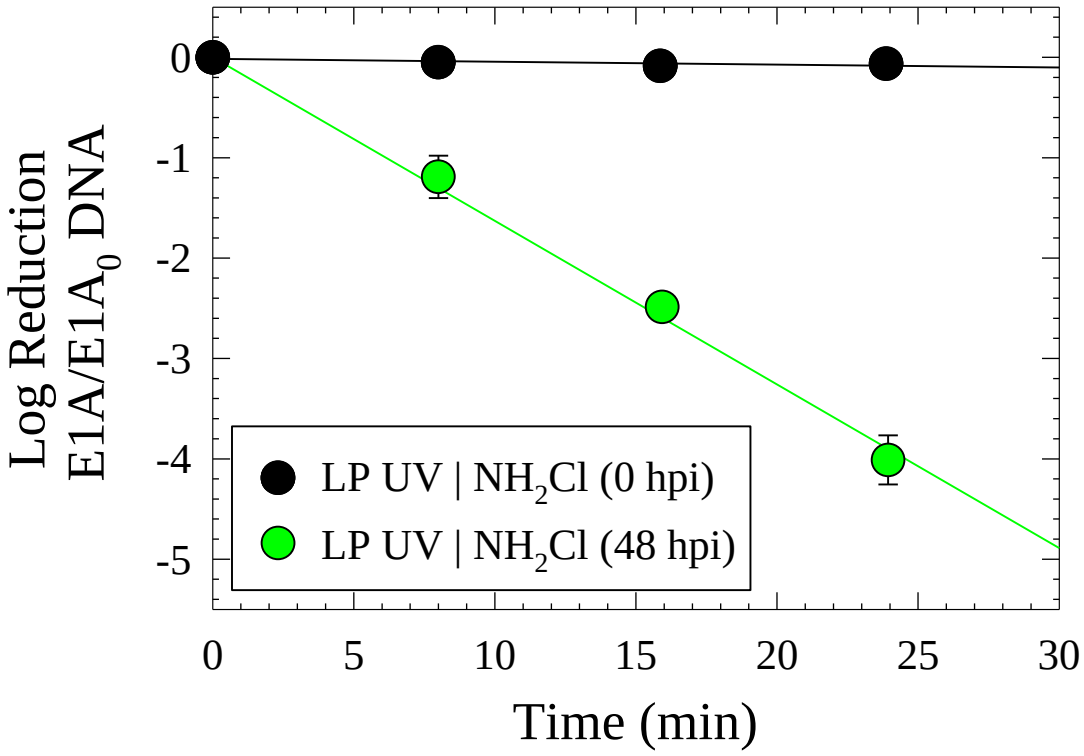

Figure 5.4. Relative expression level of E1A DNA (*E1A*/*E1A*$_0$) measured at 0 and 48 hpi (hours postinfection) normalized to the untreated sample after simultaneous exposure to low-pressure UV light and monochloramine (LP UV | NH_2Cl). Similar relative quantity of viral DNA was present at 0 hpi in all treated samples compared to the untreated control.

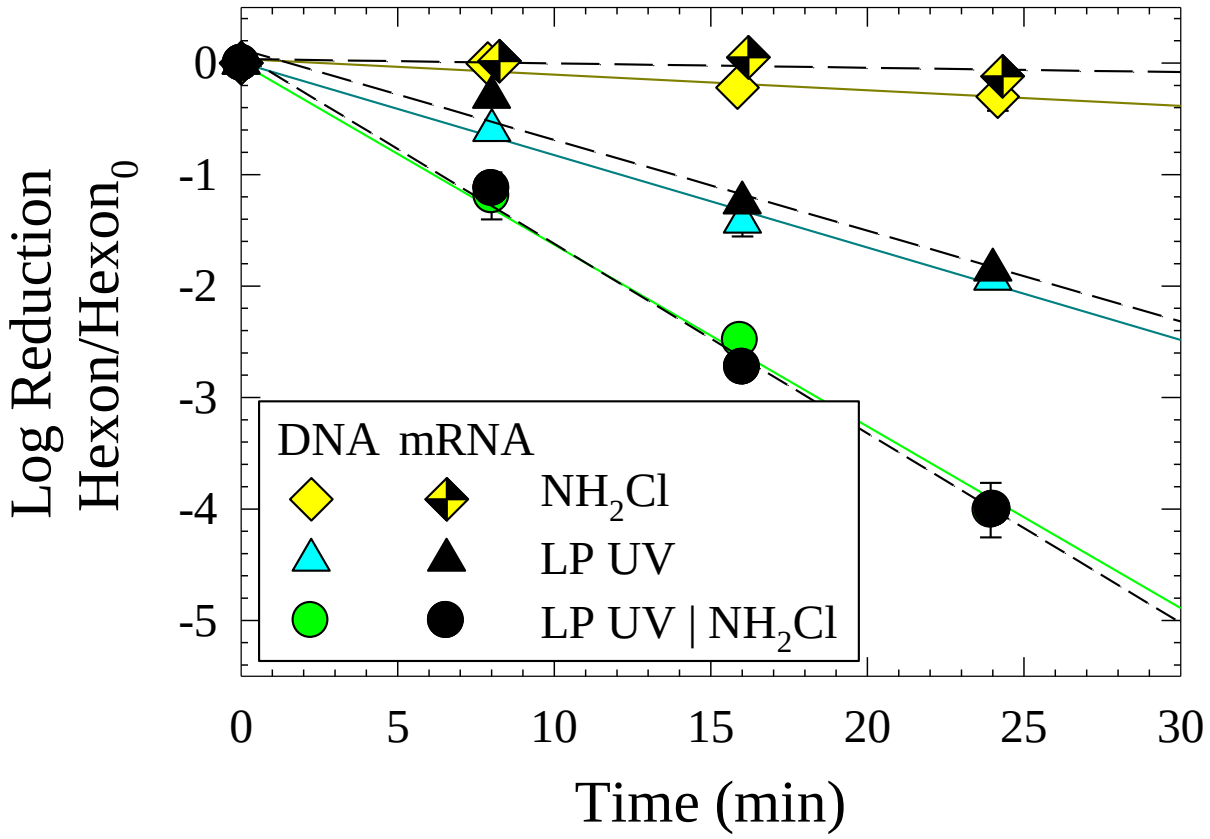

Figure 5.5. The relative expression level of Hexon mRNA synthesis (*Hexon/Hexon*$_0$) at 48 hpi (hours postinfection) normalized to the untreated sample is compared to the relative expression level of DNA replication at 48 hpi normalized to the untreated sample after exposure to monochloramine (NH_2Cl), low-pressure UV light (LP UV) or the simultaneous application of both disinfectants (LP UV | NH_2Cl). For all three disinfection conditions analyzed the linear regression of the relative decrease in mRNA synthesis and the reduction in DNA replication were not significantly different (ANCOVA, $P > 0.05$).

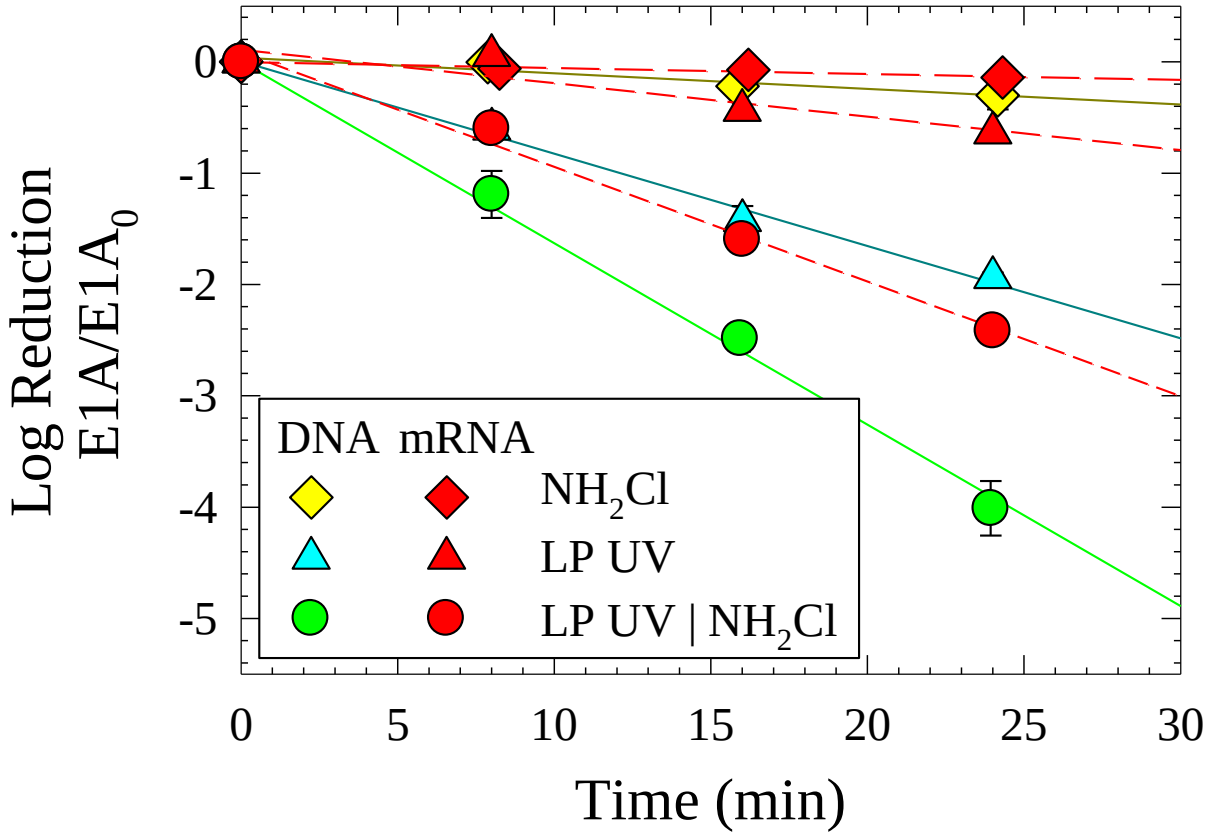

Figure 5.6. Relative expression level of E1A mRNA synthesis at 48 hpi (hours postinfection) normalized to the untreated sample (*E1A*/*E1A*$_0$ mRNA) is compared to the relative expression level of E1A DNA replication at 48 hpi normalized to the untreated sample (*E1A*/*E1A*$_0$ DNA) after exposure to monochloramine (NH_2Cl), low-pressure UV light (LP UV) or the simultaneous application of both disinfectants (LP UV | NH_2Cl). For LP UV and simultaneous LP UV | NH_2Cl the linear regression of the relative mRNA synthesis (*E1A*/*E1A*$_0$ mRNA) and the DNA replication (*E1A*/*E1A*$_0$ DNA) were significantly different (ANCOVA, $P < 0.05$).

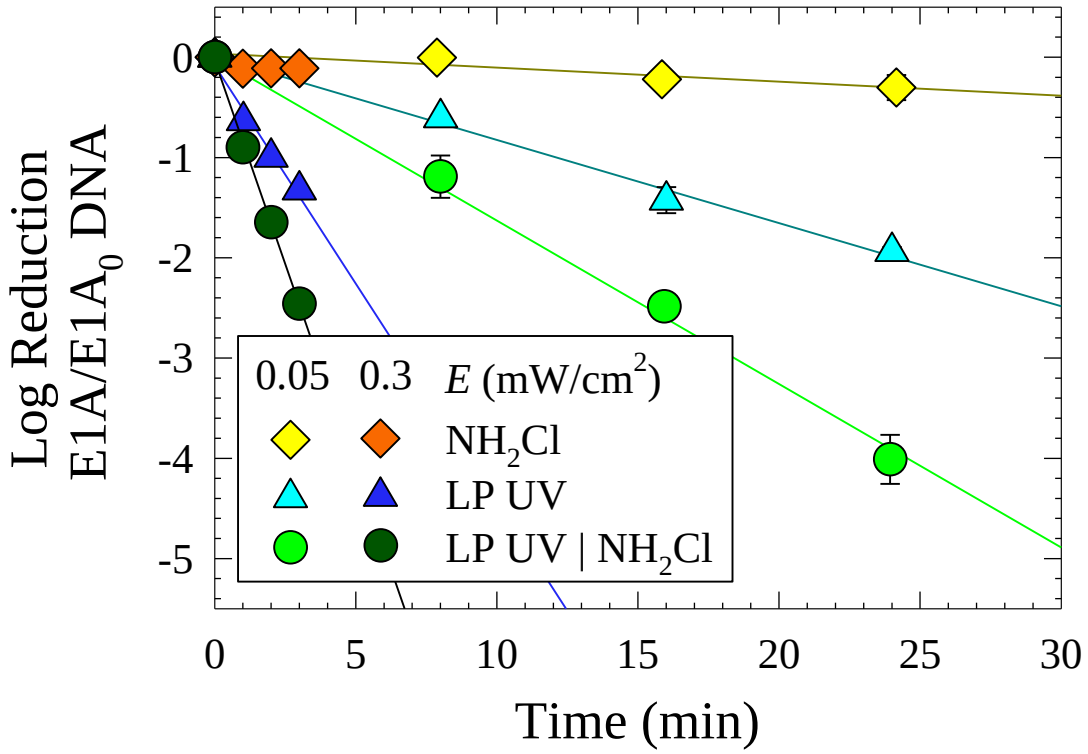

Figure 5.7. Relative expression level of E1A DNA replication at 48 hpi (hours postinfection) normalized to the untreated sample (*E1A*/*E1A*$_0$ DNA) after exposure to monochloramine (NH_2Cl), low-pressure UV light (LP UV) or the simultaneous application of both disinfectants (LP UV | NH_2Cl). The plot includes two sets of experiments in which the UV light irradiance (E) was increased from 0.05 to 0.3 mW/cm^2.

5.5 References

Ballester, N. A.; and Malley, J. P. Sequential disinfection of adenovirus type 2 with UV–chlorine–chloramine. *J. Am. Water Works Assoc*. **2004,** *96*(10): 97–103.

Baxter, C. S.; Hofmann, R.; Templeton, M. R.; Brown, M.; and Andrews, R. Inactivation of adenovirus 2, 5, and 41 in drinking water by UV light, free chlorine, and monochloramine. *J. Environ. Eng.* **2007**, *133*(1): 95–103.

Berk, A. J. Adenoviridae. In *Fields Virology*, 6th ed.; Knipe, D. M., Howley, P. M., Eds.; Lippincott Williams & Wilkins: Philadelphia, PA, **2013**; pp 1704– 1735.

Bolton, J. R.; Beck, S. E.; and Linden, K.G. Protocol for the determination of fluence (UV dose) using a low-pressure or low-pressure high-output UV lamp in bench-scale collimated beam ultraviolet experiments, *IUVA News*, **2015**. *17*(1): 11–16.

Crittenden, J. C.; Trussell, R. R.; Hand, D. W.; Howe, K. J.; Tchobanoglous, G., Disinfection. In MWH's Water Treatment: Principles and Design, Third Edition, John Wiley & Sons, Inc.: **2012**; pp 903-1032

Eischeid, A. C.; Meyer, J. N.; Linden, K. G. UV disinfection of adenoviruses: Molecular indications of DNA damage efficiency. *Appl. Environ. Microbiol.* **2009**, *75* (1), 23– 28, DOI: 10.1128/AEM.02199-08

Gall, A. M.; Shisler, J. L.; Marinas, B. J. Analysis of the viral replication cycle of adenovirus serotype 2 after inactivation by free chlorine. *Environ. Sci. Technol.* **2015**, *49* (7), 4584– 4590, DOI: 10.1021/acs.est.5b00301

Gall, A. M.; Shisler, J. L.; Mariñas B. J. Inactivation Kinetics and Replication Cycle Inhibition of Adenovirus by Monochloramine. *Environmental Science and Technology Letters*. 12 April **2016**, Vol.3 Issue 4, p185-189.

Greber, U. F.; Willetts, M.; Webster, P.; Helenius, A. Stepwise dismantling of adenovirus 2 during entry into cells. *Cell*. **1993**. 75(3):477-86.

Kim, K.; Katayama, H.; Kitajima, M.; Tohya Y.; Ohgaki, S. Development of a real-time RT-PCR assay combined with ethidium monoazide treatment for RNA viruses and its application to detect viral RNA after heat exposure. *Water Science & Technology.* **2011**, *63* (3), p. 502-507.

Linden, K. G.; Thurston, J.; Schaefer, R.; Malley, J. P. Enhanced UV inactivation of adenoviruses under polychromatic UV lamps. *Appl. Environ. Microbiol.* **2007**, *73* (23), 7571– 7574, DOI: 10.1128/AEM.01587-07

Malayeri, A. H.; Mohseni, M.; Cairns, B.; and Bolton, J. R. Fluence (UV Dose) Required to Achieve Incremental Log Inactivation of Bacteria, Protozoa, Viruses and Algae. *IUVA*, **2016**

Örmeci, B.; Ducoste, J. J.; Linden, K. G., UV disinfection of chlorinated water: impact on chlorine concentration and UV dose delivery. Journal of Water Supply: Research & Technology-AQUA. **2005**, Vol. 54 Issue 3, p189-199. 11p

Page, M. A.; Shisler, J. L.; Marinas, B. J. Mechanistic aspects of adenovirus serotype 2 inactivation with free chlorine. *Appl. Environ. Microbiol.* **2010**, *76* (9), 2946– 2954, DOI: 10.1128/AEM.02267-09

Patton, S.; Li, W.; Couch, K. D.; Mezyk, S. P.; Ishida, K. P.; and Liu, H. Impact of the Ultraviolet Photolysis of Monochloramine on 1,4-Dioxane Removal: New Insights into Potable Water Reuse *Environ. Sci. Technol. Lett*. **2017**, 4, 26−30

Rattanakul, S.; Oguma, K.; and Takizaw, S. Sequential and Simultaneous Applications of UV and Chlorine for Adenovirus Inactivation**.** *Food and Environmental Virology*. 10 September **2015**, Vol. 7 Issue 3, p295-304.

Reddy, V. S.; and Nemerow, G. R. Structures and organization of adenovirus cement proteins provide insights into the role of capsid maturation in virus entry and infection. *PNAS*. **2014**. 111(32):11715-20.

Rodriguez, R. A.; Bounty, S.; Linden, K. G. Long-range quantitative PCR for determining inactivation of adenovirus 2 by ultraviolet light. *J. Appl. Microbiol.* **2013**, *114* (6), 1854– 65, DOI: 10.1111/jam.12169

Shin, G. A., and Lee, J. K., Inactivation of human adenovirus by sequential disinfection with an alternative ultraviolet technology and monochloramine, *Can. J. Microbiol*. **2010**, 56: 606–609.

Shin, G. A.; Lee, J. K.; Linden, K. G. Enhanced effectiveness of medium-pressure ultraviolet lamps on human adenovirus 2 and its possible mechanism. *Water Sci. Technol.* **2009**, *60* (4), 851– 857, DOI: 10.2166/wst.2009.414

Sirikanchana, K.; Shisler, J. L.; Marinas, B. J., Effect of exposure to UV-C irradiation and monochloramine on adenovirus serotype 2 early protein expression and DNA replication. *Appl. Environ. Microbiol.* **2008,** *74*, (12), 3774-3782.

Rattanakul, S., and Oguma, K. Analysis of Hydroxyl Radicals and Inactivation Mechanisms of Bacteriophage MS2 in Response to a Simultaneous Application of UV and Chlorine. *Environ. Sci. Technol.* **2017**, 51, 455−462.

USEPA (U.S. Environmental Protection Agency). *Ultraviolet Disinfection Guidance Manual for the Final Long Term 2 Enhanced Surface Water Treatment Rule*; Washington, DC, **2006**.

USEPA, Drinking Water Requirements for States and Public Water Systems, Chloramines in Drinking Water, **2016**.

Wiethoff, C. M.; Wodrich, H.; Gerace, L.; Nemerow, G. R. Adenovirus protein VI mediates membrane disruption following capsid disassembly. *J Virol*. **2005**. *79*(4):1992-2000.

CHAPTER 6: CONCLUSIONS AND FUTURE WORK

6.1 Summary of Research

The overall goal of this research work was to advance the knowledge on the mechanisms by which UV light renders human adenovirus non-infectious. Additionally, the combination of different UV wavelengths of polychromatic irradiation, as well as the application of monochromatic UV light and monochloramine were evaluated in search of synergistic interactions. The approach implemented was to analyze inhibitions at different steps in the adenovirus replication cycle after exposure to the various treatment scenarios investigated to elucidate possible viral targets responsible for the reduction in infectivity. The main outcomes of this research work are summarized below:

- The adenovirus action spectrum obtained from this research work using bandpass filters to isolate narrow wavelength ranges emitted by a MP UV light is consistent with the spectrum available in the literature obtained using a UV laser emitter set at similar wavelengths (Beck et al., 2014). This replication of results served to confirm the published data and be the basis for the molecular work on the disruption at different stages of the adenovirus replication cycle.

- UV irradiation at wavelengths below 240 nm was effective to inactivate human adenovirus type 2 (HAdV-2); fluences in the range of 10-40 mJ/cm^2 provided a 4-log reduction in viral infectivity. UV irradiation at wavelengths in the 240-300 nm range showed different inactivation kinetics for HAdV-2. The slowest kinetics were observed at the wavelengths of 248, 289 and 297 nm.

- UV irradiation emitted at 3 specific wavelength ranges analyzed (224, 254 and 280 nm) inflicted different levels of damage to the adenovirus genome as indicated by qPCR amplification of a 1.1-kb fragment. UV light with peak emission at 280 nm was the most effective at inflicting genome damage among the three wavelength ranges analyzed.

- None of the 3 wavelengths ranges analyzed inhibited the ability of adenovirus to bind to the host cell, which suggested that inactivation by polychromatic UV light disrupts a replication cycle event downstream of attachment.

- UV_{224} disrupted early E1A gene synthesis to a level consistent with the decrease in viral infectivity and viral DNA replication. This inhibition is possibly induced by protein modifications of the adenovirus capsid since minor genome damage was inflicted by UV_{224} at the fluences applied to reach a 4-log HAdV-2 inactivation.

- UV_{254} reduced early E1A mRNA synthesis but not to the same level as the decrease in viral infectivity and viral DNA replication. It is possible that UV_{254} predominantly inhibited early gene transcription by UV-induced mutations to the template E1A gene, which may differ from mutations in other genome regions. For UV_{254} genome replication seemed to be the limiting step that ultimately produced the reduction in infectivity assessed by plaque assay.

- UV_{280} disrupted early mRNA synthesis to a greater extent than UV_{254} and it was the most effective among the three wavelength ranges analyzed at blocking qPCR amplification of the amplicons assessed. This aspect suggests that the faster HAdV-2 inactivation by UV_{280} (compared to UV_{254}) is likely dominated by a more effective induction of mutations on the viral genome (perhaps to DNA regions associated with core proteins), rather than modifications to structural proteins.

- The sequential application of UV light at different wavelength ranges did not show synergistic interactions in the adenovirus inactivation. These results imply that the virus inactivation by MP

UV light (200-300 nm) is the addition of the individual effects from all the wavelengths in the range covered during a given exposure time.

- The simultaneous application of monochromatic LP UV and monochloramine produced explicit synergism determined by comparison with the added contributions of both disinfectants acting independently.

- The simultaneous application of monochromatic LP UV light and monochloramine did not cause greater HAdV-2 genome damage compared to that inflicted by LP UV light acting independently. Monochloramine alone had minimal impact on the adenovirus genome integrity at the concentrations and exposure times assessed.

- The simultaneous application of LP UV light and monochloramine did not inhibit the ability of the virus to attach to the host cell. Indication of a mutagenized viral capsid that did not inhibit the ability of adenovirus to bind to the host but possibly disrupted the well-timed progression of subsequent steps was detected.

- The simultaneous application of LP UV light and monochloramine reduced early E1A mRNA synthesis but not to a level consistent with the reduction in viral infectivity. The observed decrease is possibly result from a combination of genome damage induced by the LP UV light, and less number of viruses reaching and/or translocating their genome into the nucleus due to the disruption of capsid integrity.

- The simultaneous application of LP UV light and monochloramine inhibited DNA replication and late gene hexon mRNA transcription to the same extent as the reduction in viral infectivity.

6.2 Implications

The analysis of the adenovirus replication cycle disruption after exposure to different wavelength ranges of polychromatic UV light provided important information to better understand the different mechanisms of inactivation taking place during water disinfection using MP UV light. Some of the molecular techniques utilized in this work allowed a relatively fast determination of the infectivity reduction levels attained by the different treatment approaches investigated. For all treatment approaches, results for genome replication experiments by 48 hpi consistently matched (ANCOVA, $P > 0.05$) the reduction in virus infectivity assessed by plaque assay; which requires about 10 days to be completed. This is a convenient aspect that can help to assess the effectiveness of water disinfection approaches more rapidly if adenovirus is used as the target pathogen for monitoring virus inactivation by UV light.

From the three wavelength ranges analyzed UV_{254} showed the slowest kinetics being genome damage the predominant inactivation mechanism involved. UV_{224} showed the greatest disruption of the viral capsid integrity suggesting that its enhanced effectiveness compared to UV_{254} is possibly dominated by conformational changes of the structural capsid proteins. UV_{280} displayed the greatest inhibition of the viral genome amplification by qPCR of the 1.1-kb region evaluated, suggesting a more effective induction of mutations on the viral genome (perhaps to DNA regions associated with core proteins), rather than modifications to structural proteins.

The observation that sequential application of different wavelength ranges of UV light did not show synergism suggests that the inactivation obtained by the full spectrum of a polychromatic MP UV light is likely the result of the additive independent contributions of the absorbed photons from all the wavelengths over the range covered during a given exposure time. The simultaneous application of monochloramine with an initial concentration of 4 mg/L as Cl_2 and monochromatic LP UV light showed promising results for potential application in water treatment processes for control of HAdV-2. The typical sequence in which these two disinfectants are implemented is UV disinfection followed by

monochloramine to provide residual disinfectant in the distribution line. The data obtained in this work showed that residual monochloramine decreases at a faster rate due to exposure to UV light; however the initial concentration of monochloramine and the exposure time to UV light can be adapted to provide residual monochloramine concentrations within the range usually provided in typical water treatment scenarios (2-4 mg/L). The presence of monochloramine made LP UV light as effective as MP UV light was to inactivate HAdV-2. This aspect can help water treatment facilities comply on the required viral log-reduction when using LP UV light as water disinfectant, and develop cost-effective approaches to control HAdV. A complete characterization using natural water matrices with varying environmental conditions, as well as the assessment of byproducts formed and their toxicological analysis is needed to better understand the practical implications of the synergistic interaction observed.

The fact that none of the treatment scenarios investigated in this research work showed disruption of viral association with the host cell indicates that detection methods should target modifications on structural components that are not involved in host cell attachment. The results from capsid integrity assessed by the EMA assay for UV_{224} and the simultaneous application of LP UV light with monochloramine, provided indication that mutations of the viral capsid might be affecting the timely progression of replication cycle events downstream of attachment.

It is important to note that the results presented in this work using HAdV-2 might be different for other serotypes. Different virus serotypes can show characteristics that could impact their sensitivity to the same disinfectant. There is need to develop comparable analyses with serotypes from other adenovirus species to elucidate the differences and similarities on the inactivation mechanisms. Viruses are classified in families according to several characteristics of the viral particle; capsid format, genome type, presence and type of envelope, overall size of the virion, area of the host cell in which the virus replicates, or the type of disease they cause. The species of adenoviruses are classified according to their biological properties; serology, hemagglutination, oncogenicity in rodents, transformation of cultured cells, and

genomic organization (Berk, 2013). Although all human adenoviruses are non-enveloped dsDNA viruses that have an icosahedral capsid, specifics about the molecular interactions during the replication cycle for different species are unknown (Cupelli and Stehle, 2011). The results from this work can help to develop hypothesis to be assessed regarding the inactivation mechanisms of other adenoviruses for which little information is available; like serotype 52 of species G, or HAdV-40 and HAdV-41 of species F. A complete understanding of how different viruses are inactivated will allow the development of more effective and efficient water disinfection strategies that incorporate UV technologies, as well as rapid methods for detection and monitoring of pathogens in drinking water.

6.3 Future Work Recommendations

The results from this research work indicate that for all of the different treatment approaches evaluated to inactivate HAdV-2, inhibition of a replication cycle step post-binding and prior to early gene mRNA transcription takes place. However, with exception of UV_{224} and monochloramine applied independently, different inhibition levels of early gene synthesis were observed that did not match the reduction in viral infectivity and viral genome replication. UV_{224} was the treatment approach with the lowest impact on genome integrity and therefore it is likely that the reduction in early gene transcription is not driven by genome damage. In contrast, the rest of the treatment approaches evaluated (UV_{254}, UV_{280}, LP UV, and simultaneous LP UV | NH_2Cl), showed different impacts on the viral genome integrity which likely is influencing the inhibition levels of early gene transcription detected. This research can be complemented with assessment of integrity of other genome regions that were not analyzed in this work; such as the whole region that encodes the complete E1A gene, the genome region encoding the major late promoter, and also the DNA polymerase region.

In addition, different key steps in the virus replication cycle between virus attachment and the viral genome entry into the nucleus for subsequent E1A mRNA transcription can be evaluated in continuation of this research project. Once the fiber binds to CAR it bends and the RGD-motif of penton base interacts

with αv integrin; this interaction triggers the virus internalization into an endosome through receptor-mediated endocytosis. Once in the endosome, penton base, fiber, and peripentonal hexons are removed to allow the release of protein VI from the inner surface of the virus capsid. The virus disassembly starts to occur and eventually protein VI is released, with other vertex proteins, disrupting the early endosome. Protein VI lyses the endosome and partially uncoated virions are transported along microtubules to reach the nuclear pore complex (NPC). Association of virions with proteins at the NPC facilitates further uncoating of the virion and internalize the genome into the nucleus.

One possibility is that after UV-treated adenovirus binds to the CAR receptor the bending of the fiber does not take place and interaction of the penton base and αv integrin is inhibited. Kremer and Nemerow (2015), indicated that in epithelial cells, such as A549 cells, CAR facilitates attachment but not entry; integrin ligation causes partial capsid disassembly that initiates at the vertex regions. Perhaps polychromatic UV irradiation (particularly UV_{224} and possibly UV_{280}) or the simultaneous application of LP UV and monochloramine causes protein mutations that affect the fiber flexibility and/or the penton base-integrin interaction. A previous study has shown that modifying the length of the adenoviral fiber shaft reduces virus infectivity (Wu et al., 2004). UV irradiation might be causing conformational changes that modify the capability of the fiber to bend and facilitate fiber-receptor interactions. The analysis of interaction between αv integrin and penton base in treated and untreated viruses would provide insight on whether these different treatment approaches are affecting this step in the replication cycle.

A subsequent step in the adenovirus infection cycle is the release of protein VI to lyse the endosome. Kremer and Nemerow (2015), showed that a single point mutation in the helical domain of protein VI significantly attenuates cell infection. Fluorescence microscopy has been used to elucidate how protein VI damages membranes by visualizing changes in lipid vesicles after protein VI binding. This has helped to develop a model in which protein VI binds to membranes and fragments the lipid bilayer into small highly curved structures (Kremer and Nemerow, 2015). The study by Maier et al., (2010) reported that

protein VI does not seem to form pores in the endosome, instead there is a whole reorganization of the lipid bilayer as a result of a positive membrane curvature. The synthesis of protein VI could be done following the protocols described by Maier et al., (2010). Next, the effect of the different treatment approaches evaluated in the efficiency of membrane disruption by protein VI could be assessed by a membrane permeabilization assay using fluorescence microscopy to measure the percentage of cells capturing propidium iodide (a fluorescent membrane impermeable nuclear stain) after protein VI addition. Then, the effect of increasing UV fluences or exposure to simultaneous LP UV | NH_2Cl treatment on membrane permeabilization by protein VI could be compared to viral infectivity. Another approach is the use of saporin, which is a membrane impermeable toxin whose translocation into the cytosol is facilitated by co-internalization with the virus in endosomes (Maier et al., 2010). Infected cells with treated and untreated viruses can be exposed to saporin. If the toxin reaches the cytosol via translocation mediated by adenovirus protein VI endosome disruption, the toxin will inhibit protein synthesis and ultimately result in cell death which can be quantified via yellow tetrazolium MTT (3-(4, 5-dimethylthiazolyl-2)-2, 5-diphenyltetrazolium bromide) assay. This assay would provide insight on whether certain wavelengths of UV irradiation or the combined application of LP UV and monochloramine inhibits protein VI release, disrupting endosome lysis, and subsequent docking of the virion onto the nuclear pore complex (NPC).

Finally, at the NPC level, the interaction of protein VII with the nuclear import receptors is a fundamental step for genome internalization (Kremer and Nemerow, 2015). To assess the effect of the different treatment approaches on this step, A549 cells could be infected with treated and untreated virus particles and analyzed for detection of protein VII with rabbit anti-pVII antibody by immunofluorescence; antibody staining of protein VII can only be done after nuclear import (Cassany et al., 2015). Protein VII should be detected in the nucleus of untreated viruses and any decrease on the levels of protein VII detection in treated viruses would indicate disruption of nuclear import of their genome.

Sequencing periodically the virus used is recommended to detect changes on the genome sequence throughout the duration of the study, and be able to compare to the available NCBI GenBank sequence. For HAdV-5, the mutation rate per cell infection cycle is 1.3×10^{-7} mutations per base per cell infection cycle, which is lower comparted to RNA viruses given the high replication fidelity of DNA viruses (Risso-Ballester et al., 2016). New HAdV types have been reported as a result of homologous recombination within the same subgenus acquiring different pathogenicities, and the recombination mechanisms remain unknown (Ghebremedhin, 2014).

Another important aspect to be addressed in future work is related to the UV technologies used on this research effort. The fact that LP UV and MP UV light lamps contain mercury denotes issues regarding proper disposal of the lamps at the end of their lifespan. In addition, specialized training to properly maintain and handle the lamps is required. Light-emitting diodes (LEDs) provide UV irradiation at specific narrow wavelength ranges, similar to those displayed by the bandpass filters used in this work, and present several advantages over UV lamps: do not contain mercury, have a rapid light up time, are found in compact sizes, and offer reduced heat production (Nelson et al., 2013). Mercury-vapor lamps require some time to stabilize their irradiation after they light up, are much larger in size and, a significant amount of their energy is lost in heat production (Nelson et al., 2013).

By using UV-LEDs, irradiation at specific wavelengths can be applied to have an adjusted configuration depending on the susceptibility of the target microorganism to UV light inactivation. Aoyagi et al., (2011) evaluated the inactivation efficacy of UV-LEDs operating at 280 and 255 nm using three different bacteriophages as surrogate viruses. The study concluded that the power production of the 280 nm UV-LEDs was simpler to achieve than that at 255 nm; making it a more suitable alternative for disinfection.

Another important advantage of this technology is the flexibility that allows for reactor design. The configurations that are possible with the mercury-vapor lamps are limited. UV-LEDs can facilitate design

configurations that provide optimal performance with a highly effective water treatment process. Water depth, reactor shape, and adequate sample mix, are some important factors to ensure that the irradiation from the UV-LEDs is reaching the target microorganisms in the water. These advances can be adapted for multiple contextualized applications; from the optimization of industrial water treatment processes to point-of-use approaches implemented in rural communities in developing countries.

The current disadvantages of UV-LEDs are their relatively high cost, low efficiency, and low power output requiring several of them to reach comparable UV intensities to those emitted by a mercury-vapor lamp. Nevertheless, UV-LEDs are an innovative technology in constant improvement and several studies (Chatterley and Linden, 2010; Ibrahim et al., 2014; Liu et al., 2014) project that the improvements on this technology will decrease their cost and increase their efficiency and power output making them a viable alternative to LP UV light lamps. Once these expectations are met, there is high potential for implementation of UV-LEDs, particularly in water treatment approaches at the household level.

Understanding how markets in developed and developing communities operate, UV-LED technologies can be adapted for different contexts and contribute to the economic stability of the implementation region by the empowerment of local entrepreneurs. A household level UV-LED approach could provide a safe type of technology, avoiding the risk of mercury exposure by handling fragile lamps, and would offer a sustainable alternative to traditional disinfection techniques. The future research to understand the fundamentals of this technology will have a wide range of implementation approaches that will allow a better control of important water quality parameters.

6.4 References

Aoyagi, Y.; Takeuchi, M.; Yoshida, K.; Kurouchi, M.; Yasui, N.; Kamiko, N.; Araki, T.; and Nanishi, Y. Inactivation of bacterial viruses in water using deep ultraviolet semiconductor light-emitting diode. *J. Environ. Eng*. (**2011**), 137: 1215-1218.

Beck, S. E.; Rodriguez, R. A.; Linden, K. G.; Hargy, T. M.; Larason, T. C.; Wright, H. B. Wavelength dependent UV inactivation and DNA damage of adenovirus as measured by cell culture infectivity and long range quantitative PCR. *Environ. Sci. Technol.* **2014**, *48* (1), 591– 598, DOI: 10.1021/es403850b

Berk, A. J. Adenoviridae. In *Fields Virology*, 6th ed.; Knipe, D. M., Howley, P. M., Eds.; Lippincott Williams & Wilkins: Philadelphia, PA, **2013**; pp 1704– 1735.

Cassany, A.; Ragues, J.; Guan, T.; Bégu, D.; Wodrich, H.; Kann, M.; Gerace, L. Nuclear Import of Adenovirus DNA Involves Direct Interaction of Hexon with an N-Terminal Domain of the Nucleoporin Nup214. *Journal of Virology*. **2015**.

Chatterley, C., and Linden, K. G. Demonstration and evaluation of germicidal UV-LEDs for point-of-use water disinfection. *J. Water and Health*. **2010**, 8(3): 479-486.

Cupelli, K.; T. Stehle, T. Viral attachment strategies: the many faces of adenoviruses. *Curr. Opin. Virol.*, **2011**, 1(2): pp. 84-91.

Ghebremedhin, B. Human adenovirus: Viral pathogen with increasing importance. *European Journal of Microbiology & Immunology*. 2014; 4(1):26-33. doi:10.1556/EuJMI.4.2014.1.2.

Ibrahim, M. A. S.; MacAdam, J.; Autin, O.; Jefferson, B. Evaluating the impact of LED bulb development on the economic viability of ultraviolet technology for disinfection. *Environ. Technol*. **2014,** 35:4. 400-406.

Kremer, E. J.; Nemerow, G. R. Adenovirus Tales: From the Cell Surface to the Nuclear Pore Complex. *PLoS Pathogens*, **2015**. *11*(6), e1004821.

Liu, G. Y.; Roser, D.; Corkish, R.; Ashbolt, N.; Jagals, P.; Stuetz, R. Photovoltaic powered ultraviolet and visible light emitting diodes for sustainable point-of-use disinfection of drinking waters. *Sci. Total Environ*. **2014**, 493: 185-196.

Maier, O.; Galan, D. L.; Wodrich, H.; Wiethoff, C. M. An N-terminal domain of adenovirus protein VI fragments membranes by inducing positive membrane curvature. *Virology*, **2010**. 402, 11-19.

Mathias, P.; Galleno, M.; and Nemerow, G. R. Interactions of soluble recombinant integrin αvβ5 with human adenoviruses. *J. Virol.* **1998**, 72**:**8669-8675

Nelson, K. Y.; McMartin, D. W.; Yost, C. K.; Runtz, K. J.; Ono, T. Point-of-use water disinfection using UV light-emitting diodes to reduce bacterial contamination. *Environ. Sci. Pollut. Res.*, **2013**.

Risso-Ballester, J.; Cuevas, J. M.; Sanjuán, R. Genome-Wide Estimation of the Spontaneous Mutation Rate of Human Adenovirus 5 by High-Fidelity Deep Sequencing. *PLoS Pathog*. **2016**, 12(11): e1006013. https://doi.org/10.1371/journal.ppat.1006013

Wu, E.; Pache, L.; Von Seggern, D. J.; Mullen, T.-M.; Mikyas, Y.; Stewart, P. L.; & Nemerow, G. R. Flexibility of the Adenovirus Fiber Is Required for Efficient Receptor Interaction. *Journal of Virology*, **2004**. *77*(13), 7225–7235. http://doi.org/10.1128/JVI.77.13.7225-7235.2003

APPENDIX A: INACTIVATION OF COXSACKIEVIRUS B5 AND MURINE NOROVIRUS 1 FROM EXPOSURE TO POLYCHROMATIC ULTRAVIOLET LIGHT

A.1 Introduction

UV light disinfection has been shown effective to inactivate different types of bacteria and viruses in water treatment processes. Nonetheless, microorganisms such as human adenovirus have emerged as pathogens of concern due to their resistance to UV light disinfection (Linden et al., 2009). Enteroviruses and caliciviruses are included in the U.S. Environmental Protection Agency Contaminant Candidate List 4 as microorganisms for potential future regulation (USEPA, 2016). Therefore, coxsackievirus (enterovirus) and norovirus (calicivirus) are of relevance to evaluate the effectiveness of alternative disinfection techniques, such as UV light, as a barrier in drinking water treatment systems.

Coxsackievirus, a human enterovirus in the family *Picornaviridae*, is a waterborne pathogen of concern due to its low susceptibility to chlorination. Coxsackievirus is a non-enveloped single stranded positive-sense RNA virus, about 30 nm in diameter, with an icosahedral capsid surrounding the naked RNA genome. Children are particularly susceptible to coxsackievirus infections during outbreak episodes (Chen et al., 2013). The inactivation of coxsackievirus B3, B4 and B5 by monochromatic low-pressure (LP) UV light has been assessed in a few studies showing that a fluence of about 30-36 mJ/cm^2 provided a 4-log reduction in coxsackievirus infectivity (Malayeri et al., 2016).

Human norovirus is a waterborne pathogen in the *Caliciviridae* family typically transmitted through the fecal-oral route that causes gastrointestinal illness. Norovirus is a pathogen of concern due to its low infectious dose, resistance to a variety of environmental conditions, and the absence of long-term immunity in humans (Young, 2010). Noroviruses are about 30 nm in diameter, have icosahedral shape, and are non-enveloped single stranded positive-sense RNA viruses that cause acute gastroenteritis (Bae and Schawb, 2008).

There is a lack of cultivation methods for human norovirus, thus research on this topic has been limited. Previous studies have used feline calicivirus, canine calicivirus, or poliovirus as surrogates to evaluate the inactivation of noroviruses; however, the results haven't been applicable to human norovirus due to differences in survival characteristics. Recent studies on the biology and pathogenesis of murine norovirus (MNV) suggest that it is an appropriate surrogate for studying human norovirus' resistance to disinfectants (Wobus et al., 2006; Thurston-Enriquez et al., 2003; Cannon et al., 2006; Bae and Schwab, 2008; Park et al., 2011).

A few studies have addressed the UV light inactivation for murine norovirus. Lee et al., (2008) assessed the inactivation kinetics of MNV by LP UV light and determined that a fluence of ~26 mJ/cm^2 was required for a 4-log$_{10}$ inactivation of MNV. The USEPA reported in 2005 that the UV inactivation of murine norovirus exhibited 2-log$_{10}$ and 4-log$_{10}$ reductions with fluences of 15 mJ/cm^2 and 30 mJ/cm^2, respectively. A recent study showed that the UV$_{254}$ fluence required to achieve 4-log$_{10}$ inactivation of MNV was 29 mJ/cm^2 (Park et al., 2011).

Although some studies have evaluated the inactivation of coxsackievirus and murine norovirus by LP UV light, the inactivation of these viruses by MP UV light has not been well characterized and therefore a gap in the knowledge exists regarding control of these viruses of concern. In this work coxsackievirus B5 (CVB5) and murine norovirus 1 (MNV-1) were used to elucidate their inactivation kinetics obtained from exposure to different wavelength ranges emitted by MP UV light within the 200-300 nm range.

A.2 Materials and methods

A.2.1 UV Disinfection Experiments

UV disinfection experiments were performed with a standard collimated beam apparatus equipped with a polychromatic MP UV lamp (A300014, Calgon Carbon Co., Pittsburgh, PA). Bandpass filters with a

bandwidth of about 10 nm at half of the maximum peak transmittance at 218, 224, 228, 232, 239, 248, 254, 260, 265, 270, 280, 289, and 297 nm (Andover Corporation, Salem, NH) were used to isolate specific regions within the MP UV radiation and determine the germicidal effect of those band ranges. The spectral irradiance was used as the weighting function to calculate the average germicidal irradiance in the water sample applying different correction factors as indicated in the protocol for a bench-scale UV apparatus using a polychromatic UV source by Bolton and Linden (2003). The light intensity distribution across the irradiated water surface was measured with a 1400A radiometer (International Light, Peabody, Massachusetts) and a SEL 240 detector.

During the experiment, a recirculating water jacketed reactor with 15 mL of a suspension of 1.0×10^5 to 2.0×10^6 plaque forming units (PFU) per mL of CVB5 or MNV-1 was exposed to UV light at varying doses. Continuous mixing conditions were achieved with a magnetic stir bar and plate. The irradiation was constant throughout the experiment; the applied fluence was controlled with the exposure time. The survival ratios for each virus were assessed by infectivity assay immediately after exposure to UV light.

A.2.2 Virus Propagation and Viability Assessment

Coxsackievirus

The cell line used for coxsackievirus propagation and viability assessment were buffalo green monkey kidney (BGMK) cells obtained from Diagnostic Hybrids (53-0600, Quidel, Athens, OH, USA). Upon cell arrival, 3 mL of the culture was added to 7 mL of pre-warmed cell media in a 75 cm^2 tissue-culture flask. Cell media consisted of a 50/50 mixture of MEM (with Hank's salts and L-glutamine, without sodium bicarbonate) and Leibovitz's L-15 (with L-glutamine) plus 0.75 g sodium bicarbonate per liter, along with 10% fetal bovine serum (FBS), 1% Penicillin/Streptomycin antibiotics, and 0.1% amphotericin B. The cell suspension was incubated at 37 ^oC. Cell confluence was checked every day using an inverted microscope, and when ~80-90% confluence was reached cells were used for virus propagation or harvested to prepare T-25 flasks to perform viability assessment by plaque assay

Coxsackievirus B5 (CVB5) Faulkner (VR-185) was obtained from the American Type Culture Collection (ATCC, Manassas, VA). Cell culture flasks were prepared 3 to 6 days before viral inoculation. On the day of inoculation, growth media was aspirated before addition of viruses and replaced with maintenance medium (cell media with 2 % FBS). The inoculated cell flasks were incubated at 37 °C until cytopathic effect was observed. Viral release was induced by three freeze-thaw cycles. The suspension containing the lysed cells was centrifuged at 2000 rpm for 15 min and the supernatant was removed and passed through a 0.22 µm microfilter to remove large cellular debris. Concentration and purification of the virus was done through several washes with 1mM carbonate buffer solution (CBS) using a 300 kDa ultrafiltration membrane in an Amicon stirred cell. The concentrated virus stock was aliquoted and stored at -80 °C until used for disinfection experiments. Virus titer was determined by plaque assay using a nutrient mixture and soft agar overlay on BGMK cell monolayers. Plaque formation was observed and quantified at 3 days postinfection. The CVB5 stock concentration was approximately 10^8 PFU per mL.

CVB5 viability was assessed by a soft agar overlay plaque assay using BGMK cell monolayers. Three to six days prior to plaque assay, BGMK cells were passed to 25 cm^2 tissue culture flasks and incubated at 37 °C until a monolayer with ~95-100% confluence was achieved. On the day of the plaque assay, the old cell media was removed and replaced with 1 mL of dilution broth (cell media excluding FBS). Virus suspensions were serially diluted in dilution broth. Next, 0.8 mL of virus suspension was inoculated onto the cell monolayers. The inoculated flasks were incubated at 37 °C and rocked at 15 min intervals for 80 min to distribute the suspension evenly over the cell monolayer. After 80 min, 9-mL overlay medium was added to the flask and blended with previously added virus suspension. The overlay medium consisted of 83 mL 2X MEM, 3 mL FBS, 2 mL magnesium chloride, 1 mL penicillin/streptomycin, 0.75 mL neutral red, 0.2 mL amphotericin B, and 6 ml of 7.5% (w/v) sodium bicarbonate. The nutrient mixture was combined with 100 mL of Milli-Q water containing 3 g of agar which had been previously autoclaved. The agar was then allowed to solidify in the dark. Flasks were incubated, upside-down, at 37

°C and plaque formation was observed 2-3 days postinfection. Flasks with 15-200 plaques were used for calculation of virus concentration.

Murine Norovirus

Murine Norovirus 1 (MNV-1) was provided by Dr. Herbert Virgin from the Washington University School of Medicine in St Louis, MO. MNV-1 was cultivated using RAW 264.7 cells, a macrophage-like, Abelson leukemia virus transformed cell line derived from BALB/c mice. These cells were obtained from the American Type Culture Collection (ATCC; cat. no. TIB-71; lot no. 58228175). RAW 264.7 cells were suspended in culture medium, dispensed into 75 cm^2 culture flasks, and incubated at 37 ºC in a humidified 5% CO_2 incubator. Cell media consisted of Dulbecco's modified Eagle's medium (DMEM) containing 10% fetal bovine serum (FBS), 100 units of penicillin/mL, 100 μg/mL streptomycin, 10 mM HEPES (N-2 hydroxyethylpiperazine- N9-2-ethanesulfonic acid), and 2 mM L-glutamine. All the cellular media was equilibrated for 30 min in the CO_2 incubator before use.

Cells were sub-cultured every 2-3 days by gently dislodging them from the flask surface with a cell scraper in 5 ml of culture medium. Cell suspensions were collected and centrifuged at 4000 rpm for 5 min. The supernatant was removed and the cell pellet was re-suspended in fresh equilibrated media (10% FBS). With the cell suspension new T-75 culture flasks were prepared for subsequent cell culture, and/or T-25 flasks were prepared to be used for virus viability assessment.

MNV-1 was inoculated on an 80-90% confluent RAW 264.7 cell monolayer for 2 to 3 days in a humidified 5% CO_2 incubator. After this time, cells were subjected to three freeze-thaw cycles to induce viral release and then centrifuged at 3,000 rpm for 20 min. Concentration and purification of the virus was done through several washes with 1mM carbonate buffer solution (CBS) using a 300 kDa ultrafiltration membrane in an Amicon stirred cell. The concentrated virus stock was aliquoted and stored at -80 °C.

To assess the viability of MNV-1, RAW 264.7 cells were dispensed in 25 cm^2 flasks at a density of 2 x 10^6 cells per flask and grown to 90% confluence in 3 mL of 10% FBS culture medium. The cell monolayer was inoculated with 0.5 mL of 10-fold serial dilutions of the virus prepared using culture medium. The inoculated cell flasks were incubated for 2 hours at 37 ºC in the presence of 5% CO_2. After this time, the inocula was removed and 3 mL of a solution containing 2 parts of culture medium and one part of 1.5% Sea Plaque agarose was added and allowed to solidify. The flasks were incubated for 2-3 days at 37 ºC. After this period plaques formed were counted. Flasks with 15 to 200 plaques were used to determine the virus titer in PFU per mL.

A.3 Results and Discussion

The objective of this work was to investigate the inactivation kinetics of coxsackievirus B5 (CVB5) and murine norovirus 1 (MNV-1) from exposure to different ranges of polychromatic UV irradiation emitted by MP UV light. The results from this work complement the information obtained for HAdV-2 described in the main body of this document.

A.3.1 CVB5 Inactivation Kinetics

Figure A.1 shows the CVB5 inactivation kinetics obtained after exposure to narrow band ranges of polychromatic UV light isolated from the emission of a MP UV light lamp using several bandpass filters. The horizontal axis shows the increasing applied fluences in mJ/cm^2, and the vertical axis displays in logarithmic scale the reduction of viable viruses or survival ratio (N/N_0, where N is the number of infectious viruses at a given time after UV treatment, and N_0 is the initial CVB5 concentration). Differently to what was observed with HAdV-2 (Chapter 3) the inactivation kinetics provided by most wavelength ranges are similarly effective to inactivate CVB5. The extreme wavelength ranges analyzed of 218 and 289 nm were the ones with more noticeable differences displaying the fastest and slowest

inactivation kinetics, respectively. For most of the intermediate wavelength ranges a 4-log CVB5 inactivation was achieved with 20-40 mJ/cm^2.

A.3.2 CVB5 Action Spectrum

To build the action spectrum the average fluences were calculated using the spectral irradiance from each bandpass filter as the weighting function to determine the fluence rate (Bolton and Cotton, 2008). From the linear regression analysis for each inactivation curve displayed in Figure A.1 a kinetic constant was obtained and used to determine the spectral sensitivity of CVB5 relative to its inactivation at 254 nm. The action spectrum obtained from this analysis is shown in Figure A.2. The UV absorbance of nucleic acid is included in the plot for comparison. It can be observed in Figure A.2 that at the wavelengths above 240 nm the action spectrum of CVB5 correlates with the UV absorbance of nucleic acids. This suggests that at such wavelengths the CVB5 inactivation is likely predominately driven by damage to the viral genome. At wavelengths below 240 nm, the action spectrum showed that the sensitivity of CVB5 to UV light increases beyond the UV absorbance of DNA as the wavelength decreases. Although a similar trend was observed for HAdV-2 the sensitivity of CVB5 to the lower wavelengths was not as pronounced as that observed for HAdV-2. For the lowest UV wavelength analyzed with peak emission at 218 nm CVB5 was about twice as sensitive as it was at 254 nm; while HAdV-2 was almost ten times more sensitive at that wavelength compared to UV_{254}. The action spectrum of CVB5 suggests that (similarly to HAdV) UV irradiation at wavelengths below 240 nm might cause damage to viral components different to the viral genome.

A.3.3 MNV-1 Inactivation Kinetics

Figure A.3 shows the MNV-1 inactivation kinetics obtained after exposure to narrow band ranges of polychromatic UV light isolated by using several bandpass filters. The horizontal axis indicates the increasing applied fluences in mJ/cm^2, and the vertical axis displays in logarithmic scale the reduction of viable viruses or survival ratio (N/N_0). Although the MNV-1 data is limited, the available results showed

that the inactivation kinetics of MNV-1 by the different wavelength ranges analyzed were similar to those obtained for coxsackievirus B5. The inactivation kinetics provided by most wavelength ranges show that a 4-log reduction in MNV-1 infectivity was achieved with fluences in the range of 20-40 mJ/cm^2.

A.3.4 MNV-1 Action Spectrum

The action spectrum for MNV-1 was built using the kinetic constants obtained from the linear regression analysis of the inactivation curves included in Figure A.3. The spectral sensitivity of MNV-1 relative to its inactivation at 254 nm is included in Figure A.4. The UV absorbance of nucleic acid is also included in Figure A.4 for comparison. Although the data is limited it can be observed that, similarly to the action spectrum of CVB5, at the wavelengths above 240 nm there is a good correlation between the UV absorbance of nucleic acid and the action spectrum of MNV-1. This suggests that at such wavelengths the virus inactivation is possibly driven by damage to the MNV-1 genome. At wavelengths below 240 nm, the action spectrum showed an increased sensitivity as the wavelength decreased that did not coincide with the UV absorbance of nucleic acids. Consistent with the action spectrum of CVB5 and HAdV-2, the spectrum for MNV-1 suggest that UV irradiation at wavelengths below 240 nm might cause damage to other viral components different to the viral genome. The effects of disruption of other viral components had a greater impact in human adenovirus (a dsDNA virus) compared to coxsackievirus and murine norovirus (ssRNA viruses).

A.4 Figures

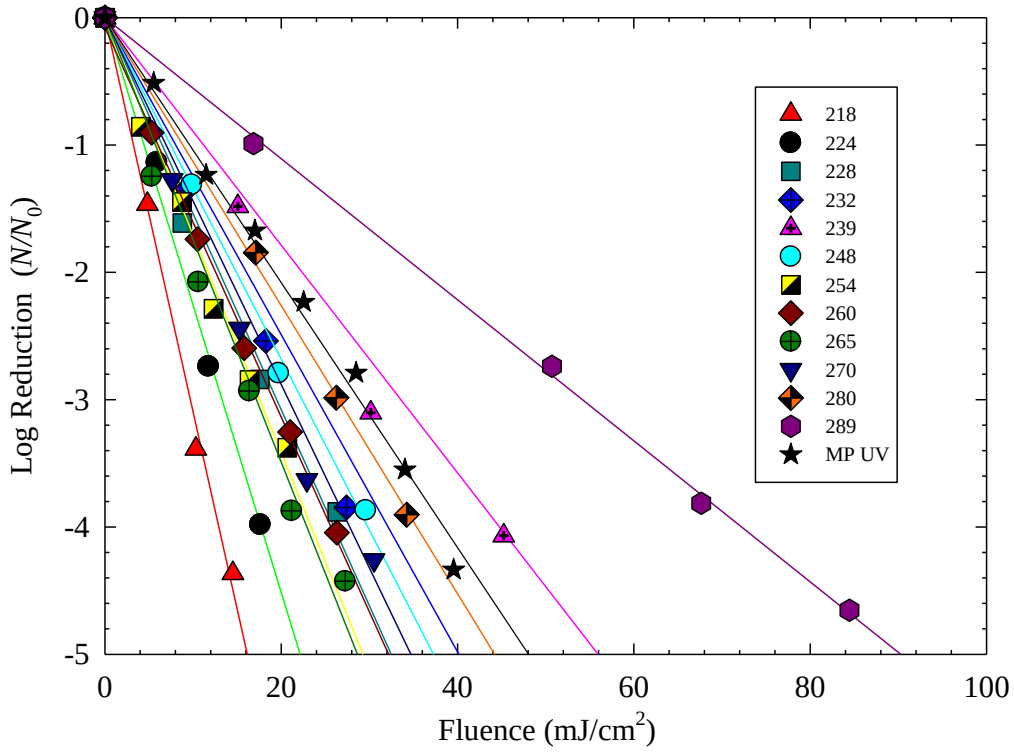

Figure A.1. Coxsackievirus B5 inactivation kinetics assessed by infectivity assay in BGMK cells after exposure to narrow bands of UV irradiation isolated using bandpass filters within the 200-300 nm range.

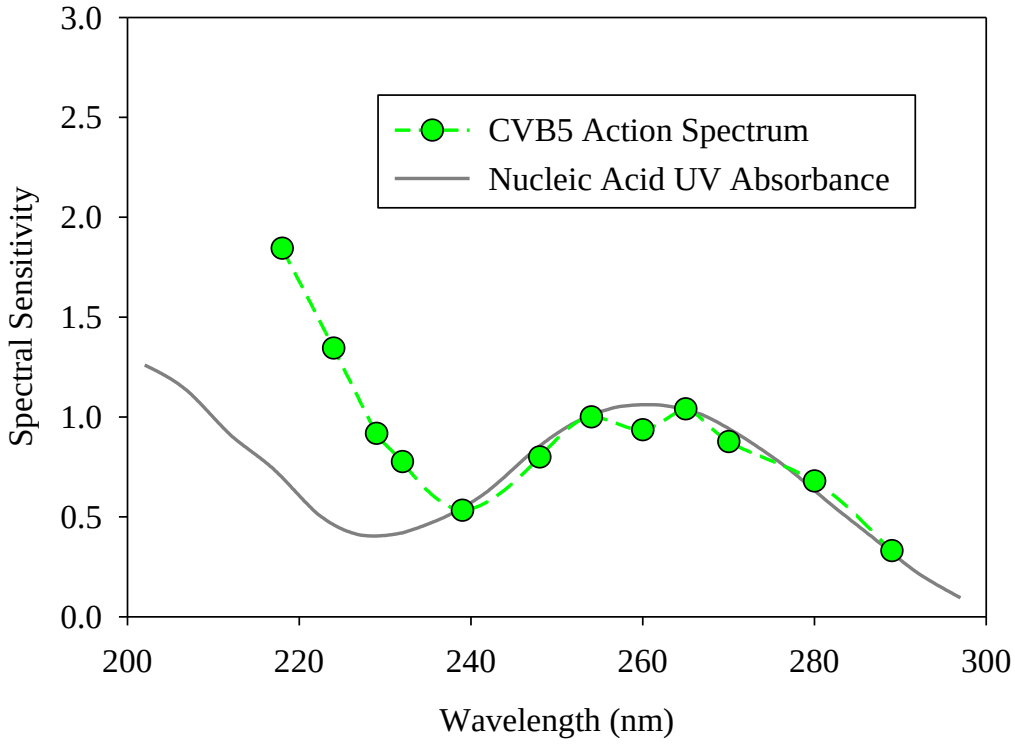

Figure A.2. Coxsackievirus B5 (CVB5) action spectrum determined by inactivation after exposure to narrow bands of UV light within the 200-300 nm range isolated with bandpass filters.

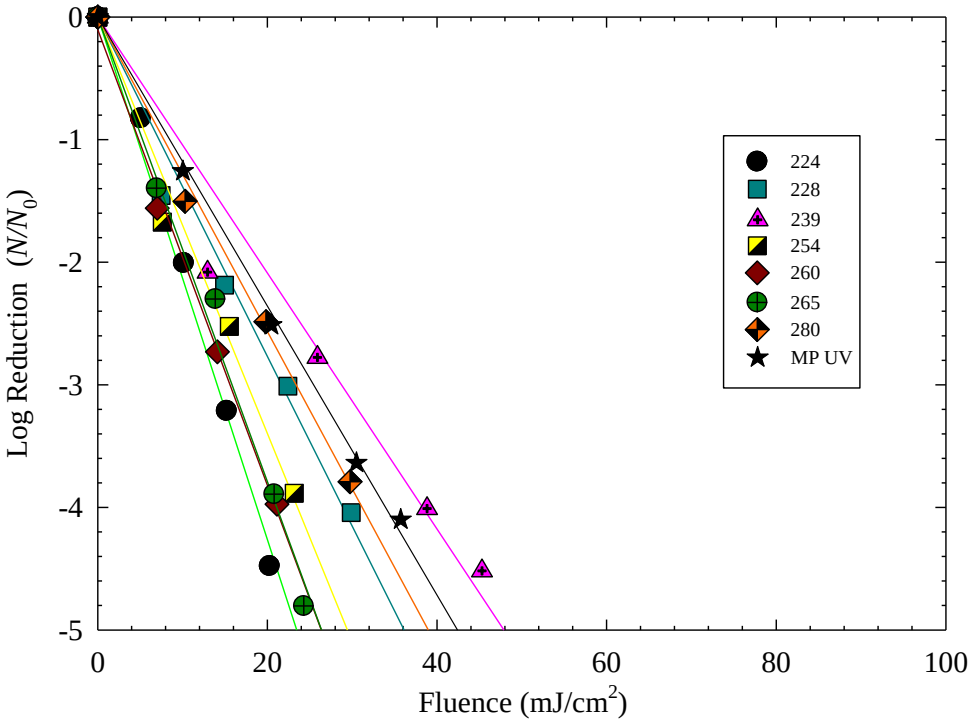

Figure A.3. Murine Norovirus 1 inactivation kinetics assessed by infectivity assay in RAW 264.7 cells after exposure to narrow bands of UV irradiation isolated using bandpass filters within the 200-300 nm range.

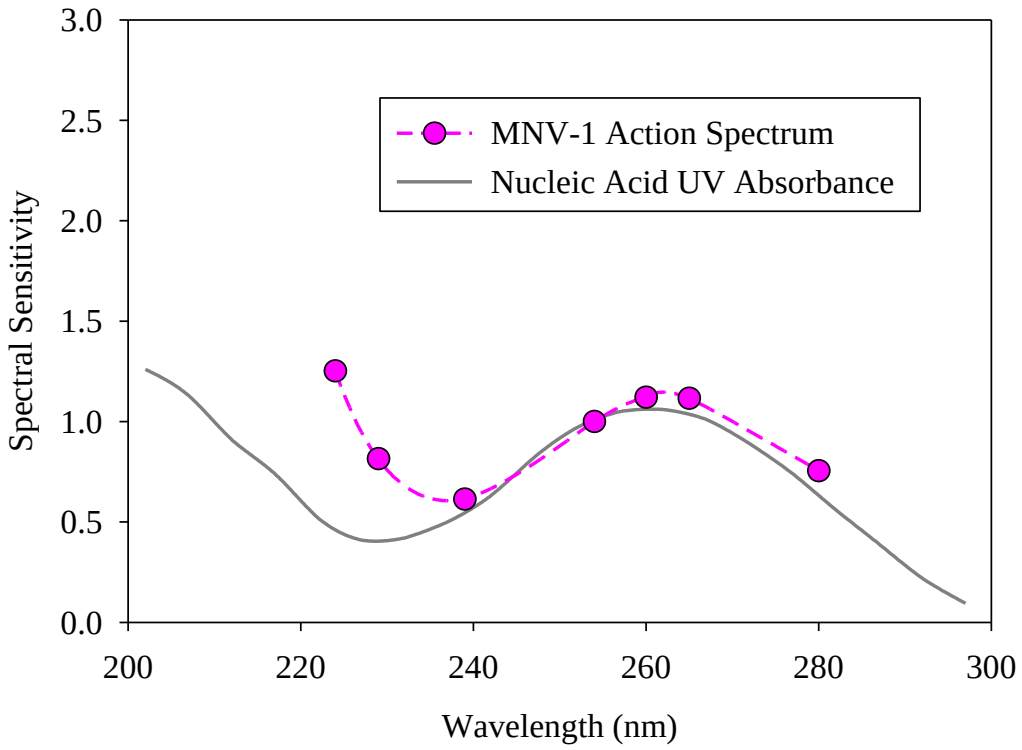

Figure A.4. Murine norovirus 1 (MNV-1) action spectrum determined by inactivation after exposure to narrow bands of UV light within the 200-300 nm range isolated with bandpass filters.

A.5 References

Bae, J.; and Schwab, K. J. Evaluation of Murine Norovirus, Feline Calicivirus, Poliovirus, and MS2 as Surrogates for Human Norovirus in a Model of Viral Persistence in Surface Water and Groundwater. *Appl. Environ. Microbiol*. January **2008** vol. 74 no. 2 477-484

Baert, L. et al., Detection of murine norovirus 1 by using plaque assay, transfection assay, and real-time reverse transcription-PCR before and after heat exposure, *Applied and Environmental Microbiology,* **2008**, *74(2)*, pp. 543-546.

Bailey, D.; Thackray, L. B., Goodfellow, I. G., A Single Amino Acid Substitution in the Murine Norovirus Capsid Protein Is Sufficient for Attenuation in Vivo, *Journal of Virology*, **2008**, *82 (15*), pp. 7725-7728.

Belliot, G.; Lavaux, A.; Souihel, D.; Agnello, D.; Pothier, P., Use of Murine Norovirus as a surrogate to evaluate resistance of Human Norovirus to disinfectants, *Applied and Environmental Microbiology*, **2008**, *74(16)*, pp. 3315-3318.

Bolton, J. R.; Linden, K. G. Standardization of methods for fluence (UV dose) determination in bench-scale UV experiments. *J. Environ. Eng.* **2003**, *129* (3), 209– 215, DOI: 10.1061/(ASCE)0733-9372(2003)129:3(209)

Cannon, J. L.; Papafragkou, E.; Park, G. W.; Osborne, J.; Jaykus, L.; Vinje, J., Surrogates for the Study of Norovirus Stability and Inactivation in the Environment: A Comparison of Murine Norovirus and Feline Calicivirus. *Journal of Food Protection*, **2006**, *69(11)*, pp. 2761-2765.

Chaudhry, Y.; Skinner, M. A.; Goodfellow, I. G., Recovery of genetically defined murine norovirus in tissue culture by using a fowlpox virus expressing T7 RNA polymerase, *Journal of General Virology*, **2007**, *88*, pp. 2091-2100.

Chen, P., Song, Y., Liu, G., Wang, H., Liu, Y., Song, L., Li, Y., Lin, X., Cui, N., and Xu, A. "A Coxsackievirus B-5-associated aseptic meningitis outbreak in Shandong Province, China in 2009." *Journal of Medical Virology*, **2013**, 85: 483-89.

Duizer, E. et al., Inactivation of caliciviruses, *Applied and Environmental Microbiology*, **2004**. *70(8)*, pp. 4538-4543.

Karst, S. M.; Wobus, C. E.; Lay, M.; Davidson, J.; Virgin IV, H.W., STAT1-Dependent Innate Immunity to a Norwalk-Like Virus, *Science*, **2003**, *299*, pp. 1575-1578.

Keller, R; Tetro J. A.; Springthorpe V. S.; Sattar S. A., The influence of temperature on norovirus inactivation by monochloramine in potable waters: testing with murine norovirus as a surrogate for human norovirus, *Food Environ Virol*, **2010**, *2*, pp. 97-100.

Kingsley, D. H.; Holliman, D. R.; Calci, K. R.; Chen, H.; Flick, G. J., Inactivation of a Norovirus by High-Pressure Processing, *Applied and Environmental Microbiology*, **2006**. *73(2)*, pp. 581-585.

Kitajma, M. et al., Chlorine inactivation of human norovirus, murine norovirus and poliovirus in drinking water", *Letters in Applied Microbiology*, **2010**. *51*, pp. *119-121.*

Lee, J.; Zoh, K.; Ko, G., Inactivation and UV disinfection of Murine Norovirus with TiO2 under various environmental conditions, *Applied and Environmental Microbiology*, **2008**. *74(7)*, pp. 2111-2117.
Linden, K. G. et al., Demonstrating 4-log adenovirus inactivation in a medium-pressure UV disinfection reactor. *American Water Works Association, Journal*. **2009**, 101(4), pp. 90.

Malayeri, A. H.; Mohseni, M.; Cairns, B.; and Bolton, J. R., Fluence (UV Dose) Required to Achieve Incremental Log Inactivation of Bacteria, Protozoa, Viruses and Algae. *IUVA*, **2016**

Park, G. W.; Linden, K. G.; Sobsey, M. D., Inactivation of murine norovirus, feline calicivirus and echovirus 12 as surrogates for human norovirus (NoV) and coliphage (F+) MS2 by ultraviolet light (254 nm) and the effect of cell association on UV inactivation, *Letters in Applied Microbiology*, **2011**. *52*, pp. 162-167.

Thurston-Enriquez, J. A. et al., Inactivation of Feline Calicivirus and Adenovirus Type 40 by UV Radiation", *Applied and Environmental Microbiology*, **2002**, *69(1)*, pp. 577-582.

U.S. Environmental Protection Agency, (**2005**), Effectiveness of UV irradiance for pathogen inactivation in surface waters. National Center for Environmental Research. RFA: Drinking water (2000).

USEPA. Drinking Water Contaminant Candidate List 4: Final. In *Federal Register*, Vol. 81, No. 222; Washington, DC, **2016**, pp 81099– 81114.

Ward, V. K.; et al., Recovery of infectious murine norovirus using pol II-driven expression of full-length cDNA, *PNAS*, **2007**. *104 (26)*, pp. 11050-11055.

Wobus, C. E. et al., Replication of Norovirus in cell culture reveals a tropism for dendritic cells and macrophages, *Plos Biology*, **2004**, *2 (12)*, pp. 2076-2084.

Wobus, C. E.; Thackray, L.B.; Virgin IV, H. W., Murine Norovirus: a Model System to Study Norovirus Biology and Pathogenesis, *Journal of Virology*, **2006**, *80(11)*, pp. 5104-5112.

Young L. M.; Kim, J. M.; and Ko, G.P., Disinfection kinetics of murine norovirus using chlorine and chlorine dioxide, *Water Research*, **2010**. *44(10)*, pp. 3243-3251.

APPENDIX B: RAW DATA

B.1 Raw Data Chapter 3

HAdV-2 vs UV_{218}

Wavelength	218 nm
Temperature	23 °C
pH	8
Solution	CBS

Virus	HAdV-2

Average irradiance through the water =	0.018431	mW/cm^2

Fluence UV Dose mJ/cm^2	Sample	Time (min)	Viability at 10^-x dilution						N pfu/ml	N/No	Log N/No
			0	-1	-2	-3	-4	-5			
0.000	Control	0.00				TNTC	64	5	800000	1.000000	0
3.502	1	3.17			TNTC	73	13		91250	0.114063	-0.94286
7.004	2	6.33			71	17			8875	0.011094	-1.95492
10.506	3	9.50		69	2				862.5	0.001078	-2.96733
14.007	4	12.67	86	10					107.5	0.000134	-3.87168

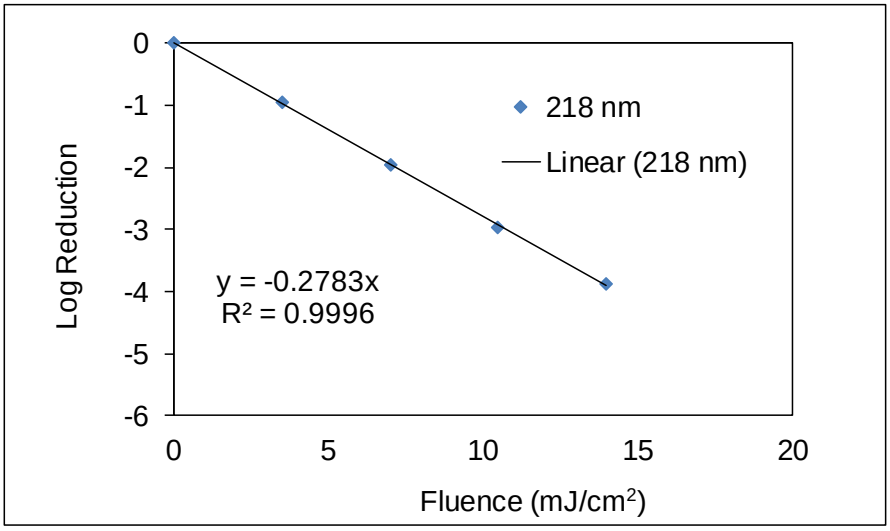

HAdV-2 vs UV_{224}

Wavelength	224 nm
Temperature	23 ℃
pH	8
Solution	CBS

Virus	HAdV-2

Average irradiance through the water =	0.011893	mW/cm^2

Fluence UV Dose mJ/cm^2	Sample	Time (min)	Viability at 10^-x dilution						N pfu/ml	N/No	Log N/No
			0	-1	-2	-3	-4	-5			
0.000	Control	0.000				TNTC	TNTC	40	5000000	1	0
3.354	1	4.700			TNTC	TNTC	170	24	2125000	0.425	-0.37161
6.708	2	9.400		TNTC	TNTC	159	45	-	380625	0.076125	-1.11847
10.074	3	14.117		TNTC	TNTC	43			53750	0.01075	-1.96859
13.427	4	18.817		TNTC	124				15500	0.0031	-2.50864
16.781	5	23.517	TNTC	221					2762.5	0.000553	-3.25767
22.038	6	30.883	TNTC	35					396.875	7.94E-05	-4.10032

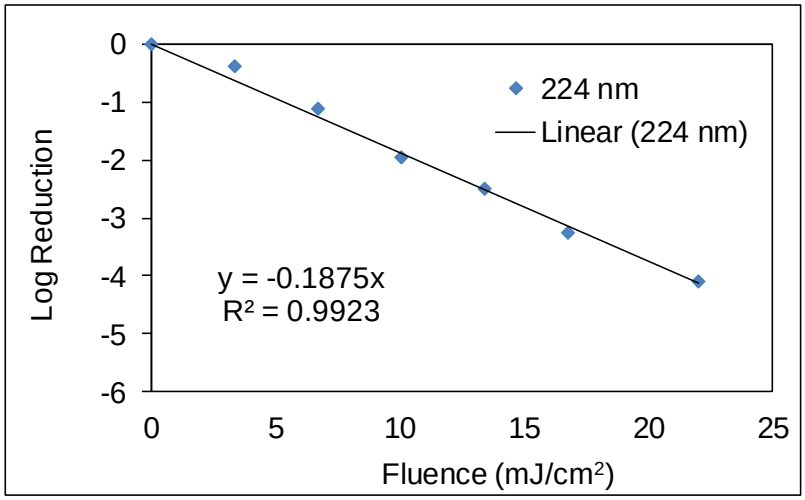

HAdV-2 vs UV_{228}

Wavelength	228 nm
Temperature	23 ℃
pH	8
Solution	CBS

Virus	HAdV-2

Average irradiance through the water =	0.051903	mW/cm^2

Fluence UV Dose mJ/cm^2	Sample	Time (min)	Viability at 10^-x dilution						N pfu/ml	N/No	Log N/No
			0	-1	-2	-3	-4	-5			
0.000	Control	0.000				429	150	12	1875000	1	0
4.464	1	1.433			TNTC	TNTC	80		1000000	0.533333	-0.273
8.875	2	2.850		TNTC	TNTC	135			168750	0.09	-1.04576
13.339	3	4.283		TNTC	209	45			41187.5	0.021967	-1.65824
17.751	4	5.700	TNTC	414	53				5900	0.003147	-2.50215
22.215	5	7.133	TNTC	71					887.5	0.000473	-3.32483
26.626	6	8.550	297	29					366.875	0.000196	-3.70848
33.737	7	10.833	37						46.25	2.47E-05	-4.60789

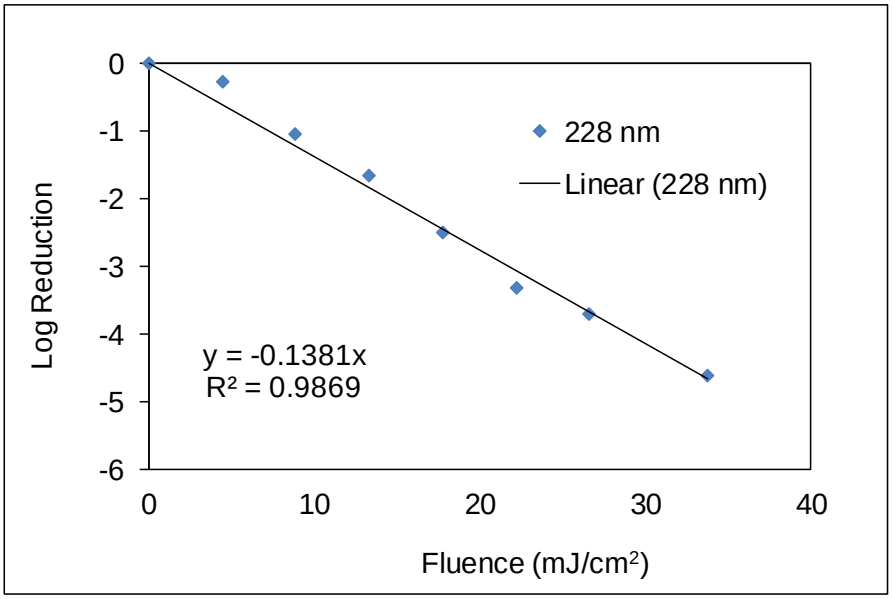

HAdV-2 vs UV_{232}

Wavelength	232 nm
Temperature	23 ℃
pH	8
Solution	CBS

Virus	HAdV-2

Average irradiance through the water =	0.063515	mW/cm^2

Fluence UV Dose mJ/cm^2	Sample	Time (min)	Viability at 10^-x dilution						N pfu/ml	N/No	Log N/No
			0	-1	-2	-3	-4	-5			
0.000	Control	0.00				TNTC	111	24	2193750	1.000000	0
7.939	1	2.08			TNTC	NA	28		350000	0.159544	-0.79712
16.196	2	4.25			TNTC	52			65000	0.029630	-1.52827
23.882	3	6.27	TNTC	284	22				3550	0.001618	-2.79096
31.821	4	8.35	TNTC	65					812.5	0.000370	-3.43136
39.824	5	10.45	116	8					145	0.000066	-4.17982

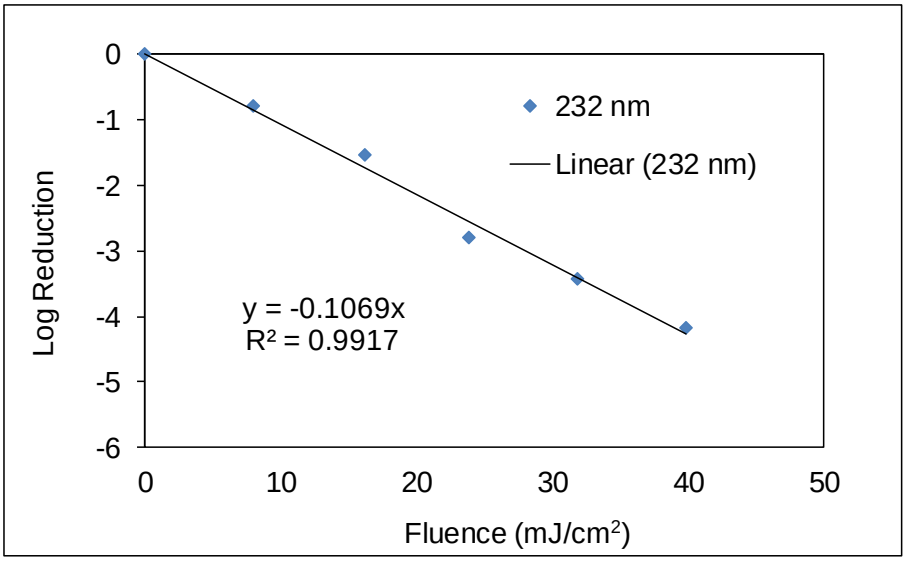

HAdV-2 vs UV_{239}

Wavelength	239 nm
Temperature	23 °C
pH	8
Solution	CBS

Virus	HAdV-2

Average irradiance through the water =	0.040262	mW/cm^2

Fluence UV Dose mJ/cm^2	Sample	Time (min)	Viability at 10^-x dilution						N pfu/ml	N/No	Log N/No
			0	-1	-2	-3	-4	-5			
0.000	Control	0.000			TNTC	TNTC	51	2	637500	1	0
22.788	1	9.433			TNTC	130	13	-	162500	0.254902	-0.59363
45.576	2	18.867		TNTC	269	19	0	-	28687.5	0.045	-1.34679
68.646	3	28.417	-	TNTC	36	1			4500	0.007059	-2.15127
91.152	4	37.733	-	103	8				1287.5	0.00202	-2.69473
113.941	5	47.167	-	35					437.5	0.000686	-3.1635

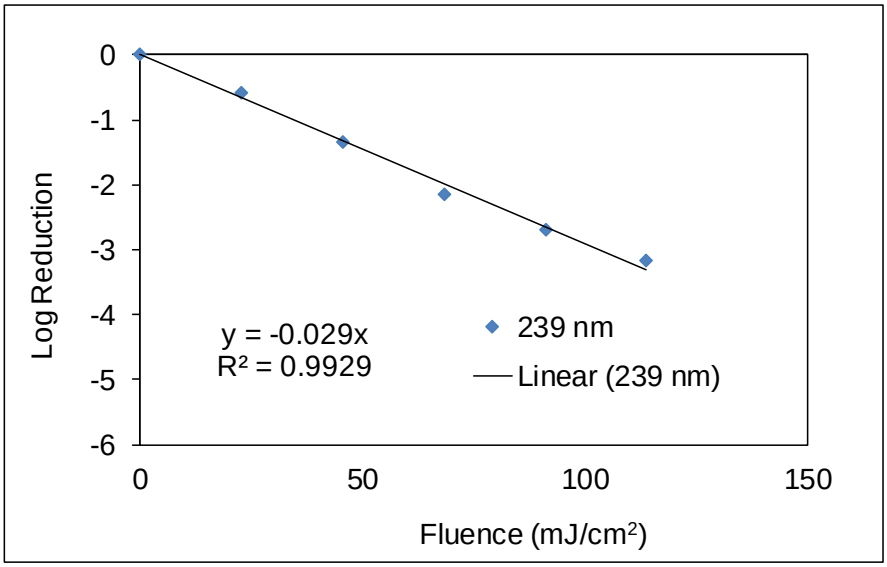

HAdV-2 vs UV_{248}

Wavelength	248 nm
Temperature	23 ℃
pH	8
Solution	CBS

Virus	HAdV-2

Average irradiance through the water =	0.038536	mW/cm^2

Fluence UV Dose mJ/cm^2	Sample	Time (min)	Viability at 10^-x dilution						N pfu/ml	N/No	Log N/No
			0	-1	-2	-3	-4	-5			
0.000	Control	0.000				TNTC	172	32	3075000	1	0
41.580	1	17.983			TNTC	147	45		373125	0.121341	-0.91599
83.160	2	35.967		TNTC	138	30			27375	0.008902	-2.05049
124.856	3	54.000	TNTC	135	9				1687.5	0.000549	-3.2606
166.475	4	72.000	120						150	4.88E-05	-4.31175

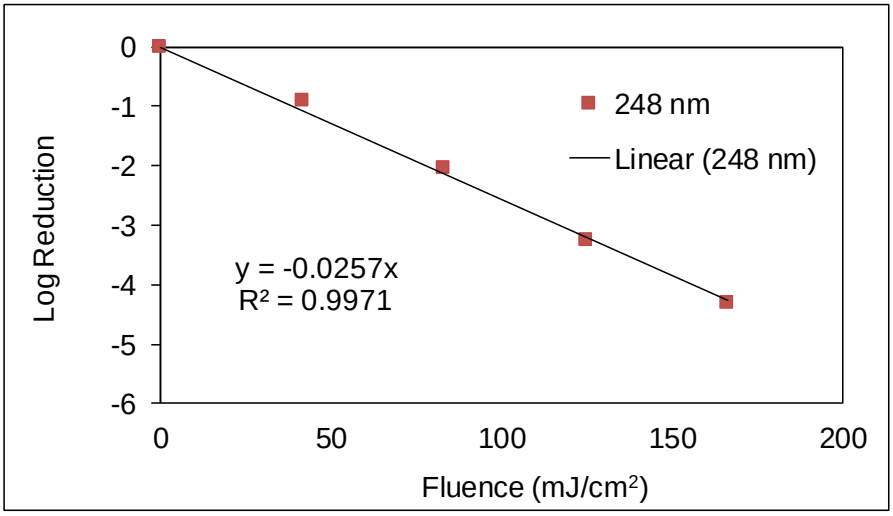

HAdV-2 vs UV_{254}

Wavelength	254 nm
Temperature	23 °C
pH	8
Solution	CBS

Virus	HAdV-2

Average irradiance through the water =	0.069629	mW/cm^2

Fluence UV Dose mJ/cm^2	Sample	Time (min)	Viability at 10^-x dilution						N pfu/ml	N/No	Log N/No
			0	-1	-2	-3	-4	-5			
0.000	Control	0.000				TNTC	TNTC	47	5875000	1	0
19.078	1	4.567			TNTC	TNTC	65		812500	0.138298	-0.85918
38.157	2	9.133		TNTC	TNTC	79			98750	0.016809	-1.77447
76.244	3	18.250		TNTC	67				8375	0.001426	-2.84602
114.401	4	27.383	TNTC	42					525	8.94E-05	-4.04885
152.558	5	36.517	34						42.5	7.23E-06	-5.14062

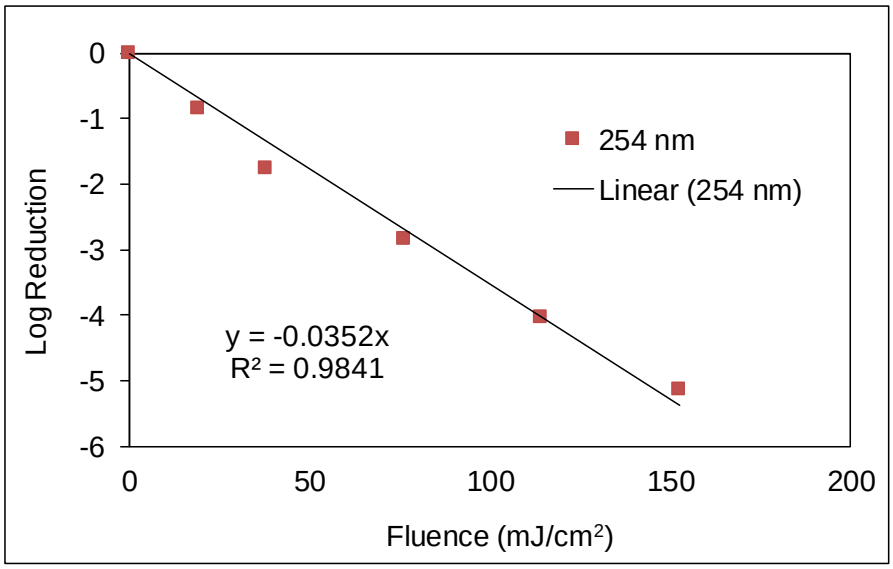

HAdV-2 vs UV_{260}

Wavelength	260 nm
Temperature	23 ℃
pH	8
Solution	CBS

Virus	HAdV-2

Average irradiance through the water =	0.094203	mW/cm^2

Fluence UV Dose mJ/cm^2	Sample	Time (min)	Viability at 10^-x dilution						N pfu/ml	N/No	Log N/No
			0	-1	-2	-3	-4	-5			
0.000	Control	0.00				TNTC	124	14	952500	1.000000	0
12.435	1	2.20				238	24		297500	0.312336	-0.50538
24.022	2	4.25				84	2		105000	0.110236	-0.95768
47.478	3	8.40		TNTC	240				30000	0.031496	-1.50174
59.348	4	10.50		TNTC	58				7250	0.007612	-2.11853
71.311	5	12.62		250+	28				3500	0.003675	-2.4348
83.652	6	14.80		57					712.5	0.000748	-3.12608
95.616	7	16.92	272	28					340	0.000357	-3.44739
110.877	8	19.62	56	6					70	0.000073	-4.13377

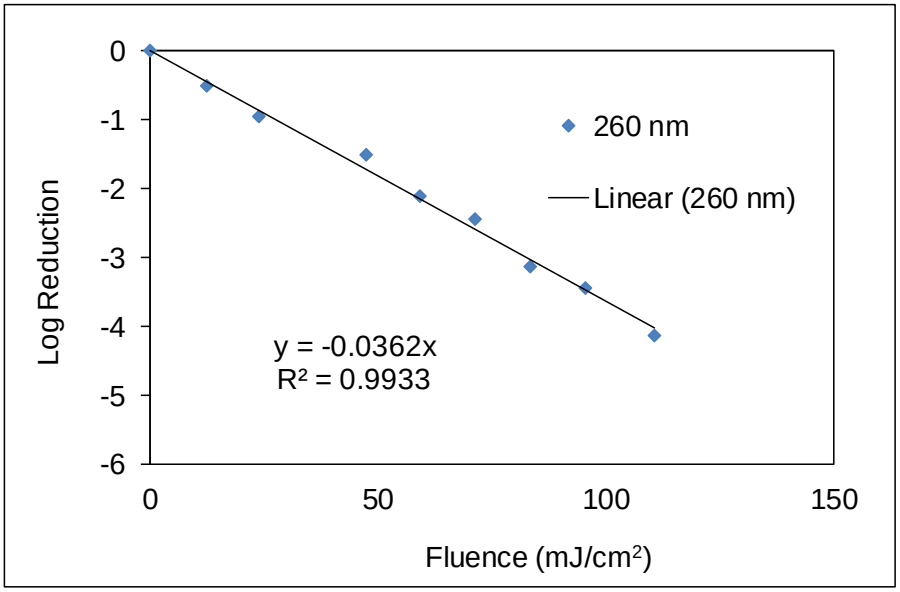

HAdV-2 vs UV_{265}

Wavelength	265 nm
Temperature	23 ℃
pH	8
Solution	CBS

Virus	HAdV-2

Average irradiance through the water =	0.091784	mW/cm^2

Fluence UV Dose mJ/cm^2	Sample	Time (min)	Viability at 10^-x dilution						N pfu/ml	N/No	Log N/No
			0	-1	-2	-3	-4	-5			
0.000	Control	0.000			TNTC	TNTC	147	16	1918750	1	0
20.927	1	3.800			TNTC	168	18		217500	0.113355	-0.94556
41.303	2	7.500		TNTC	289	65			58687.5	0.030586	-1.51447
62.413	3	11.333		TNTC	89				11125	0.005798	-2.23672
83.157	4	15.100	TNTC	131					1637.5	0.000853	-3.06884
101.881	5	18.500	224	22					280	0.000146	-3.83586

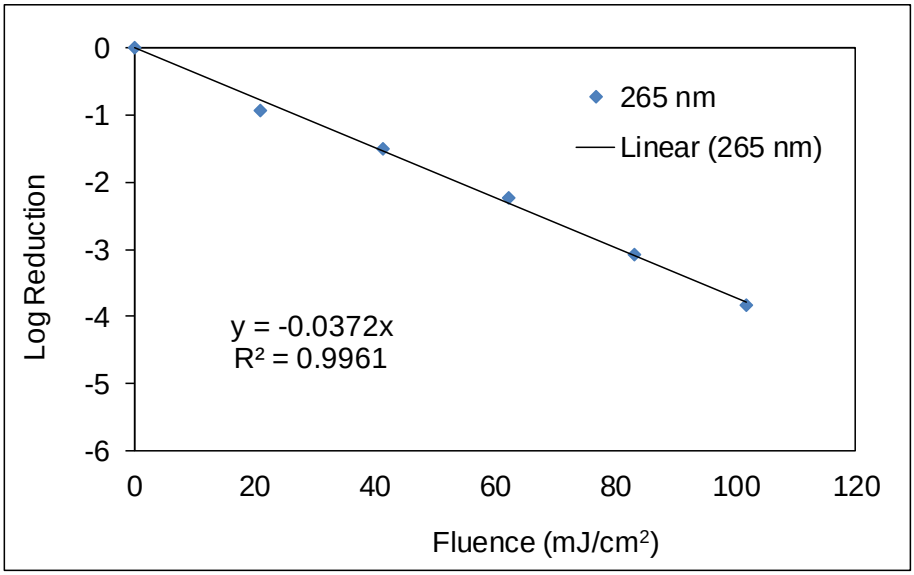

HAdV-2 vs UV_{270}

Wavelength	270 nm
Temperature	23 ℃
pH	8
Solution	CBS

Virus	HAdV-2

Average irradiance through the water =	0.05008	mW/cm^2

Fluence UV Dose mJ/cm^2	Sample	Time (min)	Viability at 10^-x dilution						N pfu/ml	N/No	Log N/No
			0	-1	-2	-3	-4	-5			
0.000	Control	0.00				TNTC	74	10	925000	1.000000	0
16.426	1	5.47				51	3		63750	0.068919	-1.16166
32.803	2	10.92			134	17			19000	0.020541	-1.68739
49.429	3	16.45		TNTC	26	2			3250	0.003514	-2.45426
65.655	4	21.85		58	4				725	0.000784	-3.1058
82.082	5	27.32	134	23					227.5	0.000246	-3.60916
98.458	6	32.77	31	4					38.75	0.000042	-4.37787

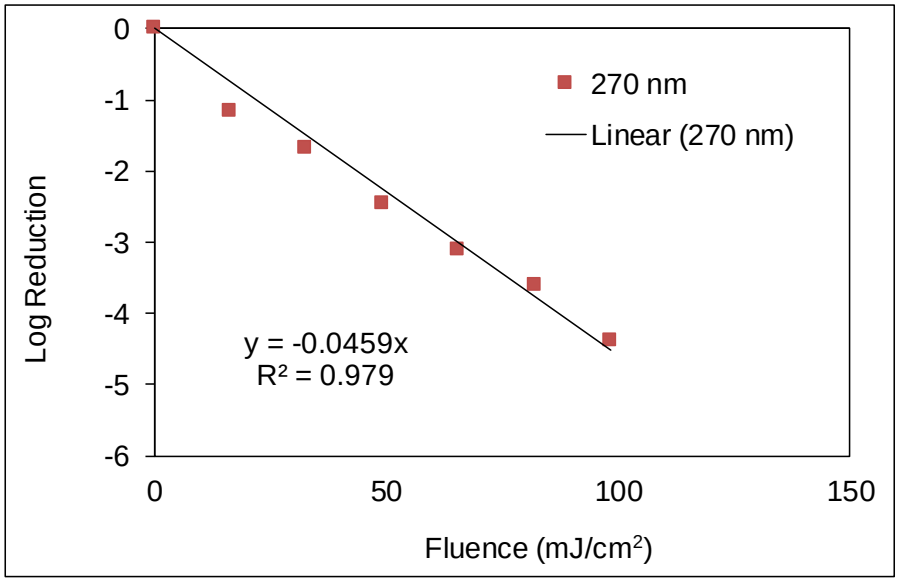

HAdV-2 vs UV_{280}

Wavelength	280 nm
Temperature	23 °C
pH	8
Solution	CBS

Virus	HAdV-2

Average irradiance through the water =	0.042253	mW/cm^2

Fluence UV Dose mJ/cm^2	Sample	Time (min)	Viability at 10^-x dilution						N pfu/ml	N/No	Log N/No
			0	-1	-2	-3	-4	-5			
0.000	Control	0.000				TNTC	107	6	1337500	1	0
19.648	1	7.750			TNTC	131	28	2	256875	0.192056	-0.71657
39.296	2	15.500		TNTC	259	37	5	-	39312.5	0.029393	-1.53176
58.943	3	23.250		TNTC	104	11			13000	0.00972	-2.01235
78.591	4	31.000		103	11	3			1287.5	0.000963	-3.01655

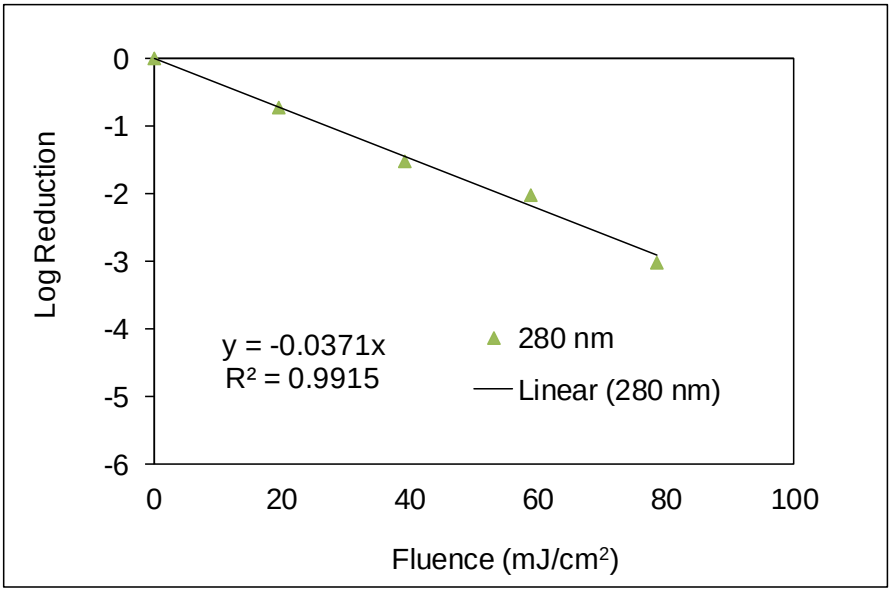

HAdV-2 vs UV_{289}

Wavelength	289 nm
Temperature	23 ℃
pH	8
Solution	CBS

Virus	HAdV-2

Average irradiance through the water =	0.041886	mW/cm^2

Fluence UV Dose (mJ/cm2)	Sample	Time (min)	Viability at 10^-x dilution						N pfu/ml	N/No	Log N/No
			0	-1	-2	-3	-4	-5			
0.000	Control	0.000				TNTC	147	40	3418750	1	0
38.954	1	15.500			TNTC	TNTC	80		1000000	0.292505	-0.53387
77.614	2	30.883			TNTC	142	15		177500	0.05192	-1.28467
116.651	3	46.417		TNTC	193	26			28312.5	0.008282	-2.08189
155.270	4	61.783	TNTC	198	27				2925	0.000856	-3.06774
196.024	5	78.000	221	16	0				276.25	8.08E-05	-4.09257
226.182	6	90.000	34	6					42.5	1.24E-05	-4.90548

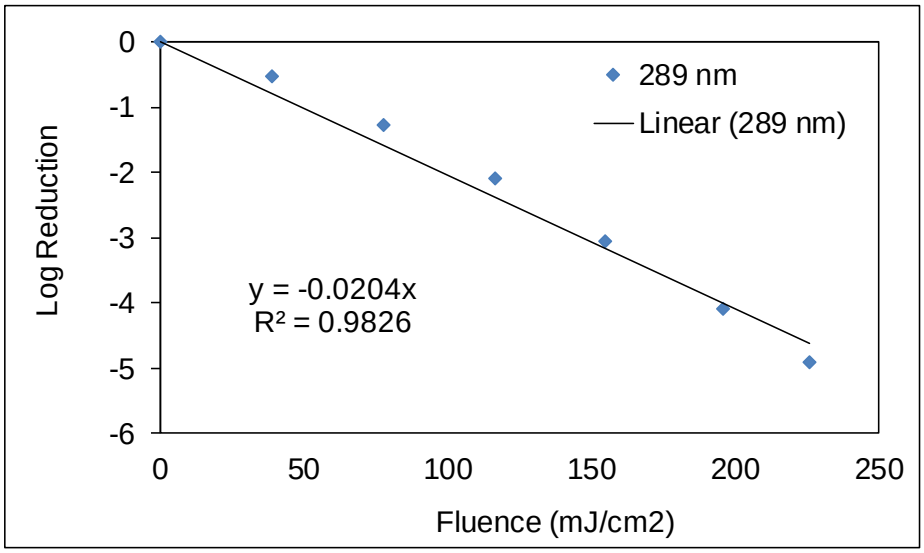

HAdV-2 vs UV_{297}

Wavelength	297 nm
Temperature	23 ℃
pH	8
Solution	CBS

Virus	HAdV-2

Average irradiance through the water =	0.05795	mW/cm^2

Fluence UV Dose mJ/cm^2	Sample	Time (min)	Viability at 10^-x dilution						N pfu/ml	N/No	Log N/No
			0	-1	-2	-3	-4	-5			
0.000	Control	0.000				TNTC	125	12	1562500	1	0
104.311	1	30.000			TNTC	328	44		480000	0.3072	-0.51258
222.530	2	64.000			TNTC	138	15		172500	0.1104	-0.95703
312.933	3	90.000		TNTC	325	51			52187.5	0.0334	-1.47625
417.243	4	120.000	TNTC	TNTC	104				13000	0.00832	-2.07988

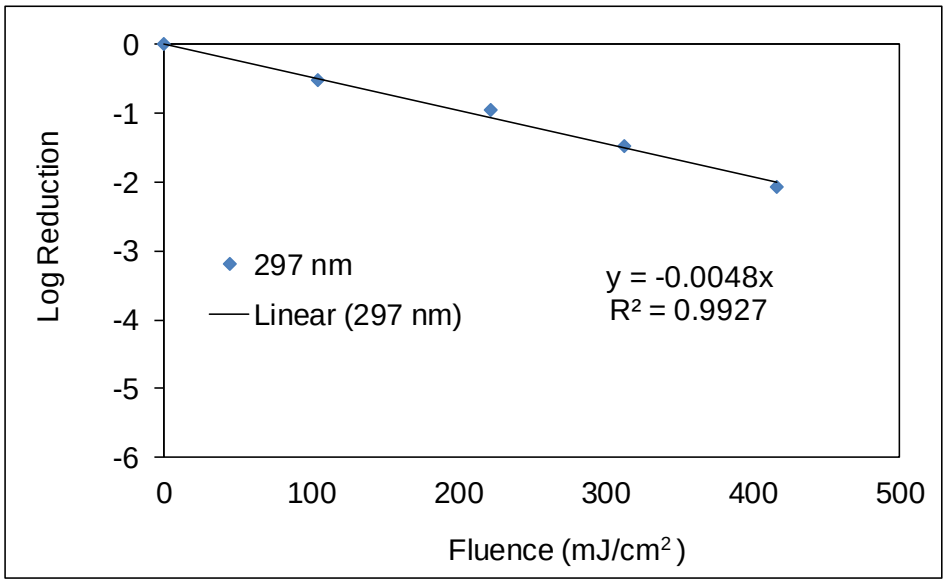

HAdV-2 vs MP UV

Wavelength	MP UV
Temperature	23 ℃
pH	8
Solution	CBS

Virus	HAdV-2

Average irradiance through the water =	0.501629	mW/cm^2

Fluence UV Dose mJ/cm^2	Sample	Time (min)	Viability at 10^-x dilution						N pfu/ml	N/No	Log N/No
			0	-1	-2	-3	-4	-5			
0.000	Control	0.00				TNTC	96	5	1200000	1.000000	0
13.042	1	0.43			TNTC	175	33		315625	0.263021	-0.58001
26.586	2	0.88			383	124			101437.5	0.084531	-1.07298
39.629	3	1.32		TNTC	105				13125	0.010938	-1.96108
53.173	4	1.77		232	37				3762.5	0.003135	-2.5037
66.215	5	2.20	TNTC	83					1037.5	0.000865	-3.06319
79.759	6	2.65	121						151.25	0.000126	-3.89949
92.801	7	3.08	40						50	0.000042	-4.38021

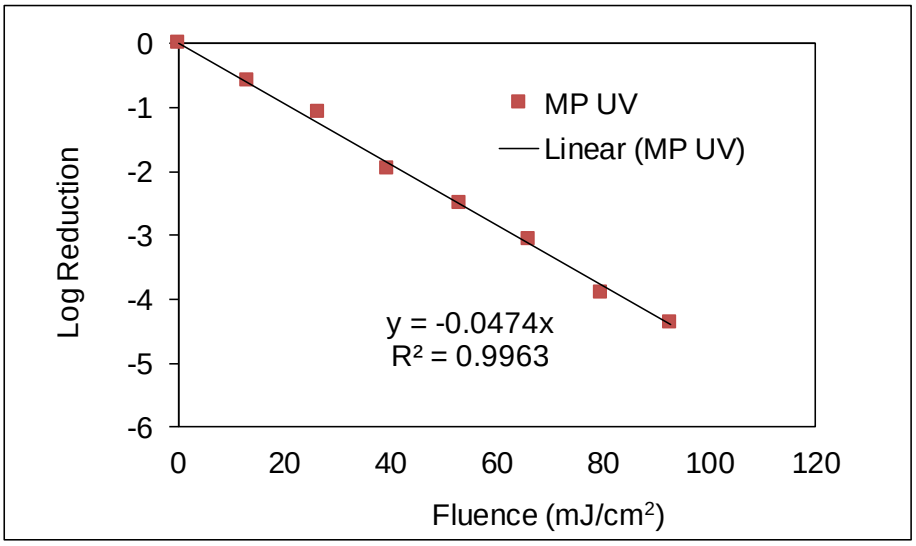

LR-qPCR 1.1-kb DNA fragment

224 nm	LR-PCR	LR-PCR
Fluence (mJ/cm2)	Average Log reduction	Standard Deviation
0	0.0000	0.0000
10	-0.2183	0.1062
20	-0.2775	0.1867
30	-0.5110	0.2147
40	-0.8619	0.0758
50	-0.7620	0.1082
75	-0.9517	0.1212
100	-1.0297	0.1753

254 nm	LR-PCR	LR-PCR
Fluence (mJ/cm2)	Average Log reduction	Standard Deviation
0	0.0000	0
20	-0.4621	
40	-0.9437	0.1233
60	-1.2700	
80	-1.9287	0.0844
100	-2.1452	
120	-2.4854	0.1536

280 nm	LR-PCR	LR-PCR
Fluence (mJ/cm2)	Average Log reduction	Standard Deviation
0	0	0
20	-0.6671	
30	-1.0676	0.0905
45	-1.6524	
60	-1.6251	0.1372
70	-2.2552	
90	-2.4487	0.0368

DNA+EMA

224 nm	224 nm	224 nm	224 nm	224 nm
Fluence (mJ/cm2)	Average Log Reduction DNA only	Standard deviation Log reduction DNA only	Average Log Reduction DNA + EMA	Standard deviation Log reduction DNA + EMA
0.0	0.0000	0.0000	0.0000	0.0000
10.0	-0.1469	0.1655	-0.4446	0.0327
15.7	0.2247	0.2585	-0.6203	0.2135
20.0	-0.0799	0.2360	-0.8803	0.1145
30.0	0.0033	0.1914	-0.9123	0.2559
34.8	0.0500	0.1636	-1.2533	0.2226
40.0	-0.0703	0.0264	-1.4949	0.3531
46.4	-0.0723	0.0130	-1.6500	0.2135

254 nm	254 nm	254 nm	254 nm	254 nm
Fluence (mJ/cm2)	Average Log Reduction DNA only	Standard deviation Log reduction DNA only	Average Log Reduction DNA + EMA	Standard deviation Log reduction DNA + EMA
0	0.0000	0.0000	0.0000	0.0000
40	0.0141	0.0686	-0.1612	0.0318
80	-0.0461	0.0768	-0.2150	0.0733
120	-0.2824	0.0187	-0.2249	0.0796
160	-0.2453	0.0508	-0.2380	0.1133

280 nm	280 nm	280 nm	280 nm	280 nm
Fluence (mJ/cm2)	Average Log Reduction DNA only	Standard deviation Log reduction DNA only	Average Log Reduction DNA + EMA	Standard deviation Log reduction DNA + EMA
0	0	0	0	0
30	-0.0221	0.1435	-0.0373	0.0203
60	-0.0556	0.0698	-0.0556	0.0698
90	-0.2006	0.0772	-0.1862	0.0442
120	-0.2982	0.0643	-0.1633	0.0727

Relative Action Spectrum

HAdV-2		
Wavelength [nm]	k [cm2/mJ]	Relative to 254 nm
218	0.2783	8.6429
224	0.1875	5.8230
228	0.1381	4.2888
232	0.1069	3.3199
239	0.0296	0.9193
248	0.0257	0.7981
254	0.0322	1.0000
260	0.0362	1.1242
265	0.0372	1.1553
270	0.0459	1.4255
280	0.0361	1.1211
289	0.0204	0.6335
297	0.0039	0.1211

UV_{224} DNA A

Fluence (mJ/cm2)	Sample	Cq E1A	Cq Hexon	Cq Actin	Relative Quantification E1A	Relative Quantification Hexon	Absolute E1A copies	Absolute Hexon copies	Absolute Actin copies	E1A/ 100ACTIN	HEXON/ 100ACTIN
0.00	224-0hrs	26.60	26.95	29.03	1.0000000	1.0000000	66169.82	100376.33	33442.45	197.86	300.15
6.71	224-0hrs	25.78	26.41	28.71	1.4142136	1.1647336	113750.70	140750.60	40802.91	278.78	344.95
10.07	224-0hrs	25.47	25.97	27.84	0.9592641	0.8645372	139606.85	185387.51	70076.49	199.22	264.55
13.43	224-0hrs	25.79	25.54	28.25	1.0210121	1.5475650	113001.61	242656.45	54310.18	208.07	446.80
16.78	224-0hrs	26.74	27.54	29.94	1.7052698	1.2483305	60323.68	69377.41	18994.06	317.59	365.26
22.04	224-0hrs	26.85	27.98	28.99	0.8179021	0.4763190	56094.98	52672.97	34284.45	163.62	153.64
0.00	224-4hrs	27.22	31.21	29.93	1.0000000	1.0000000	43929.34	6972.57	19112.50	229.85	36.48
6.71	224-4hrs	26.66	30.93	29.20	0.8888427	0.7320428	63597.98	8308.48	30088.58	211.37	27.61
10.07	224-4hrs	26.25	30.41	28.89	0.9526380	0.8467453	83385.47	11505.42	36483.38	228.56	31.54
13.43	224-4hrs	25.39	29.09	28.88	1.7171309	2.0994334	147184.56	26290.17	36710.88	400.93	71.61
16.78	224-4hrs	26.57	30.30	30.06	1.7171309	2.0562277	67494.49	12325.66	17628.70	382.87	69.92
22.04	224-4hrs	25.82	29.23	28.92	1.3103934	1.9588406	110783.82	24084.03	35809.29	309.37	67.26
0.00	224-12 hrs	27.64	28.13	29.53	1.0000000	1.0000000	33284.20	47951.79	24508.06	135.81	195.66
6.71	224-12 hrs	27.57	28.04	29.32	0.9075192	0.9201877	34859.75	50731.14	27925.72	124.83	181.66
10.07	224-12 hrs	27.09	27.37	28.66	0.8010699	0.9265881	47869.33	77168.28	42091.08	113.73	183.34
13.43	224-12 hrs	27.03	27.81	30.18	2.3949574	1.9588406	49805.12	58587.99	16361.49	304.40	358.08
16.78	224-12 hrs	27.05	27.76	30.40	2.7510836	2.3619853	49151.32	60450.92	14270.12	344.44	423.62
22.04	224-12 hrs	25.97	26.81	29.12	2.3949574	1.8790455	100330.90	109570.97	31622.78	317.27	346.49
0.00	224-16 hrs	25.85	27.47	30.26	1.0000000	1.0000000	108609.55	72485.33	15567.71	697.66	465.61
6.71	224-16 hrs	27.48	28.96	29.61	0.2058798	0.2268798	36995.53	28519.29	23319.04	158.65	122.30
10.07	224-16 hrs	27.21	28.52	29.02	0.1649385	0.2044755	44220.55	37563.75	33650.99	131.41	111.63
13.43	224-16 hrs	26.85	28.23	29.30	0.2570285	0.3035487	56094.98	45041.84	28275.08	198.39	159.30
16.78	224-16 hrs	26.73	28.30	29.96	0.4413515	0.4569157	60723.56	43110.59	18759.37	323.70	229.81
22.04	224-16 hrs	26.52	28.05	29.36	0.3368084	0.3584888	69761.45	50414.53	27239.88	256.10	185.08
0.00	224-24 hrs	20.44	21.81	29.77	1.0000000	1.0000000	3874675.12	2506859.31	21111.25	18353.60	11874.52
6.71	224-24 hrs	25.71	27.05	30.11	0.0328036	0.0334929	119135.22	94285.01	17089.19	697.14	551.72
10.07	224-24 hrs	27.60	28.30	28.91	0.0038525	0.0061296	34175.58	43110.59	36032.59	94.85	119.64
13.43	224-24 hrs	26.72	27.66	28.90	0.0070410	0.0094859	61126.10	64356.38	36257.28	168.59	177.50
16.78	224-24 hrs	26.69	27.82	29.96	0.0149885	0.0177013	62349.79	58222.35	18759.37	332.37	310.36
22.04	224-24 hrs	26.77	27.56	29.14	0.0080321	0.0120068	59139.75	68514.16	31232.05	189.36	219.37
0.00	224-36 hrs	16.95	17.94	30.31	1.0000000	1.0000000	38874965.30	28270419.03	15091.27	257599.08	187329.66
6.71	224-36 hrs	21.43	22.62	29.61	0.0275845	0.0240137	2014469.46	1509737.97	23319.04	8638.73	6474.27
10.07	224-36 hrs	24.33	25.72	29.28	0.0029399	0.0022281	296498.81	216796.47	28628.82	1035.67	757.27
13.43	224-36 hrs	26.44	27.68	29.44	0.0007609	0.0006398	73548.03	63555.61	25918.32	283.77	245.21
16.78	224-36 hrs	27.37	28.78	30.37	0.0007609	0.0005687	39784.42	31921.13	14538.75	273.64	219.56
22.04	224-36 hrs	27.53	28.68	29.58	0.0003939	0.0003525	35793.32	33983.41	23758.00	150.66	143.04
0.00	224-48 hrs	16.61	17.30	30.43	1.0000000	1.0000000	48666598.19	42202663.26	14006.46	347458.30	301308.63
6.71	224-48 hrs	19.43	20.38	29.66	0.0830429	0.0693481	7551770.45	6136605.74	22605.37	33406.97	27146.67
10.07	224-48 hrs	22.27	23.48	29.28	0.0089122	0.0062151	1156452.21	881208.84	28628.82	4039.47	3078.05
13.43	224-48 hrs	24.41	25.07	29.20	0.0019129	0.0019531	281233.75	325670.70	30088.58	934.69	1082.37
16.78	224-48 hrs	26.83	27.82	30.73	0.0010322	0.0008384	56841.15	58222.35	11623.44	489.02	500.90
22.04	224-48 hrs	27.93	28.31	29.14	0.0001600	0.0001983	27480.48	42841.55	31232.05	87.99	137.17

Irradiance (mW/cm2)	Fluence mJ/cm2		Viability at 10^-x dilution								
0.011893261		Sample	0	-1	-2	-3	-4	-5	N	N/No	
Time (min)									pfu/ml		Log reduction
0.00	0	Control				TNTC	TNTC	40	5000000	1	0
9.40	6.7077994	1		TNTC	TNTC	159	45	-	380625	0.076125	-1.118472694
14.12	10.073592	2		TNTC	TNTC	43			53750	0.01075	-1.968591536
18.82	13.427492	3		TNTC	124				15500	0.0031	-2.508638306
23.52	16.781392	4	TNTC	221					2762.5	0.0005525	-3.257667718
30.88	22.038213	5	TNTC	35					437.5	0.0000875	-4.057991947

UV_{224} DNA B

Fluence (mJ/cm2)	Sample	Cq E1A	Cq Hexon	Cq Actin	Relative Quantification E1A	Relative Quantification Hexon	Absolute E1A copies	Absolute Hexon copies	Absolute Actin copies	E1A/ 100 ACTIN	HEXON/ 100 ACTIN
0.00	224-0hrs	27.72	29.23	29.06	1.0000000	1.0000000	3.16E+04	2.41E+04	3.28E+04	96.18	73.37
7.76	224-0hrs	28.29	29.84	29.15	0.7169776	0.6973718	2.17E+04	1.64E+04	3.10E+04	69.79	52.96
11.95	224-0hrs	27.98	29.63	28.92	0.7578583	0.6877709	2.66E+04	1.87E+04	3.58E+04	74.25	52.36
15.82	224-0hrs	26.79	28.60	28.54	1.3286858	1.0792282	5.84E+04	3.57E+04	4.54E+04	128.69	78.78
19.74	224-0hrs	28.68	30.04	30.91	1.8531761	2.0562277	1.67E+04	1.45E+04	1.04E+04	161.09	139.56
0.00	224-4hrs	29.57	31.30	31.63	1.0000000	1.0000000	9.30E+03	6.59E+03	6.64E+03	139.99	99.21
7.76	224-4hrs	29.47	31.89	30.98	0.6830201	0.4233727	9.93E+03	4.56E+03	9.95E+03	99.84	45.78
11.95	224-4hrs	29.30	31.34	31.68	1.2483305	1.0069556	1.11E+04	6.43E+03	6.44E+03	172.61	99.81
15.82	224-4hrs	28.98	30.88	31.21	1.1250585	1.0000000	1.37E+04	8.57E+03	8.62E+03	159.22	99.40
19.74	224-4hrs	29.56	31.39	31.63	1.0069556	0.9395227	9.36E+03	6.23E+03	6.64E+03	140.91	93.78
0.00	224-12 hrs	26.24	27.64	29.24	1.0000000	1.0000000	8.39E+04	6.52E+04	2.93E+04	285.99	222.04
7.76	224-12 hrs	29.11	30.56	29.22	0.1349035	0.1303082	1.26E+04	1.05E+04	2.97E+04	42.41	35.25
11.95	224-12 hrs	29.32	30.83	29.84	0.1792444	0.1660857	1.10E+04	8.85E+03	2.02E+04	54.27	43.76
15.82	224-12 hrs	28.39	29.52	29.64	0.2973018	0.3584888	2.03E+04	2.01E+04	2.29E+04	88.60	87.75
19.74	224-12 hrs	29.07	30.22	30.20	0.2735734	0.3253355	1.29E+04	1.30E+04	1.62E+04	80.07	80.19
0.00	224-16 hrs	23.01	24.54	29.25	1.0000000	1.0000000	7.09E+05	4.54E+05	2.92E+04	2431.57	1555.88
7.76	224-16 hrs	28.11	29.59	29.19	0.0279695	0.0289559	2.44E+04	1.92E+04	3.03E+04	80.59	63.50
11.95	224-16 hrs	27.35	28.60	28.31	0.0257372	0.0312500	4.03E+04	3.57E+04	5.23E+04	77.05	68.29
15.82	224-16 hrs	27.71	29.34	28.91	0.0303955	0.0283600	3.18E+04	2.25E+04	3.60E+04	88.20	62.39
19.74	224-16 hrs	28.22	29.98	29.80	0.0395549	0.0337259	2.27E+04	1.51E+04	2.07E+04	109.50	72.68
0.00	224-24 hrs	19.26	20.76	30.33	1.0000000	1.0000000	8.45E+06	4.84E+06	1.49E+04	56689.57	32455.26
7.76	224-24 hrs	25.11	26.80	30.42	0.0184530	0.0161760	1.77E+05	1.10E+05	1.41E+04	1256.55	782.32
11.95	224-24 hrs	27.10	28.97	30.32	0.0043343	0.0033538	4.76E+04	2.83E+04	1.50E+04	317.08	188.97
15.82	224-24 hrs	28.02	30.04	29.35	0.0011694	0.0008155	2.59E+04	1.45E+04	2.74E+04	94.47	52.92
19.74	224-24 hrs	28.92	30.35	30.62	0.0015113	0.0015864	1.43E+04	1.19E+04	1.24E+04	114.79	95.98
0.00	224-36 hrs	17.65	18.65	30.76	1.0000000	1.0000000	2.45E+07	1.81E+07	1.14E+04	214572.35	158875.57
7.76	224-36 hrs	22.42	23.72	30.09	0.0230355	0.0187106	1.05E+06	7.58E+05	1.73E+04	6052.92	4382.33
11.95	224-36 hrs	25.82	27.50	30.02	0.0020788	0.0012975	1.11E+05	7.11E+04	1.81E+04	612.99	393.62
15.82	224-36 hrs	27.32	28.74	30.21	0.0008384	0.0006267	4.11E+04	3.27E+04	1.61E+04	256.06	203.81
19.74	224-36 hrs	28.50	29.81	30.66	0.0005055	0.0004078	1.89E+04	1.68E+04	1.21E+04	155.32	137.98
0.00	224-48 hrs	17.45	18.66	31.35	1.0000000	1.0000000	2.79E+07	1.80E+07	7.91E+03	353386.40	227837.66
7.76	224-48 hrs	20.10	21.34	29.66	0.0493776	0.0483614	4.85E+06	3.36E+06	2.26E+04	21457.77	14883.50
11.95	224-48 hrs	24.23	25.58	30.27	0.0043043	0.0039063	3.17E+05	2.37E+05	1.55E+04	2047.35	1529.65
15.82	224-48 hrs	26.85	28.23	30.28	0.0007050	0.0006267	5.61E+04	4.50E+04	1.54E+04	364.84	292.95
19.74	224-48 hrs	29.65	30.83	31.64	0.0002599	0.0002653	8.82E+03	8.85E+03	6.60E+03	133.61	133.98

Irradiance (mW/cm2)			Viability at 10^-x dilution								
0.039168451	Fluence	Sample	0	-1	-2	-3	-4	-5	N	N/No	Log Reduction
Time (min)	mJ/cm2								pfu/ml		
0.000	0	Control				TNTC	230	33	4125000	1	0
3.300	7.7553533	1			TNTC	TNTC	22		275000	0.066666667	-1.176091259
5.083	11.946378	2		TNTC	TNTC	26			32500	0.007878788	-2.103540592
6.733	15.824054	3		TNTC	26				3250	0.000787879	-3.103540592
8.4	19.740899	4		46					575	0.000139394	-3.855756108

UV_{224} mRNA A

Fluence (mJ/cm2)	Sample	Cq E1A	Cq Hexon	Cq Actin	Relative Quantification E1A	Relative Quantification Hexon	Absolute E1A	Absolute Hexon	Absolute Actin
0.00	224-4hrs	27.58		26.21	1.0000000	1.0000000	1731.51		9651.77
6.71	224-4hrs	29.52		27.20	0.5176325		480.57		5215.89
10.07	224-4hrs	32.64		26.49	0.0363979		61.16		8109.86
13.43	224-4hrs			26.66					7296.54
16.78	224-4hrs			26.53					7910.68
22.04	220-4hrs			26.14					10081.05
0.00	224-12 hrs	22.62	30.64	30.17	1.0000000	1.0000000	45884.63	498.13	823.18
6.71	224-12 hrs	25.18		30.68	0.2414841		8454.55		599.52
10.07	224-12 hrs	28.01		30.16	0.0236831		1303.28		828.31
13.43	224-12 hrs	31.69		29.45	0.0011296		114.57		1287.89
16.78	224-12 hrs			31.35					395.29
22.04	220-12 hrs			31.00					491.37
0.00	224-16 hrs	22.13	23.77	27.57	1.0000000	1.0000000	63426.37	36745.29	4144.16
6.71	224-16 hrs	24.16	30.23	26.56	0.1215819	0.0056403	16587.21	643.89	7764.52
10.07	224-16 hrs	27.30		27.06	0.0195052		2083.38		5690.17
13.43	224-16 hrs	30.64		27.28	0.0022436		229.29		4962.84
16.78	224-16 hrs	33.75		28.97	0.0008384		29.38		1735.67
22.04	220-16 hrs			27.11					5516.03
0.00	224-24 hrs	20.44	17.44	26.84	1.0000000	1.0000000	193733.76	1933061.62	6524.10
6.71	224-24 hrs	23.94	21.60	26.95	0.0953912	0.0603710	19182.32	142953.97	6092.89
10.07	224-24 hrs	27.43	27.39	25.72	0.0036195	0.0004652	1911.91	3810.40	13088.70
13.43	224-24 hrs	31.52	32.51	25.98	0.0002545	0.0000160	128.19	154.49	11135.31
16.78	224-24 hrs	33.85		27.72	0.0001691		27.50		3775.20
22.04	220-24 hrs			27.45					4465.13
0.00	224-36 hrs	21.34	16.09	27.17	1.0000000	1.0000000	106894.57	4500834.11	5314.08
6.71	224-36 hrs	24.49	19.98	27.49	0.1406323	0.0842021	13337.73	394142.24	4355.47
10.07	224-36 hrs	27.36	24.02	26.04	0.0070410	0.0018736	2002.41	31421.72	10727.62
13.43	224-36 hrs	29.84	26.42	25.64	0.0009565	0.0002690	388.98	6993.61	13756.08
16.78	224-36 hrs	33.75	30.64	28.18	0.0003700	0.0000840	29.38	498.13	2836.28
22.04	220-36 hrs		30.63	26.69		0.0000301		501.25	7161.72
0.00	224-48 hrs	22.63	15.93	29.44	1.0000000	1.0000000	45582.47	4975020.90	1295.92
6.71	224-48 hrs	24.42	19.03	28.04	0.1095757	0.0441942	13969.09	714406.73	3094.19
10.07	224-48 hrs	26.80	21.80	26.95	0.0098887	0.0030436	2898.95	126130.13	6092.89
13.43	224-48 hrs	29.41	25.79	27.47	0.0023227	0.0002747	516.79	10375.05	4409.96
16.78	224-48 hrs	32.65	29.49	28.04	0.0003650	0.0000314	60.76	1023.31	3094.19
22.04	224-48 hrs	34.16	29.54	27.85	0.0001123	0.0000266	22.40	991.78	3482.11

Irradiance	Fluence (mJ/cm2)	Viability at 10^-x dilution							
0.011893261		-1	-2	-3	-4	-5	N	N/No	
Time min							pfu/ml		Log reduction
0.00	0			TNTC	TNTC	40	5000000	1	0
9.40	6.707799386	TNTC	TNTC	159	45	-	380625	0.076125	-1.118472694
14.12	10.07359234	TNTC	TNTC	43			53750	0.01075	-1.968591536
18.82	13.42749203	TNTC	124				15500	0.0031	-2.508638306
23.52	16.78139173	221					2762.5	0.0005525	-3.257667718
30.88	22.03821323	35					437.5	0.0000875	-4.057991947

UV_{224} mRNA B

Fluence (mJ/cm2)	Sample	Cq E1A	Cq Hexon	Cq Actin	Relative Quantification E1A	Relative Quantification Hexon	Absolute E1A	Absolute Hexon	Absolute Actin
0.00	224-4hrs	25.47		27.14	1.0000000	1.0000000	6980.34		5414.11
4.79	224-4hrs	28.35		26.23	0.0722930		1041.07		9532.52
9.62	224-4hrs	30.21		25.77	0.0144779		304.62		12688.13
15.62	224-4hrs			27.34					4781.14
19.24	224-4hrs			26.88					6363.87
24.03	220-4hrs			26.33					8957.97
0.00	224-12 hrs	21.29	24.79	28.57	1.0000000	1.0000000	110484.88	19403.36	2225.66
4.79	224-12 hrs	25.02	32.10	28.07	0.0532897	0.0044561	9397.27	199.70	3037.02
9.62	224-12 hrs	26.14		26.82	0.0103087		4483.57		6605.72
15.62	224-12 hrs	28.89		27.05	0.0017972		728.67		5725.66
19.24	224-12 hrs			27.81					3569.78
24.03	224-12 hrs			26.52					7960.01
0.00	224-16 hrs	20.03	18.82	28.41	1.0000000	1.0000000	254010.90	814782.67	2458.41
4.79	224-16 hrs	24.23	26.02	27.39	0.0268302	0.0033538	15837.53	8983.72	4634.82
9.62	224-16 hrs	25.79	30.64	26.22	0.0040440	0.0000606	5650.08	498.13	9591.96
15.62	224-16 hrs	27.11		28.26	0.0066612		2362.05		2698.68
19.24	224-16 hrs	30.01		28.88	0.0013715		347.66		1835.54
24.03	224-16 hrs			27.50					4328.48
0.00	224-24 hrs	18.86	14.52	28.53	1.0000000	1.0000000	550271.34	12026947.94	2281.69
4.79	224-24 hrs	21.97	19.45	27.53	0.0579118	0.0164018	70498.67	549228.47	4248.50
9.62	224-24 hrs	24.24	24.15	27.37	0.0107464	0.0005648	15733.23	28965.74	4692.80
15.62	224-24 hrs	27.11	28.38	27.47	0.0015755	0.0000323	2362.05	2050.23	4409.96
19.24	224-24 hrs	30.03		27.44	0.0002039		343.09		4492.97
24.03	224-24 hrs			27.48					4382.63
0.00	224-36 hrs	19.06	13.31	28.54	1.0000000	1.0000000	482156.56	25653024.40	2267.55
4.79	224-36 hrs	20.97	16.83	28.22	0.2131587	0.0698304	136497.58	2832022.53	2766.63
9.62	224-36 hrs	24.24	20.54	26.65	0.0074425	0.0017972	15733.23	277585.21	7342.04
15.62	224-36 hrs	27.78	24.18	27.41	0.0010836	0.0002441	1517.18	28426.80	4577.55
19.24	224-36 hrs	28.80	27.24	27.29	0.0004917	0.0000269	773.31	4185.57	4932.08
24.03	224-36 hrs	31.69	30.53	27.29	0.0000663	0.0000028	114.57	533.64	4932.08
0.00	224-48 hrs	19.30	13.31	27.29	1.0000000	1.0000000	411454.21	25653024.40	4932.08
4.79	224-48 hrs	21.76	15.73	27.12	0.1065794	0.1660857	81259.45	5638613.00	5481.85
9.62	224-48 hrs	24.45	18.86	25.98	0.0074425	0.0086086	13694.93	794632.47	11135.31
15.62	224-48 hrs	26.18	22.31	26.75	0.0010836	0.0013433	4366.63	91655.08	6899.52
19.24	224-48 hrs	29.47	25.15	27.81	0.0003090	0.0003925	496.71	15536.64	3569.78
24.03	224-48 hrs	31.17	28.87	27.88	0.0000663	0.0000312	161.55	1508.62	3417.77

Irradiance									
0.041640321		Viability at 10^-x dilution							
Time	Fluence	0	-1	-2	-3	-4	N	N/No	Log N/No
(min)	mJ/cm2						pfu/ml		
0.0000	0.0000				TNTC	51	637500	1	0.0000
1.9167	4.7886			TNTC	82	10	102500	0.160784314	-0.7938
3.8500	9.6189		TNTC	89	10		11125	0.01745098	-1.7582
6.2500	15.6151		75	3			937.5	0.001470588	-2.8325
7.7000	19.2378	122	11				152.5	0.000239216	-3.6212
9.6167	24.0265	30					37.5	5.88235E-05	-4.2304

UV_{254} DNA A

Fluence (mJ/cm2)	Sample	Cq E1A	Cq Hexon	Cq Actin	Relative Quantification E1A	Relative Quantification Hexon	Absolute E1A copies	Absolute Hexon copies	Absolute Actin copies	E1A/ 100ACTIN	HEXON/ 100ACTIN
0.00	254-0hrs	26.72	28.47	30.08	1.000000	1.000000	6.11E+04	3.88E+04	1.74E+04	351.08	222.61
19.08	254-0hrs	26.54	28.09	29.70	0.870551	1.000000	6.88E+04	4.92E+04	2.21E+04	312.22	222.98
38.16	254-0hrs	26.12	27.75	28.84	0.641713	0.697372	9.09E+04	6.08E+04	3.76E+04	241.43	161.63
76.24	254-0hrs	26.55	28.06	29.37	0.687771	0.812252	6.84E+04	5.01E+04	2.71E+04	252.64	185.07
114.40	254-0hrs	27.26	28.68	29.75	0.547147	0.687771	4.28E+04	3.40E+04	2.14E+04	200.15	158.98
152.56	254-0hrs	27.52	29.21	29.62	0.417544	0.435275	3.60E+04	2.44E+04	2.32E+04	155.48	105.23
0.00	254-4hrs	28.03	30.08	29.03	1.000000	1.000000	2.57E+04	1.41E+04	3.34E+04	76.92	42.30
19.08	254-4hrs	28.65	29.71	30.41	0.7022224	0.5783441	1.71E+04	1.78E+04	1.42E+04	120.42	125.75
38.16	254-4hrs	28.50	29.58	29.88	0.5396141	0.4383029	1.89E+04	1.93E+04	1.97E+04	95.64	98.12
76.24	254-4hrs	28.18	30.43	28.62	0.678302	0.590496	2.33E+04	1.14E+04	4.32E+04	53.99	26.33
114.40	254-4hrs	27.51	30.32	28.27	0.846745	0.500000	3.63E+04	1.22E+04	5.36E+04	67.62	22.69
152.56	254-4hrs	27.71	30.37	28.93	1.164734	0.763130	3.18E+04	1.18E+04	3.56E+04	89.30	33.15
0.00	254-12hrs	29.45	30.60	30.44	1.000000	1.000000	1.01E+04	1.02E+04	1.39E+04	72.32	73.39
19.08	254-12hrs	27.98	29.34	28.87	0.1126563	0.0830429	2.66E+04	2.25E+04	3.69E+04	71.98	60.86
38.16	254-12hrs	26.47	27.49	27.23	0.1029489	0.0960547	7.21E+04	7.16E+04	1.02E+05	70.42	69.91
76.24	254-12hrs	30.13	31.38	29.31	0.285191	0.266093	6.42E+03	6.27E+03	2.81E+04	22.86	22.31
114.40	254-12hrs	30.09	31.56	29.57	0.351111	0.281265	6.60E+03	5.60E+03	2.39E+04	27.59	23.43
152.56	254-12hrs	29.80	31.71	30.27	0.697372	0.411796	7.99E+03	5.10E+03	1.55E+04	51.63	32.96
0.00	254-16hrs	20.94	21.60	28.98	1.000000	1.000000	2.78E+06	2.86E+06	3.45E+04	8071.72	8287.61
19.08	254-16hrs	30.21	31.06	28.93	0.0349152	0.0332616	6.09E+03	7.66E+03	3.56E+04	17.12	21.52
38.16	254-16hrs	29.46	29.78	27.48	0.0214928	0.0295643	1.00E+04	1.71E+04	8.77E+04	11.41	19.47
76.24	254-16hrs	27.75	28.69	28.24	0.005336	0.004395	3.10E+04	3.38E+04	5.46E+04	56.64	61.80
114.40	254-16hrs	29.01	29.98	28.89	0.003496	0.002820	1.35E+04	1.51E+04	3.65E+04	36.90	41.28
152.56	254-16hrs	28.76	29.74	29.06	0.004678	0.003747	1.59E+04	1.75E+04	3.28E+04	48.38	53.32
0.00	254-24hrs	17.74	18.11	29.58	1.000000	1.000000	2.31E+07	2.54E+07	2.38E+04	97089.95	106979.74
19.08	254-24hrs	25.70	26.96	29.27	0.0070410	0.0050483	1.20E+05	9.97E+04	2.88E+04	416.30	346.27
38.16	254-24hrs	27.83	29.11	29.27	0.0016086	0.0011374	2.94E+04	2.60E+04	2.88E+04	101.91	90.13
76.24	254-24hrs	28.07	28.70	28.37	0.000336	0.000280	2.51E+04	3.36E+04	5.04E+04	49.70	66.58
114.40	254-24hrs	29.54	30.21	28.21	0.000109	0.000088	9.49E+03	1.30E+04	5.57E+04	17.04	23.42
152.56	254-24hrs	28.95	29.65	28.39	0.000185	0.000147	1.40E+04	1.85E+04	4.98E+04	28.14	37.19
0.00	254-36hrs	15.95	17.23	29.48	1.0000000	1.0000000	7.53E+07	4.41E+07	2.53E+04	297718.82	174407.10
19.08	254-36hrs	18.91	19.25	28.92	0.1088188	0.1022378	1.06E+07	1.24E+07	3.58E+04	29734.73	34766.80
38.16	254-36hrs	21.73	22.35	29.06	0.0169802	0.0131390	1.65E+06	1.79E+06	3.28E+04	5033.60	5446.44
76.24	254-36hrs	25.94	27.99	28.72	0.000581	0.000341	1.02E+05	5.23E+04	4.06E+04	252.38	129.09
114.40	254-36hrs	28.12	30.44	28.76	0.000132	0.000064	2.42E+04	1.13E+04	3.96E+04	61.28	28.55
152.56	254-36hrs	28.27	30.96	28.03	0.000072	0.000027	2.20E+04	8.15E+03	6.23E+04	35.25	13.09
0.00	254-48hrs	15.59	16.67	29.97	1.0000000	1.0000000	9.55E+07	6.26E+07	1.86E+04	512148.09	335822.85
19.08	254-48hrs	17.58	18.80	29.48	0.1792444	0.1626677	2.56E+07	1.65E+07	2.53E+04	101411.57	65268.22
38.16	254-48hrs	19.47	20.77	29.16	0.0387409	0.0332616	7.35E+06	4.81E+06	3.08E+04	23843.51	15584.45
76.24	254-48hrs	23.03	24.18	29.28	0.0035697	0.0034006	7.00E+05	5.69E+05	2.86E+04	2444.82	1985.89
114.40	254-48hrs	25.86	27.03	28.73	0.0003429	0.0003221	1.08E+05	9.55E+04	4.03E+04	267.74	236.91
152.56	254-48hrs	28.21	29.11	28.40	0.0000535	0.0000606	2.28E+04	2.60E+04	4.95E+04	46.16	52.48

Irradiance		Fluence	Viability at 10^-x dilution								
mW/cm2	Time	UV Dose	0	-1	-2	-3	-4	-5	N	N/No	Log N/No
0.069629448	(min)	(mJ/cm2)							pfu/ml		
	0	0				TNTC	TNTC	36	4500000	1	0
	4.566666667	19.078469			TNTC	TNTC	65		812500	0.180555556	-0.743389144
	9.133333333	38.156938		TNTC	TNTC	79		-	98750	0.021944444	-1.658675409
	18.25	76.244246	-	TNTC	67	-			8375	0.001861111	-2.730227698
	27.38333333	114.40118	TNTC	42	-				525	0.000116667	-3.93305321
	36.51666667	152.55812	34						42.5	9.44444E-06	-5.024823584

UV_{254} DNA B

Fluence (mJ/cm2)	Sample	Cq E1A	Cq Hexon	Cq Actin	Relative Quantification E1A	Relative Quantification Hexon	Absolute E1A copies	Absolute Hexon copies	Absolute Actin copies	E1A/ 100ACTIN	HEXON/ 100ACTIN
0.00	254-0hrs	26.72	28.47	30.08	1.000000	1.000000	6.11E+04	3.88E+04	1.74E+04	351.08	222.61
19.02	254-0hrs	26.54	28.09	29.70	0.870551	1.000000	6.88E+04	4.92E+04	2.21E+04	312.22	222.98
38.04	254-0hrs	26.12	27.75	28.84	0.641713	0.697372	9.09E+04	6.08E+04	3.76E+04	241.43	161.63
76.16	254-0hrs	26.55	28.06	29.37	0.687771	0.812252	6.84E+04	5.01E+04	2.71E+04	252.64	185.07
114.03	254-0hrs	27.26	28.68	29.75	0.547147	0.687771	4.28E+04	3.40E+04	2.14E+04	200.15	158.98
152.07	254-0hrs	27.52	29.21	29.62	0.417544	0.435275	3.60E+04	2.44E+04	2.32E+04	155.48	105.23
0.00	254-4hrs	26.52	27.42	30.05	1.000000	1.000000	6.98E+04	7.48E+04	1.77E+04	393.27	421.62
19.02	254-4hrs	26.43	27.64	28.46	0.3535534	0.2851909	7.40E+04	6.52E+04	4.77E+04	155.33	136.72
38.04	254-4hrs	27.44	28.58	29.39	0.3344819	0.2832210	3.80E+04	3.62E+04	2.67E+04	142.08	135.32
76.16	254-4hrs	27.07	28.13	28.93	0.314253	0.281265	4.85E+04	4.80E+04	3.56E+04	136.30	134.74
114.03	254-4hrs	26.77	27.65	29.69	0.655197	0.664343	5.91E+04	6.48E+04	2.22E+04	266.54	291.88
152.07	254-4hrs	28.23	29.53	29.29	0.180491	0.136787	2.25E+04	2.00E+04	2.85E+04	79.22	70.16
0.00	254-12hrs	26.16	27.41	30.02	1.000000	1.000000	8.85E+04	7.53E+04	1.81E+04	489.66	416.43
19.02	254-12hrs	25.77	26.65	28.86	0.5864175	0.7578583	1.15E+05	1.21E+05	3.72E+04	308.06	325.84
38.04	254-12hrs	28.04	28.85	29.77	0.2284579	0.3099269	2.56E+04	3.06E+04	2.11E+04	121.04	144.72
76.16	254-12hrs	28.05	29.05	29.47	0.184284	0.219151	2.54E+04	2.70E+04	2.54E+04	99.79	105.96
114.03	254-12hrs	29.53	30.32	30.59	0.143587	0.197510	9.55E+03	1.22E+04	1.27E+04	75.30	95.99
152.07	254-12hrs	27.99	28.95	30.13	0.303549	0.371131	2.64E+04	2.87E+04	1.69E+04	156.49	170.03
0.00	254-16hrs	19.31	20.49	28.42	1.000000	1.000000	8.17E+06	5.73E+06	4.89E+04	16730.05	11722.92
19.02	254-16hrs	28.16	29.74	28.82	0.0028595	0.0021671	2.36E+04	1.75E+04	3.81E+04	61.95	45.93
38.04	254-16hrs	28.33	29.69	28.51	0.0020502	0.0018097	2.11E+04	1.81E+04	4.62E+04	45.66	39.08
76.16	254-16hrs	28.23	29.91	29.56	0.004550	0.003217	2.25E+04	1.57E+04	2.41E+04	93.70	65.41
114.03	254-16hrs	28.53	30.03	28.98	0.002472	0.001980	1.85E+04	1.46E+04	3.45E+04	53.59	42.31
152.07	254-16hrs	28.33	29.67	29.16	0.003217	0.002879	2.11E+04	1.83E+04	3.08E+04	68.40	59.28
0.00	254-24hrs	16.81	17.74	28.84	1.0000000	1.0000000	4.26E+07	3.20E+07	3.76E+04	113304.78	85136.48
19.02	254-24hrs	23.55	25.53	28.17	0.0058799	0.0028398	4.96E+05	2.44E+05	5.71E+04	869.68	427.79
38.04	254-24hrs	26.93	29.25	28.59	0.0007556	0.0002883	5.32E+04	2.38E+04	4.40E+04	121.03	54.10
76.16	254-24hrs	27.72	29.82	28.99	0.000577	0.000256	3.16E+04	1.66E+04	3.43E+04	92.08	48.55
114.03	254-24hrs	29.00	30.93	29.52	0.000343	0.000171	1.36E+04	8.31E+03	2.47E+04	54.95	33.69
152.07	254-24hrs	29.32	31.76	28.62	0.000147	0.000052	1.10E+04	4.94E+03	4.32E+04	25.42	11.45
0.00	254-36hrs	15.29	15.88	28.66	1.0000000	1.0000000	1.16E+08	1.03E+08	4.21E+04	276571.27	243909.76
19.02	254-36hrs	18.93	19.55	28.13	0.0555527	0.0544094	1.05E+07	1.03E+07	5.85E+04	17957.35	17632.57
38.04	254-36hrs	21.19	22.01	28.05	0.0109722	0.0093553	2.36E+06	2.21E+06	6.15E+04	3838.40	3596.46
76.16	254-36hrs	25.52	26.35	28.23	0.000618	0.000523	1.35E+05	1.46E+05	5.50E+04	245.63	265.76
114.03	254-36hrs	28.90	29.74	28.76	0.000086	0.000072	1.45E+04	1.75E+04	3.96E+04	36.60	44.25
152.07	254-36hrs	29.06	30.11	27.91	0.000043	0.000031	1.30E+04	1.39E+04	6.71E+04	19.41	20.69
0.00	254-48hrs	14.88	15.26	30.35	1.0000000	1.0000000	1.53E+08	1.51E+08	1.47E+04	1036854.04	1028164.39
19.02	254-48hrs	17.50	17.72	29.59	0.0960547	0.1073207	2.70E+07	3.24E+07	2.36E+04	114482.90	137415.97
38.04	254-48hrs	18.05	18.82	29.22	0.0507658	0.0387409	1.88E+07	1.63E+07	2.97E+04	63245.47	54836.49
76.16	254-48hrs	22.20	23.17	28.98	0.0024213	0.0016086	1.21E+06	1.07E+06	3.45E+04	3510.89	3101.46
114.03	254-48hrs	28.11	29.39	29.86	0.0000741	0.0000397	2.44E+04	2.18E+04	2.00E+04	122.22	109.15
152.07	254-48hrs	29.60	30.56	29.70	0.0000236	0.0000158	9.12E+03	1.05E+04	2.21E+04	41.34	47.50

			Viability at 10^-x dilution								
Irradiance	Fluence	Time	0	-1	-2	-3	-4	-5	N	N/No	Log N/No
mW/cm2	(mJ/cm2)	(min)							pfu/ml		
0.07957694	0	0					159	3	1987500	1	0
	19.01888855	3.9833333				114	28		350000	0.176100629	-0.75423909
	38.0377771	7.9666667			TNTC	35		-	43750	0.022012579	-1.65732908
	76.15513114	15.95		TNTC	70	-			8750	0.004402516	-2.35629908
	114.0337544	23.883333		26	-				325	0.000163522	-3.78642378
	152.0715315	31.85	30						37.5	1.88679E-05	-4.72427587

UV_{254} 48 hpi DNA

Fluence mJ/cm2	254 NEW A	Cq E1A	Cq Actin	Relative Quantification E1A	Log Reduction
0	254	13.63	27.11	1.0000000	0
19.07427414	254	15.9	26.63	0.148650889	-0.82783249
38.14854827	254	17.6	26.15	0.032803646	-1.48407788
76.2274824	254	21.42	26.55	0.003064782	-2.51360046
114.3760307	254	25.43	26.43	0.000175043	-3.75685435
152.5245789	254	28.32	26.27	2.11351E-05	-4.67499583
	254 NEW B				
0	254	12.11	25.76	1	0
20.83616987	254	14.78	25.93	0.176776695	-0.75257499
38.37547743	254	17.1	26.09	0.039554894	-1.40279978
76.68501761	254	20.56	26.09	0.003594483	-2.44436356
115.060495	254	23.68	25.9	0.000362433	-3.44077285
153.4359725	254	28.04	25.87	1.72864E-05	-4.76229453

Assay	Average Fluence mJ/cm2	Average Log Reduction	Standard Deviation (Fluence)	Standard Deviation (Log Reduction)
DNA 48 hpi E1A	**0**	**0**	0	0
	19.955222	**-0.79020374**	0.88094787	0.053215088
	38.262013	**-1.44343883**	0.11346458	0.057472295
	76.45625	**-2.47898201**	0.2287676	0.048957881
	114.71826	**-3.5988136**	0.34223218	0.223503369
	152.98028	**-4.71864518**	0.45569676	0.061729502
Plaque assay	**0**	**0**	0	0
	19.048679	**-0.74881412**	0.04212963	0.007672072
	38.339687	**-1.49168747**	0.42696458	0.288066427
	76.354618	**-2.4329434**	0.2821176	0.267333407
	114.97927	**-3.72933269**	1.33716313	0.237470142
	153.53768	**-4.84534154**	2.073453	0.158560986

Irradiance			Viability at 10^-x dilution								
0.069629448	Time	Fluence	0	-1	-2	-3	-4	-5	N	N/No	Log N/N0
mW/cm2	(min)	(mJ/cm2)							pfu/ml		
	0	0				TNTC	TNTC	36	4500000	1	0
	4.56666667	19.078469			TNTC	TNTC	65		812500	0.18055556	-0.743389144
	9.13333333	38.156938		TNTC	TNTC	79		-	98750	0.02194444	-1.658675409
	18.25	76.244246	-	TNTC	67	-			8375	0.00186111	-2.730227698
	27.3833333	114.40118	TNTC	42	-				525	0.00011667	-3.93305321
	36.5166667	152.55812	34						42.5	9.4444E-06	-5.024823584

			Viability at 10^-x dilution								
Irradiance	Time	Fluence	0	-1	-2	-3	-4	-5	N	N/No	Log N/N0
mW/cm2	(min)	(mJ/cm2)							pfu/ml		
0.072908672	0	0				TNTC	TNTC	30	3750000	1	0
	8.83333333	38.641596			TNTC	226	19		260000	0.06933333	-1.15905792
	17.5	76.554106		TNTC	184				23000	0.00613333	-2.212303432
	26.5	115.92479	-	102	12				1275	0.00034	-3.468521083
	35.4333333	155.00384	49	1	-				61.25	1.6333E-05	-4.786925175

			Viability at 10^-x dilution								
Irradiance	Time	Fluence	0	-1	-2	-3	-4	-5	N	N/No	Log N/N0
mW/cm2	(min)	(mJ/cm2)							pfu/ml		
0.07957694	0	0					159	3	1987500	1	0
	3.98333333	19.018889				114	28		350000	0.17610063	-0.754239093
	7.96666667	38.037777			TNTC	35		-	43750	0.02201258	-1.65732908
	15.95	76.155131		TNTC	70	-			8750	0.00440252	-2.356299084
	23.8833333	114.03375		26	-				325	0.00016352	-3.786423776
	31.85	152.07153	30						37.5	1.8868E-05	-4.72427587

UV_{254} mRNA A

Fluence (mJ/cm2)	Sample	Cq E1A	Cq Hexon	Cq Actin	Relative Quantification E1A	Relative Quantification Hexon	Absolute E1A	Absolute Hexon	Absolute Actin
0.00	254-4hrs	32.06		30.26	1.0000000	1.0000000	89.73		778.39
19.08	254-4hrs	32.84		29.54	0.3535534		53.59		1217.81
38.16	254-4hrs			28.94					1768.34
76.24	254-4hrs			29.35					1370.49
114.40	254-4hrs			30.06					881.44
152.56	254-4hrs			28.41					2458.41
0.00	254-12hrs	24.47	32.70	28.13	1.0000000	1.0000000	13515.15	137.17	2925.83
19.08	254-12hrs	25.87		28.52	0.4965462		5359.19		2295.92
38.16	254-12hrs	26.90		27.01	0.0853775		2713.61		5869.82
76.24	254-12hrs	28.08		27.29	0.0457527		1244.38		4932.08
114.40	254-12hrs	29.70		28.56	0.0358968		426.68		2239.54
152.56	254-12hrs	30.88		27.82	0.0094859		195.66		3547.66
0.00	254-16hrs	22.76	25.88	28.79	1.0000000	1.0000000	41830.70	9806.64	1941.17
19.08	254-16hrs	24.46		28.71	0.2911834		13604.74		2040.15
38.16	254-16hrs	25.13		28.46	0.1538931		8738.52		2383.17
76.24	254-16hrs	28.05		28.98	0.0291573		1269.29		1724.91
114.40	254-16hrs	28.56		29.56	0.0306069		906.19		1202.76
152.56	254-16hrs	29.77		27.17	0.0025241		407.40		5314.08
0.00	254-24hrs	22.16	19.95	28.97	1.0000000	1.0000000	62181.55	401614.69	1735.67
19.08	254-24hrs	23.70	28.83	28.86	0.3186402	0.0019667	22478.52	1546.87	1858.51
38.16	254-24hrs	23.55	30.79	27.16	0.1088188	0.0001556	24820.43	453.48	5347.22
76.24	254-24hrs	24.48	32.79	27.65	0.0802141	0.0000546	13426.15	129.65	3943.10
114.40	254-24hrs	26.41		27.29	0.0164018		3751.02		4932.08
152.56	254-24hrs	27.90		26.09	0.0025417		1401.53		10399.31
0.00	254-36hrs	21.25	16.64	27.05	1.0000000	1.0000000	113443.76	3189739.48	5725.66
19.08	254-36hrs	22.91	21.17	27.99	0.6070974	0.0830429	37883.80	187114.56	3191.87
38.16	254-36hrs								
76.24	254-36hrs	24.40	29.22	26.38	0.0708052	0.0001026	14154.90	1211.76	8683.82
114.40	254-36hrs	26.55		28.09	0.0521930		3419.61		2999.49
152.56	254-36hrs	28.12		26.42	0.0055243		1211.92		8470.55
0.00	254-48hrs	22.22	15.69	28.37	1.0000000	1.0000000	59764.72	5781596.30	2520.31
19.08	254-48hrs	22.16	18.05	27.52	0.5783441	0.1080672	62181.55	1319455.33	4274.99
38.16	254-48hrs	24.72	21.23	28.96	0.2660925	0.0323520	11457.37	180216.42	1746.49
76.24	254-48hrs	25.38	23.63	27.22	0.0504151	0.0018350	7408.01	40111.21	5151.44
114.40	254-48hrs	26.72	28.34	28.27	0.0412346	0.0001452	3056.30	2102.22	2681.96
152.56	254-48hrs	27.94	32.72	26.45	0.0050134	0.0000020	1364.98	135.46	8314.04

UV_{254} mRNA B

Fluence (mJ/cm2)	Sample	Cq E1A	Cq Hexon	Cq Actin	Relative Quantification E1A	Relative Quantification Hexon	Absolute E1A	Absolute Hexon	Absolute Actin
0.00	254-4hrs	24.13		27.31	1.0000000	1.0000000	16919.28		4871.14
19.02	254-4hrs	29.02		27.65	0.0426888		668.69		3943.10
38.04	254-4hrs			27.79					3614.44
76.16	254-4hrs			27.79					3614.44
114.03	254-4hrs			27.77					3659.66
152.07	254-4hrs			27.98					3211.78
0.00	254-12hrs	21.22	25.62	27.05	1.0000000	1.0000000	115714.81	11540.14	5725.66
19.02	254-12hrs	22.90	31.63	27.12	0.3275984	0.0162885	38134.93	268.02	5481.85
38.04	254-12hrs	24.03		26.56	0.1015315		18074.91		7764.52
76.16	254-12hrs	27.22		27.52	0.0216423		2196.47		4274.99
114.03	254-12hrs	29.85		28.36	0.0062584		386.42		2536.03
152.07	254-12hrs			26.88					6363.87
0.00	254-16hrs	20.75	18.67	27.52	1.0000000	1.0000000	157852.93	895003.67	4274.99
19.02	254-16hrs	22.57	29.54	27.54	0.2871746	0.0005418	47425.78	991.78	4222.17
38.04	254-16hrs	23.56	31.65	27.57	0.1476241	0.0001281	24656.98	264.69	4144.16
76.16	254-16hrs	26.55		28.15	0.0277763		3419.61		2889.68
114.03	254-16hrs	27.39		27.72	0.0115177		1963.11		3775.20
152.07	254-16hrs	29.41		27.07	0.0018097		516.79		5654.91
0.00	254-24hrs	20.65	14.37	29.06	1.0000000	1.0000000	168634.74	13211084.35	1641.23
19.02	254-24hrs	20.97	22.58	27.51	0.2735734	0.0011533	136497.58	77401.09	4301.65
38.04	254-24hrs	23.41	28.78	27.87	0.0647041	0.0000201	27225.85	1596.06	3439.09
76.16	254-24hrs	25.69		28.41	0.0193704		6036.00		2458.41
114.03	254-24hrs	26.99		29.12	0.0128686		2556.95		1581.14
152.07	254-24hrs	29.59		26.95	0.0004716		458.85		6092.89
0.00	254-36hrs	20.65	14.02	28.66	1.0000000	1.0000000	168634.74	16447461.51	2104.55
19.02	254-36hrs	20.34	17.95	27.24	0.4632940	0.0245183	206966.33	1404699.35	5087.79
38.04	254-36hrs	22.90	22.51	27.37	0.0859714	0.0011374	38134.93	80868.45	4692.80
76.16	254-36hrs	24.67	29.24	27.47	0.0270168	0.0000115	11842.19	1196.69	4409.96
114.03	254-36hrs	26.34		27.63	0.0094859		3928.58		3992.43
152.07	254-36hrs	29.02		28.38	0.0024894		668.69		2504.69
0.00	254-48hrs	20.83	14.72	29.06	1.0000000	1.0000000	149725.96	10611531.12	1641.23
19.02	254-48hrs	20.93	16.40	29.00	0.8950251	0.2993697	140153.10	3706876.09	1703.60
38.04	254-48hrs	21.43	18.53	27.73	0.2624292	0.0283600	100723.47	976987.44	3751.80
76.16	254-48hrs	23.90	23.21	28.35	0.0727958	0.0017003	19696.04	52174.50	2551.84
114.03	254-48hrs	26.12	27.80	27.86	0.0111254	0.0000503	4543.21	2947.80	3460.53
152.07	254-48hrs	28.69	31.15	27.43	0.0013907	0.0000037	831.60	361.97	4520.99

UV_{280} DNA A

Fluence (mJ/cm2)	Sample	Cq E1A	Cq Hexon	Cq Actin	Relative Quantification E1A	Relative Quantification Hexon	Absolute E1A copies	Absolute Hexon copies	Absolute Actin copies	E1A/ 100ACTIN	HEXON/ 100ACTIN
0.00	280-0hrs	27.93	30.34	30.71	1.0000000	1.0000000	27480.48	12020.84	11768.86	233.50	102.14
29.35	280-0hrs	27.46	29.44	30.27	1.0210121	1.3755418	37487.64	21117.04	15471.23	242.31	136.49
58.71	280-0hrs	27.29	29.58	29.67	0.7578583	0.8235910	41943.88	19345.00	22465.28	186.71	86.11
117.42	280-0hrs	27.69	29.62	29.85	0.6506709	0.9075192	32202.60	18866.59	20087.03	160.32	93.92
0.00	280-4hrs	29.08	29.78	29.81	1.0000000	1.0000000	12854.01	17068.34	20592.78	62.42	82.89
29.35	280-4hrs	27.81	28.84	28.47	0.9526380	0.7578583	29747.99	30744.33	47368.10	62.80	64.91
58.71	280-4hrs	27.91	28.73	28.05	0.6643429	0.6113201	27846.03	32936.14	61500.25	45.28	53.55
117.42	280-4hrs	28.50	29.58	27.85	0.3842188	0.2952482	18856.73	19345.00	69642.21	27.08	27.78
0.00	280-12hrs	28.47	29.64	28.71	1.0000000	1.0000000	19234.22	18631.83	40802.91	47.14	45.66
29.35	280-12hrs	28.65	29.60	28.25	0.6417129	0.7474246	17077.52	19104.30	54310.18	31.44	35.18
58.71	280-12hrs	28.99	29.53	27.95	0.4117955	0.6372803	13641.55	19960.12	65444.74	20.84	30.50
117.42	280-12hrs	29.94	31.21	27.89	0.2044755	0.1907824	7282.27	6972.57	67931.85	10.72	10.26
0.00	280-16hrs	22.64	23.67	28.68	1.0000000	1.0000000	905645.83	782384.68	41571.00	2178.55	1882.04
29.35	280-16hrs	29.48	30.01	28.37	0.0070410	0.0099575	9868.73	14779.42	50406.18	19.58	29.32
58.71	280-16hrs	28.78	29.39	27.27	0.0053361	0.0071393	15671.91	21788.50	99875.75	15.69	21.82
117.42	280-16hrs	30.06	31.39	29.11	0.0078668	0.0063899	6727.19	6229.50	31819.97	21.14	19.58
0.00	280-24hrs	19.42	20.54	28.68	1.0000000	1.0000000	7601831.19	5551704.20	41571.00	18286.38	13354.75
29.35	280-24hrs	27.68	28.38	27.60	0.0015430	0.0020645	32416.07	41004.65	81351.80	39.85	50.40
58.71	280-24hrs	28.82	29.57	27.54	0.0006717	0.0008680	15263.15	19466.49	84443.43	18.08	23.05
117.42	280-24hrs	30.00	31.02	27.70	0.0003312	0.0003550	6999.23	7853.29	76448.56	9.16	10.27
0.00	280-36hrs	17.40	18.47	29.31	1.0000000	1.0000000	28876542.60	20287670.91	28099.86	102764.02	72198.49
29.35	280-36hrs	21.21	22.00	27.93	0.0273939	0.0332616	2329637.66	2225724.73	66263.49	3515.72	3358.90
58.71	280-36hrs	25.43	26.88	28.77	0.0026313	0.0020220	143345.65	104872.93	39309.04	364.66	266.79
117.42	280-36hrs	29.41	30.59	27.75	0.0000822	0.0000762	10335.87	10279.29	74108.91	13.95	13.87
0.00	280-48hrs	15.20	15.92	28.33	1.0000000	1.0000000	123544124.10	100125286.96	51675.29	239077.75	193758.53
29.35	280-48hrs	18.15	18.71	27.97	0.1008302	0.1126563	17592888.87	17457390.90	64636.10	27218.36	27008.73
58.71	280-48hrs	20.99	22.12	27.25	0.0085492	0.0064343	2694114.62	2064643.27	101125.25	2664.14	2041.67
117.42	280-48hrs	29.30	30.41	27.80	0.0000394	0.0000301	11115.04	11505.42	71840.85	15.47	16.02

Average			Viability at 10^-x dilution								
Irradiance		Fluence	0	-1	-2	-3	-4	-5	N	N/No	Log N/No
mW/cm2	Time (min)	mJ/cm2							pfu/ml		
0.04193	0.000	0				TNTC	TNTC	42	5250000	1	0
	11.667	29.3542189			TNTC	TNTC	70		875000	0.166666667	-0.77815125
	23.333	58.7084378		TNTC	TNTC	48			60000	0.011428571	-1.942008053
	46.667	117.416876	73						182.5	3.47619E-05	-4.458896435

UV_{280} DNA B

Fluence (mJ/cm2)	Sample	Cq E1A	Cq Hexon	Cq Actin	Relative Quantification E1A	Relative Quantification Hexon	Absolute E1A copies	Absolute Hexon copies	Absolute Actin copies	E1A/ 100ACTIN	HEXON/ 100ACTIN
0.00	280-0hrs	27.82	29.54	29.56	1.0000000	1.0000000	2.96E+04	1.98E+04	2.41E+04	122.85	82.46
28.98	280-0hrs	28.93	30.52	29.63	0.4863275	0.5321851	1.42E+04	1.07E+04	2.30E+04	61.63	46.63
57.70	280-0hrs	29.10	31.06	29.48	0.3895823	0.3298770	1.27E+04	7.66E+03	2.53E+04	50.18	30.29
115.26	280-0hrs	29.12	31.27	29.40	0.3634931	0.2698071	1.25E+04	6.72E+03	2.66E+04	47.11	25.27
0.00	280-4hrs	28.43	29.01	28.97	1.000000	1.000000	1.97E+04	2.76E+04	3.47E+04	56.89	79.62
28.98	280-4hrs	27.84	28.43	28.28	0.9330330	0.9265881	2.92E+04	3.97E+04	5.33E+04	54.71	74.55
57.70	280-4hrs	27.57	28.53	28.08	0.9794203	0.7526234	3.49E+04	3.73E+04	6.04E+04	57.75	61.84
115.26	280-4hrs	27.31	28.21	28.27	0.742262	0.668964	4.14E+04	4.56E+04	5.36E+04	77.17	85.03
0.00	280-12hrs	27.29	27.67	27.90	1.000000	1.000000	4.19E+04	6.40E+04	6.75E+04	62.13	94.73
28.98	280-12hrs	29.51	30.68	29.20	0.5285090	0.3056601	9.68E+03	9.72E+03	3.01E+04	32.16	32.29
57.70	280-12hrs	28.28	29.57	27.86	0.4897101	0.2606164	2.18E+04	1.95E+04	6.92E+04	31.51	28.13
115.26	280-12hrs	28.37	29.17	27.84	0.186856	0.205898	2.05E+04	2.50E+04	7.01E+04	29.32	35.68
0.00	280-16hrs	24.68	25.71	29.46	1.000000	1.000000	2.35E+05	2.18E+05	2.56E+04	919.15	852.24
28.98	280-16hrs	27.19	28.33	27.26	0.0382075	0.0354026	4.48E+04	4.23E+04	1.00E+05	44.59	42.10
57.70	280-16hrs	29.83	30.58	29.25	0.0243489	0.0295643	7.83E+03	1.03E+04	2.92E+04	26.85	35.46
115.26	280-16hrs	28.97	30.04	28.30	0.006258	0.004979	1.38E+04	1.45E+04	5.26E+04	26.26	27.55
0.00	280-24hrs	19.08	19.77	27.91	1.000000	1.000000	9.52E+06	8.99E+06	6.71E+04	14184.22	13400.02
28.98	280-24hrs	27.87	28.99	27.94	0.0023066	0.0017121	2.86E+04	2.80E+04	6.59E+04	43.42	42.50
57.70	280-24hrs	29.29	30.27	28.50	0.0012708	0.0010394	1.12E+04	1.26E+04	4.65E+04	24.07	27.01
115.26	280-24hrs	28.72	29.84	27.16	0.000425	0.000292	1.63E+04	1.64E+04	1.07E+05	15.25	15.37
0.00	280-36hrs	16.33	16.60	28.17	1.000000	1.000000	5.86E+07	6.54E+07	5.71E+04	102587.83	114599.10
28.98	280-36hrs	22.00	22.51	28.43	0.0235195	0.0199150	1.38E+06	1.62E+06	4.86E+04	2846.54	3330.61
57.70	280-36hrs	26.65	27.67	28.73	0.0011533	0.0006858	6.40E+04	6.40E+04	4.03E+04	158.86	158.70
115.26	280-36hrs	28.92	29.86	28.63	0.000110	0.000094	1.43E+04	1.62E+04	4.29E+04	33.32	37.86
0.00	280-48hrs	15.42	15.87	28.29	1.000000	1.000000	1.07E+08	1.03E+08	5.30E+04	201656.55	195009.62
28.98	280-48hrs	18.39	18.85	27.88	0.0960547	0.0953912	1.50E+07	1.60E+07	6.84E+04	21963.29	23396.02
57.70	280-48hrs	22.44	23.54	28.46	0.0086685	0.0055243	1.03E+06	8.49E+05	4.77E+04	2168.51	1780.66
115.26	280-48hrs	28.92	29.86	27.54	0.000143	0.000110	1.43E+04	1.62E+04	8.44E+04	16.92	19.23

Average			Viability at 10^-x dilution								
Irradiance		Fluence	0	-1	-2	-3	-4	-5	N	N/No	Log N/No
mW/cm2	Time min	mJ/cm2							pfu/ml		
0.044589648	0.000	0				TNTC	TNTC	31	3875000	1	0
	10.833	28.98327			TNTC	TNTC	43		537500	0.138709677	-0.857893238
	21.567	57.699		TNTC	TNTC	50			62500	0.016129032	-1.792391689
	43.08333333	115.2642	150	13					187.5	4.83871E-05	-4.315270435

UV_{280} 48 hpi DNA

				Viability at 10^-x dilution								
Average irradiance mW/cm2	Time (min)	Fluence mJ/cm2	Sample	0	-1	-2	-3	-4	-5	N pfu/ml	N/No	Log reduction
0.044589648	0.000	0	Control				TNTC	TNTC	31	3875000	1	0
	10.833	28.98327127	1			TNTC	TNTC	43		537500	0.13870968	-0.85789324
	21.567	57.69900466	2		TNTC	TNTC	50			62500	0.01612903	-1.79239169
	43.0833333	115.2642404	3	150	13					187.5	4.8387E-05	-4.31527043

Average				Viability at 10^-x dilution								
Irradiance	Time	Fluence	Sample	0	-1	-2	-3	-4	-5	N	N/No	Log
mW/cm2	(min)	mJ/cm2								pfu/ml		Reduction
0.0419346	0.000	0	Control				TNTC	TNTC	42	5250000	1	0
	11.667	29.35421892	1			TNTC	TNTC	70		875000	0.16666667	-0.77815125
	23.333	58.70843784	2		TNTC	TNTC	48			60000	0.01142857	-1.94200805
	46.667	117.4168757	3	73						182.5	3.4762E-05	-4.45889643

Fluence mJ/cm2	**Sample**	**Cq E1A**	**Cq Hexon**	**Cq Actin**	**Relative Quantification E1A**	**Relative Quantification Hexon**	**Absolute E1A copies**	**Absolute Hexon copies**	**Absolute Actin copies**	**E1A/ 100ACTIN**	**HEXON/ 100ACTIN**	**Log Reduction E1A**	**Log Reduction Hexon**
0	280-48hrs	15.20	15.92	28.33	1.0000000	1.0000000	1.24E+08	1.00E+08	5.17E+04	239077.75	193758.53	0	0
29.35421892	280-48hrs	18.15	18.71	27.97	0.1008302	0.1126563	1.76E+07	1.75E+07	6.46E+04	27218.36	27008.73	-0.99640929	-0.94824449
58.70843784	280-48hrs	20.99	22.12	27.25	0.0085492	0.0064343	2.69E+06	2.06E+06	1.01E+05	2664.14	2041.67	-2.06807607	-2.19149837
117.4168757	280-48hrs	29.30	30.41	27.80	0.0000394	0.0000301	1.11E+04	1.15E+04	7.18E+04	15.47	16.02	-4.40406884	-4.52147053
0	280-48hrs	15.42	15.87	28.29	1.0000000	1.0000000	1.07E+08	1.03E+08	5.30E+04	201656.55	195009.62	0	0
28.98327127	280-48hrs	18.39	18.85	27.88	0.0960547	0.0953912	1.50E+07	1.60E+07	6.84E+04	21963.29	23396.02	-1.01748139	-1.02049169
57.69900466	280-48hrs	22.44	23.54	28.46	0.0086685	0.0055243	1.03E+06	8.49E+05	4.77E+04	2168.51	1780.66	-2.06205547	-2.25772497
115.2642404	280-48hrs	28.92	29.86	27.54	0.0000513	0.0000365	1.43E+04	1.62E+04	8.44E+04	16.92	19.23	-4.28967744	-4.43718214

Assay	Average Fluence mJ/cm2	Average Log Reduction	Standard Deviation (Fluence)	Standard Deviation (Log Reduction)
Plaque assay	0	0	0	0
	29.1687451	-0.81802224	0.185473824	0.0563861
	58.2037212	-1.86719987	0.504716591	0.105794745
	116.340558	-4.38708343	1.076317655	0.101558918

E1A DNA extraction 48 hpi	0	0	0	0
	29.1687451	-1.00694534	0.185473824	0.014900225
	58.2037212	-2.06506577	0.504716591	0.004257207
	116.340558	-4.34687314	1.076317655	0.080886933

UV_{280} mRNA A

Fluence (mJ/cm2)	Sample	Cq E1A	Cq Hexon	Cq Actin	Relative Quantification E1A	Relative Quantification Hexon	Absolute E1A	Absolute Hexon	Absolute Actin
0.00	280-4hrs	24.04		28.99	1.0000000	1.0000000	17955.88		1714.22
28.98	280-4hrs	26.17		28.99	0.2284579		4395.58		1714.22
57.70	280-4hrs	30.04		28.97	0.0154099		340.83		1735.67
115.26	280-4hrs			28.11					2962.43
0.00	280-12hrs	24.06	29.27	28.33	1.0000000	1.0000000	17720.17	1174.42	2583.76
28.98	280-12hrs	25.37		28.49	0.4506252		7457.12		2339.14
57.70	280-12hrs	29.62		28.33	0.0211969		449.84		2583.76
115.26	280-12hrs			27.29					4932.08
0.00	280-16hrs	23.64	27.27	33.05	1.0000000	1.0000000	23387.53	4107.69	137.39
28.98	280-16hrs	24.61		31.31	0.1528300		12321.08		405.24
57.70	280-16hrs	27.83		34.26	0.1267449		1467.87		64.76
115.26	280-16hrs			31.22					428.56
0.00	280-24hrs	24.05	20.56	30.60	1.0000000	1.0000000	17837.64	274131.27	630.09
28.98	280-24hrs	24.74	29.91	27.46	0.0703162	0.0001738	11306.96	786.71	4437.46
57.70	280-24hrs	25.83		27.39	0.0314674		5502.71		4634.82
115.26	280-24hrs	31.69		26.84	0.0003700		114.57		6524.10
0.00	280-36hrs	23.24	18.89	30.03	1.0000000	1.0000000	30462.25	779847.53	898.03
28.98	280-36hrs	25.05	25.64	28.57	0.1036649	0.0033771	9212.83	11396.54	2225.66
57.70	280-36hrs	27.01	32.12	27.51	0.0127797	0.0000181	2523.38	197.22	4301.65
115.26	280-36hrs	31.39		27.98	0.0008501		139.69		3211.78
0.00	280-48hrs	21.50	18.78	30.49	1.0000000	1.0000000	96171.11	835443.83	674.68
28.98	280-48hrs	25.17	24.63	30.54	0.0813339	0.0179484	8510.60	21447.61	654.03
57.70	280-48hrs	27.80	29.42	29.45	0.0061722	0.0003048	1497.26	1069.16	1287.89
115.26	280-48hrs	31.38		28.87	0.0003453		140.62		1846.99

UV_{280} mRNA B

Fluence (mJ/cm2)	Sample	Cq E1A	Cq Hexon	Cq Actin	Relative Quantification E1A	Relative Quantification Hexon	Absolute E1A	Absolute Hexon	Absolute Actin
0.00	280-4hrs	25.63		26.76	1.0000000	1.0000000	6280.09		6856.76
29.35	280-4hrs	31.12		26.91	0.0246888		166.97		6246.29
58.71	280-4hrs			25.50					15006.93
117.42	280-4hrs			25.27					17313.58
0.00	280-12hrs	21.50	23.79	29.52	1.0000000	1.0000000	96171.11	36288.07	1233.04
29.35	280-12hrs	24.86		29.34	0.0859714		10445.10		1379.03
58.71	280-12hrs	26.61		28.58	0.0150928		3286.70		2211.86
117.42	280-12hrs			28.88					1835.54
0.00	280-16hrs	20.62	18.42	28.05	1.0000000	1.0000000	172010.66	1046638.10	3075.01
29.35	280-16hrs	23.51	30.35	27.46	0.0896222	0.0001703	25485.14	597.29	4437.46
58.71	280-16hrs	26.20		26.83	0.0089742		4309.31		6564.79
117.42	280-16hrs	31.54		27.02	0.0002528		126.51		5833.44
0.00	280-24hrs	19.20	15.00	29.01	1.0000000	1.0000000	439557.72	8905323.93	1693.04
29.35	280-24hrs	22.44	27.09	27.47	0.0363979	0.0000789	51679.37	4597.66	4409.96
58.71	280-24hrs	24.45		27.21	0.0075464		13694.93		5183.57
117.42	280-24hrs	30.01		27.45	0.0001889		347.66		4465.13
0.00	280-36hrs	20.03	14.07	27.95	1.0000000	1.0000000	254010.90	15940595.22	3272.24
29.35	280-36hrs	21.73	19.50	27.80	0.2773924	0.0209051	82612.83	532302.73	3592.04
58.71	280-36hrs	23.84	26.40	27.07	0.0387409	0.0001055	20492.53	7081.73	5654.91
117.42	280-36hrs	29.53		27.07	0.0007504		477.40		5654.91
0.00	280-48hrs	18.89	12.37	26.59	1.0000000	1.0000000	539471.58	46207476.95	7621.06
29.35	280-48hrs	19.99	16.00	26.76	0.5248583	0.0908733	260813.53	4761708.73	6856.76
58.71	280-48hrs	23.78	21.92	26.69	0.0361465	0.0014298	21321.23	117001.76	7161.72
117.42	280-48hrs	29.40	31.13	26.59	0.0006858	0.0000023	520.22	366.53	7621.06

B.2 Raw Data Chapter 4

$UV_{224}+UV_{254}$

Average Irradiance mW/cm2	Time (min)	Fluence (mJ/cm2)	Cumulative Fluence (mJ/cm2)	Sample	Cq E1A	Cq Actin	Relative Quantification E1A	Absolute E1A copies	Absolute Actin copies	Log Reduction	Average Log Reduction	Standard Deviation Log Reduction
				224 A								
	0	0		224	15.27	30.73	1.0000000	1.18E+08	1.16E+04	0		
0.05789	1.6	5.557442		224	16.97	30.75	0.3120826	3.84E+07	1.15E+04	-0.5057304		
	3.2	11.11488		224	20.68	30.34	0.0179484	3.31E+06	1.48E+04	-1.745974		
	4.8	16.67233		224	25.11	31.55	0.0019262	1.77E+05	6.98E+03	-2.7152906		
	6.4	22.22977		224	27.96	30.74	0.0001524	2.69E+04	1.16E+04	-3.8170603		
				224 B								
0.0391685	0.0	0		224	17.45	31.35	1.0000000	2.79E+07	7.91E+03	0		
	3.3	7.755353		224	20.10	29.66	0.0493776	4.85E+06	2.26E+04	-1.3064702		
	5.1	11.94638		224	24.23	30.27	0.0043043	3.17E+05	1.55E+04	-2.3660958		
	6.7	15.82405		224	26.85	30.28	0.0007050	5.61E+04	1.54E+04	-3.1517841		
	8.4	19.7409		224	29.65	31.64	0.0002599	8.82E+03	6.60E+03	-3.5852672		
				254 A								
0.077514	0	0		254	13.63	27.11	1.0000000	3.49E+08	1.10E+05	0	0	0
	4.1	19.06844		254	15.9	26.63	0.1486509	7.78E+07	1.49E+05	-0.8278325	-0.7902037	0.05321509
	8.2	38.13687		254	17.6	26.15	0.0328036	2.53E+07	2.00E+05	-1.4840779	-1.4434388	0.05747229
	16.4	76.27374		254	21.42	26.55	0.0030648	2.03E+06	1.56E+05	-2.5136005	-2.478982	0.04895788
	24.6	114.4106		254	25.43	26.43	0.0001750	1.43E+05	1.68E+05	-3.7568543	-3.5988136	0.22350337
	33	153.4777		254	28.32	26.27	0.0000211	2.12E+04	1.86E+05	-4.6749958	-4.7186452	0.0617295
				254 B								
0.077514	0	0		254	12.11	25.76	1.0000000	9.52E+08	2.55E+05	0		
	4.1	20.83617		254	14.78	25.93	0.1767767	1.63E+08	2.30E+05	-0.752575		
	8.2	38.37548		254	17.1	26.09	0.0395549	3.52E+07	2.08E+05	-1.4027998		
	16.4	76.68502		254	20.56	26.09	0.0035945	3.58E+06	2.08E+05	-2.4443636		
	24.6	115.0605		254	23.68	25.9	0.0003624	4.56E+05	2.34E+05	-3.4407729		
	33	153.436		254	28.04	25.87	0.0000173	2.56E+04	2.38E+05	-4.7622945		
				224+254 A								
224	0	0	0	224+254	13.98	29.28	1.0000000	2.77E+08	2.86E+04	0	0	0
0.05789	1.6	5.557442	5.557441696	224+254	17.07	29.54	0.1406323	3.59E+07	2.44E+04	-0.8519149	-0.7836814	0.13956022
	3.2	11.11488	11.11488339	224+254	21.69	30.45	0.0107464	1.70E+06	1.38E+04	-1.9687362	-1.9065233	0.23797241
254	3.966667	18.96527	30.08015369	224+254	23.89	29.74	0.0014298	3.97E+05	2.15E+04	-2.8447335	-2.7865343	0.1034218
0.079686	7.95	38.01023	49.12510999	224+254	25.24	29.39	0.0004401	1.63E+05	2.67E+04	-3.3564845	-3.265172	0.12579789
	16.06	76.78544	87.90032228	224+254	30.17	30.33	0.0000277	6.26E+03	1.49E+04	-4.5575941	-4.3599178	0.2002321
				224+254 B								
224	0	0	0	224+254	16.04	31.42	1.0000000	7.09E+07	7.57E+03	0		
0.05789	1.6	5.557442	5.557441696	224+254	17.88	30.35	0.1330463	2.10E+07	1.47E+04	-0.8759973		
	3.2	11.11488	11.11488339	224+254	21.82	30.20	0.0078125	1.56E+06	1.62E+04	-2.10721		
254	3.966667	18.96527	30.08015369	224+254	24.68	30.60	0.0014199	2.35E+05	1.26E+04	-2.8477438		
0.079686	7.95	38.01023	49.12510999	224+254	26.33	30.69	0.0004816	7.91E+04	1.19E+04	-3.3173506		
	16.06	76.78544	87.90032228	224+254	28.64	29.52	0.0000432	1.72E+04	2.47E+04	-4.3649349		
				224+254 C								
224	0	0	0	224+254	14.89	29.11	1.0000000	1.52E+08	3.18E+04	0		
0.05789	1.6	5.557442	5.557441696	224+254	17.56	29.71	0.2381595	2.60E+07	2.19E+04	-0.6231321		
	3.2	11.11488	11.11488339	224+254	21.58	30.34	0.0227183	1.82E+06	1.48E+04	-1.6436238		
254	3.966667	18.96527	30.08015369	224+254	24.19	29.55	0.0021522	3.25E+05	2.42E+04	-2.6671258		
0.079686	7.95	38.01023	49.12510999	224+254	25.33	29.18	0.0007556	1.53E+05	3.05E+04	-3.1216811		
	16.06	76.78544	87.90032228	224+254	29.41	29.82	0.0000696	1.03E+04	2.05E+04	-4.1572242		
				254+224 A								
254	0	0	0	254+224	16.65	30.87	1.0000000	4.74E+07	1.07E+04	0	0	0
0.0847408	3.75	19.06667	19.06667109	254+224	19.00	30.92	0.2030631	1.00E+07	1.03E+04	-0.692369	-0.7540801	0.08727274
	7.5	38.13334	38.13334218	254+224	20.66	30.61	0.0518325	3.35E+06	1.25E+04	-1.2853981	-1.3666762	0.11494459
224	1.666667	5.501252	43.63459458	254+224	23.28	30.85	0.0099575	5.93E+05	1.08E+04	-2.0018495	-2.1824675	0.25543242
0.0550125	3.333333	11.0025	49.13584699	254+224	27.83	30.52	0.0003382	2.94E+04	1.32E+04	-3.4708759	-3.3986287	0.10217297
	5	16.50376	54.63709939	254+224	30.96	30.28	0.0000327	3.71E+03	1.54E+04	-4.4853469	-4.4868521	0.0021286
				254+224 B								
254	0	0	0	254+224	16.42	30.68	1.0000000	5.52E+07	1.20E+04	0		
0.0847408	3.75	19.06667	19.06667109	254+224	18.97	30.52	0.1528300	1.02E+07	1.32E+04	-0.8157913		
	7.5	38.13334	38.13334218	254+224	20.38	29.83	0.0356489	4.03E+06	2.03E+04	-1.4479543		
224	1.666667	5.501252	43.63459458	254+224	23.58	29.99	0.0043343	4.87E+05	1.84E+04	-2.3630855		
0.0550125	3.333333	11.0025	49.13584699	254+224	27.48	30.69	0.0004716	3.70E+04	1.19E+04	-3.3263815		
	5	16.50376	54.63709939	254+224	30.81	30.16	0.0000325	4.10E+03	1.66E+04	-4.4883572		

UV_{224}+UV_{280}

Average Irradiance mW/cm2	Time (min)	Fluence (mJ/cm2)	Cumulative Fluence (mJ/cm2)	Sample	Cq E1A	Cq Actin	Relative Quantification E1A	Absolute E1A copies	Absolute Actin copies	Log Reduction	Average Log Reduction	Standard Deviation Log Reduction
				224 A								
0.05789002	0	0		224	15.27	30.73	1.0000000	1.18E+08	1.16E+04	0		
	1.6	5.557441696		224	16.97	30.75	0.3120826	3.84E+07	1.15E+04	-0.50573		
	3.2	11.11488339		224	20.68	30.34	0.0179484	3.31E+06	1.48E+04	-1.745974		
	4.8	16.67232509		224	25.11	31.55	0.0019262	1.77E+05	6.98E+03	-2.715291		
	6.4	22.22976678		224	27.96	30.74	0.0001524	2.69E+04	1.16E+04	-3.81706		
				224 B								
0.03916845	0.0	0		224	17.45	31.35	1.0000000	2.79E+07	7.91E+03	0		
	3.3	7.755353272		224	20.10	29.66	0.0493776	4.85E+06	2.26E+04	-1.30647		
	5.1	11.94637752		224	24.23	30.27	0.0043043	3.17E+05	1.55E+04	-2.366096		
	6.7	15.82405415		224	26.85	30.28	0.0007050	5.61E+04	1.54E+04	-3.151784		
	8.4	19.74089924		224	29.65	31.64	0.0002599	8.82E+03	6.60E+03	-3.585267		
				280 A								
	0	0		280	15.11	29.44	1.0000000	1.31E+08	2.59E+04	0	0	0
0.04905388	9.833333	28.94178787		280	19.38	29.87	0.0698304	7.81E+06	1.98E+04	-1.155955	-1.1183264	0.05321509
	19.65	57.83452186		280	23.09	30.36	0.0074943	6.73E+05	1.46E+04	-2.125272	-2.1207563	0.00638581
	29.48333	86.77630974		280	26.53	30.07	0.0005648	6.93E+04	1.75E+04	-3.248114	-3.3399278	0.12984481
	39.31667	115.7180976		280	30.46	29.87	0.0000323	5.16E+03	1.98E+04	-4.491368	-4.2505435	0.34057656
				280 B								
	0	0		280	15.67	29.47	1.0000000	9.06E+07	2.54E+04	0		
0.04816854	9.933333	28.70845208		280	20.85	31.06	0.0830429	2.96E+06	9.47E+03	-1.080698		
	19.88333	57.46507271		280	24.61	31.38	0.0076517	2.46E+05	7.76E+03	-2.116241		
	29.81667	86.1735248		280	28.32	30.72	0.0003700	2.12E+04	1.17E+04	-3.431742		
	39.76667	114.9301454		280	30.76	31.24	0.0000978	4.24E+03	8.47E+03	-4.00972		
				224+280 A								
	0	0	0	224+280 A	16.47	30.58	1.0000000	5.34E+07	1.28E+04	0	0	0
0.05501252	1.583333	5.226189785	5.226189785	224+280 A	19.18	30.98	0.2016604	8.91E+06	9.95E+03	-0.695379	-0.6788226	0.02341464
	3.233333	10.67242967	10.67242967	224+280 A	22.92	30.68	0.0122591	7.53E+05	1.20E+04	-1.91154	-1.786613	0.17667409
	9.933333	28.70845208	39.38088175	224+280 A	27.42	30.86	0.0006138	3.85E+04	1.07E+04	-3.21199	-3.2240313	0.01702883
0.04816854	19.88333	57.46507271	68.13750238	224+280 A	31.63	30.60	0.0000277	2.38E+03	1.26E+04	-4.557594	-4.3062341	0.35547679
	29.81667	86.1735248	96.84595446	224+280 A	34.92	30.52	0.0000027	2.71E+02	1.32E+04	-5.572065	-5.1716953	0.43307884
				224+280 B								
	0	0	0	224+280 B	16.06	30.35	1.0000000	7.00E+07	1.47E+04	0		
0.05501252	1.583333	5.226189785	5.226189785	224+280 B	18.30	30.39	0.2176376	1.59E+07	1.44E+04	-0.662266		
	3.166667	10.45237957	10.45237957	224+280 B	22.07	30.84	0.0217929	1.32E+06	1.09E+04	-1.661686		
	9.933333	28.70845208	39.16083165	224+280 B	26.73	30.27	0.0005807	6.07E+04	1.55E+04	-3.236072		
0.04816854	19.88333	57.46507271	67.91745228	224+280 B	29.05	29.87	0.0000881	1.31E+04	1.98E+04	-4.054874		
	29.81667	86.1735248	96.62590437	224+280 B	31.98	30.42	0.0000169	1.89E+03	1.41E+04	-4.771325		
				280+224 A								
	0	0	0	280+224 A	16.29	31.19	1.0000000	6.01E+07	8.73E+03	0	0	0
0.04816854	9.933333	28.70845208	28.70845208	280+224 A	19.98	30.60	0.0514744	5.25E+06	1.26E+04	-1.288408	-1.0551101	0.32993354
	19.88333	57.46507271	57.46507271	280+224 A	23.05	29.98	0.0039883	6.91E+05	1.85E+04	-2.399209	-2.2261168	0.2447894
	1.666667	5.501252405	62.96632512	280+224 A	27.01	30.30	0.0003199	5.05E+04	1.52E+04	-3.494958	-3.4573295	0.05321509
0.05501252	3.333333	11.00250481	68.46757752	280+224 A	31.02	31.14	0.0000355	3.57E+03	9.01E+03	-4.449223	-4.446213	0.00425721
	5	16.50375721	73.96882993	280+224 A	34.48	30.66	0.0000023	3.63E+02	1.21E+04	-5.635282	-5.6111991	0.03405766
				280+224 B								
	0	0	0	280+224 B	15.21	29.32	1.0000000	1.23E+08	2.79E+04	0		
0.04816854	9.933333	28.70845208	28.70845208	280+224 B	19.02	30.40	0.1507260	9.90E+06	1.43E+04	-0.821812		
	19.88333	57.46507271	57.46507271	280+224 B	23.33	30.62	0.0088507	5.74E+05	1.24E+04	-2.053025		
	1.666667	5.501252405	62.96632512	280+224 B	27.11	29.86	0.0003805	4.72E+04	2.00E+04	-3.419701		
0.05501252	3.333333	11.00250481	68.46757752	280+224 B	30.47	29.82	0.0000360	5.13E+03	2.05E+04	-4.443203		
	5	16.50375721	73.96882993	280+224 B	34.58	30.13	0.0000026	3.40E+02	1.69E+04	-5.587117		

UV_{254}+UV_{280}

Average irradiance (DNA weighted) mW/cm2	Average Irradiance (Spectral Emission) mW/cm2	Time (min)	Fluence (DNA weighted) (mJ/cm2)	Fluence SE (mJ/cm2)	Cumulative fluence (unweighted)	Cumulative Fluence (mJ/cm2) DNA weighted	Sample	Cq E1A	Cq Actin	Relative Quantification E1A	Absolute E1A copies	Absolute Actin copies	Log Reduction	Average fluence DNA-weighted	Average Log Reduction	Standard Deviation Log Reduction
							280 A									
		0	0.00	0.00			280	15.11	29.44	1.0000000	1.31E+08	2.59E+04	0	0.00	0	0
0.03076108	0.04905388	9.833333	18.15	28.94			280	19.38	29.87	0.0698304	7.81E+06	1.98E+04	-1.155955183	18.08	-1.11832643	0.053215088
		19.65	36.27	57.83			280	23.09	30.36	0.0074943	6.73E+05	1.46E+04	-2.125271769	36.15	-2.12075632	0.006385811
		29.48333	54.42	86.78			280	26.53	30.07	0.0005648	6.93E+04	1.75E+04	-3.248113653	54.23	-3.3399278	0.129844814
		39.31667	72.57	115.72			280	30.46	29.87	0.0000323	5.16E+03	1.98E+04	-4.491367535	72.32	-4.25054354	0.340576562
							280 B									
		0	0.00	0.00			280	15.67	29.47	1.0000000	9.06E+07	2.54E+04	0			
0.0302059	0.04816854	9.933333	18.00	28.71			280	20.85	31.06	0.0830429	2.96E+06	9.47E+03	-1.080697684			
		19.88333	36.04	57.47			280	24.61	31.38	0.0076517	2.46E+05	7.76E+03	-2.11624087			
		29.81667	54.04	86.17			280	28.32	30.72	0.0003700	2.12E+04	1.17E+04	-3.431741951			
		39.76667	72.07	114.93			280	30.76	31.24	0.0000978	4.24E+03	8.47E+03	-4.009719542			
							254 A									
0.07830642	0.07751397	0	0.00	0.00			254	13.63	27.11	1.0000000	3.49E+08	1.10E+05	0	0.00	0	0
		4.1	19.26	19.07			254	15.9	26.63	0.1486509	7.78E+07	1.49E+05	-0.827832488	19.26	-0.79020374	0.053215088
		8.2	38.53	38.14			254	17.6	26.15	0.0328036	2.53E+07	2.00E+05	-1.484077879	38.53	-1.44343883	0.057472295
		16.4	77.05	76.27			254	21.42	26.55	0.0030648	2.03E+06	1.56E+05	-2.513600464	77.05	-2.47898201	0.048957881
		24.6	115.58	114.41			254	25.43	26.43	0.0001750	1.43E+05	1.68E+05	-3.756854346	115.58	-3.5988136	0.223503369
		33	155.05	153.48			254	28.32	26.27	0.0000211	2.12E+04	1.86E+05	-4.674995833	155.05	-4.71864518	0.061729502
							254 B									
0.07830642	0.07751397	0	0.00	0.00			254	12.11	25.76	1.0000000	9.52E+08	2.55E+05	0			
		4.1	19.26	19.07			254	14.78	25.93	0.1767767	1.63E+08	2.30E+05	-0.752574989			
		8.2	38.53	38.14			254	17.1	26.09	0.0395549	3.52E+07	2.08E+05	-1.40279978			
		16.4	77.05	76.27			254	20.56	26.09	0.0035945	3.58E+06	2.08E+05	-2.444363565			
		24.6	115.58	114.41			254	23.68	25.9	0.0003624	4.56E+05	2.34E+05	-3.44077285			
		33	155.05	153.48			254	28.04	25.87	0.0000173	2.56E+04	2.38E+05	-4.762294531			
							254+280 A									
		0	**0**	0	0	0	254+280	12.57	27.26	1.0000000	7.02E+07	1.00E+04	0	**0**	**0**	0
0.08257676	0.08174222	3.883333	**19.2403861**	19.04593657	19.04593657	19.24038614	254+280	15.03	26.96	0.1476241	1.38E+07	1.21E+04	-0.830842788	**19.29103928**	**-0.75709044**	0.104301572
		7.783333	**38.563349**	38.17361535	38.17361535	38.56334904	254+280	16.22	26.87	0.0607909	6.30E+06	1.28E+04	-1.216161182	**38.62336693**	**-1.23422298**	0.025543242
		15.55	**77.0441213**	76.26548849	76.26548849	77.04412132	254+280	18.99	27.12	0.0105985	1.01E+06	1.10E+04	-1.974756772	**77.12713904**	**-2.06958122**	0.134102021
		10.15	**17.9417832**	28.6112818	104.8767703	94.98590455	254+280	22.24	26.99	0.0010180	1.18E+05	1.19E+04	-2.992238157	**95.05599547**	**-3.00427936**	0.017028828
0.02946106	0.04698076	20.3	**35.8835665**	57.2225636	133.4880521	112.9276878	254+280	25.74	26.80	0.0000789	1.17E+04	1.34E+04	-4.103038841	**112.9989812**	**-4.20087359**	0.138359228
		30.46667	**53.8548107**	85.88082616	162.1463147	130.8989321	254+280	27.77	26.49	0.0000156	3.05E+03	1.62E+04	-4.807449031	**130.9425682**	**-4.78637693**	0.029800449
							254+280 B									
		0	**0**	0	0	0	254+280	13.24	27.00	1.0000000	4.51E+07	1.18E+04	0			
0.07830645	0.07751401	4.116667	**19.3416924**	19.14596143	19.14596143	19.34169241	254+280	15.47	26.96	0.2073299	1.03E+07	1.21E+04	-0.68333809			
		8.233333	**38.6833848**	38.29192286	38.29192286	38.68338483	254+280	17.00	26.60	0.0559391	3.76E+06	1.51E+04	-1.252284782			
		16.43333	**77.2101568**	76.42881769	76.42881769	77.21015676	254+280	19.99	26.56	0.0068485	5.22E+05	1.55E+04	-2.164405669			
		10.56667	**17.9159296**	28.57005379	104.9988715	95.1260864	254+280	22.99	26.73	0.0009631	7.19E+04	1.40E+04	-3.016320557			
0.02825856	0.04506318	21.15	**35.8601179**	57.18517075	133.6139884	113.0702746	254+280	26.81	26.29	0.0000503	5.76E+03	1.84E+04	-4.298708338			
		31.71667	**53.7760475**	85.75522454	162.1840422	130.9862043	254+280	27.88	25.81	0.0000172	2.84E+03	2.48E+04	-4.765304831			
							280+254 A									
		0	0	0	0	**0**	280+254	14.16	27.53	1.0000000	2.46E+07	8.50E+03	0	**0**	**0**	0
0.02812451	0.0448494	7.983333	13.4716381	21.48286095	21.48286095	**13.47163811**	280+254	16.21	27.45	0.2284579	6.34E+06	8.93E+03	-0.641193891	**13.55601163**	**-0.69236899**	0.072372519
		15.96667	26.9432762	42.9657219	42.9657219	**26.94327622**	280+254	18.61	27.36	0.0406669	1.30E+06	9.44E+03	-1.39075858	**27.22452127**	**-1.36366588**	0.038314863
		26.6	44.8867107	71.57963691	71.57963691	**44.8867107**	280+254	21.84	26.95	0.0032621	1.54E+05	1.22E+04	-2.486507764	**45.182018**	**-2.41426057**	0.102172969
		26.63333	44.9429597	71.6693357	71.6693357	**44.94295971**	280+254	22.03	27.27	0.0035697	1.36E+05	9.99E+03	-2.447373865	**45.25232927**	**-2.36910607**	0.110687383
		4.1	18.8896615	18.78032244	90.44965814	**63.83262124**	280+254	24.04	27.27	0.0008862	3.59E+04	9.99E+03	-3.052444156	**64.3339589**	**-2.94708366**	0.149002246
0.07678724	0.07634277	8.216667	37.8561103	37.63698765	109.3063233	**82.79907001**	280+254	25.55	26.58	0.0001929	1.32E+04	1.53E+04	-3.714710146	**83.45398216**	**-3.57623635**	0.195831523
		12.31667	56.7457718	56.41731009	128.0866458	**101.6887315**	280+254	26.86	26.88	0.0000958	5.57E+03	1.27E+04	-4.018750442	**102.5356118**	**-3.99015259**	0.040443467
		16.43333	75.7122206	75.2739753	146.943311	**120.6551803**	280+254	30.27	27.79	0.0000169	5.86E+02	7.23E+03	-4.771325431	**121.6172414**	**-4.66596493**	0.149002246
							280+254 B									
		0	0	0	0	**0**	280+254	13.86	27.29	1.0000000	2.99E+07	9.86E+03	0			
0.02812451	0.0448494	8.083333	13.6403851	21.75195733	21.75195733	**13.64038514**	280+254	16.28	27.24	0.1804911	6.05E+06	1.02E+04	-0.743544089			
		16.3	27.5057663	43.86270983	43.86270983	**27.50576633**	280+254	18.23	27.22	0.0460709	1.67E+06	1.03E+04	-1.336573181			
		26.95	45.4773253	72.52147423	72.52147423	**45.47732531**	280+254	21.02	26.67	0.0045497	2.64E+05	1.45E+04	-2.342013366			
		27	45.5616988	72.65602242	72.65602242	**45.56169883**	280+254	21.16	26.98	0.0051187	2.41E+05	1.20E+04	-2.290838267			
0.07678724	0.07634277	4.183333	19.2735977	19.16203631	91.81805873	**64.83529657**	280+254	22.40	26.39	0.0014397	1.06E+05	1.73E+04	-2.841723159			
		8.366667	38.5471955	38.32407262	110.980095	**84.10889431**	280+254	24.20	26.21	0.0003650	3.23E+04	1.93E+04	-3.43776255			
		12.55	57.8207932	57.48610893	130.1421313	**103.382492**	280+254	25.88	26.15	0.0001093	1.06E+04	2.00E+04	-3.961554743			
		16.71667	77.0176037	76.57180246	149.2278249	**122.5793025**	280+254	28.11	26.39	0.0000275	2.44E+03	1.73E+04	-4.560604434			

Plaque assays

224+254

Sample	Time (min)	Fluence UV Dose mJ/cm^2	Viability at 10^-x dilution 0	-1	-2	-3	-4	-5	N pfu/ml	N/No	Log N/No
Control	0.000	0				TNTC	63	12	1575000	1	0
1	1.600	5.557442			TNTC	159	12		397500	0.252381	-0.59794
2	3.200	11.11488		TNTC	60	15		-	15000	0.009524	-2.02119
3	3.967	30.08015		170	10				4250	0.002698	-2.56889
4	7.950	49.12511	TNTC	58					1450	0.000921	-3.03591
5	16.060	87.90032	40						100	6.35E-05	-4.19728

280+224

Sample	Time (min)	Fluence UV Dose mJ/cm^2	Viability at 10^-x dilution 0	-1	-2	-3	-4	-5	N pfu/ml	N/No	Log N/No
Control	0.000	0				TNTC	TNTC	30	7500000	1	0
1	9.933	28.70845			TNTC	TNTC	31	3	775000	0.103333	-0.98576
2	19.883	57.46507			200+	22		-	55000	0.007333	-2.1347
3	1.667	62.96633		120	11				3000	0.0004	-3.39794
4	3.333	68.46758	110	11	0				275	3.67E-05	-4.43573

B.3 Raw Data Chapter 5

Simultaneous LP UV | NH_2Cl experiments

Condition	Time (min)	IT (mJ/cm2) CT (mg/L min)	Sample	Cq E1A	Cq Actin	Relative Quantification E1A	Absolute E1A copies	Absolute Actin copies	Log Reduction E1A	Absorbance times (min)	Absorbance	NH2CL conc. mg/L
LPUV Only	**0.000**	**0.0000**	**K1**	12.41	28.08	1.0000000	7.81E+07	6.04E+03	**0**			
	8.017	**25.7702**	**K2**	14.47	28.08	0.2398160	2.00E+07	6.04E+03	**-0.6201218**			
	16.017	**51.4868**	**K3**	16.01	27.25	0.0463914	7.23E+06	1.01E+04	**-1.3335629**			
	24.000	**77.1499**	**K4**	17.85	27.19	0.0124303	2.14E+06	1.05E+04	**-1.9055199**			
NH2CL Only	**0.000**	**0.0000**	**L1**	11.96	27.14	1.0000000	1.05E+08	1.08E+04	**0**	0.000	0.168	3.9905
	8.250	**32.5297**	**L2**	11.69	26.95	1.0570180	1.26E+08	1.22E+04	**0.0240824**	7.667	0.166	3.9430
	16.200	**56.5653**	**L3**	12.63	27.24	0.6736168	6.75E+07	1.02E+04	**-0.1715871**	15.567	0.147	3.4917
	24.317	**74.5095**	**L4**	13.05	27.52	0.6113201	5.11E+07	8.55E+03	**-0.2137313**	23.750	0.129	3.0641
LPUV | NH2CL	**0.000**	**0.0000**	**M1**	12.42	27.40	1.0000000	7.75E+07	9.21E+03	**0**	0.000	0.166	3.9430
	8.000	**25.7166**	**M2**	16.48	28.00	0.0908733	5.30E+06	6.34E+03	**-1.0415638**	8.333	0.126	2.9929
	15.867	**51.0046**	**M3**	21.11	27.56	0.0027053	2.49E+05	8.34E+03	**-2.5677859**	16.200	0.113	2.6841
	23.867	**76.7212**	**M4**	25.90	26.98	0.0000654	1.05E+04	1.20E+04	**-4.1843169**	24.000	0.084	1.9952

Average Germicidal Irradiance throughout the water volume = 0.053576 mW/cm^2

Condition	Time (min)	IT (mJ/cm2) CT (mg/L min)	Sample	Cq E1A	Cq Actin	Relative Quantification E1A	Absolute E1A copies	Absolute Actin copies	Log Reduction E1A	Absorbance times (min)	Absorbance	NH2CL conc. mg/L
LPUV Only	**0.00**	**0.00**	**X1 DNA**	13.83	26.83	1.0000000	1.53E+07	6.56E+03	**0**			
	8.00	**26.00**	**X2 DNA**	15.58	26.63	0.2588162	4.81E+06	7.43E+03	**-0.587008492**			
	16.00	**52.00**	**X3 DNA**	18.05	26.01	0.0303955	9.40E+05	1.09E+04	**-1.517191178**			
	24.00	**78.00**	**X4 DNA**	19.11	25.57	0.0107464	4.66E+05	1.44E+04	**-1.968736172**			
NH2CL Only	**0.00**	**0.00**	**Z1 DNA**	12.54	26.23	1.0000000	3.58E+07	9.53E+03	**0**	0.0000	0.1730	4.1093
	7.50	**27.61**	**Z2 DNA**	12.19	25.78	0.9330330	4.51E+07	1.26E+04	**-0.030103**	8.0000	0.1550	3.6817
	15.50	**52.28**	**Z3 DNA**	12.14	24.94	0.5396141	4.66E+07	2.13E+04	**-0.267916696**	16.4333	0.1420	3.3729
	24.00	**78.10**	**Z4 DNA**	12.72	25.11	0.4061262	3.18E+07	1.91E+04	**-0.391338994**	24.9833	0.1370	3.2542
LPUV | NH2CL	**0.00**	**0.00**	**Y1 DNA**	12.75	26.89	1.0000000	3.12E+07	6.32E+03	**0**	0.0000	0.1650	3.9192
	8.00	**26.00**	**Y2 DNA**	16.19	25.88	0.0457527	3.21E+06	1.18E+04	**-1.339583481**	8.3333	0.1400	3.3254
	16.00	**52.00**	**Y3 DNA**	19.16	25.31	0.0039334	4.51E+05	1.69E+04	**-2.405229665**	16.3333	0.1190	2.8266
	24.00	**78.00**	**Y4 DNA**	23.67	25.06	0.0001452	2.29E+04	1.97E+04	**-3.838132445**	24.3333	0.0900	2.1378

Average Germicidal Irradiance throughout the water volume = 0.054166 mW/cm^2

Condition	Time (min) A	Time (min) B	Log10 E1A/E1A0 A	Log10 E1A/E1A0 B	Average Time (min)	Average Log Reduction E1A	Standard Deviation Log E1A	Absorbance times (min) A	Absorbance times (min) B	NH2CL conc. mg/L A	NH2CL conc. mg/L B	Average Abs time	Average NH2CL conc. mg/L	Standard Deviation NH2CL
LPUV Only	0.00	0.00	0	0	**0.00**	**0**	0							
	8.02	8.00	-0.62012	-0.58701	**8.01**	**-0.603565**	0.0234146							
	16.02	16.00	-1.33356	-1.51719	**16.01**	**-1.425377**	0.1298448							
	24.00	24.00	-1.90552	-1.96874	**24.00**	**-1.937128**	0.0447007							
NH2CL Only	0.00	0.00	0	0	**0.00**	**0**	0	0.00	0.00	3.990499	4.109264	**0.00**	**4.049881**	0.0839794
	8.25	7.50	0.024082	-0.0301	**7.88**	**-0.00301**	0.0383149	7.67	8.00	3.942993	3.68171	**7.83**	**3.812352**	0.1847547
	16.20	15.50	-0.17159	-0.26792	**15.85**	**-0.219752**	0.0681153	15.57	16.43	3.491686	3.372922	**16.00**	**3.432304**	0.0839794
	24.32	24.00	-0.21373	-0.39134	**24.16**	**-0.302535**	0.1255876	23.75	24.98	3.064133	3.254157	**24.37**	**3.159145**	0.1343671
LPUV | NH2CL	0.00	0.00	0	0	**0.00**	**0**	0	0.00	0.00	3.942993	3.91924	**0.00**	**3.931116**	0.0167959
	8.00	8.00	-1.04156	-1.33958	**8.00**	**-1.190574**	0.2107317	8.33	8.33	2.992874	3.325416	**8.33**	**3.159145**	0.2351424
	15.87	16.00	-2.56779	-2.40523	**15.93**	**-2.486508**	0.1149446	16.20	16.33	2.684086	2.826603	**16.27**	**2.755344**	0.1007753
	23.87	24.00	-4.18432	-3.83813	**23.93**	**-4.011225**	0.2447894	24.00	24.33	1.995249	2.137767	**24.17**	**2.066508**	0.1007753

Decrease in qPCR amplification of a 1.1-kb viral DNA fragment

Condition	Time (min)	IT (mJ/cm2) CT (mg/L min)	Sample	Cq	1.1-kb Log (copies)	Log Reduction
LPUV Only	0.000	0.0000	A1-LR-PCR	12.39	10.99559	0
	12.467	39.6749	A4 LR-PCR	15.81	9.94754	-1.04805
	24.900	79.2437	A5 LR-PCR	17.10	9.5528	-1.44279
	37.333	118.8125	A6 LR-PCR	18.18	9.22232	-1.77327
NH2CL Only	0.000		B1-LR-PCR	11.59	11.23886	0
	12.467		B4 LR-PCR	11.77	11.18378	-0.05508
	24.833		B5 LR-PCR	11.27	11.33678	0.09792
	37.400		B6 LR-PCR	11.52	11.26028	0.02142
LPUV | NH2CL	0.000	0.0000	C1-LR-PCR	11.20	11.3582	0
	8.083	25.7250	C3 LR-PCR	13.73	10.58402	-0.77418
	12.450	39.6218	C4 LR-PCR	14.19	10.44326	-0.91494
	24.883	79.1906	C5 LR-PCR	15.69	9.98426	-1.37394

Relative expression level of E1A DNA at 0 and 48 hours postinfection

Condition	Time (min)	IT (mJ/cm2) CT (mg/L min)	Sample	Cq E1A	Cq Actin	Relative Quantification E1A	Absolute E1A copies	Absolute Actin copies	Log Reduction	Absorbance times (min)	Absorbance	NH2CL conc. mg/L
LPUV | NH2CL	0.000	0.0000	M1 0h	25.78	27.21	1.0000000	1.14E+04	1.04E+04	0	0.0000	0.1660	3.9430
	8.000	25.7166	M2 0h	26.00	27.27	0.8950251	9.84E+03	9.99E+03	-0.0481648	8.3333	0.1260	2.9929
	15.867	51.0046	M3 0h	25.89	27.04	0.8235910	1.06E+04	1.15E+04	-0.0842884	16.2000	0.1130	2.6841
	23.867	76.7212	M4 0h	25.72	26.94	0.8645372	1.18E+04	1.23E+04	-0.0632163	24.0000	0.0840	1.9952
LPUV | NH2CL	0.000	0.0000	M1 48 h	12.42	27.40	1.0000000	7.75E+07	9.21E+03	0	0.0000	0.1660	3.9430
	8.000	25.7166	M2 48 h	16.48	28.00	0.0908733	5.30E+06	6.34E+03	-1.0415638	8.3333	0.1260	2.9929
	15.867	51.0046	M3 48 h	21.11	27.56	0.0027053	2.49E+05	8.34E+03	-2.5677859	16.2000	0.1130	2.6841
	23.867	76.7212	M4 48 h	25.90	26.98	0.0000654	1.05E+04	1.20E+04	-4.1843169	24.0000	0.0840	1.9952

Average Germicidal Irradiance throughout the water volume = 0.053576 mW/cm^2

Relative expression level of E1A mRNA and Hexon mRNA at 48 hours postinfection

Condition	Time (min)	IT (mJ/cm2)	Sample	Cq E1A	Cq Hexon	Cq Actin	Relative Quantification E1A	Relative Quantification Hexon	Absolute E1A copies	Absolute Hexon copies	Absolute Actin copies	Log Reduction E1A mRNA	Log Reduction Hexon mRNA
LPUV | NH2CL	0.00	0.00	Y1 mRNA	19.22	13.40	28.01	1.0000000	1.0000000	433787.50	24247599.70	3152.43	0	0
	8.00	26.00	Y2 mRNA	20.32	16.24	27.12	0.2517389	0.0753630	209719.39	4097415.18	5481.85	-0.59904969	-1.122841884
	16.00	52.00	Y3 mRNA	22.08	20.02	25.57	0.0253829	0.0018736	65556.70	384394.80	14367.90	-1.59545898	-2.727331761
	24.00	78.00	Y4 mRNA	24.39	23.84	25.16	0.0038525	0.0000998	14248.74	35169.77	18538.92	-2.41426057	-4.000688642
LPUV Only	0.00	0.00	X1 mRNA	20.90	14.49	27.67	1.0000000	1.0000000	142958.85	12254963.95	3906.51	0	0
	8.00	26.00	X2 mRNA	20.73	15.97	28.13	1.5529378	0.4948283	159952.68	4851984.82	2925.83	0.191154047	-0.305545446
	16.00	52.00	X3 mRNA	22.11	17.94	26.95	0.2633403	0.0557455	64270.07	1413520.95	6092.89	-0.57948274	-1.253789932
	24.00	78.00	X4 mRNA	21.94	19.43	26.44	0.2080497	0.0139364	71909.99	556148.51	8365.89	-0.68183294	-1.855849923
NH2CL Only	0.00		L1 mRNA	21.04	14.94	26.53	1.0000000	1.0000000	130328.34	9246192.59	7910.68	0	0
	8.25		L2 mRNA	20.91	14.55	26.20	0.8705506	1.0424658	142017.41	11803174.40	9711.96	-0.060206	0.0180618
	16.20		L3 mRNA	21.28	14.77	26.53	0.8467453	1.1250585	111217.29	10284512.43	7910.68	-0.0722472	0.051175099
	24.32		L4 mRNA	21.18	15.00	26.20	0.7219646	0.7631296	118813.75	8905323.93	9711.96	-0.1414841	-0.117401698

Average Germicidal Irradiance throughout the water volume = 0.054166 mW/cm^2

Decrease in DNA-EMA qPCR amplification after 25 min exposure to disinfectant

Condition	Time (min)	IT (mJ/cm2)	Sample	Cq	Log Copies	Absolute copies	%
LPUV Only	0.000	0.000	A1 EMA-37C	20.82	4.480042	3.02E+04	100.00
LPUV Only	24.900	79.244	A5 EMA-37C	21.08	4.405448	2.54E+04	84.22
NH2CL Only	0.000		B1 EMA-37C	20.61	4.540291	3.47E+04	100.00
NH2CL Only	24.833		B5 EMA-37C	20.82	4.480042	3.02E+04	87.05
LPUV | NH2CL	0.000	0.000	C1 EMA-37C	19.30	4.91613	8.24E+04	100.00
LPUV | NH2CL	24.883	79.191	C5 EMA-37C	22.13	4.104203	1.27E+04	15.42
LPUV Only	0.000	0.000	K1 EMA 37 E1A	20.30	4.62923	4.26E+04	100.00
LPUV Only	24.000	77.150	K4 EMA 37 E1A	20.44	4.589064	3.88E+04	91.17
NH2CL Only	0.000		L1 EMA 37 E1A	17.25	5.504275	3.19E+05	100.00
NH2CL Only	24.317		L4 EMA 37 E1A	17.32	5.484192	3.05E+05	95.48
LPUV | NH2CL	0.000	0.000	M1 EMA 37 E1A	17.97	5.297707	1.98E+05	100.00
LPUV | NH2CL	23.867	76.721	M4 EMA 37 E1A	20.04	4.703824	5.06E+04	25.48
LPUV Only	0.000	0.000	1.1kb EMA 37C A1	20.87	8.40E+00	2.51E+08	100.00
LPUV Only	24.900	79.244	1.1kb EMA 37C A5	20.96	8.37E+00	2.35E+08	93.86
NH2CL Only	0.000		1.1kb EMA 37C B1	19.53	8.81E+00	6.44E+08	100.00
NH2CL Only	24.833		1.1kb EMA 37C B5	19.07	8.95E+00	8.91E+08	138.28
LPUV | NH2CL	0.000	0.000	1.1kb EMA 37C C1	19.14	8.93E+00	8.48E+08	100.00
LPUV | NH2CL	24.883	79.191	1.1kb EMA 37C C5	23.36	7.64E+00	4.34E+07	5.11
LPUV | NH2CL	0.000	0.000	1.1kb EMA 37C M1	17.32	9.49E+00	3.06E+09	100.00
LPUV | NH2CL	23.867	75.955	1.1kb EMA 37C M4	21.12	8.32E+00	2.10E+08	6.87

Condition	Average %	Standard Deviation
Untreated	100.00	0.000
LP UV treated	87.69	4.913
NH2CL treated	91.26	5.964
LP UV | NH2CL treated	20.45	7.110

Increased UV irradiance

Condition	Time (min)	IT (mJ/cm2) CT (mg/L min)	Sample	Cq E1A	Cq Actin	Relative Quantification E1A	Absolute E1A copies	Absolute Actin copies	Log Reduction E1A
LPUV Only	0.000	0	N1	13.41	29.87	1.0000000	4.03E+07	1.98E+03	0
	1.017	18.64343	N2	15.35	29.71	0.2332582	1.12E+07	2.19E+03	-0.632163
	2.000	36.6756	N3	16.28	29.43	0.1008302	6.05E+06	2.61E+03	-0.9964093
	3.000	55.0134	N4	17.29	29.35	0.0473661	3.11E+06	2.74E+03	-1.324532
NH2CL Only	0.000		Q1	12.73	29.88	1.0000000	6.32E+07	1.97E+03	0
	1.000		Q2	12.76	29.53	0.7684376	6.19E+07	2.45E+03	-0.1143914
	2.000		Q3	12.35	29.13	0.7737825	8.12E+07	3.14E+03	-0.1113811
	3.000		Q4	12.12	28.90	0.7737825	9.45E+07	3.63E+03	-0.1113811
LPUV | NH2CL	0.000	0	O1	12.77	29.50	1.0000000	6.15E+07	2.50E+03	0
	1.000	18.3378	O2	15.80	29.54	0.1258694	8.31E+06	2.44E+03	-0.9000797
	2.000	36.6756	O3	17.60	28.86	0.0225614	2.53E+06	3.72E+03	-1.6466341
	3.000	55.0134	O4	20.57	29.13	0.0034720	3.56E+05	3.14E+03	-2.4594151

Average Germicidal Irradiance throughout the water volume = 0.305630 mW/cm^2

B.4 Raw Data Inactivation Kinetics CVB5 and MNV-1

CVB5 vs UV_{218}

Wavelength	218 nm
Temperature	23 °C
pH	8
Solution	CBS

Virus	CVB5

Average irradiance through the water =	0.007197	mW/cm^2

Fluence UV Dose mJ/cm^2	Sample	Time (min)	Viability at 10^-x dilution						N pfu/ml	N/No	Log N/No
			0	-1	-2	-3	-4	-5			
0.000	Control	0.00				TNTC	TNTC	56	7000000	1.000000	0
4.815	1	11.15				192	13		240000	0.034286	-1.46489
10.320	2	23.90			23	1			2875	0.000411	-3.38646
14.516	3	33.62	242	18					302.5	0.000043	-4.36437

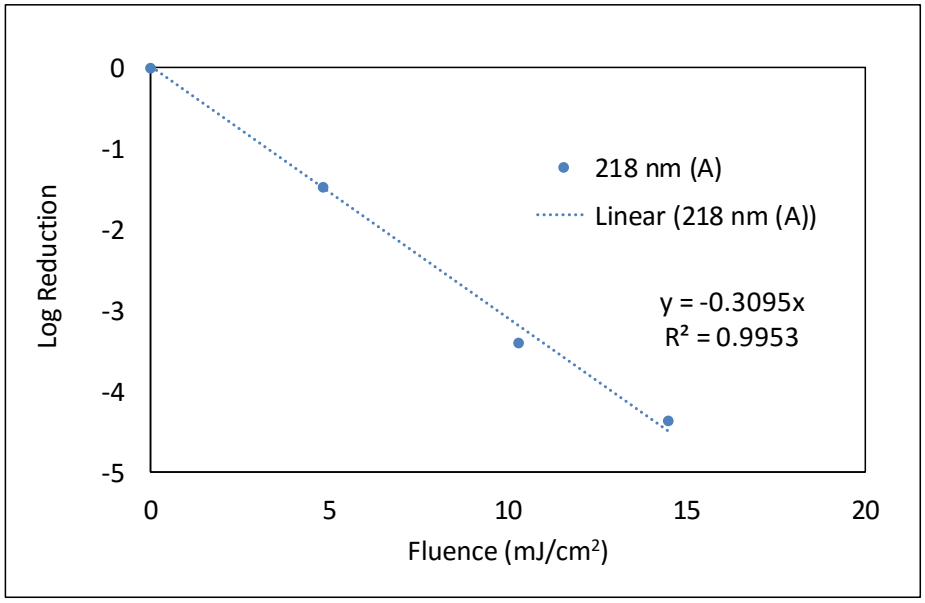

CVB5 vs UV_{224}

Wavelength	224 nm
Temperature	23 °C
pH	8
Solution	CBS

Virus	CVB5

Average irradiance through the water =	0.019024	mW/cm^2

Fluence UV Dose mJ/cm^2	Sample	Time (min)	Viability at 10^-x dilution						N pfu/ml	N/No	Log N/No
			0	-1	-2	-3	-4	-5			
0.000	Control	0.00					TNTC	41	5125000	1.000000	0
5.878	1	5.15				TNTC	30		375000	0.073171	-1.13566
11.738	2	10.28			75	12			9375	0.001829	-2.73772
17.616	3	15.43		43	3				537.5	0.000105	-3.97932

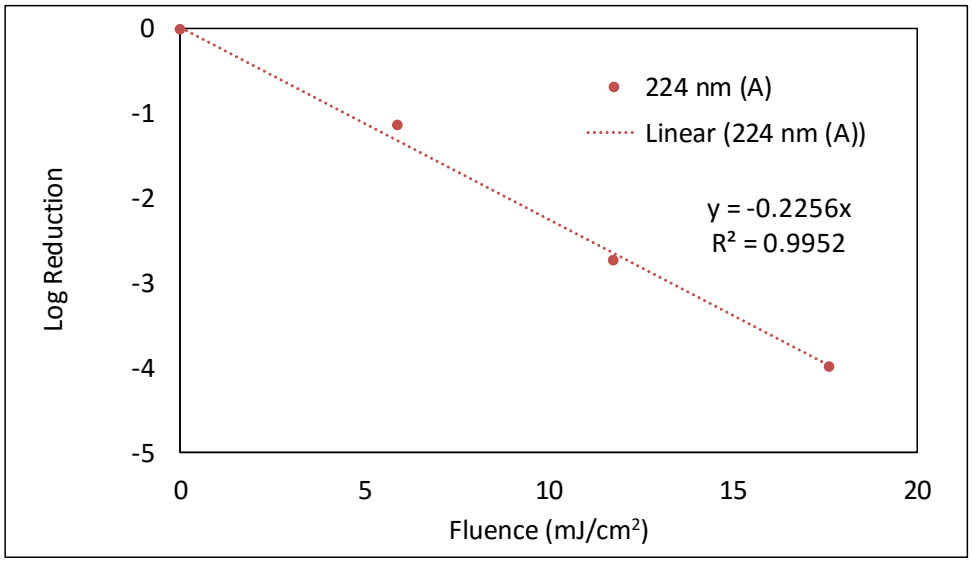

CVB5 vs UV_{224}

Wavelength	224 nm
Temperature	23 ℃
pH	8
Solution	CBS

Virus	CVB5

Average irradiance through the water =	0.019347	mW/cm^2

Fluence UV Dose mJ/cm^2	Sample	Time (min)	Viability at 10^-x dilution						N pfu/ml	N/No	Log N/No
			0	-1	-2	-3	-4	-5			
0.000	Control	0.00				TNTC	TNTC	94	11750000	1.000000	0
2.051	1	1.77				TNTC	319		3987500	0.339362	-0.46934
10.254	2	8.83	TNTC	TNTC	TNTC	64			80000	0.006809	-2.16695
15.477	3	13.33	TNTC	TNTC	54				6750	0.000574	-3.24073

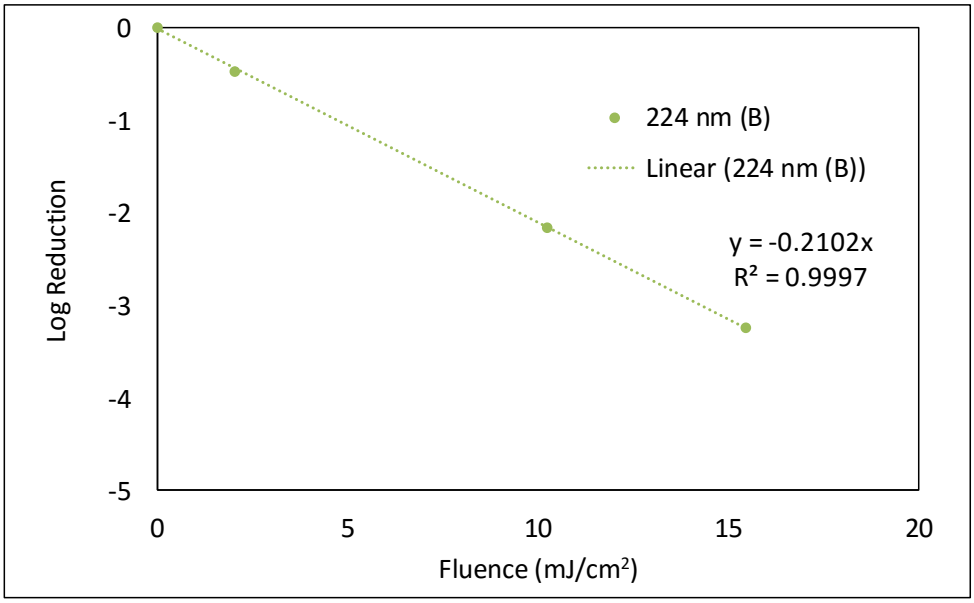

CVB5 vs UV_{228}

Wavelength	228 nm
Temperature	23 ℃
pH	8
Solution	CBS

Virus	CVB5

Average irradiance through the water =	0.034452	mW/cm^2

Fluence UV Dose mJ/cm^2	Sample	Time (min)	Viability at 10^-x dilution						N pfu/ml	N/No	Log N/No
			0	-1	-2	-3	-4	-5			
0.000	Control	0.00					TNTC	70	8750000	1.000000	0
8.785	1	4.25			TNTC	171	18		213750	0.024429	-1.6121
17.571	2	8.50		TNTC	101	7			12625	0.001443	-2.84078
26.356	3	12.75	TNTC	92	11				1150	0.000131	-3.88131

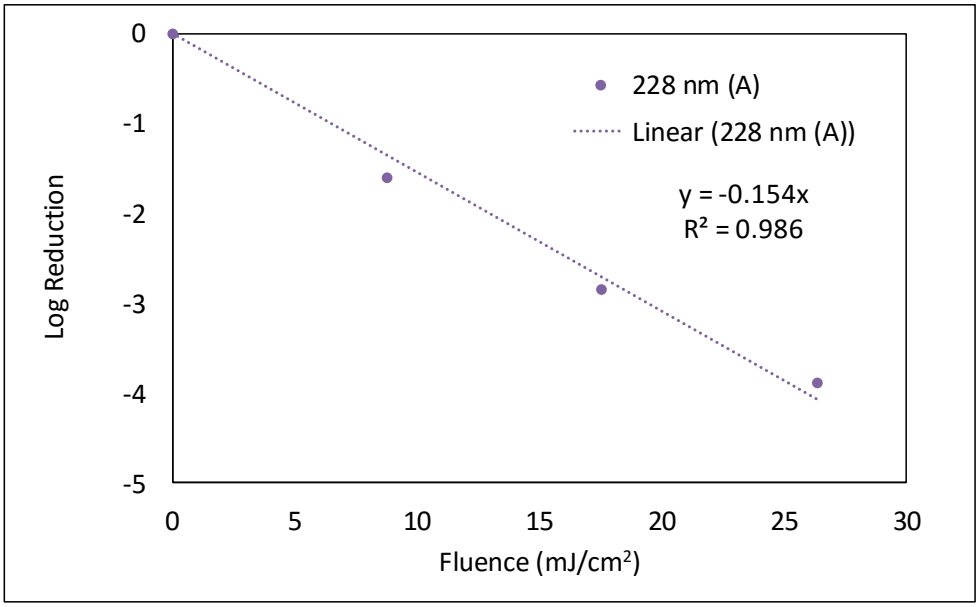

CVB5 vs UV_{232}

Wavelength	232 nm
Temperature	23 ℃
pH	8
Solution	CBS

Virus	CVB5

Average irradiance through the water =	0.042679	mW/cm^2

Fluence UV Dose mJ/cm^2	Sample	Time (min)	Viability at 10^-x dilution						N pfu/ml	N/No	Log N/No
			0	-1	-2	-3	-4	-5			
0.000	Control	0.00					TNTC	47	5875000	1.000000	0
9.133	1	3.57			TNTC	182	23		257500	0.043830	-1.35823
18.266	2	7.13		TNTC	72	20			17000	0.002894	-2.53856
27.400	3	10.70	TNTC	67	11	1			837.5	0.000143	-3.84602
45.666	4	17.83	27	0					33.75	0.000006	-5.24073

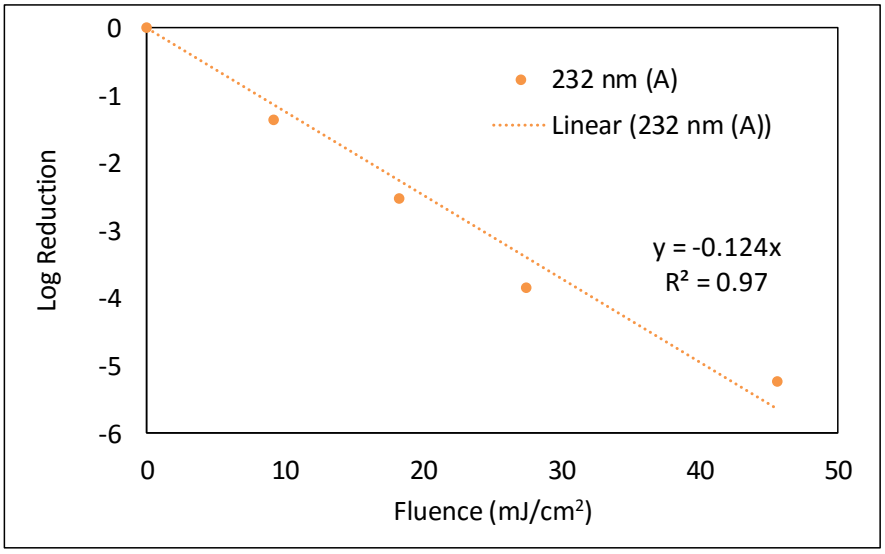

CVB5 vs UV_{232}

Wavelength	232 nm
Temperature	23 °C
pH	8
Solution	CBS

Virus	CVB5

Average irradiance through the water =	0.040745	mW/cm^2

Fluence UV Dose mJ/cm^2	Sample	Time (min)	Viability at 10^-x dilution						N pfu/ml	N/No	Log N/No
			0	-1	-2	-3	-4	-5			
0.000	Control	0.00				TNTC	81	15	1012500	1.000000	0
8.679	1	3.55			TNTC	42	4		52500	0.051852	-1.28524
17.358	2	7.10		141	19	4			2068.75	0.002043	-2.68969
26.036	3	10.65	TNTC	37	0				462.5	0.000457	-3.34028
34.756	4	14.22	40	2					50	0.000049	-4.30643

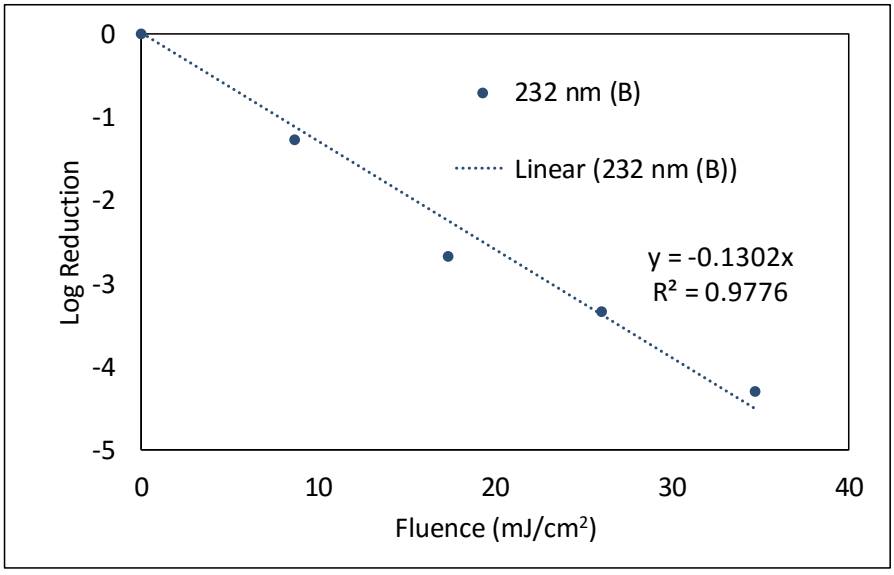

CVB5 vs UV_{239}

Wavelength	239 nm
Temperature	23 ℃
pH	8
Solution	CBS

Virus	CVB5

Average irradiance through the water =	0.033415	mW/cm^2

Fluence UV Dose mJ/cm^2	Sample	Time (min)	Viability at 10^-x dilution						N pfu/ml	N/No	Log N/No
			0	-1	-2	-3	-4	-5			
0.000	Control	0.00					TNTC	24	3000000	1.000000	0
10.158	1	5.07				TNTC	35	12	437500	0.145833	-0.83614
21.720	2	10.83				24	4		30000	0.010000	-2
33.415	3	16.67	TNTC	167	6				2087.5	0.000696	-3.15749
43.473	4	21.68	TNTC	31	1				387.5	0.000129	-3.88885
53.597	5	26.73	123	8					153.75	0.000051	-4.29031
58.342	6	29.10	48	5					60	0.000020	-4.69897

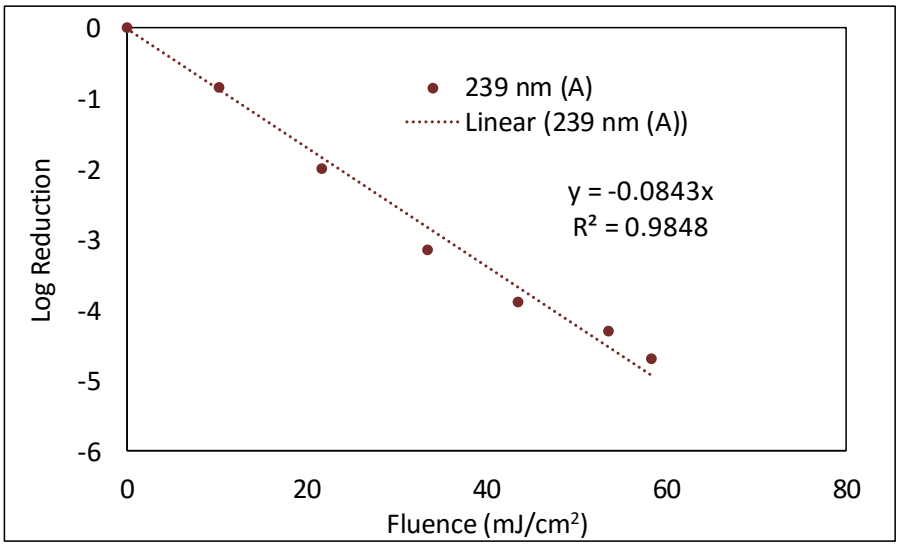

CVB5 vs UV_{239}

Wavelength	239 nm
Temperature	23 ℃
pH	8
Solution	CBS

Virus	CVB5

Average irradiance through the water =	0.032566	mW/cm^2

Fluence UV Dose mJ/cm^2	Sample	Time (min)	Viability at 10^-x dilution						N pfu/ml	N/No	Log N/No
			0	-1	-2	-3	-4	-5			
0.000	Control	0.00				TNTC	269	41	4243750	1.000000	0
15.078	1	7.72			TNTC	112	14		140000	0.032990	-1.48162
30.156	2	15.43		256	28				3350	0.000789	-3.1027
45.234	3	23.15	TNTC	29					362.5	0.000085	-4.06844
60.312	4	30.87	25						31.25	0.000007	-5.1329

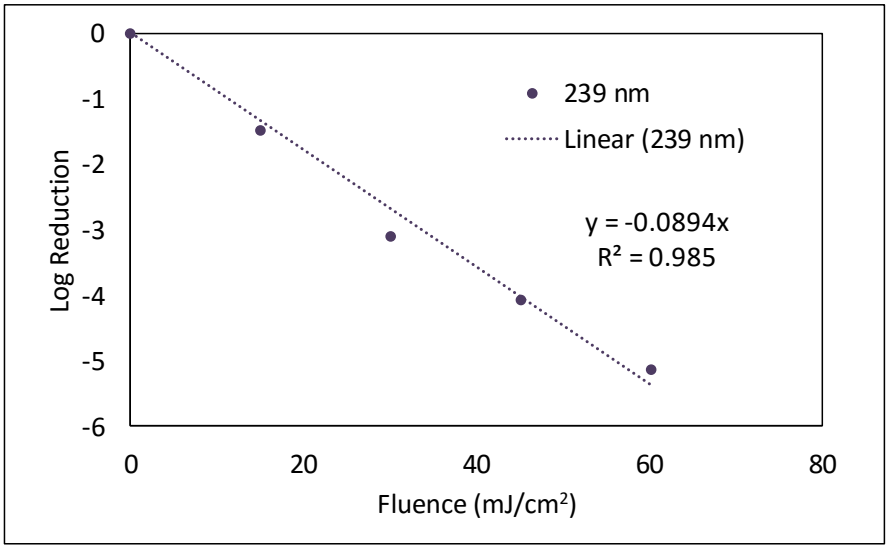

CVB5 vs UV_{248}

Wavelength	248 nm
Temperature	23 ºC
pH	8
Solution	CBS

Virus	CVB5

Average irradiance through the water =	0.0326	mW/cm^2

Fluence UV Dose mJ/cm^2	Sample	Time (min)	Viability at 10^-x dilution						N pfu/ml	N/No	Log N/No
			0	-1	-2	-3	-4	-5			
0.000	Control	0.00					TNTC	34	4250000	1.000000	0
9.845	1	5.03				102	23		207500	0.048824	-1.31137
19.690	2	10.07		TNTC	55				6875	0.001618	-2.79112
29.568	3	15.12	TNTC	46	3				575	0.000135	-3.86872

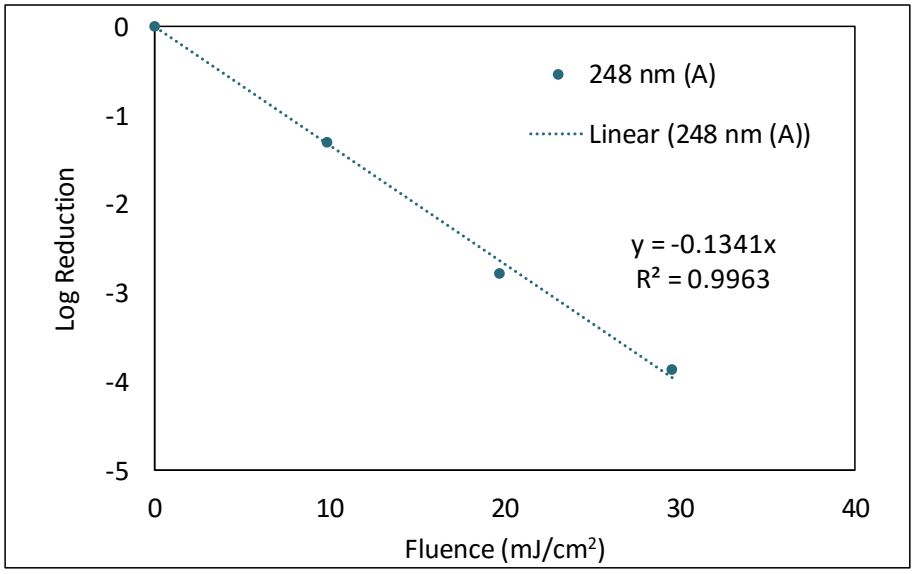

CVB5 vs UV_{248}

Wavelength	248 nm
Temperature	23 ℃
pH	8
Solution	CBS

Virus	CVB5

Average irradiance through the water =	0.0326	mW/cm^2

Fluence UV Dose mJ/cm^2	Sample	Time (min)	Viability at 10^-x dilution						N pfu/ml	N/No	Log N/No
			0	-1	-2	-3	-4	-5			
0.000	Control	0.00					256	40	4100000	1.000000	0
9.845	1	5.00				118	10		147500	0.035976	-1.44399
19.690	2	10.00		TNTC	67	4			8375	0.002043	-2.6898
29.568	3	15.00	TNTC	51	7				637.5	0.000155	-3.8083

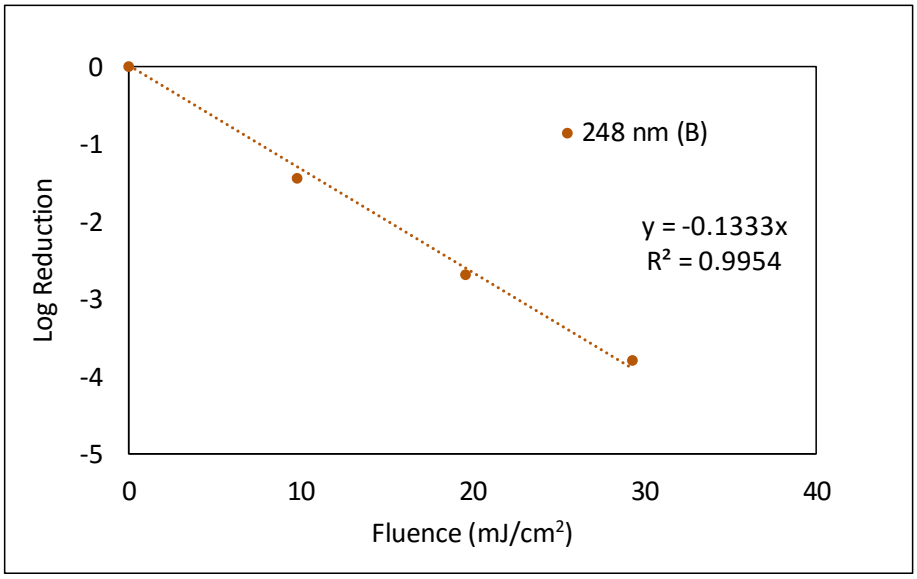

CVB5 vs UV_{254}

Wavelength	254 nm
Temperature	23 ℃
pH	8
Solution	CBS

Virus	CVB5

Average irradiance through the water =	0.063822	mW/cm^2

Fluence UV Dose mJ/cm^2	Sample	Time (min)	Viability at 10^-x dilution						N pfu/ml	N/No	Log N/No
			0	-1	-2	-3	-4	-5			
0.000	Control	0.00				TNTC	TNTC	112	14000000	1.000000	0
4.085	1	1.07				TNTC	156	13	1950000	0.139286	-0.85609
8.744	2	2.28			TNTC	TNTC	40		500000	0.035714	-1.44716
12.318	3	3.22		TNTC	TNTC	58			72500	0.005179	-2.28579
16.402	4	4.28		TNTC	160	13			20000	0.001429	-2.8451
20.678	5	5.40	TNTC	TNTC	47				5875	0.000420	-3.37712
24.572	6	6.42	TNTC	80					1000	0.000071	-4.14613
29.103	7	7.60	190						237.5	0.000017	-4.77046

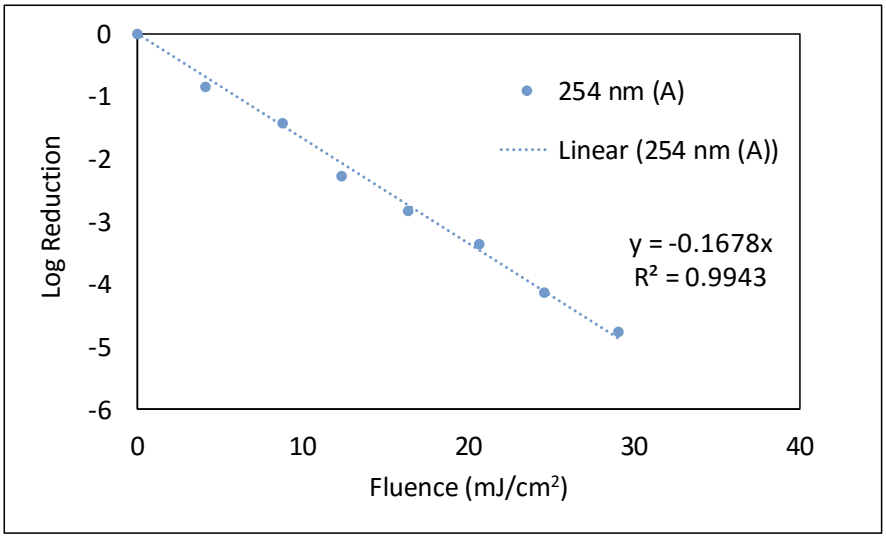

CVB5 vs UV_{260}

Wavelength	260 nm
Temperature	23 ℃
pH	8
Solution	CBS

Virus	CVB5

Average irradiance through the water =	0.085396	mW/cm^2

Fluence UV Dose mJ/cm^2	Sample	Time (min)	Viability at 10^-x dilution						N pfu/ml	N/No	Log N/No
			0	-1	-2	-3	-4	-5			
0.000	Control	0.00				TNTC	230+	28	3500000	1.000000	0
5.295	1	1.03				TNTC	35	1	437500	0.125000	-0.90309
10.504	2	2.05			TNTC	51	6		63750	0.018214	-1.73959
15.798	3	3.08		TNTC	71	3			8875	0.002536	-2.5959
21.007	4	4.10	TNTC	156	14				1950	0.000557	-3.25403
26.302	5	5.13	226	28					316.25	0.000090	-4.04404

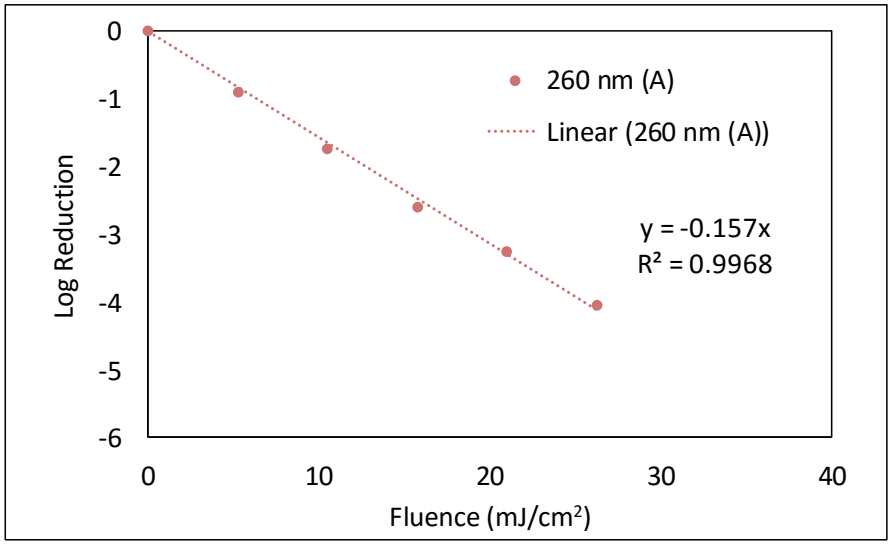

CVB5 vs UV_{265}

Wavelength	265 nm
Temperature	23 °C
pH	8
Solution	CBS

Virus	CVB5

Average irradiance through the water =	0.079008	mW/cm^2

Fluence UV Dose mJ/cm^2	Sample	Time (min)	Viability at 10^-x dilution						N pfu/ml	N/No	Log N/No
			0	-1	-2	-3	-4	-5			
0.000	Control	0.00				TNTC	TNTC	88	11000000	1.000000	0
5.294	1	1.12				TNTC	50		625000	0.056818	-1.24551
10.587	2	2.23			TNTC	74	6		92500	0.008409	-2.07525
16.355	3	3.45		TNTC	103				12875	0.001170	-2.93165
21.174	4	4.47	TNTC	118	8				1475	0.000134	-3.8726
27.258	5	5.75	330						412.5	0.000038	-4.42597

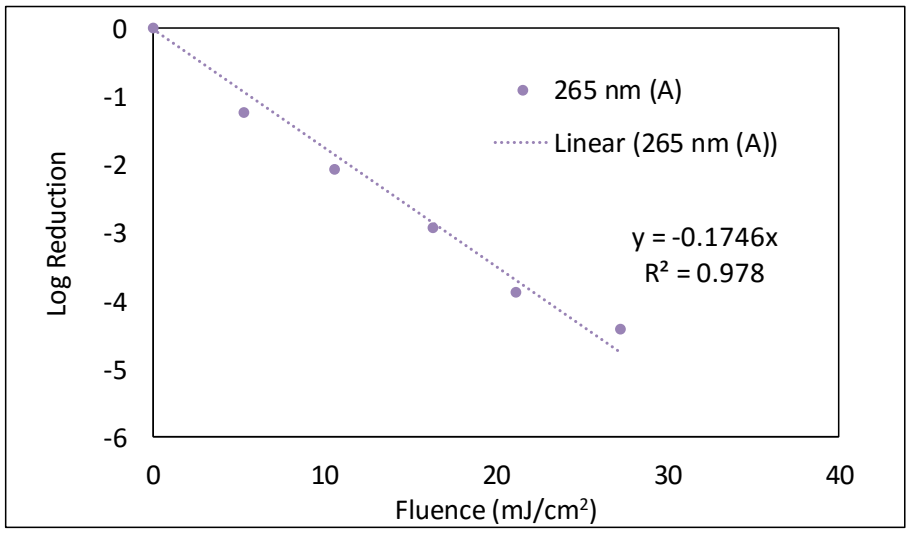

CVB5 vs UV_{270}

Wavelength	270 nm
Temperature	23 °C
pH	8
Solution	CBS

Virus	CVB5

Average irradiance through the water =	0.047052	mW/cm^2

Fluence UV Dose mJ/cm^2	Sample	Time (min)	Viability at 10^-x dilution						N pfu/ml	N/No	Log N/No
			0	-1	-2	-3	-4	-5			
0.000	Control	0.00				TNTC	145	7	1812500	1.000000	0
7.764	1	2.75			TNTC	52	11		101250	0.055862	-1.25288
15.951	2	5.65		TNTC	92	13			11500	0.006345	-2.19758
23.291	3	8.25	TNTC	77					962.5	0.000531	-3.27488
31.054	4	11.00	27						33.75	0.000019	-4.73

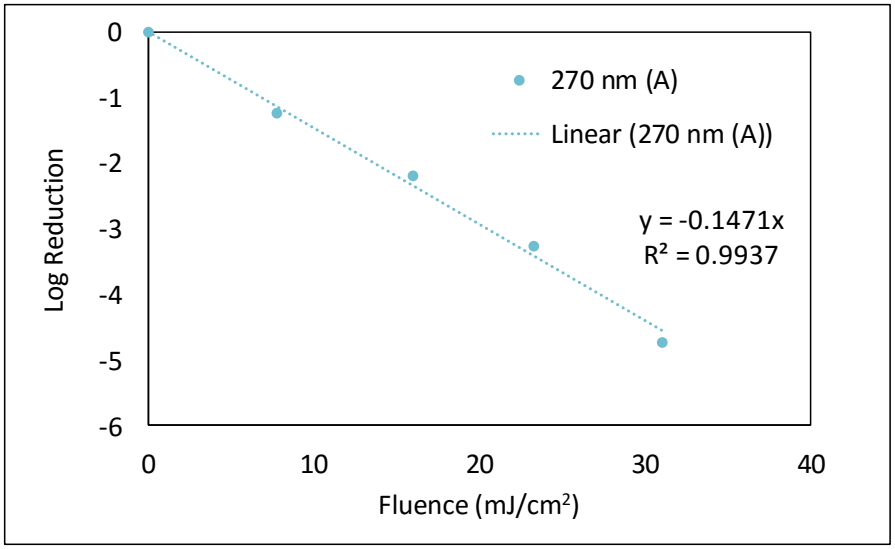

CVB5 vs UV_{280}

Wavelength	280 nm
Temperature	23 °C
pH	8
Solution	CBS

Virus	CVB5

Average irradiance through the water =	0.033822	mW/cm^2

Fluence UV Dose mJ/cm^2	Sample	Time (min)	Viability at 10^-x dilution						N pfu/ml	N/No	Log N/No
			0	-1	-2	-3	-4	-5			
0.000	Control	0.00					TNTC	56	7000000	1.000000	0
17.114	1	8.43				80	8		100000	0.014286	-1.8451
26.246	2	12.93			58	1			7250	0.001036	-2.98476
34.228	3	16.87		70	8				875	0.000125	-3.90309
43.359	4	21.37	57	0					71.25	0.000010	-4.99231

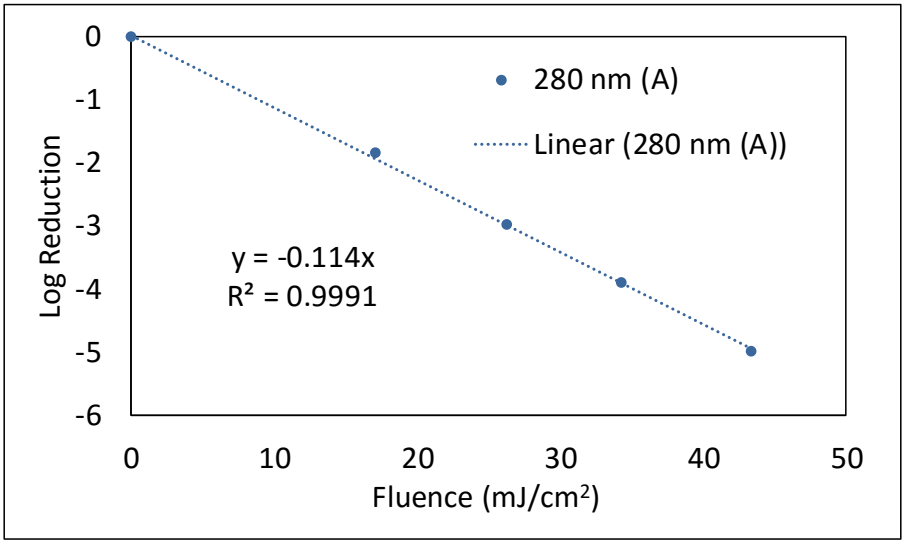

CVB5 vs UV_{289}

Wavelength	289 nm
Temperature	23 °C
pH	8
Solution	CBS

Virus	CVB5

Average irradiance through the water =	0.035636	mW/cm^2

Fluence UV Dose mJ/cm^2	Sample	Time (min)	Viability at 10^-x dilution						N pfu/ml	N/No	Log N/No
			0	-1	-2	-3	-4	-5			
0.000	Control	0.00					TNTC	41	5125000	1.000000	0
16.856	1	7.88				TNTC	42	10	525000	0.102439	-0.98953
50.709	2	23.72		TNTC	75	7			9375	0.001829	-2.73772
67.636	3	31.63	TNTC	63	11				787.5	0.000154	-3.81344
84.456	4	39.50	91	4					113.75	0.000022	-4.65374

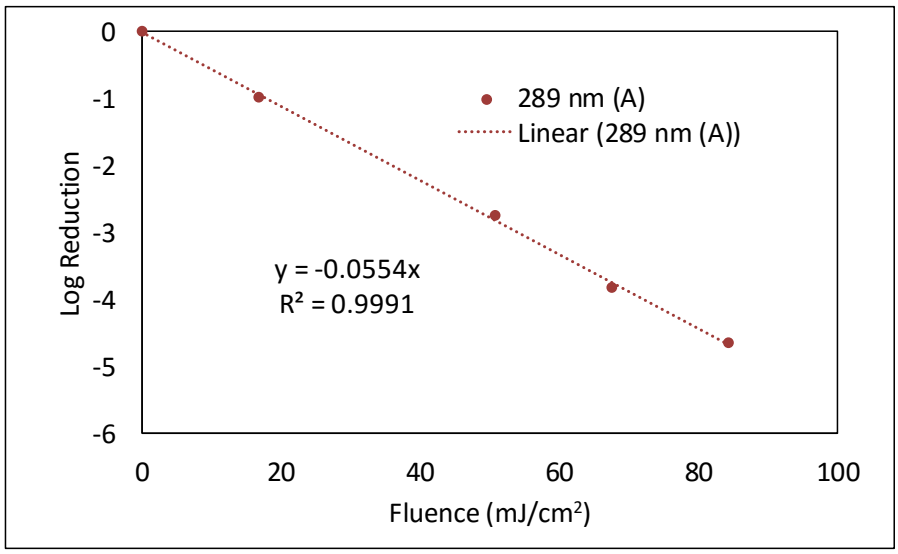

CVB5 vs MP UV

Wavelength	MP UV
Temperature	23 ℃
pH	8
Solution	CBS

Virus	CVB5

Average irradiance through the water =	0.425309	mW/cm^2

Fluence UV Dose mJ/cm^2	Sample	Time (min)	Viability at 10^-x dilution						N pfu/ml	N/No	Log N/No
			0	-1	-2	-3	-4	-5			
0.000	Control	0.00				TNTC	TNTC	40	5000000	1.000000	0
5.529	1	0.22				TNTC	123	11	1537500	0.307500	-0.51215
11.483	2	0.45			TNTC	206	26		291250	0.058250	-1.2347
17.012	3	0.67		TNTC	TNTC	85			106250	0.021250	-1.67264
22.541	4	0.88		TNTC	218	25			29250	0.005850	-2.23284
28.496	5	1.12	TNTC	TNTC	65				8125	0.001625	-2.78915
34.025	6	1.33	TNTC	113					1412.5	0.000283	-3.54898
39.554	7	1.55	185						231.25	0.000046	-4.33489

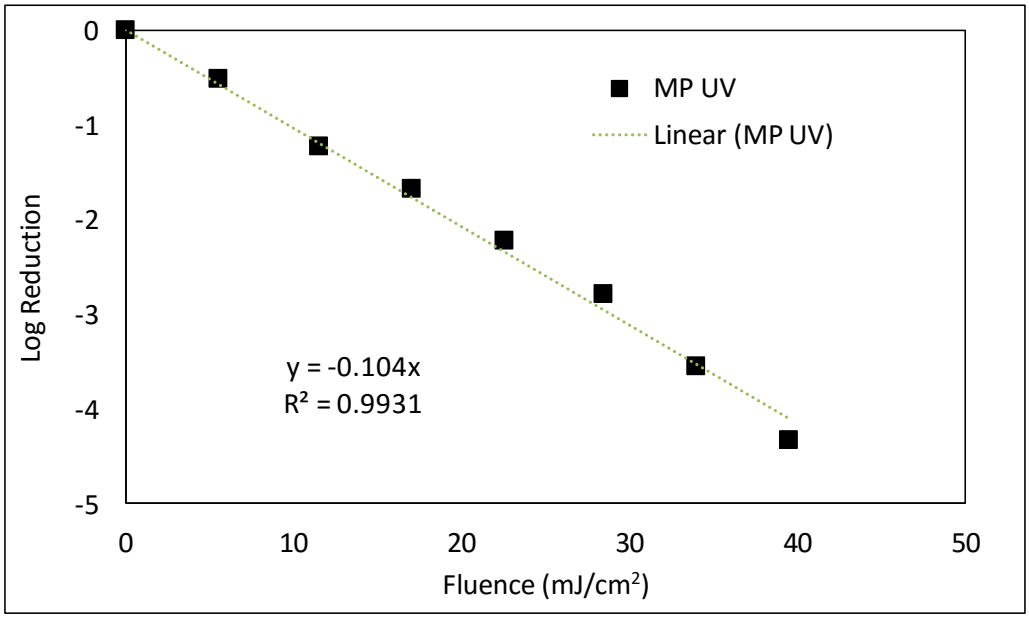

MNV-1 vs UV_{224}

Wavelength	224 nm
Temperature	23 °C
pH	8
Solution	CBS

Virus	MNV-1

Average irradiance through the water =	0.018692	mW/cm^2

Fluence UV Dose mJ/cm^2	Sample	Time (min)	Viability at 10^-x dilution						N pfu/ml	N/No	Log N/No
			0	-1	-2	-3	-4	-5			
0.000	Control	0.00				TNTC	78	16	975000	1.000000	0
5.065	1	4.52		TNTC	TNTC	117	7		146250	0.150000	-0.82391
10.131	2	9.03		TNTC	77	7			9625	0.009872	-2.0056
15.196	4	13.55	TNTC	48	7				600	0.000615	-3.21085
20.262	5	18.07	27	5					33.75	0.000035	-4.46073

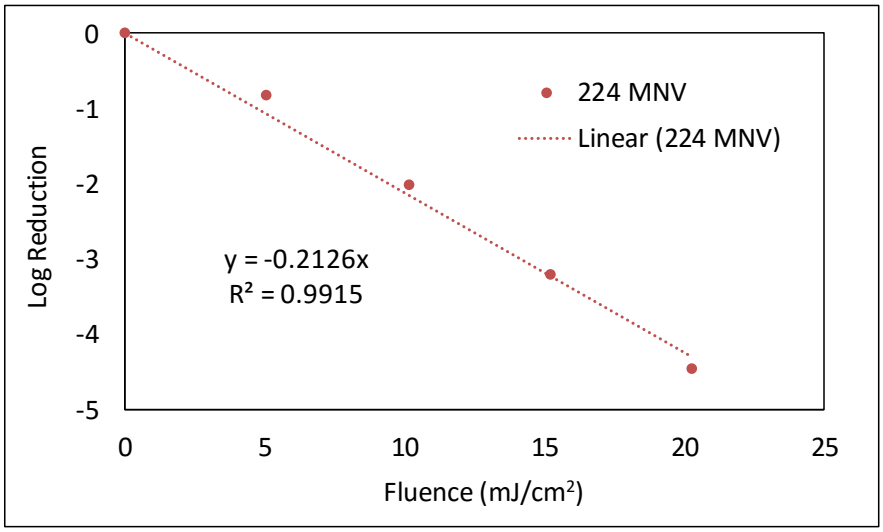

MNV-1 vs UV_{228}

Wavelength	228 nm
Temperature	23 ℃
pH	8
Solution	CBS

Virus	MNV-1

Average irradiance through the water =	0.031801	mW/cm^2

Fluence UV Dose mJ/cm^2	Sample	Time (min)	Viability at 10^-x dilution						N pfu/ml	N/No	Log N/No
			0	-1	-2	-3	-4	-5			
0.000	Control	0.00				TNTC	203	38	3643750	1.000000	0
7.473	1	3.92			TNTC	102	10		127500	0.034991	-1.45604
14.947	2	7.83		TNTC	139	24			23687.5	0.006501	-2.18703
22.420	3	11.75	TNTC	284					3550	0.000974	-3.01132
29.893	4	15.67	229	30					330.625	0.000091	-4.04221

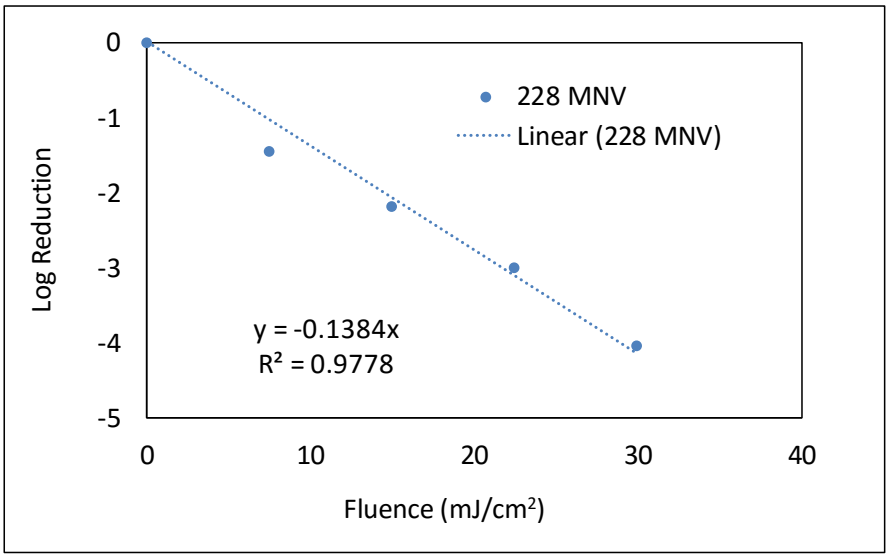

MNV-1 vs UV_{239}

Wavelength	239 nm
Temperature	23 ºC
pH	8
Solution	CBS

Virus	MNV-1

Average irradiance through the water =	0.030837	mW/cm^2

Fluence UV Dose mJ/cm^2	Sample	Time (min)	Viability at 10^-x dilution						N pfu/ml	N/No	Log N/No
			0	-1	-2	-3	-4	-5			
0.000	Control	0.00				TNTC	168	24	2550000	1.000000	0
12.952	1	7.00			199	14			24875	0.009755	-2.01078
25.903	2	14.00		243	44	4			4268.75	0.001674	-2.77624
38.824	3	20.98	189	21					249.375	0.000098	-4.00969
45.300	4	24.48	62	0					77.5	0.000030	-4.51724

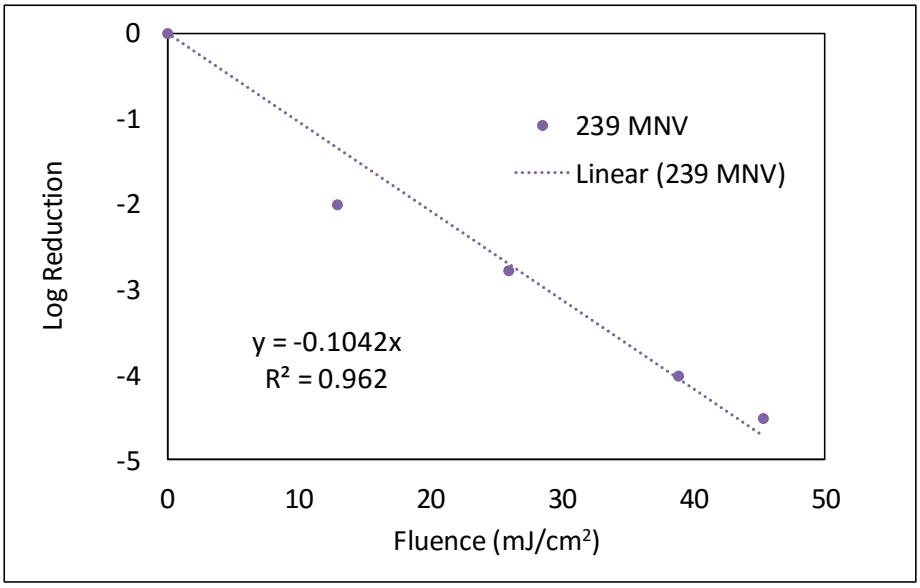

MNV-1 vs UV_{254}

Wavelength	254 nm
Temperature	23 ºC
pH	8
Solution	CBS

Virus	MNV-1

Average irradiance through the water =	0.052056	mW/cm^2

Fluence UV Dose mJ/cm^2	Sample	Time (min)	Viability at 10^-x dilution						N pfu/ml	N/No	Log N/No
			0	-1	-2	-3	-4	-5			
0.000	Control	0.00				TNTC	88	8	1100000	1.000000	0
7.600	1	2.43		TNTC	187	17	3		23375	0.021250	-1.67264
15.513	2	4.97	TNTC	188	34	3			3300	0.003000	-2.52288
23.165	3	7.42	60	17	0				143.75	0.000131	-3.88378

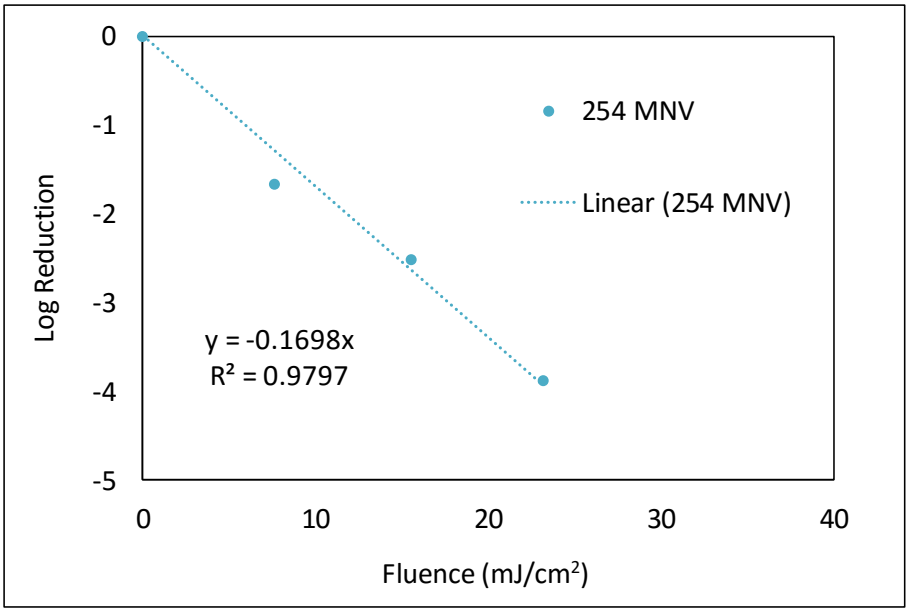

MNV-1 vs UV_{260}

Wavelength	260 nm
Temperature	23 °C
pH	8
Solution	CBS

Virus	MNV-1

Average irradiance through the water =	0.084519	mW/cm^2

Fluence UV Dose mJ/cm^2	Sample	Time (min)	Viability at 10^-x dilution						N pfu/ml	N/No	Log N/No
			0	-1	-2	-3	-4	-5			
0.000	Control	0.00				TNTC	177	20	2356250	1.000000	0
7.015	1	1.38			TNTC	52			65000	0.027586	-1.55931
14.115	2	2.78		TNTC	35	2			4375	0.001857	-2.73124
21.130	3	4.17	TNTC	30					375	0.000159	-3.79819
24.933	4	4.92	27	2					33.75	0.000014	-4.84395

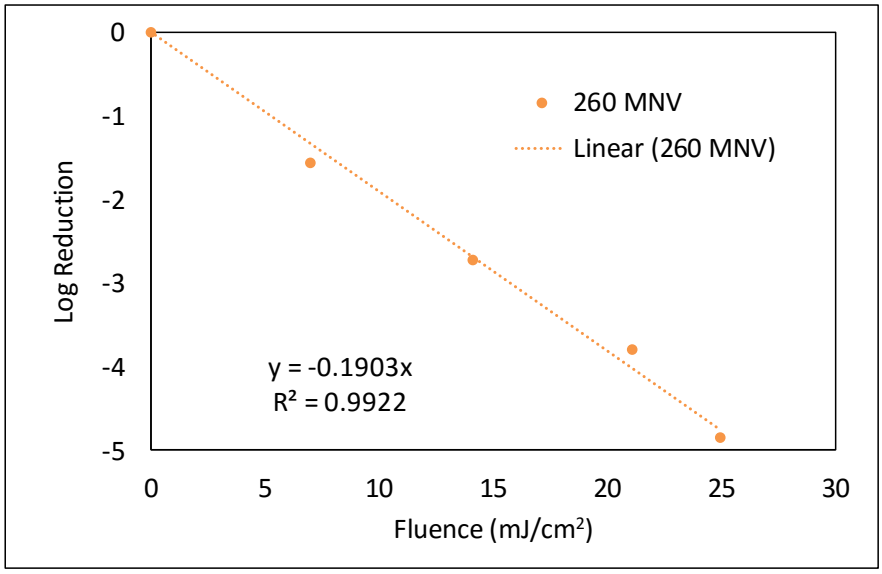

MNV-1 vs UV_{265}

Wavelength	265 nm
Temperature	23 °C
pH	8
Solution	CBS

Virus	MNV-1

Average irradiance through the water =	0.077871	mW/cm^2

Fluence UV Dose mJ/cm^2	Sample	Time (min)	Viability at 10^-x dilution						N pfu/ml	N/No	Log N/No
			0	-1	-2	-3	-4	-5			
0.000	Control	0.00				TNTC	173	31	3018750	1.000000	0
6.931	1	1.48			TNTC	97			121250	0.040166	-1.39615
13.861	2	2.97		TNTC	121				15125	0.005010	-2.30013
20.792	3	4.45	300	31					387.5	0.000128	-3.89156
24.296	4	5.20	38	0					47.5	0.000016	-4.80313

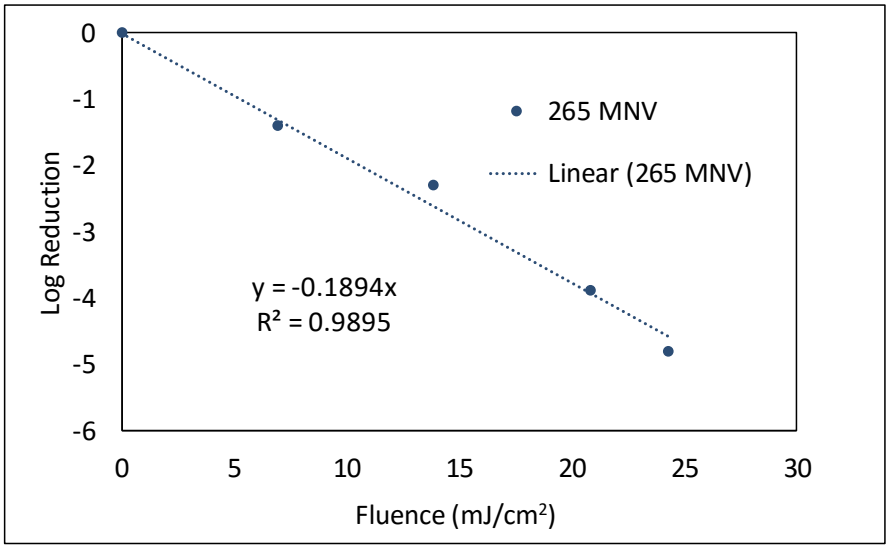

MNV-1 vs UV_{280}

Wavelength	280 nm
Temperature	23 ℃
pH	8
Solution	CBS

Virus	MNV-1

Average irradiance through the water =	0.030319	mW/cm^2

Fluence UV Dose mJ/cm^2	Sample	Time (min)	Viability at 10^-x dilution						N pfu/ml	N/No	Log N/No
			0	-1	-2	-3	-4	-5			
0.000	Control	0.00				TNTC	152	30	2825000	1.000000	0
10.309	1	5.67			TNTC	71			88750	0.031416	-1.50285
19.829	2	10.90		TNTC	74				9250	0.003274	-2.48488
29.743	3	16.35	322	41					457.5	0.000162	-3.79063

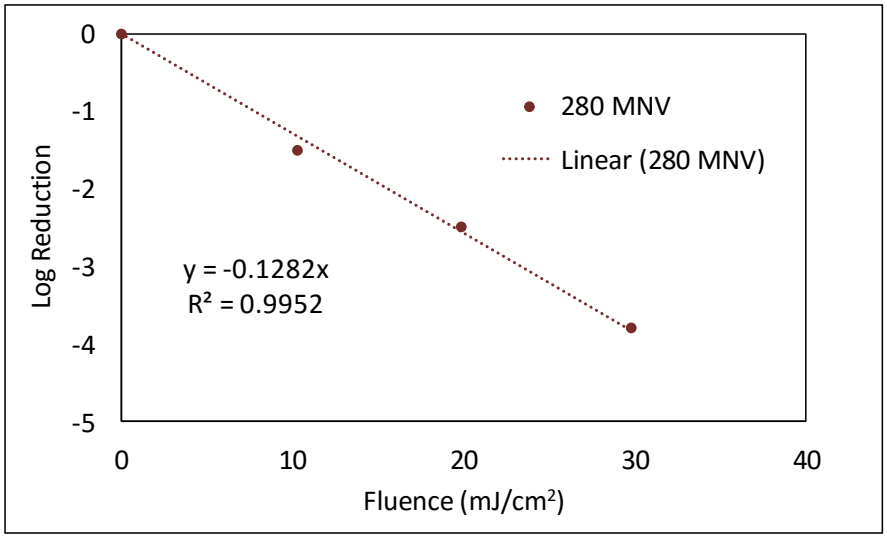

MP UV vs MNV-1

Wavelength	MP UV
Temperature	23 ℃
pH	8
Solution	CBS

Virus	MNV-1

Average irradiance through the water =	0.401353	mW/cm^2

Fluence UV Dose mJ/cm^2	Sample	Time (min)	Viability at 10^-x dilution						N pfu/ml	N/No	Log N/No
			0	-1	-2	-3	-4	-5			
0.000	Control	0.00					227	30	3293750	1.000000	0
10.034	1	0.42	_		TNTC	142	15		182500	0.055408	-1.25643
20.469	2	0.85	_	TNTC	81	9			10125	0.003074	-2.5123
30.503	3	1.27		61	8				762.5	0.000231	-3.63545
35.720	4	1.48	210	20					262.5	0.000080	-4.09856

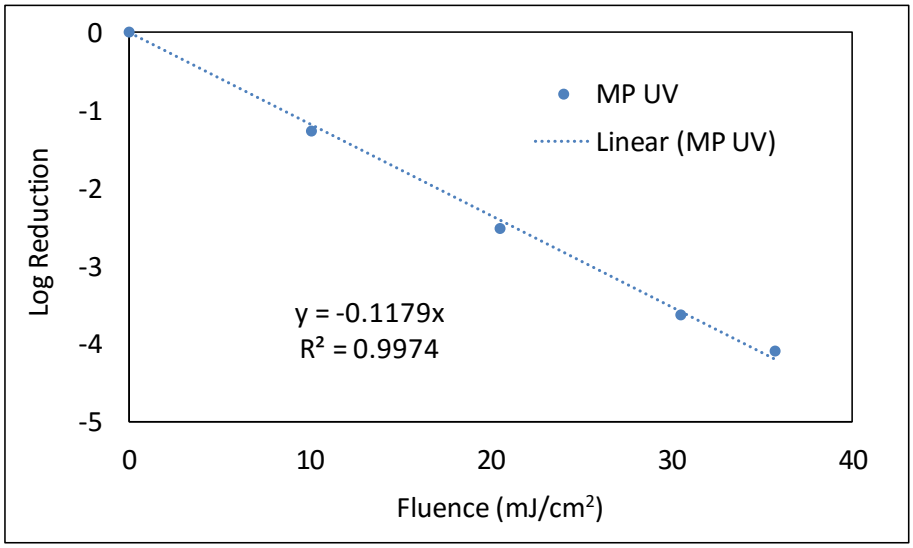

Relative Inactivation for Action Spectrum

CVB5		
Wavelength [nm]	k [cm2/mJ]	Relative to 254 nm
218	0.3095	1.8445
224	0.2256	1.3445
228	0.1540	0.9178
232	0.1302	0.7759
239	0.0894	0.5328
248	0.1341	0.7992
254	0.1678	1.0000
260	0.1570	0.9356
265	0.1746	1.0405
270	0.1471	0.8766
280	0.1140	0.6794
289	0.0554	0.3302

MNV-1		
Wavelength [nm]	k [cm2/mJ]	Relative to 254 nm
224	0.2126	1.2521
228	0.1384	0.8151
239	0.1042	0.6137
254	0.1698	1.0000
260	0.1903	1.1207
265	0.1894	1.1154
280	0.1282	0.7550